ANTI-ASTHMATIC AND AIRWAY SMOOTH MUSCLE RELAXATION EFFECTS OF POLYSACCHARIDES FROM *Lignosus rhinocerotis* IN ANIMAL MODELS

ABUBAKAR BISHIR DAKU

UNIVERSITI SAINS MALAYSIA

2025

ANTI-ASTHMATIC AND AIRWAY SMOOTH MUSCLE RELAXATION EFFECTS OF POLYSACCHARIDES FROM *Lignosus rhinocerotis* IN ANIMAL MODELS

by

ABUBAKAR BISHIR DAKU

**Thesis submitted in fulfilment of the requirements
for the degree of
Doctor of Philosophy**

May 2025

ACKNOWLEDGEMENT

TABLE OF CONTENTS

LIST OF TABLES

LIST OF FIGURES

LIST OF ABBREVIATIONS

AC	Adenyl-cyclase
ACH	Acetylcholine
ACO	Asthma COPD Overlap
ADAM	Metallopeptidase Domain
AHR	Airway Hyperresponsiveness
ANOVA	One-Way Analysis of Variance
APSD	Aerodynamic Particle Size Distribution
ASM	Airway Smooth Muscles
BALF	Bronchoalveolar Lavage Fluid
CAE	Cellulose Assisted Extraction
COPD	Chronic Obstructive Pulmonary Disease
CRD	Chronic Respiratory Diseases
DEAE	Diethylaminoethyl
Dexa	Dexamethasone
dH_2O	Distilled Water
DLC	Differentiation Leukocyte Count
DPI	Dry Powder Inhalation
DRC	Dose-Response Curve
EC_{50}	Concentration of Agonist that produces 50% maximal response
EAE	Enzyme Assisted Extraction
EF	Emitted Fraction
Emax	Concentration of agonist with maximal response
FPF	Fine Particle Fraction
GOPOD	Glucose Oxidase/ Peroxidase
GPT	Guinea-Pig Trachea
GSD	Geometric Standard Deviation
H&E	Haematoxylin and Eosin
HPLC	High Performance Liquid Chromatography
HWE	Hot Water Extraction
IC_{50}	Concentration of antagonist that produces 50% maximal response
IgE	Immunoglobin E

IL	Interleukin
IP	Intraperitoneal
LR	Lignosus rhinocerotis
LRE	Lignosus rhinocerotis extract
LRP	Lignosus rhinocerotis polysaccharide
MAE	Microwave Assisted Extraction
MB	Mass Balance
MFI	Mean Fluorescence Intensity
MMAD	Median Mass Aerodynamic Diameter
MOC	Micro Orifice Contactor
MP	Mushroom Polysaccharide
NGI	Next-Generation Impactor
OD	Optical Density
OVA	Ovalbumin
PAS	Periodic-acid Schiff
PBS	Phosphate Buffer Saline
PDD	Pulmonary Drug Delivery
RNA	Ribonucleic Acid
ROS	Reactive Oxygen Species
RT	Room Temperature
RWE	Room-temperature Water Extraction
SD	Standard Deviation
SEM	Standard Error of Mean
UAE	Ultrasound Assisted Extraction
WHO	World Health Organization

LIST OF APPENDICES

KESAN ANTI-ASMA DAN RELAKSASI OTOT LEMBUT SALURAN PERNAFASAN DARI POLISAKARIDA *Lignosus rhinocerotis* DALAM MODEL HAIWAN

ABSTRAK

Asma merupakan penyakit saluran pernafasan yang kronik yang dikaitkan dengan beberapa ciri termasuk bronkokonstriksi, vasodilatasi saluran udara, edema, pengaktifan saraf deria, dan hipersensitiviti. Kortikosteroid sistemik sangat penting dalam pengurusan asma dari peringkat sederhana sehingga ke peringkat yang lebih teruk, akan tetapi ia juga dikaitkan dengan pelbagai kesan sampingan apabila digunakan dalam jangka masa panjang. Hal ini telah mendorong para penyelidik untuk meneroka intervensi anti-asma melalui kaedah alternatif dan komplementari yang lebih selamat untuk mengurangkan tindak balas imun yang berlebihan ini. Polisakarida cendawan (MP) dilaporkan mengandungi sebatian β-glukan dan kompleks polisakarida-protein, yang diketahui mempunyai pelbagai kesan bioaktiviti, termasuk anti-radang, imunomodulator, antitumor dan antioksidan, seperti yang ditunjukkan dalam banyak kajian *in vivo* dan *in vitro*. Namun, potensi polisakarida *Lignosus rhinocerotis* (LRP) dalam memperbaiki patofisiologi asma masih belum diketahui, dan penyelidikan semasa mengenai sifat bioaktifnya masih terhad. Oleh itu, kajian ini bertujuan untuk (i) mengasingkan dan menentukan komposisi polisakarida LR, (ii) menentukan pemberian LRP melalui kaedah sedutan, (iii) mewujudkan model mencit BALB/c alahan asma yang diaruh OVA dan menentukan kesan LRP terhadap patofisiologi asma, dan (iv) menentukan kesan LRP terhadap pengecutan reseptor saluran udara pada cincin trakea tikus belanda (GPT). Elusi lajur DEAE-cellulose dan Sephadex G-100 LRP menghasilkan satu puncak simetri tunggal, menunjukkan

pengasingan sebatian polisakarida yang diperoleh dalam bentuk serbuk kuning muda. Ujian β-glukan megazyme menunjukkan bahawa peratusan α- dan β-glukan dalam LRP masing-masing adalah 21.52% ($\pm$ 0.53) dan 21.08% $\pm$ (2.19). Analisis HPLC mendedahkahkan bahawa LRP adalah heteropolisakarida lazim yang terdiri dari manosa, ribosa, rhamnosa, glukosa, galaktosa, xilosa, dan arabinosa. LRP sedutan serbuk kering menunjukkan sifat yang tidak stabil kerana ketumpatannya yang rendah dan higroskopik. Penebulaan larutan LRP menghasilkan aerosol dalam julat yang boleh disedut untuk penghantaran ke paru-paru, pemendapan aerosol *in vitro* menggunakan NGI menunjukkan fine particle fraction (FPF) adalah 62.84, mean median aerodynamic distribution (MMAD) adalah 4.16, dan geometric standard deviation (GSD) adalah 1.83. Rawatan penebulaan polisakarida LR (4, 8, dan 40 mg/ml) pada model mencit asma yang diinduksi OVA secara signifikan menghalang penyusupan sel radang ke dalam paru-paru, hiperplasia sel goblet, sitokin Th2 pro-radang, dan ekspresi gen radang paru-paru Cox-2, iNOS, and ADAM33 ($p<0,05$), dengan kumpulan rawatan 8 dan 40 mg/ml menunjukkan kesan yang paling ketara. Selain itu, LRP menunjukkan kesan relaksasi saluran udara yang diperhatikan tidak bergantung kepada reseptor beta, namun berpotensi melalui antagonisme reseptor muskarinik dan histamin pada cincin GPT yang dikecutkan oleh EC_{40} carbachol and EC_{50} histamine ($p <0,05$). Penemuan ini menunjukkan potensi terapeutik polisakarida LR sebagai alternatif pelengkap dalam pengurusan alahan asma.

ANTI-ASTHMATIC AND AIRWAY SMOOTH MUSCLE RELAXATION EFFECTS OF POLYSACCHARIDES FROM LIGNOSUS RHINOCEROTIS IN ANIMAL MODELS

ABSTRACT

Asthma is a chronic airway disease which is associated with several characteristics including bronchoconstriction, airway vasodilation, oedema, sensory nerve activation, and hypersensitivity. Systemic corticosteroids are crucial for managing moderate-to-severe asthma but are associated with various adverse effects with long-term use. This has driven researchers to explore safer complementary and alternative anti-asthmatic interventions to mitigate these exaggerated immune responses. Mushroom polysaccharides (MP) have been reported to contain β-glucan compounds and polysaccharide-protein complexes, which are known to exhibit several bioactivities, including anti-inflammatory, immunomodulatory, antitumor, and antioxidant properties, as demonstrated in numerous *in vivo* and *in vitro* studies. However, the potential of inhaled *Lignosus rhinocerotis* polysaccharide (LRP) to ameliorate asthma pathophysiology remains undetermined, and current research on its bioactive properties is limited. Therefore, this study aimed to (i) isolate and determine the polysaccharide composition of LR mushrooms, (ii) determine LRP inhalation delivery, (iii) establish a BALB/c mouse model of OVA-challenged allergic asthma and determine the effect of LRP on asthma pathophysiology, and (iv) determine the effect of LRP on airway receptor contractility in guinea pig tracheal (GPT) rings. The LRP DEAE-cellulose and Sephadex G-100 column elution exhibited a single symmetrical peak fractionated polysaccharide fraction. The megazyme β-glucan assay revealed that the percentages of α- and β-glucans in LRP were 21.52% (±0.53) and

21.07% ± (2.19), respectively. HPLC analysis revealed that LRP was a typical heteropolysaccharide composed of mannose, ribose, rhamnose, glucose, galactose, xylose, and arabinose. LRP spray drying was shown to produce unstable LRP powders due to its volatility and hygroscopic nature. Nebulization of the LRP solution-produced inhalable aerosols for lung delivery, the *in vitro* aerosol deposition using NGI demonstrated fine particle fraction (FPF) of 62.84, mean median aerodynamic distribution (MMAD) of 4.16, and geometric standard deviation (GSD) of 1.83. LRP nebulization treatment (4, 8, and 40 mg/ml) in an OVA-challenged mouse model of asthma significantly inhibited airway inflammation, and Cox-2, iNOS, and ADAM33 lung inflammatory gene expression ($p < 0.05$), with 8 and 40 mg/ml treatment groups expressing the most significant effect. Furthermore, LRP demonstrated an airway relaxation effect independent of beta receptors, potentially through muscarinic and histamine receptor antagonism in carbachol-and histamine-pre-contracted GPT rings ($p < 0.05$). These findings suggest the therapeutic potential of LR mushroom polysaccharides as complementary alternatives for the management of allergic asthma.

CHAPTER 1

INTRODUCTION

1.1   Background of the study

Chronic Respiratory Diseases (CRDs) are the third leading cause of death globally, causing 4.0 million deaths and accounting for a prevalence of 454.6 million cases. In recent decades, the prevalence of CRDs has increased from 28.5% in 1990 to around 39.8% in 2019 (Momtazmanesh *et al.*, 2023). CRDs remain a leading cause of morbidity, mortality, and disability-adjusted life years (DALY) worldwide (Chen *et al.*, 2023). The most prevalent CRDs are chronic obstructive pulmonary disease (COPD) and asthma accounting for 212.3 million and 262.4 million cases, respectively (Momtazmanesh *et al.*, 2023). According to Song *et al.* (2022), the prevalence of asthma among individuals aged 5-69 years in Southeast Asia is approximately 8.8%. Additionally, the National Health and Morbidity Survey (IPH, 2008) reported a prevalence of 4.2% in Malaysia. In a recent population-based cross-sectional study, Tan *et al.* (2022) reported a prevalence of 3.8% in a semi-urban and rural Malaysian populations.

Asthma is associated with genetic and environmental factors (including air pollution, workplace exposure to chemicals, fumes, or dust, house dust mites and moulds), leading to significant morbidity and mortality (To *et al.*, 2012; OMS, 2013). It involves inhalation via environmental exposure followed by a pathological inflammatory immune response. Asthma is a chronic allergic airway inflammatory response orchestrated by activation of inflammatory cells and the release of pro-inflammatory mediators. These effects lead to narrowing of the airways, dilation of blood vessels, swelling in the respiratory passages, and stimulation of sensory nerve

1

endings, and is characterized by airway hyper-responsiveness (AHR) (Barnes, 2016; Athari *et al.*, 2017). This inflammatory responses cause acute respiratory symptoms referred to as exacerbations including cough, wheeze, chest dyspnoea and tightness (Andrew, Brian and David, 2020).

Owing to its complex pathophysiology and various triggers, multiple asthma phenotypes have been recognized. Atopic asthma, also referred to as extrinsic asthma, T2 asthma or type 2 asthma is mediated by T-helper 2 (Th2) inflammatory responses characterized by increased Th2 cells, Th2 cytokines, eosinophils, IgE-producing B cells, and activated type-2 innate lymphocytes (ILC-2 cells) (Fahy, 2015; Barnes, 2016). The atopic phenotype accounts for approximately 60% of asthma cases and is often responsive to inhaled corticosteroids (ICS) (Narendra, Blixt and Hanania, 2019). Non-atopic asthma is characterized by the absence of Th2 inflammation, which is associated with neutrophilic and TH17 cells mediated inflammatory pathway activation (Anto *et al.*, 2017; Narendra, Blixt and Hanania, 2019).

Respiratory exacerbations of acute asthma include cough, wheezing, chest dyspnea, chest tightness, and other symptoms that can be graded as mild, moderate, severe, or even life-threatening (Barnes, 2016; Andrew, Brian and David, 2020). During an asthma attack, immediate airway narrowing occurs, which lasts for approximately 1 h, or even 4–6 h into the late phase in more sensitive individuals, and the late phase of airway compromise is induced by chronic inflammation that lasts from hours to days (Lee, Lim, *et al.*, 2018).

Various medications, including corticosteroids, β_2-agonists, muscarinic receptor antagonists, leukotriene modifiers, long-acting phosphodiesterase-4 inhibitors, and biologics, are presently used in the management of asthma, in addition to non-pharmacological measures such as cessation of smoking, controlling allergen

exposure, physical activity, and breathing exercises (GINA, 2024). Systemic corticosteroids (SCS) are necessary for the control of asthma in patients with moderate-to-severe asthma (Haida *et al.*, 2020). However, a clear link exists between chronic SCS use and the risk of SCS-related complications in patients with severe asthma, where corticosteroids are linked to cause cardiovascular complications (Lefebvre *et al.*, 2015). The long-term use of asthma medications is associated with adverse effects such as tachycardia, anxiety, osteoporosis, stunting of growth in children, and cataract formation (Newnham, 2001) and has been reported to be associated with a 3.1 and 2.7 folds higher rate of developing osteoporotic fracture and pneumonia, respectively (Price *et al.*, 2018).

Mushrooms, a group of fungal species, have a long history of being used as universal remedy in various cultures worldwide. These species can be categorized into edible and non-edible, with the former being used for nutritional or therapeutic purposes and the latter being mostly toxic. According to Zhou et al. (2020), only about half of the mushrooms traditionally used have been scientifically studied; thus, there is a need for further investigation in this research field to harness their phytochemical benefits. Studies have been conducted on the potential health and nutritional benefits of various mushrooms, as well as on the therapeutic use of their crude extracts and isolated bioactive compounds. The macrofungal species Ascomycota and Basidiomycota are known to produce various biological macromolecules. In addition to their traditional medicinal uses, mushrooms are currently used as a source of nutrients, additives, and cosmeceuticals.

Lignosus rhinocerotis, often referred to as "tiger milk mushroom" by indigenous communities in Malaysia, has a long history of use in Southeast Asia, this

mushroom species has gained attention for its potential health and medicinal benefits (Lee, Chang and Noraswati, 2009; Lau *et al.*, 2013). Morphologically, LR has a tea-brown pileus with a woody and rigid umbrella-shaped stipe projecting from an underground sclerotium (Lau *et al.*, 2015; Usuldin, 2020). These sclerotia have been reported to be potential sources of nutrition and medicine (Choong *et al.*, 2016).

Different traditional medicine preparation methods for LR have been reported, including boiling or maceration-like methods, macerated (aqueous preparations), grated, dewed, and sometimes mixed with other herbs or burned and applied to the chest (Lau *et al.*, 2015). Although the medicinal preparation methods of LR vary, it is also consumed orally in raw or decoction form (Lee, Lim, *et al.*, 2018). LR has traditionally been used to treat a wide range of conditions, such as liver cancer, chronic hepatitis, gastric ulcers (Lai, Wong and Cheung, 2008), cancer, fever, chronic cough, and inflammation-related disorders (Chang and Lee, 2004; Lau *et al.*, 2015) among others.

Recently, a significant portion of the research on medicinal mushrooms has concentrated on the therapeutic effects of isolated bioactive compounds rather than on crude extracts. Various bioactive compounds, such as polysaccharides, polysaccharide-protein complexes, lectins, flavonoids, fatty acids, terpenoids, and alkaloids have been identified in a wide range of mushroom species, and these compounds have been investigated for their various health-promoting bioactivities. A large body of scientific research has been conducted and reported the bioactive properties of LR extracts, including bronchodilation (Lee, Lim, *et al.*, 2018), anti-asthmatic (Johnathan *et al.*, 2016; Muhamad *et al.*, 2019), immunomodulatory, anti-inflammatory effects (Guo, Wong and Cheung, 2011; Lee *et al.*, 2014), antioxidant, anti-proliferative (Jamil *et al.*, 2018; Yap *et al.*, 2018b) anti-diabetic (Yap *et al.*,

2018a), neuroprotective (Yeo *et al.*, 2019; Kittimongkolsuk, Pattarachotanant, *et al.*, 2021) and antimicrobial activities (Mohanarji, Dharmalingam and Kalusalingam, 2012; Sillapachaiyaporn and Chuchawankul, 2020).

Previous studies by Lee *et al.,* (2012) and Lee *et al.*, (Lee *et al.*, 2014) analyzed the anti-inflammatory effects of LR sclerotium extracts. The aqueous extracts demonstrated the most potent anti-inflammatory activity, particularly the high-molecular-weight (HMW) fraction, which contains a mixture of carbohydrates and proteins. Similarly, LR extract displayed strong inhibitory effects on TNF-α and exhibited antiproliferative activity against both human breast carcinoma (MCF-7) and human lung carcinoma (A549) cells. In another study, intranasal administration of LR extract was found to significantly suppress inflammatory cells counts in BALF, CD4+ T cells in lung draining lymph nodes, serum IgE and Th2 cytokines in BALF, and leukocyte infiltration and mucus production in the lungs in an OVA-challenged asthma model (Muhamad *et al.*, 2019).

Several mushrooms have been extensively studied for their polysaccharides content, which is known to provide a range of therapeutic benefits. Polysaccharides are fundamental components of mushroom cell walls and mushroom polysaccharides (MP) are generally classified into homo- polysaccharides or hetero- polysaccharides. These classifications are based on their bond types - homolinkages or heterolinkages and the type and sequence of their monosaccharide units resulting in a broad range of structural variations among MPs (Ruthes, Smiderle and Iacomini, 2016). β-glucan being the most abundant polysaccharides in the mushroom cell walls (Volman *et al.*, 2010; Li *et al.*, 2015; Wang *et al.*, 2017) have been studied extensively. These complex carbohydrates are found in various mushrooms, including *in Lignosus rhinocerotis*. In recent years, the most effective clinical application of medicinal mushrooms has been

in the prevention and treatment of immune system disorders, particularly in immunodeficient and immunocompromised patients (Wasser, 2014).

1.2 Problem Statement

Various factors, including tobacco smoking, air pollution, occupational chemical hazards, and genetics have been linked to pulmonary diseases. According to estimates, approximately 2 billion people are exposed to indoor toxic smoke, 1 billion to outdoor pollutant air, and another 1 billion to tobacco smoke (Levine *et al.*, 2021), these prolonged exposures may lead to pulmonary diseases. The global epidemiology and prevalence of asthma have increased markedly in recent decades, which is part of the global increase in chronic respiratory diseases that are now leading causes of disability and reduced life expectancy worldwide (Ehteshami-Afshar *et al.*, 2016).

The economic burden of asthma is significant and multifaceted, encompassing both direct costs, such as healthcare services and increased emergency department visits, and indirect costs, including productivity losses due to missed work or school days (Loftus and Wise, 2015; Zannetos *et al.*, 2017). Notably, although the overall economic burden of asthma is increasing, there is considerable variation in the per capita annual costs of asthma across different regions and countries (Ehteshami-Afshar *et al.*, 2016).

Longitudinal, open-cohort, observational studies on asthma management observed that long-term use of SCS led to adverse complications and increased costs (Lefebvre *et al.*, 2015). Long-term use of SCS often leads to adrenal insufficiency (AI), potentially necessitating hydrocortisone replacement therapy (Haida *et al.*, 2020). The study found a 15% prevalence of AI among asthmatic patients on high-dose oral corticosteroids (OCS) and recommends thorough assessment and

treatment for cases with underlying AI. In addition, these complications are reported to be more pronounced in elderly asthmatic patients. Side effects of β_2-agonists include cardiotoxicity, whereas corticosteroids can result in osteoporosis, skin bruising, and cataracts (Reed, 2010). Therefore, scientists have become more motivated to research safe anti-asthmatic interventions as a useful approach to mitigate these exaggerated immune responses.

LR mushrooms contain various chemical constituents, as previous studies have revealed the presence of alkanes, fatty acids, benzene, dicarboxylic acid, phenolics (Lau *et al.*, 2013; Johnathan *et al.*, 2016), flavonoids (Jamil *et al.*, 2018), proteins (Lee *et al.*, 2014; Yap *et al.*, 2018a), polysaccharides and polysaccharide–protein complexes (Lai *et al.*, 2011; Lau, Abdullah and Aminudin, 2013; Mohd Jamil *et al.*, 2013; Lai, Zainal and Daud, 2014; Jamil *et al.*, 2018; Sum *et al.*, 2020) in their sclerotia. Previous studies have proposed that polysaccharides and protein complexes are the major bioactive components that determine LR bioactivity (Lai, Wong and Cheung, 2008; Wong, Lai and Cheung, 2011; Lee *et al.*, 2012).

1.3   Justification

The identification and discovery of new therapeutics from natural products have gained attention because of their cost-effectiveness and safety, and there is a need for natural alternatives to reduce the negative consequences of long-term medication dependence in respiratory conditions, such as asthma. LR extracts have been reported to mitigate allergic airway inflammation and hyperresponsiveness in an asthmatic model. Despite the traditional use of LR for respiratory ailments and studies supporting its efficacy, evidence identifying the phytochemicals responsible for its purported

benefits remains limited and the active anti-asthmatic constituent is currently undetermined.

Therefore, the isolation and characterisation of LR mushroom bioactive compounds will help elucidate their traditional medicinal claims, determine the receptors involved in the LR antiasthma mechanism, and provide a direction for further studies on their medicinal potential. Although several studies have investigated the polysaccharide constituents in mushroom species, few have focused on the fractionation and isolation of polysaccharides from LR.

The traditional application of LR is likely based on its potential efficacy and affinity for airway inflammatory and immunomodulatory targets. The anti-asthmatic effect of LR crude extracts (LRE) reduced serum IgE levels and significantly suppressed Th2 cytokines and inflammatory cell counts in BALF, as well as ameliorated airway remodelling have been previously reported (Muhamad *et al.*, 2019, 2023; Johnathan *et al.*, 2021). The purpose of this study was to build upon previous anti-asthmatic effect studies of LRE and determine whether it can be a viable complementary therapy for managing asthma. This research was conducted to investigate the effects of LR polysaccharides in mitigating the pathogenesis of asthma-related airway inflammation, airway receptor effect, and to assess its potential for lung inhalation delivery.

1.4   Objective

1.4.1   General objectives

This study aimed to isolate polysaccharide constituents from *Lignosus rhinocerotis* and to determine its anti-asthmatic effects in OVA-challenged mouse

model of asthma, as well as its bronchodilator effect on isolated guinea pig trachea (GPT) rings.

1.4.2   Specific objectives

i.   To isolate and characterise polysaccharide constituent of LR

ii.   To determine inhalation formulation and aerodynamic characterization for *Lignosus rhinocerotis* polysaccharides (LRP)

iii.   To establish OVA-challenged mouse asthma model and to determine the optimal inhalation dose of LRP on selected airway inflammation parameters

iv.   To determine immunological parameters (serum IgE; BALF IL-4, IL-5 and IL-13 levels; and lung gene expression of iNOS, COX-2, ADAM33 and IL-22) in the OVA-challenged mouse model of asthma treated with LRP.

v.   To determine the histological changes in airway inflammation (inflammatory cells infiltration, goblet cell hyperplasia, and BALF differential leukocyte count) in the OVA-challenged mouse model of asthma treated with LRP.

vi.   To determine the effect of LRP on ASM contractility in isolated Guinea Pig Trachea (GPT) rings.

1.5   Research hypotheses.

i.   LRP has no effect on asthma related immunological and histological parameters.

ii.   LRP has no effects on GPT airway contractility.

CHAPTER 2

LITERATURE REVIEW

2.1 An overview of asthma

Respiratory diseases are a broad spectrum of conditions affecting the lungs and airways. These disorders can be classified as either obstructive or restrictive. Obstructive respiratory disorders, such as asthma and COPD, are characterized by limited airflow resulting from inflammation and constriction of the airways (Alhajery, 2024). Conversely, restrictive respiratory disorders, exemplified by interstitial lung disease (ILD), are distinguished by reduced lung capacity due to inflammation or scarring of lung tissue. These conditions are characterized by restrictive ventilatory defects and impaired gas exchange (Clement and Eber, 2008; Xu, 2019).

By breathing air, the lungs are continuously in contact with inhaled outdoor pollutants and antigens, mostly non-pathogenic, and therefore do not elicit or induce an immune response. However, this is not true for allergic conditions, such as asthma, where air pollutants, viruses, and allergen sensitization trigger subsequent asthma exacerbations (Sears, 2008). Asthma is a chronic allergic inflammatory response in all airways, from the trachea to the terminal bronchioles (Barnes, 2016), and is characterized by the presence of inflammatory cells and the release of proinflammatory mediators (Rawy and Mansour, 2015). Asthma is also characterized by airway hyper-responsiveness (AHR) (Athari *et al.*, 2017) and release of pro-inflammatory and anti-inflammatory cytokines (Bodkhe *et al.*, 2020) with reversible airflow obstruction (Steinke and Borish, 2001; Athari *et al.*, 2017).

2.1.1 Epidemiology of asthma

It is estimated that approximately 2 billion people are exposed to indoor toxic smoke, 1 billion to outdoor pollutant air, and another 1 billion to tobacco smoke (Levine *et al.*, 2021), leading to pulmonary diseases that impose an immense worldwide health burden (Lallukka *et al.*, 2017). Chronic Respiratory Diseases (CRDs) are the third leading cause of death globally, causing 4.0 million deaths and accounting for a prevalence of 454.6 million cases. In recent decades, the prevalence of CRDs has increased from 28.5% in 1990 to 39.8% in 2019 (Momtazmanesh *et al.*, 2023). These diseases include asthma, COPD, pulmonary hypertension, cystic and idiopathic pulmonary fibrosis, and lung cancer. Factors such as tobacco smoke, air pollution, occupational chemicals, and genetics are linked to pulmonary diseases, which are characterized by inflammation, airflow limitation, and excessive mucus secretion (Mehtaa *et al.*, 2018; Aminu *et al.*, 2020).

Chronic respiratory diseases together account for approximately 4.7% of global disability-adjusted life years (Högman *et al.*, 2018). Asthma is the most common long-term respiratory disease (Menzies-Gow *et al.*, 2019), affecting all age groups and most frequently affecting patients with allergic diseases (Antoniu, 2011). Asthma affects approximately 300-339 million individuals globally (Lallukka *et al.*, 2017; Network GA, 2018) representing an estimated 4.3% of the world's population. The disease is associated with genetic and environmental factors, and is characterized by significant morbidity and mortality (To *et al.*, 2012).
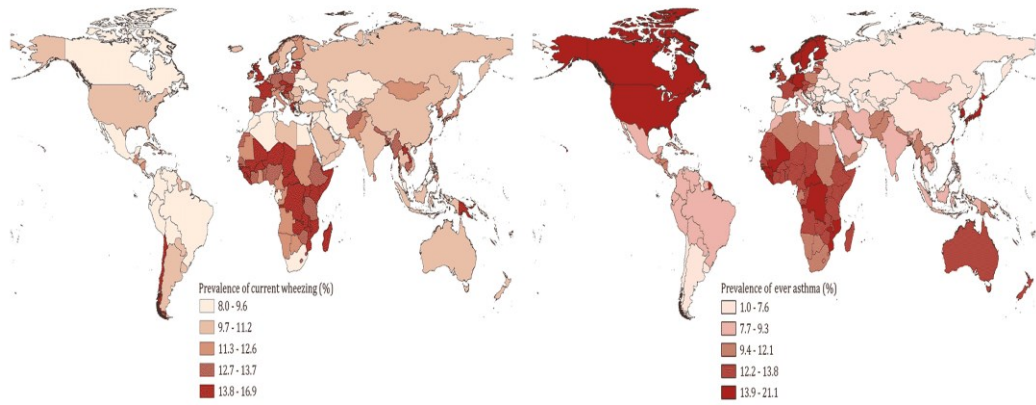
Figure 2.1   Global asthma prevalence (Adopted from Song *et al.*, 2022)

A systematic analysis of asthma population-based studies by Song et al. (2022) indicated that asthma affects approximately 8.8% of people aged between 5 and 69 years in Southeast Asia. Furthermore, the National Health and Morbidity Survey (IPH, 2008) reported a prevalence rate of 4.2% in Malaysia. In a recent population-based cross-sectional study, Tan et al. (2022) reported a prevalence of 3.8% in semi-urban and rural Malaysian populations.

Based on gender, a reverse association was reported with greater asthma incidence and prevalence among boys before puberty, and higher in females after puberty (Schatz, Clark and Camargo, 2006), which postulates a hormonal influence on asthma exacerbations (Sears, 2008). Similarly, the use of oral contraceptives has been reported to reduce airway hyperresponsiveness (Tan, McFarlane and Lipworth, 1997), while hormone replacement therapy post menopause has been associated with increase asthma and exacerbations (Troisi *et al.*, 1995; Barr *et al.*, 2004). Joks et al. (2020) demonstrated a possible hereditary link between cancer and asthma. Their study found a higher prevalence of cancer in families of asthmatic subjects or allergies than in families of subjects without asthma or allergies, implying a heritable trait that predisposes to both cancer and allergy-asthma.

In low- and middle-income countries, atopy was observed to have less influence on the prevalence of asthma symptoms, while breastfeeding exerts a protective effect on non-atopic asthma (Asher, 2010). The International Study of Asthma and Allergies in Childhood (ISAAC) cross-sectional study, involving children from two school-age groups 13–14 years adolescents and 6–7 years children from 233 collaborating centres across 98 countries, demonstrated global prevalence rates of current asthma of 14.1% and 11.7%, respectively. Notably, there was substantial variation in prevalence and severity across centres, regions, and countries (Mallol *et al.*, 2013).

As stated, the determinants of diseases are majorly economic and social (Rose, 1992), accordingly environmental factors influence the prevalence of asthma, rhino-conjunctivitis, and eczema; therefore, analysis of the population environment is paramount in asthma epidemic assessment (Asher, 2010). An epidemiology and Natural History of Asthma: Outcomes and Treatment Regimens (TENOR II) multicentre observational study reported a continued increase in morbidity, allergic sensitization, exacerbations, very poorly controlled asthma, and reduced lung function (Chipps *et al.*, 2018). The prevalence of asthma symptoms tends to be higher in high-income countries but severe in low- and middle-income countries. These trends in asthma epidemics in developed nations over the past decades were observed to gradually affect developing countries as they become more urbanized (Asher, 2010).

Furthermore, the prevalence of asthma-COPD overlap (ACO) varies widely in the general population, ranging from 0.9% to 11.1% according to previous studies (Uchida, Sakaue and Inoue, 2018); with approximately 15–25% of obstructive airway diseases are ACO conditions (Bodkhe *et al.*, 2020).

2.1.2 Asthma Phenotypes

Owing to its complex pathophysiology and variant triggers, multiple asthma phenotypes are recognized with some under consideration, the most common of which include:

2.1.2(a) Atopic asthma

Atopic asthma, also referred to as extrinsic T2 or Th2 high asthma, is mediated by T helper 2 (Th2) inflammatory responses and is characterized by increased Th2 cells, Th2 cytokines, and eosinophils (Anto *et al.*, 2017) or activated type 2 innate lymphocytes (ILC-2 cells) (Fahy, 2015). Hence, it is referred to as Type 2 asthma (Bodkhe *et al.*, 2020). Atopy can be determined by measuring the total and antigen-specific serum IgE levels or assessing immediate cutaneous reactions to panels of antigens through allergen skin testing (Burrows. B. et al., 1989). The atopic phenotype asthma accounts for about 60% of asthma cases and is often responsive to inhaled corticosteroids (ICS) (Narendra, Blixt and Hanania, 2019). The majority of asthma patients exhibit allergic airway inflammation (Bodkhe *et al.*, 2020). Allergic asthma is characterized by recurrent wheezing, shortness of breath, chest tightness, and coughing (Barnes, 2016).

Upon reaching the airway, allergens are taken up by DCs and presented to Th lymphocytes by the extracellular major histocompatibility complex (MHC) class II (Barnes, 2016). In atopic asthma models, re-exposure to allergens led to an IgE-mediated inflammatory cascade in the airways with airway eosinophils infiltration; increase levels of IgE, airway mucus production and T-helper 2 cytokines levels, (Johnathan *et al.*, 2016; Kim, Song and Lee, 2019; Muhamad *et al.*, 2019).

2.1.2(b)   Non-atopic (intrinsic) asthma

Non-atopic asthma is characterized by the absence of Th2 inflammation, and is hence referred to as non-type-2 (Fahy, 2015), T2 low, non-T2 (Narendra, Blixt and Hanania, 2019), or non-atopic asthma, which is a more severe type of asthma disease (Wong, Lai and Cheung, 2011). Non-atopic asthma is associated with neutrophilic inflammation (Anto *et al.*, 2017), TH17 cells mediated inflammatory pathway activation (Narendra, Blixt and Hanania, 2019), and paucigranulocytic airway inflammation (Anto *et al.*, 2017; Narendra, Blixt and Hanania, 2019). The subtypes of T2 Low or non-atopic asthma include neutrophilic asthma associated with smoke exposure, elderly asthma, and late-onset obese asthma (Narendra, Blixt and Hanania, 2019).

2.1.2(c)   Asthma-COPD overlap (ACO)

Asthma-COPD overlap (ACO) is a condition characterized by persistent airflow limitation, with clinical features of both asthma and COPD (Hikichi, Hashimoto and Gon, 2018; Uchida, Sakaue and Inoue, 2018). Asthma is characterized by eosinophilic and major Th2 lymphocyte-mediated responses, while COPD is characterized by neutrophilic, macrophage inflammation, and majorly Th1 mediated (Barnes, 2008; Erick Bateman, 2016). Etiologically, asthma is an allergic disease due to airway hyper-responsiveness leading to reversible airflow obstruction (Erick Bateman, 2016; Bodkhe *et al.*, 2020), while COPD is caused by tobacco smoking, leading to progressive and irreversible (Högman *et al.*, 2018) or not fully reversible airflow obstruction (Zuo *et al.*, 2019). Certain patients manifest features of both neutrophil-based COPD and eosinophil-based asthma inflammation (Bodkhe *et al.*, 2020). However, each disease condition can express heterogeneity and overlap

between both conditions in clinical practice (Uchida, Sakaue and Inoue, 2018); hence, the condition is referred to as ACO.

Other Subtypes of asthma include early onset allergic asthma, late-onset eosinophilic disease, and aspirin-exacerbated respiratory disease (AERD) (Narendra, Blixt and Hanania, 2019).

2.1.3   Risk factors of asthma

Asthma involves inhalation of environmental adjuvants or antigens that trigger a pathological inflammatory immune response to that exposure. The strongest risk factor for asthma is atopy, which is an exaggerated symptomatic immune response against common environmental antigens (Porter *et al.*, 2011) and is a genetically controlled hypersensitivity to antigens (Kabesch M. et al., 2006). Single nucleotide polymorphisms at the IL4 and IL13 loci (Demenais *et al.*, 2018) and their epigenetic modifications are associated with asthma (Seumois *et al.*, 2014).

Asthma inflammation is associated with airway hyper-responsiveness (AHR) induced by upper respiratory tract viral infections, allergens, exercise, cold air, SO2, or particulate exposure (Barnes, 2016). According to Porter et al. (2011) many human allergens in fungi, pollen, bacteria, dust mites, and others share a common proteinase activity that is both structurally and biochemically similar.

During acute asthma exacerbation, allergic sensitization is likely triggered by the synergistic interaction of allergens with respiratory viruses (Murray, Simpson and Custovic, 2004; Porter *et al.*, 2011). Several viral infections have been implicated in triggering asthma exacerbation, including Rhinovirus (Johnston NW *et al.*, 2005; Murray *et al.*, 2006) and human metapneumovirus (Sears, 2008). Active fungal infections are believed to partly trigger asthma and related respiratory tract allergic diseases (Porter *et al.*, 2011), therefore highlighting the potential relevance of

antifungals in asthma management (Denning. D.W. et al., 2009; Pasqualotto A.C. et al., 2009; Vicencio. A.G. et al., 2010).

However, several other risk factors are associated with asthma prevalence. Factors such as thunderstorms and extreme weather conditions (Marks *et al.*, 2001), fungal spores (Atkinson *et al.*, 2006; Porter *et al.*, 2011), Maternal tobacco (Peden, 2003), psychological stress (Sandberg *et al.*, 2004) have been associated with epidemics of asthma exacerbations. At the population level, these risk factors act as either direct causes of disease or as effect modifiers or determinants of exposure to individual risk factors (Asher, 2010).

Genetic analysis has associated asthma and COPD with certain common susceptibility genes: A Disintegrin and Metalloprotease Domain (ADAM33), ADAM8, and orosomucoid-like protein 3 (ORMDL3). Accordingly, genetic airway hyperreactivity, high IL-17 levels, and viral infections during early childhood are risk factors for the development of both asthma and COPD. Both the intrauterine and external environments influence pulmonary hypoplasia, which is a risk factor for both asthma and COPD (Hikichi, Hashimoto and Gon, 2018). Thus, these risk factors increase an individual's tendency to develop ACO.

2.1.4 Pathogenesis and pathophysiology of asthma
2.1.4(a) Pathogenesis of asthma

Asthma responses are mediated through the interaction of inflammatory mediators with their respective cellular receptors on the airway tissues and inflammatory cells. Adjuvants and allergens that trigger these inflammatory responses are recognised by immune cell receptors based on their structural features, such as microbial cell wall components, nucleic acids, and certain proteins, referred to as pathogen-associated molecular patterns (PAMPs) (Ramet M et al., 2001; Kim *et al.*,

2008). Examples are the toll-like receptors (TLRs), which are integral membrane glycoproteins located on the cell surface that sense microbial antigens or intracellular vesicles that sense microbial nucleic acids, following which TLR stimulate the immune system towards a pro- or anti-allergic response (Akira and Takeda, 2004).

Nuclear Factor Kappa-B (NF-κB) is the main signal controlling factor of the TLRs pathway, causing the production of different pro- or anti-allergic inflammatory cytokines and chemokines (Akira, Uematsu and Takeuchi, 2006; Gon, 2008). Therefore, TLR stimulation can mediate tissue damage or repair, depending on the type of TLR-activated signalling pathway (Athari *et al.*, 2017). The TLRs are specific Pattern-Recognition Receptors (PRRs) that allow the innate immune system to recognize some microbial antigenic molecules of PAMP (Akira and Takeda, 2004). The T helper type 2 (Th2) immune response is crucial for protection against pathogens and the orchestration of humoral immunity. However, excessive Th2 response can lead to the development of asthma and other allergic diseases (Liu and Liu, 2022).

For allergen scanning and recognition, DCs possess PRRs, including toll-like receptors (TLRs), C-type lectin receptors, NOD-like receptors, and RIG-I-like receptors, for sensing the local environment (Wills-Karp, 2010; Gregory and Lloyd, 2011). DCs are also activated by epithelial cells, especially in the case of environmental adjuvants (diesel particles, dust particles, and toxic gases) that sensitise Th2/Th17 cells through DCs (Schuijs *et al.*, 2013). This occurs either by producing DAMPs in response to allergens or by producing the cytokines IL-33, IL-25, and GM-CSF in a TLR-dependent manner. In sensitised individuals, the nasal mucosa contains high levels of IgE-binding mast cells that traverse the epithelium into the mucosal region and degranulate upon allergen exposure and recognition (Enerback, Pipkorn and Granerus, 1986).

Nevertheless, it is crucial to acknowledge that the Th2-dominant concept alone is insufficient to elucidate all the aspects of asthma pathogenesis. Recent investigations have emphasised the significance of the airway epithelium in asthma development, particularly through the secretion of alarmins, which induce type 2 innate lymphoid cells (ILC2s) (Singh *et al.*, 2023).

Furthermore, asthma exhibits a hereditary component, although the specific genes involved remain unclear. Certain asthma phenotypes demonstrate strong hereditary associations, and their inheritance patterns are complex and appear non-Mendelian. It is probable that multiple genes contribute to asthma, with locus heterogeneity and polygenic inheritance resulting in the multifaceted expression of the condition (Sinyor and Perez, 2023). ADAM33 and ADAM8 are genes significantly associated with susceptibility to asthma and its progression, with ADAM33 polymorphism significantly associated with an increased risk of childhood asthma (Sun *et al.*, 2017). Genome-wide association studies have identified IL33 and IL-1 receptor-like 1 (IL1RL1) genes as substantial contributors to asthma (Grotenboer *et al.*, 2013). The expression of ADAM33 and ADAM8 increases with asthma severity, indicating their roles in airway remodelling and disease progression (Foley *et al.*, 2007; Tripathi *et al.*, 2013). Furthermore, RORA, which encodes a transcription factor crucial for the differentiation of type 2 innate lymphoid cells, has also been associated with susceptibility to asthma (Grotenboer *et al.*, 2013).

2.1.4(b)   Pathophysiology of asthma

The pathophysiology of asthma involves inhalation of environmental exposure, followed by a pathological inflammatory immune response (Porter *et al.*, 2011), with mobilisation and migration of inflammatory cells into the peribronchiolar and perivascular regions of the airways (Curtis *et al.*, 1990; Lambrecht and Hammad,

2015). Many inflammatory cells are involved in asthma pathophysiology, including dendritic cells, lymphocytes, eosinophils, mast cells, macrophages, and neutrophil inflammatory cells, together with airway structural cells such as epithelial fibroblasts and smooth muscle cells, which secrete mediators that orchestrate a complex network of inflammatory cytokines with positive or negative feedback on each other (Barnes, 2016), comprising a series of interconnected and concurrent physiological processes in asthma pathophysiology.

The recognition and presentation of antigen derivatives to Th2 triggers the secretion of Th2 cytokines that mediate eosinophils (Barnes, 2016; Athari *et al.*, 2017), mast cells, basophil activation and migration into the airways, and increased IgE production (Fahy, 2015; Barnes, 2016; Caminati *et al.*, 2018). Upon activation, these cells rapidly release inflammatory mediators and reactive oxygen species (ROS), which initiate asthma-related inflammatory responses. The release of mediators such as Ach, histamine, and leukotrienes mediates stimulation of airway smooth muscle muscarinic and histamine receptors mobilises extracellular and intracellular Ca^{2+}, resulting in airway smooth muscle contraction and manifesting as bronchoconstriction, a characteristic feature of asthma (Erle and Sheppard, 2014; Dale *et al.*, 2018; Williams and Rubin, 2018).

In addition to ASM contraction, inflammatory mediators sensitise airway sensory nerve endings, causing reflex cholinergic bronchoconstriction. Airway epithelial and mast cells also release neutrophil-like nerve growth factor (NGF), causing the proliferation and sensitisation of airway sensory nerves (Barnes, 2016; Lambrecht, Hammad and Fahy, 2019). These factors, together with the effects of released inflammatory mediators, result in airway hyper-responsiveness, wherein

stimuli and antigens elicit a bronchoconstrictor response at levels that do not typically induce such an effect (Fahy, 2015).

Vascular endothelial growth factor (VEGF) plays a central role in mediating angiogenesis in asthma pathophysiology and is elevated in individuals with asthma (Tsai *et al.*, 2015; Elkholy *et al.*, 2019). The major secretion of VEGF is from the airway smooth muscle (ASM). VEGF, in conjunction with other proangiogenic factors such as angiopoietin-1 and angiogenin (Simcock *et al.*, 2012), stimulates the proliferation and differentiation of endothelial cells, induces vascular leakage and permeability, and enhances allergic sensitisation (Bakakos, Patentalakis and Papi, 2016). Angiogenesis in response to inflammatory mediators and growth factors causes increased airway mucosal blood flow in asthma, resulting in airway narrowing, oedema, and plasma exudation (Barnes, 2016).

Pathological changes in the airway epithelium and submucosal layers result in what is termed airway remodelling in asthma, including subepithelial fibrosis, increased ASM volume, and goblet cell hyperplasia (Fahy, 2015). The characteristic hypertrophy and hyperplasia of airway smooth muscle are believed to be stimulated by a platelet-derived growth factor orendothelin-1 released from inflammatory and epithelial cells (Black *et al.*, 2012). Eosinophil infiltration and the release of a profibrotic mediator, transforming growth factor beta (TGFβ), causes airway remodelling through the deposition of type III and V collagen beneath the airway epithelial basement membrane, resulting in thickened subepithelial fibrosis (Barnes, 2016). Therefore, proangiogenic factors in combination with inflammatory mediators promote vascular remodelling in asthma. In addition, submucosal gland hyperplasia and increased numbers of epithelial goblet cells cause mucus hypersecretion, which sometimes further occludes asthmatic airways (Barnes, 2016).

Over time, these recurrent exposures and inflammation lead to hyperplasia and hypertrophy of airway blood vessels and mucus cells, as well as airway remodelling features, such as friability and fibrosis of airway epithelial cells. This results in airway bronchospasm, plasma exudation, mucus secretion, and structural changes (Barnes, 2016; Lambrecht, Hammad and Fahy, 2019). Furthermore, recurrent exacerbations cause airway epithelial damage, impairing epithelial functions, including loss of barrier function allowing more penetration of allergens, loss of enzymes such as endopeptidase that degrades certain peptide inflammatory mediators, loss of epithelial-derived relaxant factor, and exposure of sensory nerves causing reflex neural effects on the airways, all of which together lead to increased AHR in asthma (Brightling, Saha and Hollins, 2010).

2.1.5 Sign and symptoms of asthma

Asthma is characterised by acute respiratory symptoms referred to as exacerbations (Andrew, Brian and David, 2020), which can be graded as mild, moderate, severe, or life-threatening (Sears, 2008). In early phase asthma attacks in sensitised individuals, allergens in the respiratory tract are recognised by IgE antibodies on mast cells and basophils, eliciting the release of mediators such as histamine and leukotrienes. These mediators induce arteriolar dilation, increased vascular permeability, enhanced mucus production, and contraction of airway smooth muscles, typically occurring within minutes of exposure (Dykewicz and Hamilos, 2010).

Acute airway constriction occurs during asthma exacerbation, persisting for approximately 1 h or extending to 4–6 h into the late phase in more susceptible individuals. The late phase of airway compromise is precipitated by chronic

inflammation, which may persist for a duration ranging from one hour to one day (Lee, Lim, *et al.*, 2018) due to the released mediators and cytokines that elicit a delayed cellular inflammatory response, resulting in the severe recurrence of symptoms (Dykewicz and Hamilos, 2010).

Asthma symptoms include cough, wheezing, chest dyspnoea, and tightness (Barnes, 2016). Asthmatic patients often have clinical manifestations of coughing; it is the predominant initial symptom in some asthmatic patients, whereas wheezing is the predominant symptom in others (Lai, 2016). Various ion channels, including transient receptor potential channels on the airway sensory nerves, have been suggested to mediate coughing in asthma and systemic reflexes, such as sneezing (Naclerio, 1991). Collectively, the manifestations of asthmatic inflammation include bronchoconstriction, vasodilation, airway oedema, and the activation of sensory nerve endings (Barnes, 2016), with patients experiencing chest tightness and shortness of breath.

2.1.6   Inflammatory cells in Asthma

The development of asthma involves mobilization and migration of cells into the peribronchiolar and perivascular regions (Curtis *et al.*, 1990). In sensitized individuals, the nasal mucosa contains high levels of IgE-binding mast cells that traverse the epithelium into the mucosal region and degranulate after allergen exposure and recognition (Enerback, Pipkorn and Granerus, 1986). Immunoglobulin E (IgE), leukotrienes, cholinergic transmitters, and oxidative stress have been implicated in the pathophysiology of asthma. The inflammatory mediators attract and activate more Th2 cells (Athari *et al.*, 2017; Sinyor and Perez, 2023), mast cells, basophils into the airway, and production of IgE (Caminati *et al.*, 2018).

The T helper 2 (Th2) cytokines IL-4, IL-5, IL-9, and IL-13 mediate allergic inflammation, whereas tumour necrosis factor alpha (TNFα) and IL-1β amplify the inflammatory response. Lung epithelial cells release thymic stromal lymphopoietin (TSLP), an upstream cytokine that mediates the release of several chemokines further attracts Th2 cells (Barnes, 2016). Therefore, many inflammatory cells are involved in the pathophysiology of asthma, including:

2.1.6(a)   Dendritic cells (DCs)

As the immune system is constantly exposed to various antigens, the ability to differentiate between harmful and non-harmful antigens is important (van-Helden and Lambrecht, 2013). For allergens to induce an immune response, they need to cross the innate immune barriers through the airway epithelial and mucous membranes to reach adaptive immune cells. DCs at mucosal surfaces are among the first contacts (Nguyen Hoang *et al.*, 2012; Farache *et al.*, 2013).

DCs are specialized macrophage-like cells in the airway epithelium (Barnes, 2016), located at the lung basolateral site. Dendritic cells constantly scan the body for the presence of pathogens, expressing antigen specification with particular types of DCs for specific antigens (van-Helden and Lambrecht, 2013), which are the major antigen-presenting cells (APCs) in the airways (Barnes, 2016), and initiate a protective immune response against pathogens (Guilliams, Lambrecht and Hammad, 2013). Therefore in asthma DCs play a central role in initiating a cascade of immune responses against harmless allergens (Lambrecht and Hammad, 2012).

Dendritic cells uptake allergens, migrate to local lymph nodes, and present the allergenic peptides to naive uncommitted T lymphocytes that differentiate into allergen-specific T cells (van-Helden and Lambrecht, 2013; Barnes, 2016). In

addition, epithelial thymic stromal lymphopoietin (TSLP) triggers dendritic cells to also release Th2 cells attracting chemokines (Hammad and Lambrecht, 2015).

2.1.6(b)   Lymphocytes

The predominant lymphocytes in allergic asthma are Th2 in atopic asthma and innate lymphoid cells (ILC) in non-allergic asthma, as well as gamma delta T-cells, Th9, and Th17 cells in severe asthma. Th2 differentiation is activated by IL-4, whereas Th1 differentiation is activated by IL-12, IL-23, IL-6, and TGF-β (van-Helden and Lambrecht, 2013). These Th2 cytokines regulate the activation and survival of eosinophils and mast cells in the airways,

Similarly, Th2 cytokines are also produced by type 2 innate lymphoid cells (ILC2s), especially IL-5 and IL-13 (Hardman, Panova and McKenzie, 2012; Klein *et al.*, 2012; Barnes, 2016). ILC2s are inflammatory cells void of T cell receptors, which are regulated by the epithelial cell cytokines IL-25 and IL-33. Th17 cells are also associated with neutrophilic inflammation (Barnes, 2016).

2.1.6(c)   Eosinophils

Eosinophilic inflammation is a characteristic feature of atopic asthma, Th-2 lymphocytes mediate the activation, growth, and differentiation of eosinophils (Bradding, Walls and Holgate, 2006); they migrate by chemotaxis, adhere to airway vascular endothelial cells via adhesion molecules, and infiltrate the airway submucosa for activation, and prolong survival (Barnes, 2016).

The release of certain basic proteins and oxygen-derived free radicals by eosinophils has been linked to the development of AHR in asthma. Eosinophils and basophils have been reported to exhibit sufficient antigen-presenting capacity to induce allergic responses, independent of DCs. The known cytokine activators of

eosinophils include IL-5, IL-13, and prostaglandin-D2 (PG-D2) produced by Th2, ILC, and mast cells (Barnes, 2008; Perrigoue *et al.*, 2009; Yoshimoto *et al.*, 2009).

2.1.6(d)   Mast cells

Mast cells are another group of inflammatory cells activated by IgE binding to high-affinity IgE receptors on mast cells, after which they infiltrate the airway surface and smooth muscles. Other factors, such as exercise and hyperventilation, activate mast cells by an increase in airway lining fluid osmolality (Barnes, 2016). Secretions from activated mast cells include histamine, PG-D2, cysteinyl leukotrienes, growth factors, neurotrophins, and proteases, which are majorly bronchoconstrictors, and cause further activation and infiltration of Th2 cells, eosinophils, and basophils into the airways (Barnes, 2008).

2.1.6(e)   Macrophages

Similar to mast cells, macrophages are activated by low-affinity IgE receptors (FcεRII). In addition to Th2 cells, ILC2, basophils and mast cells, the macrophages are also implicated in the production of IL-4 and IL-13, which play a central role in asthmatic inflammation. However, macrophages secrete both pro- and anti-inflammatory cytokines, making their role in asthma unclear (Barnes, 2016; Gordon *et al.*, 2016). Macrophages have been reported to exert an inhibitory effect on DCs activation, promoting tolerance to inhaled allergens (van-Helden and Lambrecht, 2013).

2.1.6(f)   Neutrophils

Neutrophils are less implicated in atopic asthma, which is predominantly of eosinophilic inflammation. However, increased numbers of activated neutrophils are also found in the sputum and airways of some severe asthmatic patients, asthmatics

who smoke, during exacerbations, and in Asthma-COPD Overlap (ACO) (Barnes, 2016; Russjan and Kaczyńska, 2018).

2.1.7 Inflammatory mediators of asthma

Asthma mediators are secreted by both inflammatory cells and airway structural cells, such as epithelial cells, fibroblasts, and smooth muscle cells. Th2 lymphocytes released IL-4, IL-5, IL-9, IL-13 referred to as T2 cytokines, that mediate allergic inflammation, whereas tumour necrosis factor alpha (TNFα) and IL-1b amplify the inflammatory response (Barnes, 2008). In the ovalbumin (OVA)-sensitized animal models, a typical model of asthma, allergen exposure causes dendritic cell activation of Th-2 cells to release IL-4, IL-5 and IL-13 cytokines (Shin, Takeda and Gelfand, 2009; Kim, Song and Lee, 2019). Furthermore, airway epithelial cells release an upstream cytokine, thymic stromal lymphopoietin (TSLP), which attracts Th2 cells (Barnes, 2016).

Multiple mediators are involved in asthma pathophysiology, with several major factors implicated, including the following.

2.1.7(a) IL-4

IL-4 is involved in B lymphocyte differentiation towards IgE synthesis (Fish *et al.*, 2005; Bradding, Walls and Holgate, 2006), and is also involved in increasing the Th-2 cell population and eosinophil exotaxis from airways (Wynn, 2015; Lambrecht, Hammad and Fahy, 2019). IL-4 and IL-13 are two functionally overlapping and major mediators of allergic response (Andrew, Brian and David, 2020) that mediate the production and release of IgE and transforming growth factor β (TGF-β) (Shin, Takeda and Gelfand, 2009). Similarly, IL-4 and IL-13 also play a central role in T2 mediated comorbidities, such as nasal polyposis, atopic dermatitis, and allergic rhinitis, which are also Th 2 inflammations (Boulet, 2009).

27

2.1.7(b)   IL-5:

IL-5 is involved in eosinophil activation, development from bone marrow, recruitment into the lung interstitial mucosa, and their release into peripheral circulation (Collins *et al.*, 1995; Shin, Takeda and Gelfand, 2009). IL-5 also enhances eosinophil survival at sites of inflammation (Farahi *et al.*, 2007).

2.1.7(c)   IL-13

IL-13 plays a central role in mediating allergic asthma and stimulates airway hyperresponsiveness (Wills-Karp *et al.*, 1998; Brightling, Saha and Hollins, 2010). In similar role to IL-5, IL-13 mediate eosinophil chemotaxis and migration (Wynn, 2015; Lambrecht, Hammad and Fahy, 2019) and induce the up-regulation of adhesion molecules, goblet cell hyperplasia, and barrier dysfunction, including airway remodelling (Boulet, 2009; Brightling, Saha and Hollins, 2010). However, IL-13 is reported to have an asthma regulatory mechanism independent of IgE, as eosinophil activity is not affected by IL-13 inhibition in mouse models (Wills-Karp, 2004).

2.1.7(d)   IL-17

Th17 cells release IL-17 and IL-22, which are reported to regulate neutrophilic inflammation (Halwani, Al-Muhsen and Hamid, 2013), especially in non-atopic asthma. Generally, in allergic inflammation, a dominance of Th2 cytokines (IL-4, IL-5 and IL-13) over Th1 cytokines is observed, while certain anti-inflammatory cytokines (IL-10 and IL-12) can be deficient in asthma (Hwang *et al.*, 2013; Barnes, 2016), causing a regulatory imbalance towards pro-inflammatory mediators.

2.1.7(e)   IL-22

Various inflammatory cells such as Th17 cells and type 3 ILCs generate IL-22, involve in the progression of allergic airway inflammation and has important

biological functions. IL-22 may enhance the production of proinflammatory mediators triggered by TNF and IL-17 (Sabat, Ouyang and Wolk, 2013). However, studies have shown that IL-22 plays a dual role: it can induce lung epithelial cells to produce antioxidants and simultaneously act on non-hematopoietic cells, including mucosal surface epithelial cells, to promote airway remodelling (Ito, Hirose and Nakajima, 2019).

2.1.7(f)   iNOS

Inducible nitric oxide synthase (iNOS) is responsible for producing substantial quantities of nitric oxide (NO) within the bronchial epithelium. In asthma, iNOS overexpression results in elevated NO levels, contributing to bronchial hyperreactivity, mucus hypersecretion, increased vascular permeability, and airway inflammation (Escamilla-Gil, Fernandez-Nieto and Acevedo, 2022).

Increased production of nitric oxide (NO) by bronchial epithelial cells elevated fractional exhaled nitric oxide (FENO) levels (Narendra, Blixt and Hanania, 2019). Consequently, the measurement of FENO is a validated method for diagnosing and monitoring asthmatic inflammation (Barnes, 2008; Dweik *et al.*, 2011; Rawy and Mansour, 2015).

2.1.7(g)   COX-2

Cyclooxygenase-2 (COX-2) enzyme plays a crucial role in the biosynthesis of prostaglandin D2 (PGD2), a potent pro-inflammatory lipid mediator derived from arachidonic acid within the COX-2 pathway. Prostaglandin D2 (PGD2) is primarily released from mast cells, but it is also secreted by other immune cells, including Th2 cells and dendritic cells. This mediator induces significant chemotaxis and

degranulation of inflammatory cells, leading to tissue remodelling, mucus production, and airway structural damage (Domingo *et al.*, 2018).

Prostaglandin D$_2$ (PGD$_2$) serves as a significant and potent activator of ILC2 through the Chemoattractant Receptor-Homologous Molecule Expressed on Th2 Cells (CRTH2) present on human ILC2s. This interaction mediates robust pro-allergic inflammatory responses, including the release of classical Th2 cytokines and IgE-mediated mast cell degranulation. (Xue *et al.*, 2014). The enzymes iNOS and COX-2 are involved in the inflammatory response associated with asthma and exhibit increased expression in animal models of allergic asthma (Kim *et al.*, 2022; Zhang *et al.*, 2022).

2.1.7(h)   IgE

In asthmatic airway inflammations, B lymphocytes are major source of IgE production, the released IgE is involved in mast cell degranulation (Lambrecht and Hammad, 2015; Barnes, 2016; Athari *et al.*, 2017).
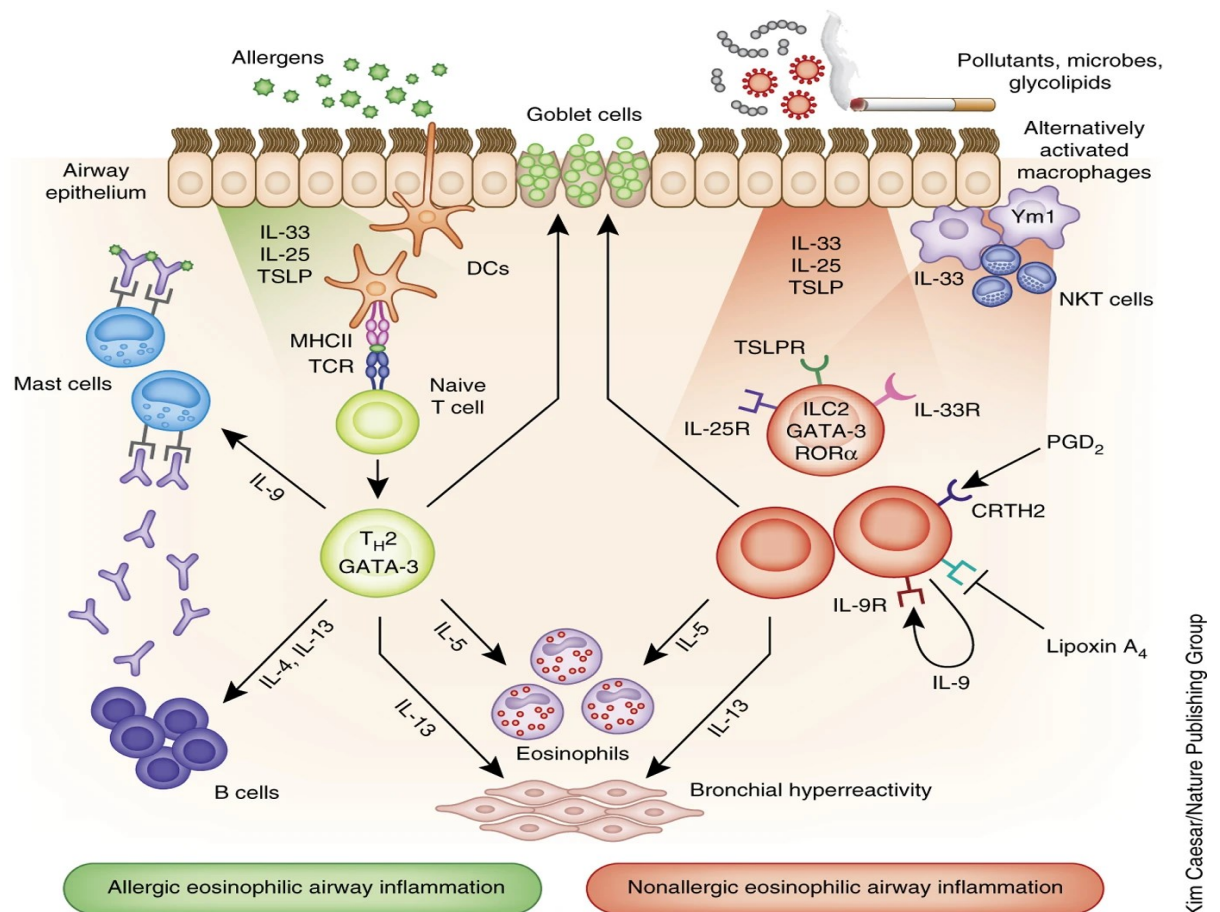
Figure 2.2   Overview of Allergic and Non-Allergic Inflammation Pathways in Asthma Pathogenesis via Th2 and ILC2 cells (Adopted from Lambrecht and Hammad, 2015).

2.1.8   Asthma inflammatory biomarkers

2.1.8(a)   IgE level

Increased IgE levels correlate with the incidence of wheezing, severity of asthma, and associated presence of sputum eosinophilic inflammation (Schleich, Demarche and Louis, 2016). Allergic profiles of individuals can be identified by Allergen-specific IgE level measurements and can be used to identify patients suitable for anti-IgE therapy (Narendra, Blixt and Hanania, 2019).

2.1.8(b)   Eosinophil count

Both eosinophil measurements and blood IgE are minimally invasive evaluations. The eosinophil count can predict asthma exacerbations, poor control, and

airway obstruction. Th2 phenotype asthma is characterized by an increased eosinophil count. An increase in blood and sputum eosinophil counts has been reported to correlate with the clinical severity and pulmonary function in asthma (Rawy and Mansour, 2015). Sputum eosinophils are known to predict the response to corticosteroids and biologics therapies (Narendra, Blixt and Hanania, 2019).

Furthermore, eosinophils and related measurements from various tissues, such as blood eosinophils, sputum eosinophils, eosinophil cationic protein (ECP), Eosinophil-Derived Neurotoxin (EDN), and eosinophil peroxide (EPX), have been considered potential biomarkers for asthma (Narendra, Blixt and Hanania, 2019).

2.1.8(c)   Fractional Exhaled Nitric Oxide (FENO)

Different cells within the respiratory airways produce NO through NO synthase conversion from the amino acid L-arginine to L-citrulline and NO (Nathan and Xie, 1994). NO plays a signalling role in both physiological and pathophysiological processes of the airway (Rawy and Mansour, 2015) and is involved in the recruitment and activation of eosinophilic granulocytes and bronchial vasodilation (Prado *et al.*, 2006; Barnes, 2016).

FENO measurements can be performed in the absence of bronchial challenge and/or spirometry (Rawy & Mansour, 2015). Owing to increased nitric oxide (NO) production by bronchial epithelial cells, elevated fractional exhaled nitric oxide (FENO) levels >50 ppb in adults or >35 ppb in children, can be utilized as a diagnostic indicator for asthma. (Narendra, Blixt and Hanania, 2019). FENO measurement is a validated diagnostic and monitoring biomarker of asthmatic inflammation, which is simple, immediate, and non-invasive (Barnes, 2008; Dweik *et al.*, 2011; Rawy and Mansour, 2015).

2.1.8(d)   H₂S

Mammalian tissues produce H_2S by H_2S-generating enzymes or redox oxidation of glucose with elemental sulphur (Suzuki *et al.*, 2021). H_2S has been recognized as a gas signal biomarker of asthma, which can be detected in serum, sputum, or exhaled breath. In the lungs, H_2S reduces pro-inflammatory eosinophils, neutrophils, and the type-2 inflammatory cytokines IL-5 and IL-13 eotaxin-1, together with the inhibition of AHR (Zhang *et al.*, 2013; Roviezzo *et al.*, 2015). In animal model experiments, H_2S has been reported to exhibit roles such as improvement of lung function (Roviezzo *et al.*, 2015), prevention of oxidative stress (Benetti *et al.*, 2013), and relaxation of airway smooth muscle through the KATP channel (Suzuki *et al.*, 2021).

The measurement of sputum H_2S levels can be a marker of neutrophilic inflammation, chronic airflow obstruction, and a reflection of response to β2 agonist bronchodilators, thereby serving as a predictor of asthma control status (Suzuki *et al.*, 2021). Serum H_2S levels of asthmatics have been reported to be lower than those of non-asthmatic individuals and may be further reduced in cases of acute and severe inflammation (Wu *et al.*, 2008; M. Tian *et al.*, 2012; Suzuki *et al.*, 2021). However, higher Sputum H_2S levels are observed in asthmatic individuals than in non-asthmatic subjects, suggesting a serum:sputum H_2S ratio predicting asthma exacerbation biomarkers, and is found to be more predictive than FENO (Suzuki *et al.*, 2021).

2.1.8(e)   Urine

Multiple urine metabolites, such as bromotyrosine, leukotriene E4 (LTE4), prostaglandin D2 (PGD2), and its metabolite 11 β prostaglandin F2α (11βPGF2), and metabolomics by NMR analysis of human urine measurements are under consideration as biomarkers of asthma (Narendra, Blixt and Hanania, 2019).

2.1.8(f)   Lipid profile

Considering the involvement of Lipids in many important biological functions, such as energy storage, material transport, signal transduction, and molecular recognition processes; abnormal lipid metabolism has been reported in patients with asthma. Abnormal lipid metabolism determined by LC-MS lipidomics has been reported to correlate well with asthma severity and IgE levels (Jiang *et al.*, 2021).

2.1.8(g)   Serum dipeptidyl peptidase (DDP-4) and Periostin

DDP-4 is associated with aspirin-exacerbated respiratory disease that stimulates bronchial smooth muscle proliferation and fibronectin production (Narendra, Blixt and Hanania, 2019). Whereas bronchial epithelial cells secrete periostin, which is a matricellular protein, in response to IL-13. Periostin serum levels may represent IL-13 activity (Izuhara *et al.*, 2016).

DDP-4 and periostin production are induced by IL-13 and are therefore potential biomarkers of IL-13 pathway activation (Narendra, Blixt and Hanania, 2019). However, periostin levels are elevated in many diseases, such as atopic dermatitis, eosinophilic otitis media, eosinophilic-esophagitis, idiopathic pulmonary fibrosis, scleroderma, diabetic nephropathy, cancer, cardiovascular disease, pre-eclampsia, and lupus nephritis, which limits its use as a standalone asthma biomarker (Izuhara *et al.*, 2016). Therefore, periostin showed predictive, prognostic, and pharmacodynamic properties as an asthma investigational biomarker in combination with other rather than standalone biomarkers (Narendra, Blixt and Hanania, 2019).

There is unlikely a single biomarker to reflect the pathophysiology of different asthma phenotypes, considering the heterogeneity of the disease; hence, combining biomarkers may increase their predictive capability (Narendra, Blixt and Hanania, 2019). Of great significance, ongoing research studies have investigated additional

emerging biomarkers of asthma, and numerous candidates have been reported, including Chitinases, Biomarkers in exhaled breath condensate (EBC), genomics by gene expression biomarker signature, ezrin, volatile organic compounds, and the use of an electronic nose (eNose) to detect volatile organic compound biomarkers) (Narendra, Blixt and Hanania, 2019), microRNAs (miR-582-5p) from the nasal epithelium (Trifunovic *et al.*, 2020), IL-6 (Jackson *et al.*, 2019), and C-reactive protein (CRP) (Rawy and Mansour, 2015).

2.1.9   Management of asthma

The aetiology of asthma encompasses not only IgE-mediated allergic reactions but also innate immune responses elicited by endotoxins and trypsin-like proteases. Consequently, the assessment and regulation of environmental exposure plays a crucial role in the effective management of this condition (Reed, 2010). In asthma diagnosis, a history of exacerbation episodes in terms of airway hyper-responsiveness, variable airflow limitation, symptoms of recurrent coughing and wheezing and reversibility in response to bronchodilators, should be considered. Bronchial hyper-responsiveness can be assessed by inhalation challenges (Uchida, Sakaue and Inoue, 2018; GINA, 2024). Asthma diagnosis is mostly based on symptoms and therefore routine chest radiographs are not recommended for the management of acute asthma exacerbations, except in severe cases or in the presence of related complications such as pneumothorax (Mowbray *et al.*, 2020).

The identification of specific treatment targets to improve disease symptoms is paramount in asthma management (Bodkhe *et al.*, 2020). Different management options and relevant guidelines are available for asthma treatment. Various medications are currently being utilized for the management of asthma, whereas others are in development. Current medications include the following.

2.1.9(a)   Corticosteroids

Corticosteroids are the most commonly used medications in asthma management administered in the form of Inhaled Corticosteroids (ICS), Oral Corticosteroids (OCS), and Systemic Corticosteroids. They are potent anti-asthmatic medications recommended as first-line therapy for severe acute exacerbations (Liang, Wang, Hua, Liao, & Chen, 2020). Corticosteroids inhibit airway structural changes associated with fibrosis in animal models as well as target eosinophil activation and subsequent infiltration (Trifilieff, El-Hashim and Bertrand, 2000; Andrew, Brian and David, 2020). Inhaled corticosteroids (ICSs) are effective in suppressing chronic airway inflammation (Barnes and Adcock, 2003), and their nebulization is reported to be effective in children aged five years or younger (Murphy *et al.*, 2020).

On the other hand, systemic corticosteroids are central to acute asthma therapy and reduce markers of type-2 inflammation (Busby *et al.*, 2020), improve lung function, reduce the rate of acute emergencies, and relapse of asthma attack (Alangari, 2014; GINA, 2024). Short-course OCSs improve asthma symptoms and control in moderate to severe persistent asthma (Expert Panel Report 3 (EPR-3), 2007) and are more effective in patients with increased type-2 markers, suggesting the use of type-2 biomarkers to identify better OCS treatment targets (Busby *et al.*, 2020). In the clinical setting, corticosteroids are beneficial within one hour of asthma emergency presentation (Mowbray *et al.*, 2020).

2.1.9(b) β_2 agonist

β_2-Agonist directly activate beta adrenergic receptors, causing smooth muscle relaxation in the airways (Gans and Gavrilova, 2020). There are Short Acting β_2 Agonist (SABA) and Long Acting β_2 Agonist (LABA).

2.1.9(c)   Long-acting muscarinic receptor antagonists (LAMA)

LAMAs competitively antagonize M3 muscarinic receptors, thereby preventing acetylcholine-mediated bronchoconstriction of the airway (Côté, Godbout and Boulet, 2020). The anticholinergic drugs ipratropium and tiotropium bromide are used for control of airway smooth muscle tone, mucus secretion, vasodilation, and inflammation (Buels and Fryer, 2012). In children and adolescents with moderate-to-severe symptomatic asthma, tiotropium once daily was found to improve lung function (FEV1) with long-acting bronchodilation (Sunther, Marchon and Gupta, 2021).

2.1.9(d)   Leukotriene inhibitors (LTI)

LTIs competitively block Cysteinyl Leukotrienes, thereby decreasing inflammation and Th2 response, LTI are more effective in preventing the Th2 and Th17 pathways, sparing the Th1 pathway (Gans and Gavrilova, 2020).

2.1.9(e)   PDE4 inhibitors

In the airways, Phosphodiesterase- 4 is an isoenzyme that catalyses the inactivation of the unstable second messenger signalling molecule, cyclic adenosine monophosphate (cAMP), by hydrolysis, and most airway tissues and inflammatory cells are influenced by PDE4 (Al-sajee, Yin and Gauvreau, 2019; Zuo *et al.*, 2019; Bodkhe *et al.*, 2020). Phosphodiesterase- 4 is expressed in airway smooth muscle, epithelium, and inflammatory cells (Antoniu, 2011; Zuo *et al.*, 2019). PDE4 inhibition causes the accumulation of cellular cAMP, thereby mediating smooth muscle relaxation and inhibition of inflammation (Kawamatawong, 2017).

Phosphodiesterase-4 inhibitors (PDE4) have a wide range of anti-inflammatory effects. Roflumilast is a long-acting selective PDE4 inhibitor that inhibits both pulmonary and systemic inflammation. It significantly reduces AHR, lowers IL-6 and tumour necrosis factor-α (TNF-α) levels, and is reported to reduce airway

inflammatory cell infiltration, FEV1, and airway remodelling (Bodkhe *et al.*, 2020). Roflumilast is an effective and safe anti-inflammatory drug (Antoniu, 2011).

2.1.9(f)   Biologics

Most biologics therapies in asthma management are therapies targeting Th2 cytokines, and biological therapeutics are recommended for patients with uncontrolled persistent asthma. The related and central role of IL-4, IL-5 and IL-13 in asthma pathophysiology makes their blockade an important approach in modifying type 2 inflammatory disease (Andrew, Brian and David, 2020). Examples include IL-5 antagonists that either bind to the anti-IL-5 ligand (mepolizumab and reslizumab) or bind to the IL-5 receptor (benralizumab). Others are anti-IgE (omalizumab); anti-IL-4/IL-13 (dupilumab) and IL-13 blockade (lebrikizumab) (Bateman *et al.*, 2019).

Bateman et al. (2019) compared the efficacy of dupilumab versus anti-IL-5 and anti-IgE therapies using the endpoints of annualized severe asthma exacerbation rates and changes in pre-bronchodilator forced expiratory volume in 1 s (FEV1). The study found that dupilumab improved FEV1 more than the other biologics. Biologics blocking IL-5 causes a sustained reduction in circulating and sputum eosinophils, which is independent of reduced AHR or asthma symptoms (Barnes, 2016). Similarly, Omalizumab acts as an anti-IgE agent by binding to IgE and downregulating FcεRI on mast cells, basophils, and epidermal Langerhans cells, thereby making these inflammatory cells less responsive to allergen stimulation (Ochiai *et al.*, 1994; Holgate *et al.*, 2005).

In addition to the aforementioned, other biologics including rolipram, ezepelumab, and PDE4 inhibitors are being investigated. Others agents include tezepelumab, cilomilast, apremilast which targets thymic stromal lymphopoietin (TSLP) and prevents its receptor binding (Verstraete *et al.*, 2017).

Furthermore, ORMDL3 overexpression was observed to aid airway epithelial cell repair by regulating IL-33 expression (Li *et al.*, 2020) highlighting potentials of gene therapy in asthma. The use of TLR ligands or manipulation of Treg functions on the Th1/Th2 balance are postulated approaches for better control or prevention of allergic asthma (Athari *et al.*, 2017). Oxidation-specific epitopes (OSE) and their accumulation, which lead to cell death, inflammation, and tissue dysfunction, may serve as potential therapeutic targets in asthma and related inflammatory conditions (Pascoe, Vaghasiya and Halayko, 2020).

Overall, decrease environmental exposure to air pollutants is associated with improved health outcomes, for instance decreasing ambient air pollutant levels by decreasing fossil fuels use (Peden, 2005). Emerging therapies for asthma management include theophylline, bronchial thermoplasty, and macrolide treatment (Barnes, 2012).

2.1.9(g)   Combination and add-on therapies

Different stepwise international guidelines for asthma management across age groups and severity are available (Powell, White and Primhak, 1993; Erick Bateman, 2016; Network GA, 2018). In situations where a single medication is insufficiently effective, increased ICS dosage, leukotriene receptor antagonist, combinations of ICS and long-acting beta-2 agonist (LABA), ICS, LABA, LAMA are recommended (GINA, 2024). A combination of low-dose budesonide and formoterol reduces the exacerbation risk in mild asthma (Foster *et al.*, 2020). Liang et al. (2020), found ICS-LABA therapy as adequate initial treatment for asthma control in majority of patients in their study, while add-on short course oral corticosteroids provided no significant clinical benefit over ICS. ACO management currently relies mainly on ICS, LAMA, LABA, and PDE4 inhibitors (Generoso and Oppenheimer, 2020).

Nevertheless, available evidence suggests that restoration of epithelial health may attenuate asthmatic symptoms. Consequently, a strategy focusing on the epithelium and utilization of agents that protect epithelial cells may enhance the barrier function of the airway epithelium and protect against external irritants and allergens. This approach could potentially reduce the frequency and severity of asthma, leading to improved management (Singh *et al.*, 2023).

2.1.9(h)   Challenges in present asthma management

Many studies have reported challenges associated with current asthma medications. These include patient medication noncompliance, β2-adrenoceptor agonist tolerance due to long-term use, and steroid side effects (Lavorini, 2013). Specifically, persistent use of ICSs at high doses is associated with complications such as candidiasis, osteoporosis, growth retardation, cataracts, and pharyngitis (Li, 2011), whereas systemic corticosteroid exposure is associated cardiovascular and cerebrovascular impairments, cataracts, sleep apnoea, renal impairment, depression, anxiety, type 2 diabetes, and weight gain (Newnham, 2001; Price *et al.*, 2018). The side effects of β2-agonists include cardiotoxicity, whereas corticosteroids can result in osteoporosis, skin bruising, and cataracts (Reed, 2010).

The long-term use of systemic corticosteroids (SCS) often leads to adrenal insufficiency (AI), potentially necessitating hydrocortisone replacement therapy. A 15% prevalence of AI was reported among asthmatic patients receiving high-dose oral corticosteroids (OCS) (Haida et al., 2020). A longitudinal, open-cohort, observational study on asthma management observed that the long-term use of SCS led to adverse complications and increased costs (Lefebvre *et al.*, 2015) and these complications are more pronounced in elderly patients with asthma (Reed, 2010). In addition, OCSs are associated with 3.1- and 2.7-folds higher rate of osteoporotic fractures and pneumonia,

respectively (Price *et al.*, 2018). These challenges necessitate the exploration of alternative and/or complementary options for current asthma medications, underscoring the importance of investigating additional phytochemical alternatives.

2.1.10   Asthma experimental animal models

Given the complexity of multiple concurrent and interrelated biological processes in asthma pathophysiology, the selection of an appropriate animal model is as critical as assessing the bioactivity potential of the test compound. Researchers have employed animal models to elucidate the pathophysiological mechanisms of asthma and evaluate potential therapeutic interventions.

Diverse animal models have been used in asthma research, each of which has distinct advantages and limitations. Experimental studies on asthma typically comprise two phases: sensitization and challenge. Sensitization is frequently conducted via intraperitoneal or subcutaneous routes, whereas challenges are administered through aerosol, intranasal, or intratracheal instillation (Aun *et al.*, 2017). Animal models of asthma are used to replicate the pathophysiology of asthma in humans. Various animal species have been used in experimental models of asthma, including Drosophila, rats, rabbits, guinea pigs, cats, dogs, pigs, primates, and equines (Aun *et al.*, 2017; MERUERT *et al.*, 2023). However, the predominant species studied in the past two decades have been mice, particularly the BALB/c strain (Aun *et al.*, 2017).

2.1.10(a)   Atopic asthma models

The most extensively studied models of atopic asthma are ovalbumin and lipopolysaccharide (LPS) models. OVA is the most commonly used allergen for these purposes. The use of egg ovalbumin (OVA), a prevalent human allergen, renders OVA-challenged asthma models highly relevant to asthma research (Aun *et al.*, 2017). It is derived from chicken eggs shell and can be produced in large quantities, making

it cost effective. Chicken egg ovalbumin (OVA) is an inert protein that requires systemic injection in the presence of an adjuvant to induce Th2 sensitization in mice.

OVA mouse model of asthma has several advantages, including reproducibility, as it consistently replicates asthma characteristics such as elevated serum immunoglobulin E (IgE), airway inflammation, and hyperresponsiveness (AHR) (Kim, Song and Lee, 2019). Mice can be readily bred and maintained with the availability of genetically engineered transgenic or gene-knockout variants, which are particularly effective for investigating Th2-mediated immune responses. These responses are essential to elucidate the mechanisms underlying allergic asthma. Consequently, these factors render OVA mice asthma models the most widely utilized(Aun *et al.*, 2017; MERUERT *et al.*, 2023). Moreover, a wide array of specific reagents and assays are available for analysing cellular and humoral responses in mice.

Thakur et al., (2019) reported an experimental model of asthma in rats using a combination of ovalbumin (OVA) and lipopolysaccharide (LPS) allergens to simulate clinical asthma more accurately. The OVA-LPS model effectively replicated the severe asthma phenotypes, demonstrating significant eosinophilic, neutrophilic, and lymphocytic inflammation. The rats model exhibited significantly decreased tidal volume and airflow rate, as well as increased respiration rate, thus suitable for preclinical evaluation of antiasthmatic therapies.

Although ovalbumin and LPS are conventionally utilized, house dust mites are increasingly being employed because of their relevance to human asthma (Debeuf *et al.*, 2016; Aun *et al.*, 2017). Additional allergens, including cockroach extracts and the fungus Alternaria alternata, have been used to induce asthma in animal models (Debeuf *et al.*, 2016).

2.1.10(b)   Non-atopic asthma model

Conversely, although numerous animal models have focused on allergic asthma, researchers are developing and refining models for non-atopic asthma. These include hapten-induced, endotoxin administration, and maternal transmission models. Hapten-induced asthma models are particularly advantageous for investigating the mechanisms of non-atopic and occupational asthma. These models employ sensitizing haptens to elicit asthma-like symptoms in the absence of allergic predisposition (Russjan and Kaczyńska, 2018).

Exposure to particulate matter (PM) 2.5 induced bronchial asthma and fibrosis in male rats. This approach results in oxidative stress, macrophage activation, and immune imbalance through pathways such as JAK/STAT and PI3K/Akt. High-concentration intermittent PM exposure demonstrated greater detrimental effects than continuous low-concentration exposure (H. Liu *et al.*, 2022). Additional methods for inducing non-atopic asthma include the utilization of air pollutants, exposure to cold air inhalation, and strenuous physical activity.

Despite their widespread utilization, mice present certain limitations as asthma research models, owing to their small size and anatomical differences from humans (Bates et al., 2009). Although no single animal model perfectly replicates all aspects of human asthma, existing experimental models have significantly enhanced the understanding of asthma pathophysiology and have facilitated the development of novel treatments. The selection of an animal model depends on the specific research objectives, with each model offering distinct advantages and limitations.
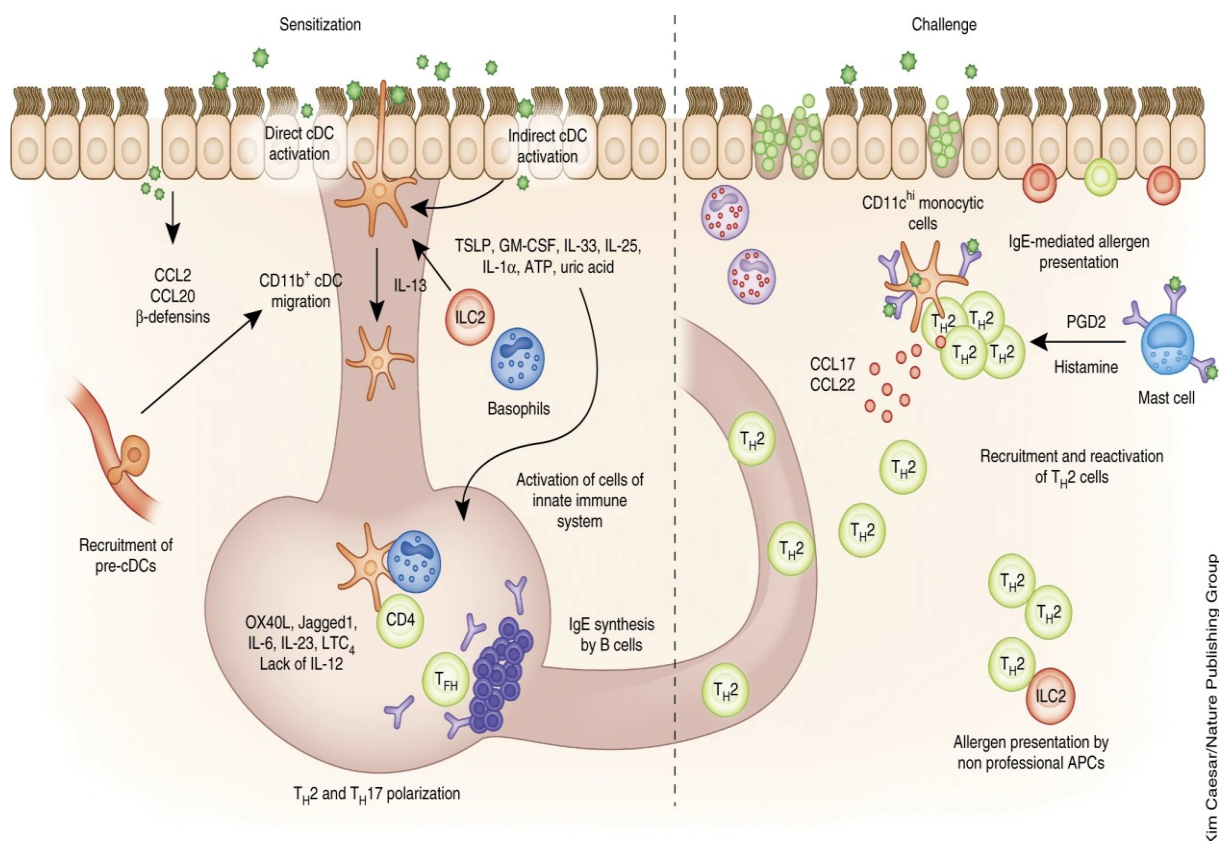
Figure 2.3   Dendritic cell (DC) activation during sensitization and challenge phases in experimental asthma models (Adopted from Lambrecht and Hammad, 2015).

2.2   Tiger Milk Mushroom and its medicinal use

2.2.1   *Lignosus rhinocerotis* (Tiger Milk Mushroom)

Mushrooms are eukaryotic, non-photosynthetic, aerobic macrofungi with a characteristic fruiting bodies (Sabaratnam *et al.*, 2013). diverse group of mushrooms have been consumed for centuries owing to their nutritional and medicinal properties. The macrofungal species Ascomycota and Basidiomycota produce various biological macromolecules. These mushrooms can be broadly classified into edible species eaten for their health benefits and non-edible species.

Lignosus rhinocerotis (LR) belongs to the Lignosus spp. mushroom family, with other identified members, including *L. dimiticus*, *L. ekombitii*, *L. goetzii*, *L. sacer*,

L. hainanensis, *L. tigris*, and *L. cameronensis* (Lau *et al.*, 2015), and is locally known as the Tiger Milk mushroom by indigenous communities in Malaysia (Abdullah *et al.*, 2013). By morphology, LR is made up of underground sclerotium, stipe supporting the central pileus (Lai *et al.*, 2013; Lau *et al.*, 2015).
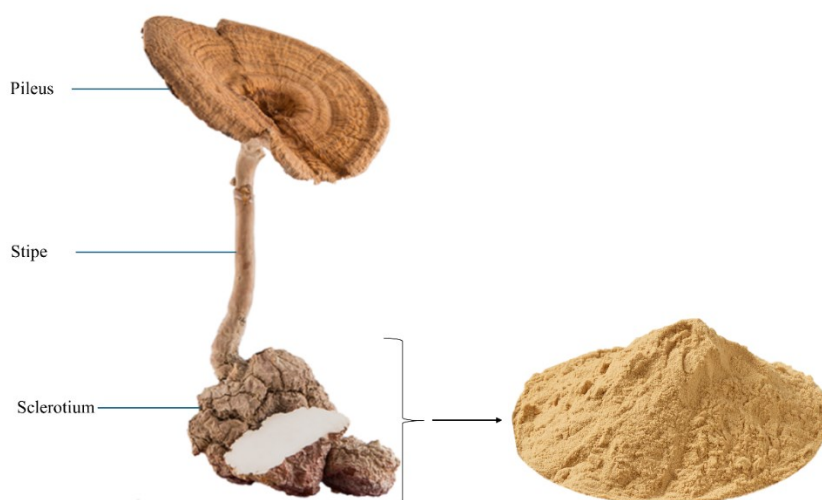
Figure 2.4   *Lignosus rhinocerotis*

2.2.2   Medicinal and bioactive properties of LR

Many macrofungus are known for their medicinal value, according to Qin & Han (2014) about 140,000 mushrooms are recognise as fungal species, with around 2,000 of them are edible and among which over 200 are utilized for food or traditional medicine. In addition, many macrofungus sclerotia are well-known medicinal herbs, health food and nutritional supplements (Choong *et al.*, 2016). *Lignosus rhinocerotis* (Cooke) Ryvarden is a medicinal mushroom used for centuries in Southeast Asia and Southern China (Lee, Lim, *et al.*, 2018; Sillapachaiyaporn and Chuchawankul, 2020). There is a large volume of published studies describing the medicinal role of several mushrooms. It is estimated that only less than half of the traditionally used mushrooms

have been scientifically studied for their medicinal claim (Wang *et al.*, 2020). LR has been traditionally utilized for the treatment of various ailments. These include asthma, chronic cough, inflammatory diseases, cancer, fever (Chang and Lee, 2004), liver cancer, chronic hepatitis, gastric ulcers (Wong and Cheung, 2008), breast cancer, stomach cancer, food poisoning, and wound healing (Eik *et al.*, 2012). Therefore, contemporary scientific studies on LR have investigated and documented a wide range of bioactive properties and effects.

Previous studies on LR reported its extracts to exhibit various bioactive properties, including the following:

2.2.2(a)   Anti-asthmatic

Extracts from LR mushrooms have been demonstrated to mitigate airway inflammation in OVA-challenged asthma mouse models. This effect is achieved through multiple mechanisms: suppression of inflammatory cells, inhibition of the release of pro-inflammatory Th2 cytokines (IL-4, IL-5, and IL-13) in BALF, and reduction of serum IgE levels. LR extract attenuated airway remodelling by decreasing smooth muscle thickness and diminishing the expression of TGF-β1 and Activin A-positive cells in the lung tissues (Muhamad *et al.*, 2023).

The intranasal administration of LR extract is reported to significantly suppress BALF inflammatory cell counts, CD4+ T-cells in lung draining lymph nodes, Th2 cytokines in BALF and serum IgE in OVA-induced asthma model, as well ameliorating leukocytes infiltration and mucus production in the lungs (Muhamad *et al.*, 2019). Furthermore, hot water extract of LR was reported to significantly ameliorate the increased total serum IgE, IL-4, IL-5 and IL-13 levels in BALF and effectively suppressed eosinophils numbers in BALF at the same time attenuating lungs eosinophil infiltrations in rat asthma model (Johnathan *et al.*, 2016).

2.2.2(b)　Anti-inflammatory effect

The acute anti-inflammatory activity of hot aqueous, cold aqueous and methanol extracts of LR sclerotia was investigated using carrageenan-induced paw oedema and cotton pellet-induced granuloma models in SD rats. The cold and hot water extracts exhibited strong anti-acute inflammatory activity and inhibitory effects on TNF-α production in RAW 264.7 macrophage cells. *In vivo* the three extracts exhibited effective anti-inflammatory activity at 200 mg/kg, with the cold aqueous extract being the most potent attributed to its high molecular weight (HMW) fraction, that demonstrated significant inhibition of TNF-α production (Lee *et al.*, 2014).

2.2.2(c)　Cytotoxic and immunomodulatory effect

Best clinical applications of medicinal mushrooms are as supplements for preventing and treating immune disorders, particularly in immunodeficient and immunosuppressed patients (Wasser, 2014). LR hot water extracts exhibited cytotoxic activity against human lung cancer cell line (A549) (IC$_{50}$: 65.50 ± 2.12 μg/mL) and against human breast cancer cell line (MCF7) (IC$_{50}$:19.35 ± 0.11 μg mL) (Jamil *et al.*, 2018). Also, LR extracts exhibited minimal cytotoxicity against seven selected mammalian cell lines, at IC$_{50}$ value exceeding 200 mg/ml after 72 hours of exposure (Lau *et al.*, 2014).

The cultivated strain of LR exhibits a more nutritious composition, enhanced antioxidant capacity, and more potent antiproliferative effects on MCF-7 cells than the wild type. The study demonstrated that the LR cultivar TM02 sclerotium displays superior antioxidant and antiproliferative activities, as well as a higher protein content, relative to the wild type (Yap *et al.*, 2013). Furthermore, the hot water extract of the sclerotium of *Polyporus rhinocerus* demonstrates an immunomodulatory effect mediated by macrophage activation via the NF-kappa-B signalling pathway and

decreased expression of the cell surface receptor Dectin-1 in RAW 264.7 cells and primary macrophages (Guo, Wong and Cheung, 2011).

2.2.2(d)   Antioxidant effect

Significant antioxidant properties were observed in aqueous methanol extracts derived from LR sclerotium, mycelium, and culture broth. These properties were evidenced by the extracts' capacity to scavenge free radicals, chelate metals, and inhibit lipid peroxidation (Lau *et al.*, 2014). Also, LR mycelium hot water extract exhibited antioxidant activity with DPPH scavenging and ferrous ion-chelating abilities. The extract improved the lipid profile *in vivo*, thereby mitigating liver damage in a plant-based HFD-induced non-alcoholic fatty liver disease (NAFLD) hamster model. These effects are potentially due to decreased reactive oxygen species and reduced mononuclear cell infiltration in the liver (Tsai *et al.*, 2022).

Similarly, the antioxidant activity of the LR hot water extract was evaluated using DPPH scavenging activity. The cultivated sclerotia extract exhibited an IC_{50} value of 760 μg/mL, whereas the wild-type LR sclerotia extract demonstrated an IC_{50} value of 840 μg/mL to achieve an equivalent level of inhibition (Jamil *et al.*, 2018).

2.2.2(e)   Other bioactivities of LR

LR extracts (ethanol, cold, and hot water extracts) exhibit anti-aging properties by reducing intracellular ROS through the DAF-16/FOXO pathway, resulting in increased stress resistance, decreased intracellular ROS accumulation, and an extended lifespan in Caenorhabditis elegans (Kittimongkolsuk, Roxo, *et al.*, 2021). The antimicrobial activity of four distinct LR extracts was investigated using the disc diffusion method against 15 bacterial and four fungal species. The zone of inhibition (mm) of the extracts (30 mg/ml) against the selected microorganisms demonstrated

that LR extracts exhibited mild-to-moderate antibacterial and antifungal properties (Mohanarji, Dharmalingam and Kalusalingam, 2012).

Eik et al. (2012) reported the neurite-stimulating activities of LR sclerotium extract, specifically examining neurite outgrowth activity in the PC-12Adh cell line. The combination of neurotrophin (NGF) and sclerotium extract demonstrated additive effects and enhanced neurite outgrowth. In addition, LR extracts have also been reported to exhibit bioactivities of Anti-viral activity (Sabaratnam *et al.*, 2013; Ellan *et al.*, 2019; Sillapachaiyaporn and Chuchawankul, 2020)

2.2.3   Mushroom polysaccharides

Considering the bioactivity of LR mushroom extracts, studies have been conducted to elucidate the potential medicinal properties of LR constituents. The multi-effect nature of LR reported thus far suggests the presence of multiple compound constituents potentially with diverse bioactivities. As knowledge of its active therapeutic compounds remains unclear, limited plausible data are available regarding the mechanisms of these effects. Research studies have documented the presence of proteins, carbohydrates, carbohydrate-protein complexes (Wong, Lai and Cheung, 2011; Lau *et al.*, 2015; Lee, Lim, *et al.*, 2018), fatty acids, triterpenoids, sterols, sugars, amides, amino acids, phenolics, and methyl esters (Lau, Abdullah and Aminudin, 2013; Lau *et al.*, 2014; Johnathan *et al.*, 2016; Sillapachaiyaporn and Chuchawankul, 2020; Tsai *et al.*, 2022), as constituents in LR.

Previous LR studies have proposed that polysaccharides and protein complexes are a major bioactive component that determine LR bioactivity. Polysaccharides are long-chain sugar polymers with glycosidic linkages. Polysaccharides are also classified based on the sequences and composition of their monosaccharides; these polysaccharides are either homopolysaccharides or heteropolysaccharides, having

homo or hetero glycosidic structures and linkages (Wang *et al.*, 2017). The fungal cell wall consists of glucans (50-60%), glycoproteins (20-30%), lesser chitin (10-20%), and proteins. Chitin microfibrils are arranged near plasma membranes and may be covalently linked to β- (1 → 3) glucans, forming bonds or weak interactions with mannanoproteins and branched β- (1 → 6) glucan networks, which contributes to the cell-wall structure maintenance (Kang *et al.*, 2018).The chemical composition of these mushroom polysaccharides varies depending on the fungal species and extraction methodology employed. The structural characteristics of polysaccharides derived from mushrooms include β-, α-, or both α- and β-linked glucan backbones, manifesting diverse patterns and degrees of branching (Wang *et al.*, 2017; Kang *et al.*, 2018; Seedevi *et al.*, 2019).

Even though several mushroom polysaccharides have been examined for bioactivities and have been reported and summarised in several reviews (Ruthes, Smiderle and Iacomini, 2015, 2016; Rosdan Bushra and Nurul, 2022); however, there are relatively few studies in the area of LR polysaccharides composition, which have not been extensively isolated and characterized thus far. Few studies have elucidated various biological effects of LR carbohydrates and polysaccharides fractions, including their anti-inflammatory, antioxidant, and immunomodulatory properties. LR sclerotia polysaccharides fractionated by hot water and sonication-assisted alkali extraction from *Polyporus rhinocerus* exhibit different chemical structures, such as polysaccharide-protein complexes and pure β-glucans, and demonstrate distinct immunomodulatory effects. The hot water extracts elicited a significant increase in spleen weight in both healthy BALB/c mice and healthy athymic nude mice, whereas this effect was less pronounced for the sonication fraction. *In vivo* immunomodulatory studies have shown that innate immune cells and T-helper cells are activated by LR

sclerotia polysaccharides (Lai, Wong and Cheung, 2008; Wong, Lai and Cheung, 2011). Similarly, high-molecular-weight proteins or protein-carbohydrate complexes were fractionated by Sephadex G-50 gel filtration from the L. R cold-water extract and were reported to exhibit cytotoxic antiproliferative effects against human breast carcinoma (MCF-7) and human lung carcinoma (A549) (Lee *et al.*, 2012).

The aforementioned and other reported bioactivities of LR carbohydrates, polysaccharides, and protein complexes are summarized in Table 2.1.

Table 2.1 Reported fractionated LR carbohydrate, polysaccharide and protein complex

Source	Extraction and isolation methods	Extract/isolate	Bioactive effect and properties	Reference
Sclerotia (Polyporus rhinocerus Cooke)	Hot water extraction and sonication-assisted alkali extraction	Hot water- (PR-HW) and a cold alkaline (PR-CA)-soluble polysaccharides	Antiproliferative PR-HW significantly inhibited the growth of human acute promyelocytic leukemia cells (HL-60), chronic myelogenous leukemia cells (K562), and human acute monocytic leukemia cells (THP-1) in vitro via cell cycle arrest of G1 phase-induced apoptosis. However, PR-CA showed no such inhibitory effect.	(Lai, Wong and Cheung, 2008)
Sclerotia (Polyporus rhinocerus Cooke)	Hot water extraction	Polysaccharide-protein complexes and a β-glucan	Antiproliferative LR extracts significantly enhanced the proliferation of NK-92MI cells, CD56+ natural killer (NK) cells, and human normal spleen monocytes/macrophages (MD) cells, concomitantly increasing the expression of cytokines IL-2 and I-309 chemokines, as well as Dectin-1 expression.	(Wong, Lai and Cheung, 2009)
Sclerotia (Polyporus Rhinocerus Cooke)	Hot water extraction and sonication-assisted alkali extraction	Polysaccharide-protein complex and β -glucan	Immunomodulatory LR hot water extract fractions demonstrated significant immunomodulatory effects (p <0.05) through an increase in spleen weight in both healthy BALB/c mice and healthy athymic nude mice, whereas this effect was less pronounced in the sonication fraction.	(Wong, Lai and Cheung, 2011)
Sclerotia	cold-water extraction Sephadex G-50 gel filtration	High-molecular-weight fraction (carbohydrate (68.7%) and protein (3.6%) complex	Antiproliferative LR proteins and protein-carbohydrate complexes exhibited cytotoxic antiproliferative effects against human breast carcinoma (MCF-7) with an IC50 of 96.7 µg/mL and human lung carcinoma (A549) with an IC50 of 466.7 µg/mL.	(Lee et al., 2012)
LR Cap	Hot water extraction and 1.25MNaOH alkali extraction ethanol precipitation	β-D-glucan and Lentinan-Like β-D-Glucan.	The alkaline solution extracted more β-D-glucan than hot water but altered the retention time and conformation of the compound. This indicates that different solvents affect both the yield and the structural properties of the isolated β-D-glucan.	(Mohd Jamil et al., 2013)

Table 2.1 Continued

Source	Extraction and isolation methods	Extract/isolate	Bioactive effect and properties	Reference
Sclerotia	Hot and cold aqueous extraction	β-glucans, water-soluble protein/peptides	Cytotoxicity The cytotoxicity of the cold aqueous extract was significantly more potent (IC50:37–355 mg/ml) than that of the hot aqueous extract (IC50: >500 mg/ml). However, the cold aqueous extract demonstrated a lack of specificity, as it exhibited cytotoxic effects in both cancerous and normal cell lines. The LR extracts exhibited a presence of 37-38.93 mg/g w/w β-glucan..	(Lau *et al.*, 2013)
Sclerotia	4% (w/v) NaOH alkali extraction 80°C Ethanol precipitation	Crude polysaccharides	Neurogenesis L. rhinocerotis sclerotium crude extracts and polysaccharides demonstrate NGF-like activity via the MEK/ERK1/2 signaling pathway in rat pheochromocytoma (PC-12) cells, promoting neuritogenesis without eliciting NGF production.	(Seow *et al.*, 2015)
Polyporus rhinocerotis Sclerotia	Hot water extraction ethanol precipitation	Highly branched heteropolysaccharide–protein complex	Immunomodulatory LR extract induced NO production, enhanced cytokine release, and triggered ERK phosphorylation to activate macrophages.	(C. Liu *et al.*, 2016)
Sclerotia	ethyl acetate and acetone defatting, 0.5 M NaOH alkali extraction	(1 - 3)-β-glucan backbone with hyperbranched side chains.	LR polysaccharides exhibit high branching in a compact coil conformation, representing an intermediate structure between the hard sphere and fully swollen branched structure.	(Hu, Huang, Wong, Yang, *et al.*, 2017)
Sclerotia	Hot aqueous extraction	Crude polysaccharides	Cytotoxicity The Hot Aqueous Extract inhibit NO production and demonstrated lowest cytotoxicity towards BV2 microglia, with IC_{50} values of 176.23 ± 2.64 mg/mL at 24 h of incubation and 20.01 ± 1.69 mg/mL at 48 h of incubation.	(Seow *et al.*, 2017)

Table 2.1 Continued

Source	Extraction and isolation methods	Extract/isolate	Bioactive effect and properties	Reference
Sclerotia	25, 95 and 120°C hot water extraction and 1.0 M NaOH at 4°C Ethanol precipitation	Polysaccharide-protein complexes and β-d-glucan	Immunomodulation LRP fractions demonstrated protective effects against Cy-induced immunosuppression in mice by stimulating the release of the major cytokines, TNF-α and INF-γ.	(Hu, Huang, Wong and Yang, 2017)
Sclerotia	Hot water extraction	β-d-glucan	Cytotoxicity LR β-D-glucan extracts exhibited cytotoxic activity against a human lung cancer cell line (A549) (IC_{50} 57.78 ± 2.29 μg/mL) and a human breast cancer cell line (MCF7) (IC50 33.50 ± 1.41 μg/mL).	(Jamil *et al.*, 2018)
Sclerotia	Cold water extraction	β-glucans, polysaccharides and glycoproteins and derivatives of adenosine	Bronchodilation The LR extract induces complete relaxation of both the trachea and bronchus, a process mediated by the calcium signaling pathway downstream of Gαq-coupled protein receptors. Furthermore, preincubation with the extract significantly attenuated the maximum response to carbachol-induced contractions.	(Lee, Lim, *et al.*, 2018)
Sclerotia	Hot water extraction Ethanol precipitation	Ultrasound LR polysaccharide-selenium nanoparticles (LRP-SeNPs)	Antioxidant Under ultrasonic conditions, selenium nanoparticles (SeNPs) were incorporated into the LR polysaccharide, which enhanced its antioxidant properties, as assessed by DPPH and ABTS+ radical-scavenging assays.	(Cai *et al.*, 2018)
Sclerotia	Cold water extraction Sephadex G-50 fractionation and Ammonium sulfate Proteins precipitation	LR Proteins fraction F5	Antitumour F5 fraction selectively inhibited the growth of MCF7 cells through the induction of apoptosis, potentially via crosstalk between the extrinsic and intrinsic apoptotic pathways in MCF7 cells.	(Yap *et al.*, 2018b)

Table 2.1 Continued

Source	Extraction and isolation methods	Extract/isolate	Bioactive effect and properties	Reference
Mycelia	Cold water extraction Ethanol precipitation	(1,3) - β - D - glucan	Antioxidant LR β-D-glucan fraction exhibits antioxidant properties, as demonstrated through analyses of DPPH radical scavenging ability and ferric ion reduction capacity.	(Ahmad Usuldin *et al.*, 2020)
Mycelial Biomass	Cold water extraction Ethanol precipitation	Exopolysaccharides and bioreactor-grown biomass extracts	Cytotoxicity Neither extract demonstrated toxicity, as assessed using the zebrafish embryo toxicity (ZFET) model, indicating the safety of the LR polysaccharide extracts.	(Usuldin *et al.*, 2021)

2.2.4 Extraction and isolation of MPs

MPs are typically extracted from mushroom fruiting bodies, mycelia, sclerotia, and fermentation broth. MP extraction methods are important for the isolation and purification of these bioactive mushroom compounds. This process constitutes a crucial step in obtaining high-quality MPs and investigating their bioactive properties. LR for traditional medicinal purposes is conventionally utilized in various forms, such as a decoction, which is sliced or grated, boiled, or prepared through maceration methods (Lau *et al.*, 2013). However, in scientific studies, there are several methods to extract MPs, including conventional methods such as hot water extraction (HWE), acid hydrolysis, and enzyme hydrolysis, and more modern techniques such as ultrasound assisted extraction (UAE), microwave assisted extraction (MAE), enzyme assisted extraction (EAE), Ultrasonic microwave synergistic extraction, and supercritical fluid extraction.

Fungal polysaccharides can be classified according to their cellular location: intracellular polysaccharides found in fruiting bodies and cultured mycelia, and exopolysaccharides present in fermentation broth. Generally, most exopolysaccharides are water-soluble and can be extracted directly using aqueous, acidic, or alkaline solutions (Hsu and Cheng, 2018; Tang *et al.*, 2020; Leong, Yang and Chang, 2021).
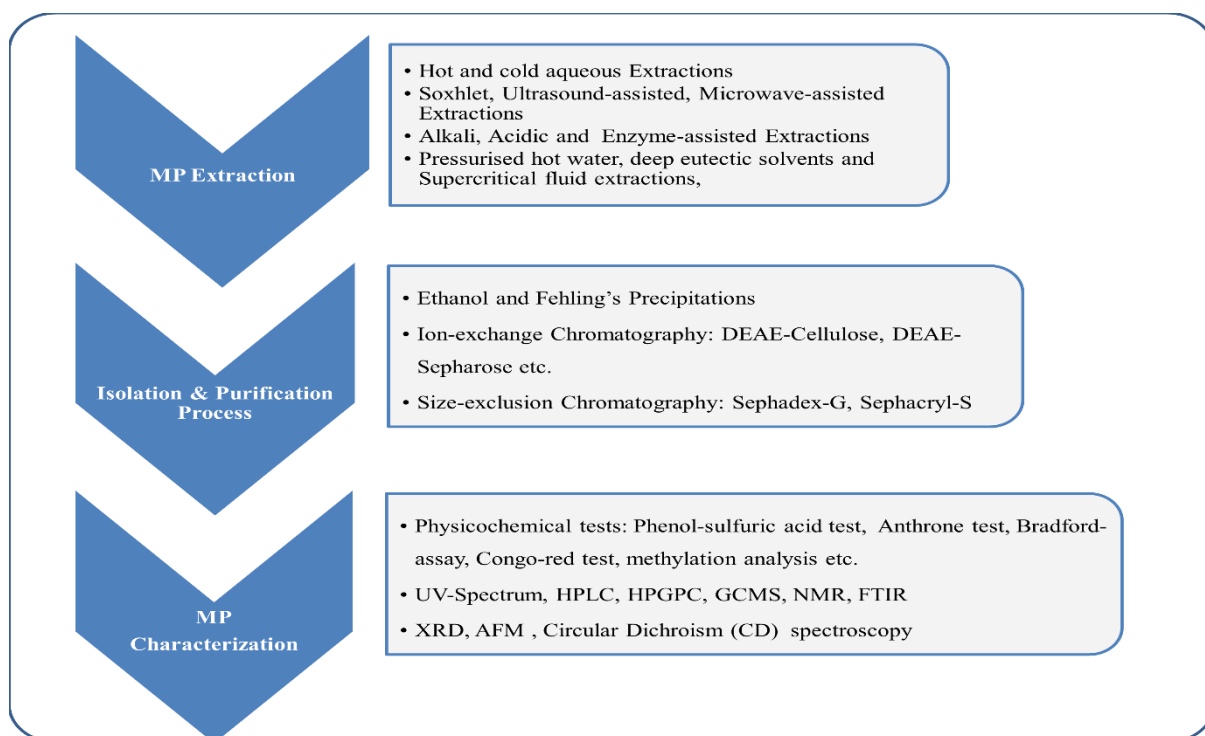
Figure 2.5   Mushroom polysaccharides isolation process

In addition to the extraction process, the importance of selecting appropriate and efficient methods for isolating MPs from mushrooms is significant factor of consideration. MPs are mostly extracted through aqueous extraction, wherein mushroom powder may undergo pre-treatment with organic solvents to remove polar components, such as lipids, phenols, and terpenes, thereby facilitating the complete separation of polysaccharides from other compounds.

Mushroom polysaccharides (MP) macromolecules are typically bound to the cell walls of mushrooms, necessitating efficient extraction techniques to penetrate narrow channels and dissolve and recover these metabolites (Zhang *et al.*, 2016). Moreover, a higher solvent-to-solid ratio is essential for generating concentration gradients that facilitate the transfer of these macronutrients from the cell wall of the fungus (Prakash Maran *et al.*, 2017). The most common method for extracting mushroom polysaccharides is hot water extraction, which is cost-effective and requires minimal equipment (Parniakov *et al.*, 2014; H. Wang *et al.*, 2022).

Aqueous extracted solutions can be further subjected to alkaline extraction and ethanol precipitations to obtain polysaccharide supernatants (Parniakov *et al.*, 2014; Ruthes, Smiderle and Iacomini, 2016). For MP isolation, ethanol precipitation involves the stepwise addition of ethanol, which fractionates the extracted mixture into an alcohol-insoluble polysaccharide fraction and other alcohol-soluble fractions that are subsequently centrifugation.

Also, ion-exchange chromatography and size-exclusion chromatography are extensively utilized techniques for the isolation and purification of MPs. These methods have been used in numerous studies to isolate bioactive compounds from mushrooms. The process is based on varying degrees of electrostatic interactions between the stationary phase media and isolation solutes as they traverse through the stationary column composed of appropriate cation- and/or anion-exchange chromatography media.

The combination of ion-exchange chromatography and size-exclusion chromatography is particularly effective for separating charged polysaccharides. These methods can be employed independently or in conjunction with other purification techniques to obtain high-purity MP for subsequent applications. (Zhao *et al.*, 2019; Ma, 2024). Ion exchange and size exclusion chromatography in mushroom polysaccharides isolation provides a versatile approach for isolating and purifying these bioactive compounds, and has been utilized in numerous MP isolation studies (Moon *et al.*, 2013; Gunasekaran, Govindan and Ramani, 2021; Q. Liu *et al.*, 2022).

Additional reviews have provided a comprehensive overview of MP extraction (Ruthes, Smiderle and Iacomini, 2015, 2016; Leong, Yang and Chang, 2021).

2.2.5   *Lignosus rhinocerotis* toxicity

Renowned for their nutritional properties, mushrooms are valued as a culinary delicacy. Even though many mushroom species are edible, many researches to determine the toxicity or otherwise of different mushroom species were reported, including on *Lignosus rhinocerotis*. LR hot water extract treatment demonstrated no treatment-related toxicity regarding the fertility of male and female rats and did not elicit teratogenic effects on the pups of treated rats (Hamzah *et al.*, 2022). LR extract administered orally to rats at doses up to 1000 mg/kg of both TM02 and wild type LR sclerotia powder for 28 days (sub-acute) and chronic exposure toxicity studies did not elicit any adverse toxicity effects (Lee *et al.*, 2011; S. S. Lee *et al.*, 2013). Both mycelium and sclerotium forms are reported to be safe for consumption (Lee *et al.*, 2011; Lau *et al.*, 2015). A similar finding was reported by Jhou et al. (2017), who observed that rats exposed to doses of up to 3400 mg/kg/day LR mycelium extract did not exhibit any adverse reproductive or developmental effects when assessed for reproductive and developmental toxicity.

In general, the *in vitro* non-cytotoxicity of LR extracts has been demonstrated through cell culture incubation on panel of human cell lines, including the normal human colon (CCD-18Co), kidney (HEK-293), nasopharyngeal (NP 69), oral (OKF6), rat kidney (NRK-52E), and Vero cell lines (Lau *et al.*, 2013, 2014; Suziana Zaila *et al.*, 2013); embryonic fibroblasts (NIH/3T3), mouse neuroblastoma (Neuro-2a) cells, normal human breast (184B5), and lung (NL20) cells (Lee *et al.*, 2012) and PC-12 cells (Eik *et al.*, 2012). Chen et al. (2013) investigated the mutagenicity of LR mycelium from liquid fermentation using a chromosome aberration test in Chinese Hamster Ovary (CHO-K1) cells, their study reported insignificant mutagenic activity of the LR extracts.

Furthermore, a study investigating LR supplementation in human subjects was conducted on 50 participants who were administered 300 mg of LR extract twice daily over a three-month period. The results indicated that LRE significantly suppressed IL-1β, IL-8, and MDA levels as well as respiratory symptoms. LR supplementation results in a significant increase in IgA levels, total antioxidant capacity, and pulmonary function (Tan, Leo and Tan, 2021). The toxicity of the LR exopolysaccharides isolate was evaluated using a zebrafish embryo toxicity (ZFET) model. The polysaccharides isolate exhibited an LC_{50} of 0.41 mg/mL, which is considered practically non-toxic (Usuldin *et al.*, 2021).

Therefore, considering its historical and traditional applications, bioactivity, and safety, as evidenced by numerous research findings, investigation of LR in phytochemical-complementary medicine is of significant importance.

2.3   Pulmonary inhalation drug delivery

Targeted drug delivery aims to enhance the presence of the therapeutic agent at specific desired sites within the body while minimizing nonspecific adverse effects (Pattni and Torchilin, 2015). Respiratory diseases are a major cause of morbidity and mortality worldwide. The development of effective drug delivery systems for respiratory diseases is essential to improve therapeutic outcomes.

Regarding the importance of polysaccharides in drug delivery, biopolymers have garnered considerable attention in recent years because of their potential applications in this field as natural polysaccharides have several advantages over synthetic polymers in drug delivery systems. Polysaccharides exhibit a range of properties that render them suitable for drug delivery applications. These natural polymers can function as drug carriers or excipients to enhance drug solubility,

stability, and bioavailability. Polysaccharides offer additional benefits, of biocompatibility, biodegradability, and mucoadhesion (Barclay et al., 2019; Islam & Ferro, 2016). Previous studies have investigated mushroom polysaccharides as a potential method for targeted drug delivery in various nano formulations. Mushroom polysaccharide nanoparticle formulations have been successfully developed and reported in the scientific literature (Cai *et al.*, 2018; Keshavarz-Rezaei *et al.*, 2022; Luk *et al.*, 2023).

Inhalation formulations have various clinical applications in which medications for asthma and COPD can be administered via inhalation. However, limited studies have been conducted on the inhalation of phytochemicals. This represents a potentially interesting area of research, wherein naturally occurring bioactive compounds for therapeutic applications could be delivered to the respiratory system.

2.3.1 Inhalation devices

Drug delivery to the respiratory system presents a significant challenge owing to the complex anatomy and physiology of the lungs. The efficacy of inhalation therapy is contingent not only on the potency of the active pharmaceutical ingredient but also on the effectiveness of the delivery system and formulation. These components are instrumental in ensuring efficient administration of inhaled medications.

Furthermore, it is essential to consider the physicochemical properties of drug particles in inhalation formulations which can be evaluated using various analytical techniques. Aerodynamic Particle Size Distribution (APSD) properties such as particles size, morphology, density, surface charge, and cohesive forces are assessed to determine the distribution and inhalation performance of the particles. Inhalation

products can be broadly categorized into two major forms: those based on dry powder formulations, and those utilizing solution formulations. The devices utilized for the administration of these formulations included the following:

2.3.1(a)   Dry powder inhalers

Dry powder formulations suitable for inhalation are commonly produced using spray drying (SD) and milling methods. The SD technique involves dissolving the desired solutes in suitable solvent and using a compressed gas (typically air or N_2) to atomize the liquid through a nozzle, creating fine droplets. These droplets are then dried, resulting in small particles that are collected as dry powders (Sou *et al.*, 2013; Büchi, 2020). One advantage of spray drying is its ability to modify the content or composition of the feed solution by incorporating excipients. This allows for the alteration of the dry powder formulation properties, enabling the production of various DPI formulations (Sou et al., 2013). The SD technique is recognized for its capability to generate particles with appropriate dimensions and morphologies for inhalation applications.

Dry powder inhalers (DPIs) generate medication aerosols using patient's respiratory effort. This process necessitates individuals to inhale forcefully and completely to produce the required inspiratory airflow within a specified range for optimal medication delivery (Zhang *et al.*, 2020).

2.3.1(b)   Nebulizers

In contrast, nebulizers use an external power supply to deliver solution formulations by generating liquid aerosols. Nebulization is an alternative methodology for administering medications in aerosol form. This process employs nebulizer devices to convert liquid drug formulations into fine-droplet aerosols.

Nebulizers do not incorporate any propellants (Muralidharan *et al.*, 2014). Compressed air is forced through apertures to create accelerated fluid particles (Kaur *et al.*, 2012). Nebulization is frequently utilized in the treatment of respiratory diseases, as it facilitates the administration of large volume of medication solution in fine droplets that can be readily inhaled, particularly in paediatric patients.

2.3.1(c) Pressurized metered dose inhalers (pMDI)

The metered-dose inhaler (pMDI) facilitates the delivery of the active pharmaceutical ingredient (API) to the lungs through dispersion or dissolution in a propellant at high vapor pressure. The device provides precise measurements of doses ranging from tens to hundreds of micrograms, are the most frequently used pulmonary drug-delivery devices (Thorat and Meshram, 2015).

pMDIs operate as pressurized systems containing propellants, flavour enhancers, surfactants, and preservatives, with API (Chandel *et al.*, 2019). pMDIs provide advantages such as portability, independence from external power sources, and consistent dosage delivery. Nevertheless, patients using pMDIs need to synchronize the device's activation with their inhalation (Zhang *et al.*, 2020).

2.3.1(d) Soft-mist inhalers (SMI)

Soft mist inhalers (SMIs) are devices that also administer medication to patients without propellants. These inhalers generate a low-velocity mist of drug aerosols via mechanical aerodynamic mechanisms. A spring-powered mechanism in a soft mist inhaler produces a slow, sustained aerosol, which helps patients synchronize their inhalation with the device's activation (Zhang *et al.*, 2020). SMIs can dispense single or multiple doses of medication in the form of fine mist, which is designed to facilitate inhalation into the respiratory system. As a category of solution based

inhalers, SMIs produce a slow-moving cloud of aerosol particles that can effectively penetrate a patient's airways (Komalla *et al.*, 2023).

2.3.2   Inhalation formulation characterization

Research on inhalation formulations also emphasizes the use of sophisticated analytical methods to evaluate the aerodynamic characteristics of inhaled aerosols. The development of inhalation drug delivery formulations aims to enhance the efficacy of drug administration to the lungs. Several critical factors must be considered in the formulation of inhalation therapies, including the particle size and morphology, surface area, electrostatic charge, and aerodynamic diameter (Paranjpe and MüllerGoymann, 2014). Various methodologies can be employed to evaluate the inhalation properties of dry powder and nebulized formulations designed for pulmonary administration.

For the purpose of inhalation characterisations, the US and European Pharmacopoeia protocols provides a standardised method and techniques for assessing the aerodynamic properties of inhalations, including DPIs and nebulised aerosol in terms of APSD, Emitted Fraction (EF), Median Mass Aerodynamic Diameter (MMAD) and Geometric Standard Deviation (GSD).

Various methodologies are employed to evaluate the performance of inhalation formulations and devices, each providing distinct insights into their efficacy and functionality. Cascade impactors, slit sampler impactors and twin impingers are the most commonly used to assess the APSD of the intended inhalation products.

2.3.2(a)   Twin impingers

Twin impinger evaluates drug delivery for oral inhalation formulations through a two-stage separation process. The released aerosol is propelled through a simulated oropharynx and an impinger stage with a specific particle size cut-off point,

subsequently collecting the fine particle fraction in a lower impinger component. This process facilitates the assessment of formulations for pulmonary delivery (Hallworth and Westmoreland, 1987). Notwithstanding the twin impinger demonstrates limitations in comparison to multistage impactors with respect to characterising finer fractions of the particle size distribution. An ideal two-stage instrument exhibits insufficient capacity to discern the critical features of the aerosol size distribution, thereby constraining its efficacy in certain applications (Miller *et al.*, 1992).

Although more sophisticated impactors may be preferred for precise APSD analysis, the twin impinger remains a crucial instrument for routine quality assessment during product development, stability studies, and comparisons of commercial formulations (Hallworth and Westmoreland, 1987; Omer, Husein and Hamadameen, 2019). The twin-impinger apparatus offers advantages in terms of simplicity and cost-effectiveness, particularly for basic performance evaluation of inhalation formulations and devices.

2.3.2(b)   Andersen cascade impactors

Andersen cascade impactors assess formulations based on APSD of their aerosols and deposition patterns within the respiratory system. Cascade impactors segregate aerosol particles into discrete categories based on their aerodynamic characteristics, facilitating the evaluation of their aerodynamic properties. The impactors utilize particle inertia, which is influenced by size and velocity, to separate samples. Air containing the sample is drawn through the impactor stages at a constant flow rate control by the vacuum pump. The aerosols are propelled through multiple nozzles and subsequently deposited onto a collection surface, such as a filter medium or agar plate (Annadurai *et al.*, 2024). Each stage comprised a plate with specific nozzles and collection surface. As the stage number increased, the nozzle size and total

area decreased. At each stage, particles of decreasing size acquired sufficient inertia to deviate from the airflow and impact the collection surface (Copley, 2018).

2.3.2(c)   Next Generation impactor (NGI)

Comprising a cascade impactor system, NGI characterizes inhalation formulations by determining the APSD of dispersed aerosols and estimating the deposition pattern across various regions of the respiratory tract. The NGI system comprises seven stages that operates with an inlet flow rate ranging from 30 to 100 L/min, encompassing a cut size spectrum between 0.24-µm to 11.7-µm aerodynamic diameter (Marple, Hochrainer, *et al.*, 2003).

NGI operates on the principle of inertial impaction, a methodology that segregates particles based on their dimensions and aerodynamic properties. This device comprises multiple stages that simulate the various components of the respiratory system, enabling researchers to assess the distribution of drug particles in the lungs and other targeted anatomical regions (Copley, 2018). These factors make NGI an extensively utilized impactor for assessing the inhalation characteristics of diverse devices and formulations, facilitating the evaluation of the delivery performance of inhalation system.

NGI systematically size fractionate aerosols through stages with one or more nozzles. The effective diameter of the nozzles in the multi-nozzle stage correlates with the cut-point size, establishing a relationship with the aerodynamic diameter. NGI characterization of inhalation aerosols entails impactor classification, particle size distribution, and aerodynamic diameter measurements, NGI demonstrates superior *in vitro*/*in vivo* correlations (IVIVCs) through the incorporation of a more anatomically accurate inhalation-impactor interface. (Copley, 2018).
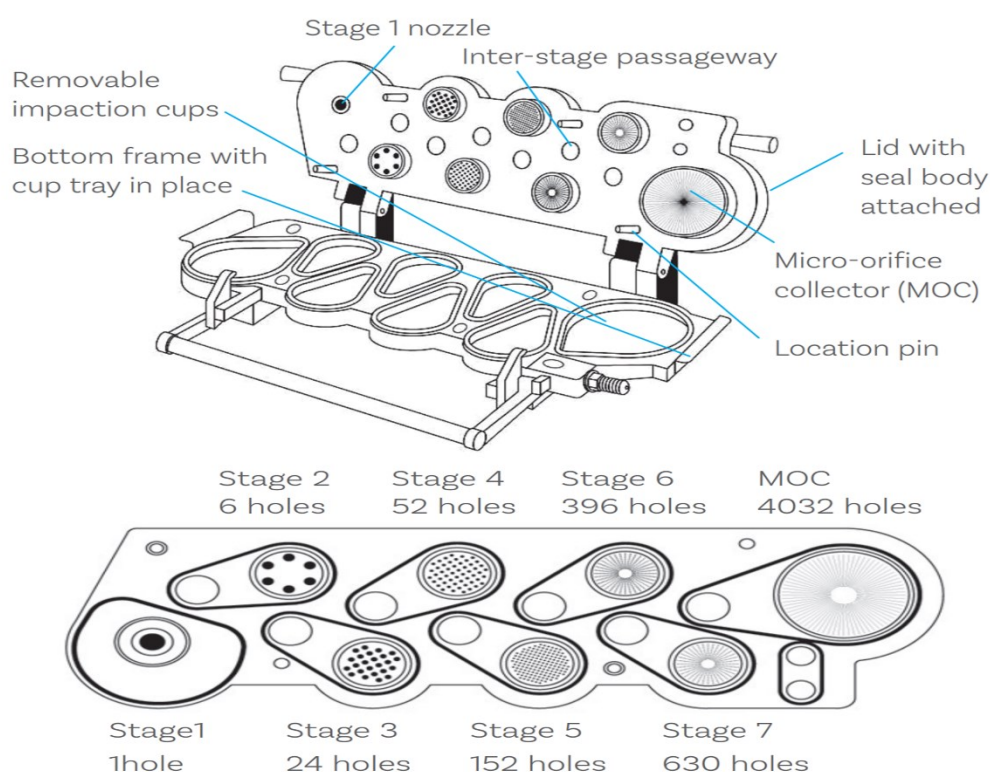
Figure 2.6   Schematic representation of next-generation impactor (NGI), comprising seven multi-nozzle stages (1-7) and a micro-orifice collector (MOC), arranged in order of decreasing cut-point sizes (Adopted from Copley Scientific, 2024).

The accuracy and reliability of results in inhalation delivery performance assessments can be significantly influenced by errors and insufficient precautions. NGI critical precaution protocols encompass proper equipment calibration, the maintenance of consistent airflow during testing procedures, and precise impactor positioning for accurate particle collection, stage mensuration checks to ensure that each stage remains within the manufacturer's specified tolerances (Roberts and Mitchell, 2019). During the passage of aerosols through an impactor, heat transfer from the device to the aqueous particles can result in droplet evaporation, leading to underestimation of the aerosol size. To mitigate this issue, the pharmacopeia recommends cooling the impactor to 5°C. By maintaining the NGI impactor temperature below that of the aerosol, particle condensation can be prevented (Schuschnig, Heine and Knoch, 2022).

2.3.2(d) Other forms of inhalation characterization methods

Alternative inhalation drug delivery assessment methodologies, including Acoustic Emission-Multivariate Data Analysis (AE-MVDA) (Boberg *et al.*, 2019), Laser diffraction spectrometry (Cyr and Tagnit-Hamou, 2001), three-dimensional positron emission tomography (PET) imaging (Dolovich and Bailey, 2012), and Computational fluid dynamic models (Shur *et al.*, 2012; Ari and Alhamad, 2023) have been studied and documented in the scientific literature.

2.4 Regulation of airway smooth muscle (ASM) tone

The regulation of respiration is predominantly dependent on the fundamental physiological mechanisms of airway relaxation and contraction. The precise equilibrium between the relaxing and contracting airways facilitates the modulation of airflow during respiration, ensuring optimal respiratory function. The physiological processes of airway contractions and relaxation play a crucial role in regulating the flow of air within the lungs, thereby significantly contributing to overall respiratory function.

Previous studies have demonstrated that polysaccharides derived from mushrooms exhibit promising biological activities including immunomodulatory, anti-inflammatory, and bronchodilation effects. These properties render them a subject of interest for investigating their potential to induce airway relaxation.

2.4.1 Airway smooth muscle receptor mechanism

Airway dilation is essential for maintaining optimal respiratory function, especially in pathological conditions, such as asthma. The regulation of airway relaxation and contraction is a complex process that involves multiple physiological pathways processes. Various factors and mechanisms, including the autonomic

nervous system, hormones, and inflammatory mediators regulate airway dilation and constriction. The neural regulation of the airways involves both sympathetic and parasympathetic innervations (Pera and Penn, 2014). The overall control of airway dynamics is influenced by the sophisticated interplay between these factors and regulatory systems.

Smooth muscle cells are responsible for regulating the contraction and relaxation of airway walls, which subsequently influences airway diameter and airflow. During airway relaxation, a reduction in smooth muscle tone occurs, accompanied by an increase in airway diameter, thereby facilitating an enhanced airflow in to the lung. Conversely, airway contraction results in an increase smooth muscle tone, leading to a reduce airway diameter and, therefore reducing airflow, especially during the exhalation phase.

Previous studies have provided significant insights into the roles of smooth muscle cells, neurotransmitters, inflammatory mediators, and other factors in airway contractility. Multiple investigations have demonstrated the involvement of diverse receptor pathway mechanisms in regulating ASM contraction and relaxation, with some exhibiting crosstalk and varying degrees of influence.

2.4.1(a)   Muscarinic receptors pathway

In asthma, parasympathetic nerves innervating the lungs significantly contribute to airway narrowing and mucus secretion (Scott and Fryer, 2012). The cholinergic system of the airways comprises three subtypes of muscarinic receptors, which mediate distinct activities upon activation (Barnes, 2016). Airway smooth muscle expresses both M2 and M3 muscarinic receptors, with the majority of the receptors being of the M2 subtype (Roffel, Elzinga and Zaagsma, 1990). These M2 and M3 muscarinic receptor subtypes are abundantly expressed by the airway smooth

muscle at a ratio of approximately 4:1 (Roffel *et al.*, 1988; Gosens *et al.*, 2006). The M3 muscarinic receptor subtype has been identified as the primary mediator of ASM contraction in both central and peripheral airways.

Acetylcholine (Ach) is the predominant parasympathetic neurotransmitter in the airways (Kolahian and Gosens, 2012), Ach released by vagal nerve endings stimulates muscarinic receptors, resulting in increased ASM tone and subsequent bronchoconstriction (Pieper, 2012). The muscarinic receptor influences ASM contractions, predominantly via Gq proteins coupled M3 receptors activation of phospholipase C (PLC) and inositol phosphates for intracellular Ca2+ release, as well as protein kinase C (PKC) activation for diacylglycerol formation, all of which cause ASM contractions (Dale *et al.*, 2014; Pera and Penn, 2014).

Recent studies have indicated that Ach is synthesized not only by neurons but also by diverse inflammatory cells. These cells, including lymphocytes, macrophages, mast cells, eosinophils, and neutrophils, infiltrate bronchial tissue during chronic inflammatory conditions such as asthma (Koarai and Ichinose, 2018). Investigations have elucidated this component of the cholinergic system referred to the non-neuronal cholinergic system (Pieper, 2012; Scott and Fryer, 2012). In asthma the increase stimulation by non-neuronal Ach intensify cholinergic activity in the lungs, potentially resulting in inflammation, structural alterations, excessive mucus secretion, and persistent cough (Pieper, 2012).

Therefore, acetylcholine also plays a role in airway inflammation via autocrine/paracrine mechanisms (Montalbano *et al.*, 2016) through muscarinic M3 receptor, rather than the M1 or M2 receptors, mediates the role of acetylcholine, causing allergen-induced remodelling and increased smooth muscle mass (Kistemaker *et al.*, 2014).

In conclusion, the muscarinic regulation of ASM tone involves multiple mechanisms, including direct contraction through M3 receptors, inhibition of relaxation via M2 receptors, and modulation of cAMP signaling. The interplay between cholinergic and adrenergic signaling, as well as the involvement of non-neuronal cholinergic systems, plays a critical role in determining ASM tone (Pieper, 2012).

2.4.1(b)   Histamine receptors pathway

Histamine receptor stimulation elicits its effects through four distinct receptor subtypes, H_1, H_2, H_3, and H_4, which are predominantly G protein-coupled receptors (Ince and Ruether, 2021). Histamine serves as a critical mediator in asthmatic reactions, eliciting significant and occasionally acute changes in airway smooth muscle tension, regulating airway smooth muscle tone primarily causing bronchoconstriction effects. It acts directly on airway smooth muscles by stimulating H1-receptors, resulting in ASM contraction.

Histamine is primarily synthesized and secreted by mast cells and basophils (Ince and Ruether, 2021). Histamine receptors are $G_{q/11}$ coupled receptors, and when stimulated, cause activation of PLC-β for inositol triphosphate (IP3) messenger activation to trigger the release of Ca2+ from the sarcoplasmic reticulum (Dale *et al.*, 2018; Ince and Ruether, 2021).

2.4.1(c)   β-receptor pathway

Conversely, activation of the adrenergic pathway results in the release of adrenaline neurotransmitters, which subsequently induce relaxation of the airway. $β_2$-adrenergic receptors are predominantly located in the ASM. Additional $β_2$- receptors they are present in type II pneumocytes, endothelial, epithelial, and mast cells (Yusuf, Prayle and Yanney, 2019).

Relaxation through the beta-receptor pathway is mediated by the activation of cAMP and protein kinase A (PKA) (Dale *et al.*, 2018). When a specific agonist binds to β2-receptors, adenylyl cyclase (AC) activation increases cAMP to stimulate receptor-coupled Gs-proteins. These mediate both the opening of Ca^{2+}-activated potassium channels and the activation of PKA to inhibit phosphorylation of IP3R in the sarcoplasmic reticulum, promote repolarisation and decreasing Ca^{2+} levels for relaxation (Barisione *et al.*, 2010; Dale *et al.*, 2018). According to Morgan (2014), the primary mechanism for ASM relaxation induced by β-agonists is PKA rather than the exchange protein activated by cAMP (Epac).

2.4.1(d)   The pathway cross talk mechanism in ASM contractility:

Airway contractility is mediated by multiple interacting receptor pathways. However, the primary interaction influencing ASM tone occurs between the airway muscarinic, histamine, and β2 receptor pathways, and their crosstalk interplay has been extensively studied.

On one hand, β-receptor-activated PKA promotes M3 receptor desensitization by phosphorylation of the Gq subunit or PLC, which decreases IP3 release. The decrease in IP3 generation, coupled with the phosphorylation of membrane KCa^{2+} channels, lowers Ca^{2+} levels from both sarcoplasmic and extracellular influx (Pera and Penn, 2014). Furthermore, the influence of the β-receptor pathway on the histamine pathway has been reported. This interaction occurs through selective inhibition of histamine-evoked Ca^{2+} signals via hyperactive cAMP junctions (Dale *et al.*, 2018).

Conversely, M2 regulation induces functional antagonism of β2-receptors. The muscarinic crosstalk desensitization of the β2-pathway results in contractions exhibiting greater resistance to relaxation induced by β2-adrenoceptors, compared to contractions caused by agonists that do not involve muscarinic receptor stimulation

(Dale *et al.*, 2014). Chronic activation of muscarinic receptors mediates the chronic activation of PKC in conditions such as asthma, which can lead to decreased AC activity, these alterations in neuronal M2 receptor function contribute to airway hyper-responsiveness in asthma (Buels and Fryer, 2012). Consequently, these factors potentially reduce the effectiveness of bronchodilators that function through cAMP elevation (Schears *et al.*, 1997; Emala, Clancy-Keen and Hirshman, 2000), which is attributable to ligand-directed desensitization of the β_2 receptors (Goral *et al.*, 2011). This clinical manifestation is observed in asthma patients, wherein the regular administration of short-acting β_2-agonists (SABA) is associated with the development of β_2-agonist tachyphylaxis (Michele, Zhao and Sahajwalla, 2012).

In overall, these mechanisms suggest a complex interaction between the signalling pathways in the regulation of ASM tone, highlighting the intricate balance of various mediators in regulating airway tone. Given that these pathways compete with one another, the pathogenic upregulation of muscarinic pro-contractile, pro-remodelling signalling in combination with β_2-pathway desensitization alters the balance of the signalling in disease conditions like asthma and COPD towards increased ASM tone (Pera and Penn, 2014).
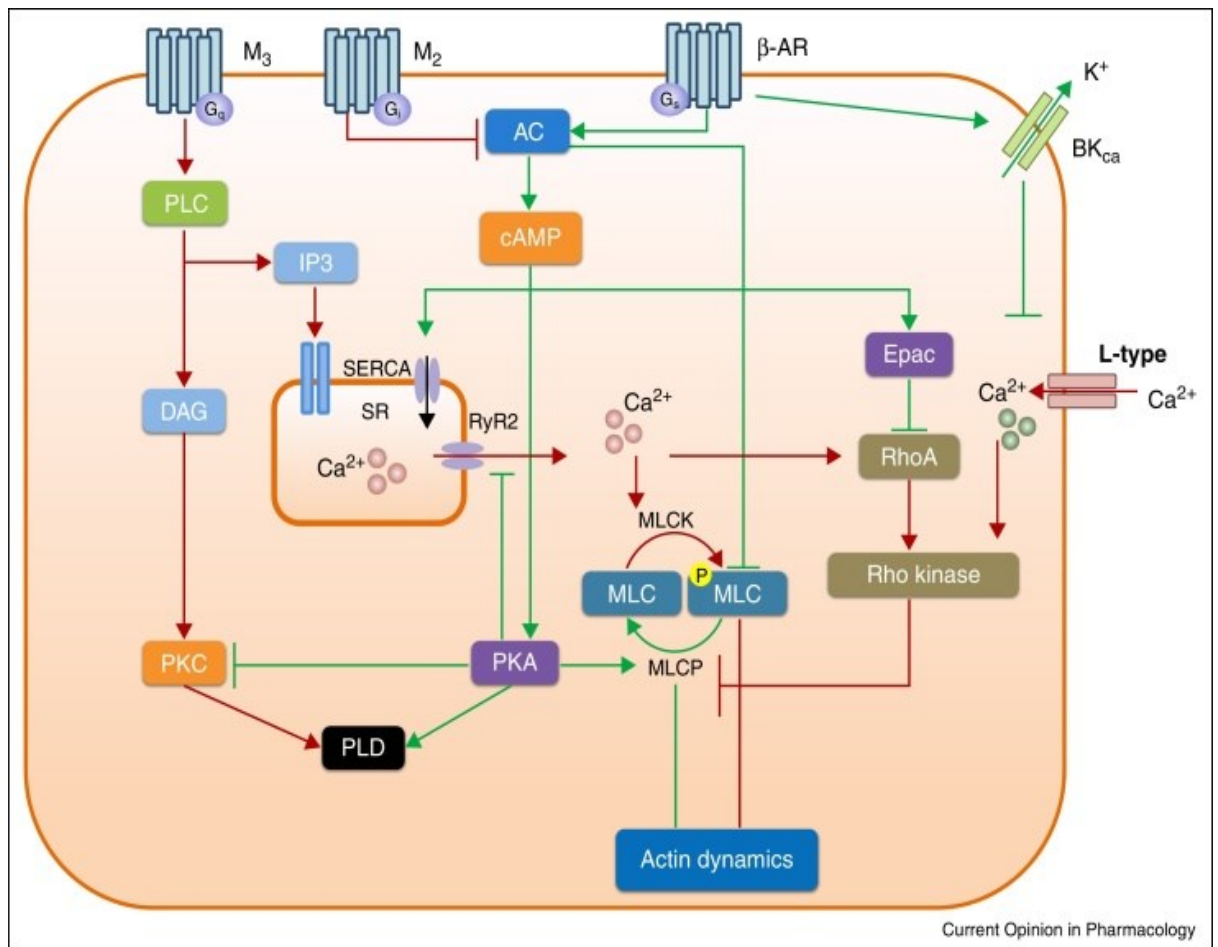
Figure 2.7   Illustration of the mechanisms and signalling cascades involved in regulating airway smooth muscle (ASM) contractility through muscarinic, histamine, and β-adrenergic receptor-mediated pathways (Adopted from Dale *et al.*, 2014).

2.4.1(e)   Other ASM contractility pathways

In addition to the aforementioned receptors, extensive literature has also identified role of other mediator pathways that influence airway contractility, including: E-Prostanoid receptor (Säfholm *et al.*, 2015), Prostaglandins receptors (Kamal *et al.*, 2013; Säfholm *et al.*, 2015), Cysteinyl LT receptor 1 (Rovati *et al.*, 2006; Okunishi and Peters-Golden, 2011), Purinergic receptors (Gui *et al.*, 2011) and the downstream central role of Phosphodiesterase (PDE) (Townsend and Emala, 2013; Zuo *et al.*, 2019; Rehman *et al.*, 2022).

2.4.2   ASM contractility assessment

Constriction of ASM is a characteristic feature of respiratory disorders. Diverse experimental methodologies have been used to assess ASM contractility, providing valuable insights into the complex physiology of ASM in both normal and pathological states.   The direct evaluation of airway contractions *in vivo* presents significant challenges. Consequently, most measurements rely on *ex vivo* and in vitro methodologies to directly assess isolated airway tissues. The extant literature described various approaches for quantifying airway contractility, with a predominant focus on the response of the ASM to diverse substances by measuring and comparison of contractile and relaxation responses.

Techniques and devices encompassing *in vitro, ex vivo,* and *in vivo* methodologies have been used to evaluate ASM contractility. These methods are used to investigate the response of ASM to a diverse array of stimuli, including pharmacological agents, chemicals, electric field stimulation, transmural pressure, and phytochemical extracts. These approaches facilitate measurement of ASM contractility under controlled and relatively constant physiological conditions.

2.4.2(a)   *In vitro* ASM contractility assessment methods

In vitro studies have used isolated tissues and cells to quantify contractile responses to diverse stimuli. Current methodologies for in vitro airway remodelling simulation include microfluidic chip technology and organoids, monolayer cultures of respiratory cell lines and primary cells, and co-cultures of various cell subpopulations (Zhou, Duan and Yang, 2023). As these methodologies have evolved, recent in vitro approaches include multi-well organ baths, which utilize 96-well standard plates, facilitating simultaneous camera and bi-telecentric optic airway tissue evaluations

through computer-controlled optical measurements of muscle contraction and relaxation (Borges, 2022).

2.4.2(b) *In vivo* ASM contractility assessment

In vivo methods involve functional respiratory studies using animal models. It is arguable that compared to reduced or isolated systems of in vitro models, integrated systems with various cell types and a comprehensive in situ mechanical environment are more suitable for accurate ASM contractility assessments.

Plethysmography offers a non-invasive method for assessing airway obstructions, and whole-body barometric plethysmography allows for non-invasive measurement of airway obstruction in conscious, unrestrained animals (Hamelmann *et al.*, 1997). Various studies have demonstrated the use of plethysmography use in measuring lung function and AHR in experimental animals (Glaab *et al.*, 2001; Albertine *et al.*, 2002; Muhamad *et al.*, 2019; Dixon, Bedenice and Mazan, 2021)

2.4.2(c) *Ex vivo* ASM contractility assessment methods

To overcome *in vivo* complex mechanical environments and mitigate the influence of different cell types, bronchial and tracheal rings are positioned on force transducers and length-sensing levers within organ baths (Wright *et al.*, 2013), thus enabling the physical evaluation of airway excitability and contractility independent of micro-environmental influences.

Significantly, airway segments maintain the mechanical properties of the airway wall as well as several advantages of an integrated system, including the epithelial layer, parasympathetic neurons, and nitrergic neurons (Wright *et al.*, 2013). However, the quality and reproducibility of data obtained from *ex vivo* ASM experiments on isolated airways are primarily influenced by two factors: the

researcher's technical skills and availability of suitable tissue samples (Calzetta *et al.*, 2024). *Ex vivo* techniques measure responses in isolated airway segments and smooth muscle strips enabling rigorous protocols that are not feasible with intact animals *in vivo*, thereby providing the ability to compare central and peripheral airways, apply electric field stimulation, and selectively evaluate pharmacological responses to drugs (Wright *et al.*, 2013).

In conclusion, numerous experimental approaches in this field have focused on quantifying and comparing the degree of contraction and relaxation in response to various stimuli agents, including *in vivo* small animals, *ex vivo* airway segments, thin-lung slices, ASM strips and rings, *in vitro* cell cultures, *ex vivo* videomicroscopy with visual imaging, and engineered tissues. Each approach possesses distinct advantages and limitations, which are predominantly influenced by the level of cell-type integration and complexity of the mechanical environment. Consequently, each model exhibits specific limitations and benefits.

2.4.3   Myography technique

This technique is also employed to examine the contractile function of muscle tissues in an experimental setting in which the tissue is isolated and mounted externally (Del Campo and Ferrer, 2015). Myograph methods facilitate the observation of the lateral isometric force generated by airway and blood vessel segments in response to various physiological and pathological stimuli ex vivo.

The wire myography technique enables *ex vivo* assessment of the functional and mechanical responses of isolated muscle tissue. Isolated bronchial and tracheal rings are positioned on force transducers and length-sensing levers within organ baths (Wright *et al.*, 2013), thereby allowing the physical evaluation of airway excitability and contractility. Therefore, prior to experiments, normalization of tissue segments is

important. The goal of normalization is to return isolated tissue to its initial resting tension (McPherson, 1992) to reflect *in vivo* parameters such as connective tissue tethering, altered pressure-length, and pressure-diameter correlations (Lew & Angus, 1992).

In asthma, airway hyper-responsiveness and inflammation induce excessive bronchial smooth muscle contraction, resulting in airway narrowing and increased airflow resistance. The adrenergic and muscarinic systems have been extensively investigated with respect to airway contractility. The multichannel myography facilitates precise stimulation of parasympathetic and sympathetic pathways, enabling specific examination of the roles of their respective receptors in bronchodilation and bronchoconstriction. Myography primarily focuses on comparing the mechanical responses elicited by pathway receptor stimulation *ex vivo* and quantifying the mechanical contraction response.

2.4.4   Isolated Guinea pig airway study model

For airway research studies, guinea pig are a better model for human airway pharmacology than rat or mouse airway, as similar receptor pharmacological responses to human lungs are expressed in guinea pigs (Ressmeyer *et al.*, 2006). Studies have indicated that guinea pigs exhibit superior anatomical and physiological similarities to human airways compared to mice. This is particularly evident in aspects such as airway branching, neurophysiology, pulmonary circulation, smooth muscle distribution, mast cell localization, and mediator secretions (Adner *et al.*, 2020).

Research has demonstrated that guinea pigs exhibit comparable potency and efficacy of agonists and antagonists to human airways, and display numerous similarities in their physiological mechanisms that govern airway autonomic control and responses to allergens (Canning and Chou, 2008). When activated, muscarinic M3,

neurokininNK2, leukotriene cysLT1, endothelin ETB receptors, and thromboxane/prostanoid TP receptors that can elicit ASM contraction in human airways also elicit guinea pigs ASM contraction in in vitro airway preparations and *in vivo* bronchospasm (Adner *et al.*, 2020).

In conclusion, myography evaluates *ex vivo* smooth muscle responses to various agents, wherein the assessment of their pharmacological parameters is utilized to compare bioactivity and potency to determine the therapeutic role of drugs and agents, such as organic extracts. Most research studies have employed a combination of these assessment methods of *in vivo, ex vivo, and/or in vitro* approaches to correlate results interpretation for an enhanced understanding of bioactive effects. A substantial body of literature has investigated the influence of various extracts on the airway smooth muscle response of guinea pigs.

.

CHAPTER 3

MATERIALS AND METHODS

The data utilised in this investigation were obtained using the following materials, and the results were examined and analysed using the following methodologies.

3.1 Study flow chart

Figure 3.1 describes the overall flow chart of the study starting from the extraction, fractionation and characterisation of LRP, followed by assessment of the anti-asthmatic effects of LRP in ovalbumin-induced allergy asthma mouse model and airway contractility study in guinea pig trachea.
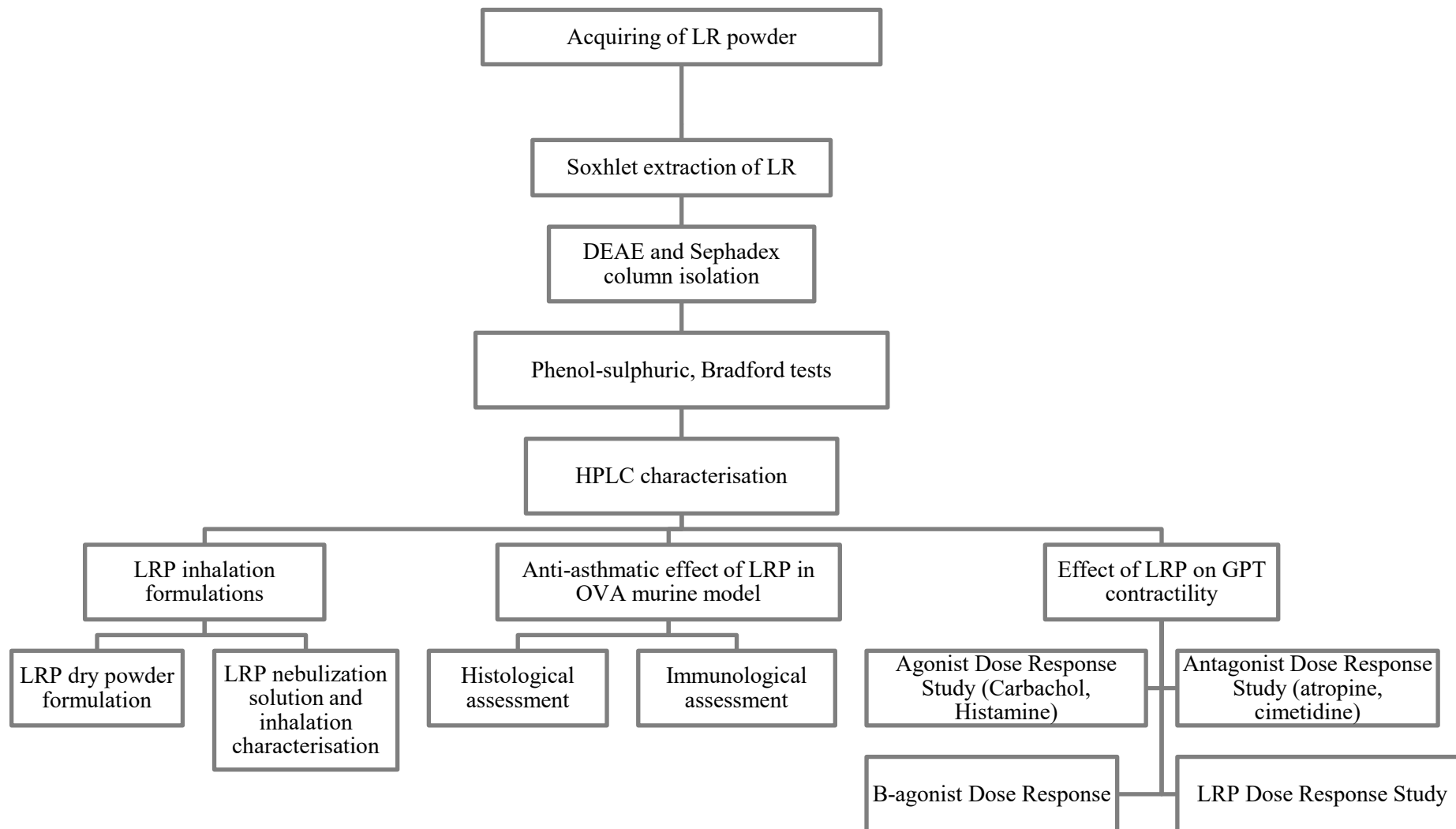
Figure 3.1   The overall flow chart of study

3.2 Materials

Table 3.1 List of chemicals and reagents

Items	Manufacturer
1-phenyl-3-methyl-5-pyrazolone (PMP)	Sigma-Aldrich, Germany
Acetonitrile	Fisher Scientific, USA
Albumin Hydroxide	Naclai tesque, Japan
Aluminium hydroxide	Naclai tesque, Japan
Ammonia	VWR Chemicals, UK
Ammonium acetate	Sigma-Aldrich, Germany
Atropine	Agros organics, Belgium
Bovine serum albumin	gibco, Fisher Scientific, USA
Bradford reagent	BIO-RAD, USA
Carbachol	Sigma Aldrich, USA
Chloroform	Fisher Scientific, USA
Cimetidine	Sigma Aldrich, USA
Cover slip	Menzel-Glaser, Thermofisher, Germany
DEAE-cellulose	ChemCruz, USA
Dexamethasone	Naclai tesque, Japan
D-glucose	ChemPur-SYSTERM, Malaysia
di-n-butyl phthalate (DPX)	Chemiz, Selangor Malaysia
Eosin	Sigma-Aldrich, Japan
Ethanol	VWR Chemicals, UK
Fetal bovine serum (FBS)	Thermo Fisher, UK
Formalin	SYSTERM, Malaysia
Giemsa Stain	Merck KGaA, Germany
Glacial acetic acid	Chemiz, Selangor Malaysia
Haematoxylin	Epredia, Thermofisher, UK
Histamine	Sigma Aldrich, USA
Hydrochloric acid	VWR Chemicals, UK
Immersion oil	SYSTERM, Malaysia
Isopropanol	Fisher Scientific, USA
Kreb's solution: Sodium chloride (NaCl), Potassium chloride (KCl), Calcium chloride solution (CaCl2), Magnesium sulphate ($MgSO_4$), Potassium dihydrogen phosphate (KH_2PO_4), D(+)-glucose and Sodium hydrogen carbonate (NaHCO3)	Merck KGaA, Darmstadt, Germany
Lactose	ChemPur-SYSTERM, Malaysia
L-Fucose	Supelco, USA
L-leucine	EMD Millipore, USA
Methanol	VWR Chemicals, UK
Monosaccharide standards	Sigma-Aldrich, Germany
Ovalbumin	TCI, USA
Periodic acid Schiff stain kit	Epredia, Thermofisher, UK
Phenol	GR ACS Reag, Merck, Germany
Phosphate buffer saline (PBS)	1st BASE, Malaysia

Items	Manufacturer
Propranolol	Sigma Aldrich, USA
RNA hold	TransGen, China
Salbutamol	MedChemExpress, USA
Sephadex G-50	GE Healthcare, Sweden
Sodium chloride	Fisher Scientific, UK
Sodium hydroxide	Merck KGaA, Darmstadt, Germany
Sodium pentobarbitone	Dorminal 20%, Alfasan Woerden-Holland
Sulphuric Acid	UNIVAR, AJAX chemicals, Australia
Trifluoroacetic acid (TFA)	Sigma-Aldrich, Germany
Trizol	ambion, Thermo Fisher, UK
Tween-20	Sigma-Aldrich, Japan
Xylene	VWR Chemicals, UK

Table 3.2   List of consumables and Kits

Items	Manufacturer
70% alcohol	SYSTERM, Malaysia
Cannula (18G, 22G)	SURGICO, Malaysia
Cellulose extraction thimble (CT43123)	FAVORIT, PLT Scientific, Malaysia
Centrifuge tubes (15ml, 50ml)	Fisher Scientific, UK
Cotton wool	Tani Segar, Malaysia
Cover slip (24 X 60 mm)	MENZEL-GLASER, USA
Cuvettes	Square Cuvette, Evergreen, Malaysia
Disposable Face mask	Zhejiang juhao Med. Tech., China
Disposable gloves	Zhejiang juhao Med. Tech., China
Distiled water	UPMS, USM Kelantan Kampus
Elisa Plate	Wuxi NEST, Jiangsu, China.
Foil paper	AYL indust, Malaysia
HiScript III 1st Strand cDNA Synthesis Kit (+gDNA wiper)	VazymE, China
Injection needles (27G, 25G, 23G)	TERUMO, USA
IgE Elisa kit	Elisa Max Delux, Biolegend, USA
Luna® Universal qPCR Master Mix	NEB #M3003S, BioLabs, UK
Micro centrifuge tubes (50µl, 200µl, 1.5ml)	aras 1, Malaysia
Micro pipettes	Wuxi NEST, China
Microscope slides	Sail Brand, China
Mouse IgE ELISA kit	ELISA MAX™ Deluxe Set, USA
Mouse IL-4 ELISA kit Quantikine™	Biotechne, R&D Systems USA
Mouse Magnetic Luminex Screening Assay 4-plex kit (GZ-LXSAMSM-04)	R&D Systems, Minneapolis, USA
Paraffin wax	Fisher Scientific, UK
Parafilm	Parafilm M, Bemis Company, USA
Pipette tips	BIOLOGIX, USA
qPCR tubes (Low profile clear Caps)	NOVAS BIO, USA

Table 3.2 Continued

Items	Manufacturer
Sterile hand gloves	CLEANGUARD, LYNK Malaysia
RNase Quiet	Naclai tesque, Japan
Syringes (1ml)	TERUMO, USA
Tissue cassette	CITOTEST, China
Urine bottles	PlasDispo, PorLab, China

Table 3.3   List of devices and Lab equipment

Items	Manufacturer
-80 freezer	ilShin, Korea
Autoclave	HIRAYAMA HV-110, Japan
Biological safety cabinet	RICO Scientific, India
Bright Light microscope	Olympus BX41, USA
Carbogen gas	Linde Gases, Malaysia
Centrifuge machine	eppendorf 5810R, Germany
Cold plate	EG1130, Leica microsystems, Germany
Deep freezer	NR-BL347NSMY, Panasonic, Malaysia
Dissecting kit	Gold Cross, Malaysia
Dissection microscope	OLYMPUS SZ61, USA
Freeze dryer	Ilshin, Korea
Glass wares (beakers, test-tubes, glass bottles, funnels,)	
Heating mantle	MS-E, MTOPO, Republic of Korea
HPLC column	Naclai Tesque, Japan
Laminar flow Cabinet	ERLA Technologies, Malaysia
Luminex 200 system	Luminex Inc., Austin, TX, USA
Magnetic microplate washer	BioTek ELx50, USA
Magnetic stirrer	Merck, Darmstadt, Germany
Microplate reader	NanoQuant, Tecan, Switzerland
Microplate shaker	MS1 Minishaker, IKA malaysia
Microtome	RM2235, Leica Biosystem, Germany
Multichannel-Myograph System - DMT 620M	Danish Myo Technology, Denmark
NanoDrop 2000c Spectrophotometer	Thermo Scientifics, US
Nebuliser	N80 RossMax, Switzerland
Next Generation Impactor (NGI)	Copley Scientific, United Kingdom
Paraffin dispenser	EG1120, Leica Biosystems, Germany
PCR thermo cycler	Veriti, Applied Biosystems, UK
pH meter	HANNA pH 211, Italy
qPCR machine	CFX Opus 96, RT-PCR System, USA
Rotary evapourator	Laborota 4000-efficient, Heidolph, USA
Slide storage box	Citotest, China
Slide warmer	Leica Microsystem, Germany
Soxhlet apparatus	BUCHI, USA
Spectrophotometer	Eppendorf, Biophotometer plus, USA
Spray dryer	B-290, Büchi, Switzerland

Table 3.3 Continued

Items	Manufacturer
Stop watch	Elabscience, USA
Test tube racks	Heathrow Scientific, Malaysia
Stop watch	Elabscience, USA
Test tube racks	Heathrow Scientific, Malaysia
Tissue embedding	Leica Biosystem, USA
Tissue floatation bath	Thermos Shandon, UK
Tissue processor	Leica Biosystem, Germany
Vortex mixer	MS1 Minishaker, IKA Malaysia
Water bath	DAIHAN scientific, South Korea
Weighing scale	HR-251AZ, A&D, Japan

Table 3.4   List of computer Applications and software

Items	Manufacturer
Data acquisition unit	PowerLab, ADInstruments Ltd, US
Data acquiring programme	LabChat 7, ADInstruments Ltd, US
Desktop computer system	Hewlett Packard, US
GraphPad Prism	Version 8, Dotmatics US

3.3   Solutions and buffers preparation

3.3.1   Ethanol (50%)

To prepare 50% ethanol, 500 ml of absolute ethanol was mixed with 500 ml of distilled water (dH_2O) to form a 1 L solution. The solution was stored at room temperature.

3.3.2   Ethanol (70%)

To prepare a 70% ethanol solution, 700 ml of absolute ethanol was diluted with 300 ml of distilled water. The solution was stored at room temperature.

3.3.3   Ethanol (80%)

To prepare 80% ethanol, 800 ml of absolute ethanol was mixed with 200 ml of distilled water. The solution was stored at room temperature.

3.3.4   Ethanol (90%)

To prepare a 90% ethanol solution, 900 ml of absolute ethanol was diluted with 100 ml of distilled water. The solution was stored at room temperature.

3.3.5   0.2 % ammonia water

To prepare a 0.2 % aqueous ammonia solution, 4 ml of absolute ammonia was diluted into 996 ml dH2O and stored at room temperature.

3.3.6   1 % acid alcohol

To prepare 1 % acid alcohol, 10 ml of absolute HCL was diluted with 290 ml of dH2O and 700 ml of ethanol and stored at room temperature.

3.3.7   Phosphate buffer saline (PBS)

PBS was prepared by dissolving 100 ml 10X-PBS solution in 900 ml of dH2O. Sterilisation was performed by autoclaving at 115 °C, followed by storage at 4^0C.

3.3.8   Stop solution

The stop solution was prepared by dissolving 54 ml of 98% 2N H_2SO_4 in 950 ml dH2O. The solution was stored at room temperature.

3.3.9   Wash buffer

The wash buffer was prepared by dissolving 0.5 ml Tween-20 in 1 L of 1X PBS. The solution was stored at room temperature.

3.3.10   Kreb solution

Kreb–Henseleit solution (Henseleit and Adolf Krebs, 1932) was prepared every morning of the experiment day with the following composition:

Table 3.5   Kreb–Henseleit solution composition

Components	g/L
Sodium Chloride	6.92
Sodium Hydrogen carbonate	2.1
D-Glucose	2.0
Potassium Chloride	0.35
Magnesium Sulphate	0.29
Potassium Phosphate Monobasic	0.16
Calcium chloride	2.5ml

To prepare the Krebs solution, 500 mL of distilled water was added to a 1 L bottle. Subsequently, each constituent of the Krebs solution was weighed on a scale according to Table 3.5 and added to 1 L of distilled water. The volume was adjusted to 1 L using distilled water.

3.4   *Lignosus rhinocerotis* polysaccharides (LRP) isolation and characterisation

Sclerotia powder of cultivated *L. rhinocerotis* was obtained from Ligno Biotech Sdn. Bhd. Official mushroom identification was performed by the Institute of Agricultural Research and Development, Malaysia, and mushroom authentication was conducted using the internal transcribed spacer (ITS) regions of their ribosomal RNA (Tan *et al.*, 2010).

3.4.1 Lignosus rhinocerotis extraction

For the extraction of LR, 42 g of TM02 sclerotia powder was weighed into a 43 × 123 mm Soxhlet thimble for hot aqueous extraction. The Soxhlet apparatus was subsequently assembled, and the extraction process was carried out using distilled water, heated at a temperature of 110°C in a Florence flask, with steam passing through the Soxhlet apparatus per cycle for 24 h. After each cycle, the LR extracts were collected as *Lignosus rhinocerotis* extract (LRE), concentrated using a rotary evaporator, freeze-dried, and stored at -20°C for further use.

The yields of LR extraction and polysaccharides isolation processes were calculated using the following equations:

$$\text{LRE yield} = \frac{\text{LR powder (g)} - \text{LR extract (g)}}{\text{LR powder (g)}} \qquad 1$$

$$\text{LRP yield} = \frac{\text{LR powder (g)} - \text{LR polysaccharides (g)}}{\text{LR powder (g)}} \qquad 2$$

3.4.2 *Lignosus rhinocerotis* polysaccharides isolation

LRP was fractionated from LRE through ion exchange chromatography using a DEAE-cellulose prepared following the manufacturer's instructions. Activated DEAE-cellulose was suspended in a 46 × 14 cm column. For each isolation cycle, 500 mg of the crude LRE extract was dissolved in 10 ml of distilled water and then added to the column. The flow rate of the column was adjusted to 1 ml/min and eluted with distilled water before being eluted with an increasing ionic gradient of NaCl solution (0.1M-1M). The eluents were collected in 10 ml test tubes and analysed for polysaccharides content using the phenol-sulfuric acid test. After each cycle, the column was washed with 200 ml of 1M NaCl and 500 ml of distilled water to remove impurities. High-concentration fractions were collected and concentrated at 45°C

using a rotary evaporator before further purification using size-exclusion chromatography.

The fractionated polysaccharides fraction was further purified using size exclusion chromatography on a 78 x 4.5 cm column. Approximately 20 ml of the fractionated fraction was loaded into a Sephadex column and eluted with double deionised water at a flow rate of 1 ml/min. After each cycle, the Sephadex G-100 column was washed with 200 ml of distilled water to remove impurities. Both column isolations were performed at room temperature. *Lignosus rhinocerotis* polysaccharides isolate (LRP) was freeze-dried and stored at 40°C until further use.

3.4.3   LRP carbohydrate and protein assay

Developed by Dubois et al. (1956) and Bradford (MM and Bradford, 1976), the Phenol-sulfuric acid and Bradford assays are commonly used in biochemical experiments to detect and quantify sugars and proteins. These assays are widely used in the field. In this study, these methods were employed to determine the levels and concentrations of carbohydrates and proteins in the LRP.

3.4.3(a)   Carbohydrate estimation in LRP using phenol-sulfuric acid procedure:

For the phenol-sulphuric acid procedure, a series of serial dilutions was prepared, ranging from 0.01 mg/ml to 0.2 mg/ml, using glucose standards of known concentrations.

$$200 \; \mu l \; _{standard/sample} + 400 \; \mu l \; _{phenol} + 200 \; \mu l \; _{water}, + 2 \; ml \; H_2SO_4 \qquad 3$$

The test tubes were left to stand for ten minutes before adding sulphuric acid. This was followed by vortexing for ten seconds at a medium speed. Subsequently, the tubes were placed in a water bath at temperatures ranging from to 25-30°C for 20 min. The spectrophotometer was then auto-zeroed using distilled water to obtain a blank

reading. Absorbance values were obtained by reading the samples in triplicates at a wavelength of 490 nm in the ultraviolet spectrum.

3.4.3(b)   Protein concentration estimation in LRP using Bradford procedure:

Briefly, the dilution series for bovine serum albumin (BSA) standard solutions (0.2 mg/ml to 2 mg/ml) was prepared using distilled water. For this purpose, Bradford reagent was freshly prepared, and 1 ml of Bradford reagent was added to an equal volume of the fractionated LRP solution. The mixture was then incubated in the dark for 5 min and gently vortexed for 10 s at a medium speed. Similarly, the autozeroing procedure for spectrophotometry was performed using distilled water to obtain a blank reading. Subsequently, the absorbance values were measured three times at a wavelength of 595 nm within the ultraviolet spectrum.

Standard curves were plotted using the absorbance values of the standard solutions relative to their corresponding sugar and protein concentrations. The LRP sugar and protein concentrations were estimated by comparing the absorbance values with the standard curves obtained from the glucose and BSA standard solutions.

3.4.3(c)   LRP monosaccharide composition analysis (HPLC)

This study adopted previous methodologies of qualitative and quantitative analyses for LRP according to Bushra et al. (2025). Derivatization was carried out prior to column separation, followed by reverse-phase high-performance liquid chromatography (RP-HPLC) to identify and quantify the monosaccharides present in the LRP.

LRP was initially subjected to hydrolysis using trifluoroacetic acid for 6 h, after which it was dried and dissolved in double deionised water. Subsequently, the LRP and monosaccharide standards were derivatised with 1-phenyl-3-methyl-5-pyrazolone (PMP) before injection into the HPLC column for separation, the HPLC parameters

for LRP monosaccharide characterisation are presented in Table 3.6. Equal volumes of hydrolysed LRP product or standards were combined with equal volumes of NaOH and PMP, and the mixture was vortexed and allowed to react for 120 min. The resulting mixture was separated using chloroform, and the aqueous layer was used for the HPLC analysis. HPLC analysis was performed using the following parameters:

Table 3.6   HPLC parameters for LRP monosaccharide characterisation

Column	Cosmosil 5C18-MS-II column (250 X 4.6 mm, I.D: 5 μm
UV detection	DAD at 254 nm
Monosaccharide standards	Mannose, ribose, rhamnose, glucose, galactose, xylose, arabinose and fucose
Duration	45 min
Mobile phase	Ammonium acetate buffer (A) and Acetonitrile (B)
Flow rate	1.0 mL/min
Oven temperature	30°C
Injection volume at	10 μL

3.4.3(d)   LRP total glucan and β-Glucan assay

The Megazyme β-Glucan Assay Kit (Yeast and Mushroom) was utilised to quantify LRP β-Glucan via spectrophotometry in accordance with the manufacturer's protocol. Specifically, exo-1,3-β-Glucanase plus β-Glucosidase enzymes (Bottle 1) were prepared through dilution with 200 mM sodium acetate, while the GOPOD enzyme was reconstituted using the GOPOD buffer provided in the kit.

The total glucan assay was conducted using 50 mg LRP, LRE, and kit control, hydrolysed with 2 ml cold H_2SO_4 12 M for 2 h on ice with intermittent vortexing. Further hydrolysis was performed in H_2SO_4 2 M for 2 h at 100°C in boiling water for complete hydrolysis of β-glucan, after which tube caps were loosened for cooling to room temperature. Subsequently, the content of each tube was transferred and diluted

to 100 ml using sodium acetate 200 mM and NaOH 8 M in labelled 100 ml volumetric flasks. Aliquots of 2 ml were centrifuged at 1300 rpm for 5 min, from which 0.1 ml was transferred to the bottom of test tubes in duplicate. These were treated with 0.1 ml exo-1,3-β-Glucanase + β-Glucosidase enzymes (Bottle 1) to hydrolyse any remaining glucans. To all tubes, including the standards, 0.1 ml sodium acetate 200 mM and 3 ml GOPOD reagent were added to samples and controls. The tubes were vortexed and incubated in a 40°C water bath for 60 min.

The α-glucan assay was also conducted using 50 mg LRP, LRE, and kit control. Tubes were solubilised with sodium hydroxide 1.7 M and placed in an ice bath with magnetic stirring for 20 min to dissolve the phytoglycogens. Hydrolysis was then performed using amyloglucosidase plus invertase enzymes and 0.05 mL of Trehalase (Bottle 7). Aliquots of 2 ml were centrifuged at 1300 rpm for 5 min, from which 0.1 ml was transferred to the bottom of test tubes in duplicate. These were treated with 0.1 ml sodium acetate 200 mM and 3 ml GOPOD reagent, followed by incubation of the tubes at 40°C for 60 min.

In both total and α-glucan assays, optical density absorbance was measured using a cuvette spectrophotometer at 510 nm against a blank. Readings were compared to kit standard D-glucose and blank solutions. The samples' total glucan, alpha-glucan, and beta-glucan were calculated utilising a Mega-Calc™ Excel spreadsheet. The β-glucan content was determined by subtracting the α-glucan from the total glucan content and the percentage concentration (w/w) was calculated using the formular below. All determinations were performed in triplicate.

$$\text{Total } \beta \text{ glucan (\% w/w)} = \frac{\text{Total glucan} - \text{Total } \alpha-\text{D}-\text{glucan}}{\text{Total glucan}} \times 100\% \qquad 4$$

3.5 LRP inhalation formulation and characterization

3.5.1 LRP inhalation formulation

In this study, two inhalation forms, DPI and nebulization solution, were attempted for LRP.

3.5.1(a) LRP Dry Powder Inhalation (DPI) Formulation

The spray-drying method was tested to achieve inhalable aerodynamic powder aerosols. The Next Generation Impactor (NGI) was used to characterise the aerodynamic properties of the intended formulations.

The LRP DPI formulation was first formulated in dry powder inhalation form using the spray drying method. For the initial approach, the LRP solution was spray dried without any excipients to determine its drying behaviour. The spray drying parameters used to dry the solution are detailed in Table 3.7.

Table 3.7   LRP spray drying parameters

Parameters	Conditions
Inlet temperature	120°C
Outlet temperature	90°C
Spray gas flow	60 L/min
Pump	5%
Aspirator	100%
Feed flow rate	2 ml/min
Solution concentration	2 mg/ml a) 200 mg LRP + 200mg lactose in 200 mL distilled water b) 400 mg LRP in 200 mL distilled water

3.5.1(b) LRP nebulization solution

The suitability and feasibility of delivering the LRP using a nebuliser in a nebulisation solution form were assessed. The nebulisation solution was prepared by dissolving 80 mg of freeze-dried LRP powder in 20 ml of distilled water (4 mg/ml). Each nebulisation uses only the prepared LRP solution from the freeze-dried powder.

The quantification of polysaccharides in the LRP solution was performed to determine amount of polysaccharides in the sample. The phenol-sulfuric acid test (Dubois *et al.*, 1956) was used for LRP quantification, followed by absorbance reading using a UV spectrophotometer at 490 nm wavelength. Using LRP standards, a linear standard calibration curve was made at different concentrations in three replicates.

3.5.2   LRP inhalation characterization

The study of the inhalation characteristics of the LRP solution for nebulization was carried out using the Next Generation Impactor (NGI) in accordance with the protocol outlined in General Chapter 1601 of the United States Pharmacopoeia. The aim was to evaluate the aerodynamic properties of the nebulised mist. To begin, the NGI apparatus was pre-cooled at a temperature of 5°C for 90 min and assembled with the internal terminal filter in place, with the pre-separator removed. The mouthpiece of the nebulizer was attached to the NGI induction port via a silicon rubber adaptor, then aerosols were generated from the nebuliser compressed air and introduced into the NGI. The airflow through equipment was adjusted to a flow rate of 15 L/min using a vacuum pump and flow meter (Copley 4043: DFM 2000). The flow meter was then removed, and the nebuliser mouthpiece was inserted into the mouthpiece adaptor, which was attached to the induction port. Finally, the compressor for the nebuliser was switched on, and nebulization was performed.

Nebulization of the LRP solution was carried out using a RossMax N80 jet nebuliser connected to the NGI induction port with the aid of an adaptor. The maximum stage volume capacity (T_0) was established to prevent overflow of the stages. A solution of 6 ml of LRP was nebulised to complete dryness at a flowrate of 0.3 ml/min (Figure 3.2). Following this, the nebuliser bottle, induction port, stages 1-

7, and micro-orifice filter were cleaned with distilled water, and the deposited LRP concentration was estimated.
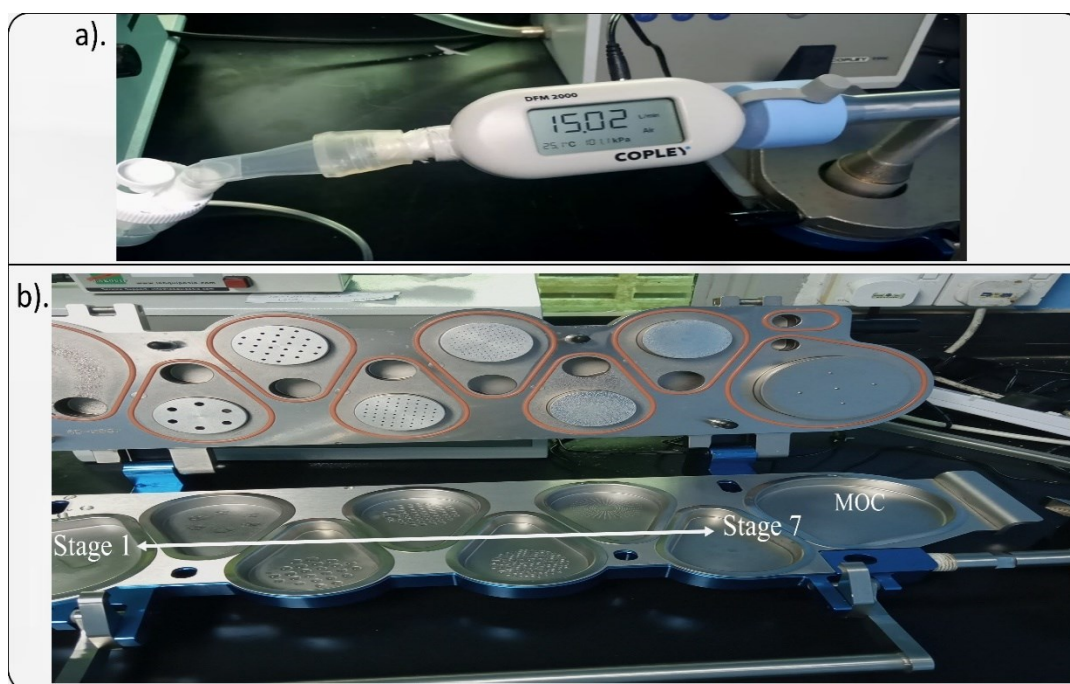
Figure 3.2   LRP nebulization on NGI: a). NGI airflow rate setting using vacuum pump and flow meter; b). nebulised LRP deposition along the NGI stages 1-7 and MOC.

The aerodynamic particle size distribution (APSD) parameters of nebulised LRP were determined using the following equations, and the values are reported as the mean ± standard deviation of three experiments:

a. Nebulisation Rate:

$$\text{Nebulisation Rate} = \frac{\text{Nebulized volume (mL)}}{\text{Nebulization time (min)}} \times 100 \qquad 5$$

b. Mass balance (MB)

$$\text{Mass balance (MB)} = \frac{\text{Total amount of drug collected in NGI and nebuliser (mg)}}{\text{Intial amount of drug in nebulised solution (mg)}} \times 100 \qquad 6$$

c. Emitted Fraction (EF)

$$\text{Emitted Fraction (EF)} = \frac{\text{Total amount of drug collected in NGI(mg)}}{\text{Total amount of drug collected in NGI and nebuliser (mg)}} \times 100 \qquad 7$$

d. **Geometric Standard Deviation (GSD)**

$$\text{GSD} = \sqrt{\frac{d_{84.1}}{d_{15.9}}} \qquad \text{or} \qquad \left(\frac{d_{84}}{MMAD}\right) \qquad\qquad 8$$

$d_{84.1}$: Particle diameter intercepts at cumulative mass 84.1%
$d_{15.9}$: Particle diameter intercepts at cumulative mass 15.9%
MMAD: Mass median aerodynamic diameter

Precautionary measures were taken during the procedure, including proper calibration of the equipment, adequate device cooling, proper positioning of the impactor to adequately collect particles, and consistent airflow during testing.

3.6 Anti-asthmatic effect of LRP in ovalbumin asthma mice model

3.6.1 Animals holding and preparation

Female Balb/c mice, aged 6-8 weeks and weighing 20–25 g, were obtained from the Universiti Sains Malaysia (USM) Kelantan Kampus, Malaysia. These mice were acclimatised for 7 days prior to the commencement of the study and housed in polystyrene cages in an air-controlled room at the Animal Research and Service Centre (ARASC) of the Universiti Sains Malaysia Health Campus, Kubang Kerian Kelantan. The facility provided 12-hour light-dark cycles, and water and pellets were provided to the animals ad libitum. The study protocol was approved by the Institutional Animal Care and Use Committee of Universiti Sains Malaysia (USM/IACUC/2021/(128)(1139)). The experimental design of LRP anti-asthmatic study in OVA-challenged mouse model is described in Figure 3.3.

Prior to the commencement of the asthma study, a pilot study was conducted to determine the optimal concentration and duration of LRP inhalation that improve specific asthma pathophysiology-related parameters, including inflammatory cells counts in BALF and lung inflammatory cells infiltration in OVA-challenged asthmatic mice. The pilot study evaluated three different LRP nebulisation solution concentrations of 4mg to 40mg and durations, ranging from 15 to 30 min for 7 days

which were given once a day treatment (days 21-27), with Dexa group receiving 7

days dexamethasone treatment 3mg/kg intraperitoneally (IP).
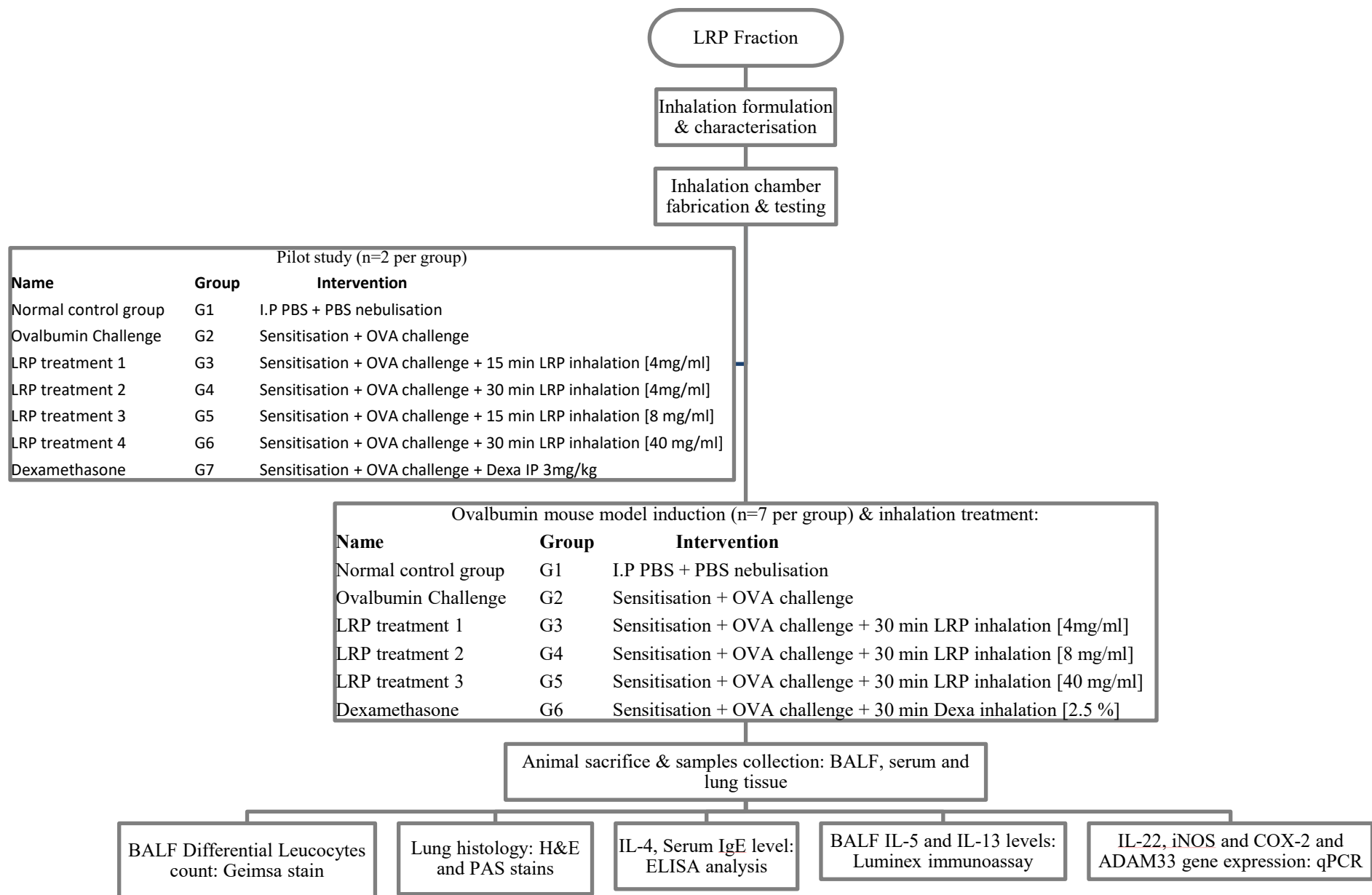
Figure 3.3   Experimental design of anti-asthmatic study

3.6.2   Inhalation chamber

The inhalation chamber utilised in this study was modelled following Kaur et al. (2020), who described a simple, reliable, and cost-effective nose-only inhalation chamber for rodents that can be used to nebulise drugs for preclinical experimental studies. Nebulised air is delivered directly and continuously from the central chamber to mouthpieces, creating an aerosol cloud for rodents to inhale. *In vivo* studies demonstrated the successful exposure of mice to nebulization using the developed prototype (Kaur *et al.*, 2020).

For this study, a central inhalation chamber was devised utilising a 5-way splitter tube, with one end connected to a conducting tube from the nebuliser and the other four ends each attached to a 5 cm long and 3 cm diameter urine bottle serving as a mouthpiece. 50 ml centrifuge tubes were used as mouse restrainer connected to the urine bottles. Mice were positioned in the holding chamber with cotton wool, allowing only sideward movements or rolling but not backward turning (Figure 3.4).
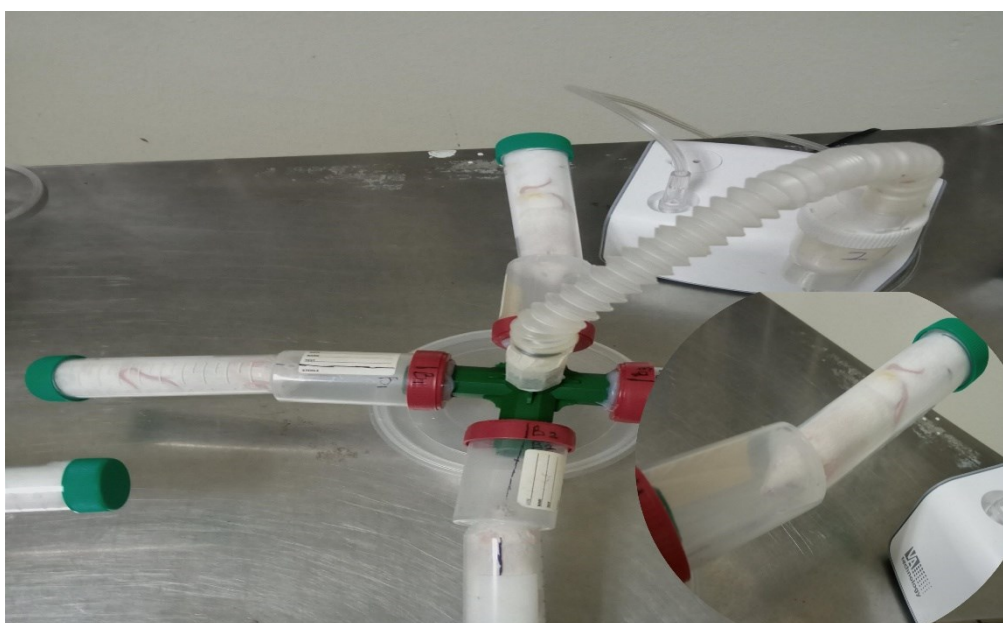
Figure 3.4   The mice inhalation chamber

3.6.3   Ovalbumin-induced asthmatic mouse model

Immunological parameters in mouse models of asthma exhibit sexual dimorphism, with female mice typically having higher Th2 inflammation than male mice, female mice have significantly higher OVA-specific IgE during sensitization (Chiarella et al., 2023), long-term OVA-challenged airway remodelling and higher OVA-specific immunoglobulin E (IgE) and serum IgA levels (Takeda et al., 2013). These increased effects are reported to be influenced by 17β-oestradiol-mediated CD103+ dendritic cells that promote female-predominant Th2 cytokine production (Masuda et al., 2018).

For the main study, 42 female BALB/c mice were randomly divided into six groups of seven mice per group (n=7 per group). The mice were sensitised by intraperitoneal (I.P) injection of a 0.2 ml mixture containing 100 μg ovalbumin and 4 mg of aluminium hydroxide [Al(OH)$_3$] as adjuvant in 1x PBS solution on days 0, 7, and 14 (Jin *et al.*, 2019; Kim, Song and Lee, 2019; Song *et al.*, 2023). After sensitisation, the mice were challenged with 1% OVA aerosols with a jet nebuliser for 20 min on days 21-27 once daily. The normal control group was injected and nebulised PBS alone instead of OVA. The OVA-challenged asthma protocol is described in Figure 3.5.

Considering the established dosage range for nebulizer feeds in inhalation studies, with doses ranging from 1 mg/mL for potent compounds to 40 mg/mL for less potent compounds (Phillips et al., 2017), and that previous LRP inhalation deposition study utilized a nebulizer feed concentration of 4 mg/mL LRP for NGI deposition quantification, which also falls within the reported concentration range for animal inhalation nebulization experiments. Therefore, 4-40 mg/mL concentration range was selected for the LRP anti-asthma study in an OVA-challenged asthma mouse model.

It was determined that the 4-40 mg/mL range is a suitable concentration range for the study, encompassing for both potent and less potent compounds. This dose range is consistent with the doses utilized or reported in nebulization studies (Song *et al.*, 2016; Sarhan *et al.*, 2018; Adorni *et al.*, 2019; Chang *et al.*, 2019, 2020) and demonstrated efficacy in the LRP anti-asthma pilot study based on the DLC and H&E results.

Furthermore, given the established role of inhaled corticosteroids in asthma management, the nebulizer-based administration of both the experimental compound and dexamethasone approach was deemed appropriate, aligning with the administration route of the experimental compound in this study. Inhaled dexamethasone (20 mg/ml) administered to male guinea pigs (200–300 g) inhibited OVA-induced inflammatory responses more effectively than LPS alone or combined OVA and LPS-induced asthma (Lowe *et al.*, 2017). Consequently, inhaled dexamethasone 2.5% in PBS was selected as the positive control to validate the study methodology and to assess the efficacy of the LRP against a known standard care.

Nebulise inhalation treatment with LRP was given one hour after OVA challenge, whereas the normal group was administered PBS solution. The choice of LRP nebulization duration and experimental dose in this study was determined by the outcomes of preceding optimisation pilot study. Twenty-four hours after the last challenge and treatment, the mice were sacrificed on day 28 using pentobarbitone (200 mg/kg).

day 0   7   14   21, 22, 23,24,25,26,27   28

Sensitisation   2nd sensitisation   3rd sensitisation   Sacrifice
100µg OVA + 4mg Al(OH)₃

1% OVA challenge
± LRP inhalations
± Dexamethasone inhalation
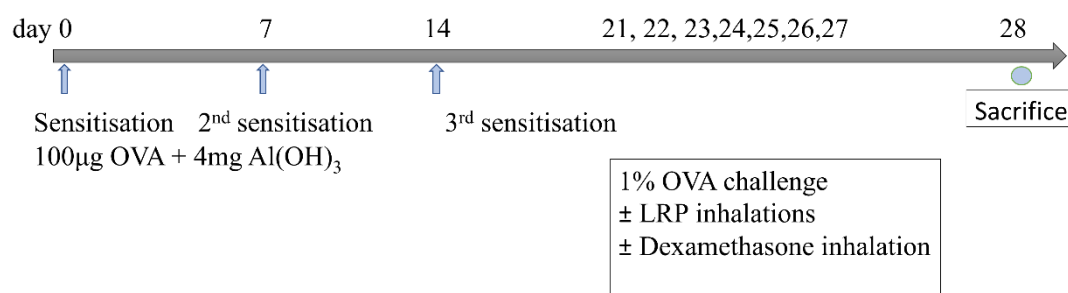
Figure 3.5   OVA-challenged model protocol

3.6.4   Samples collection

3.6.4(a)   Serum collection

Twenty-four hours after the final treatment, the mice were anaesthetised, longitudinal incision was made along the mediastinum and 0.5-1 ml of blood was collected via cardiac puncture. This blood was allowed to clot for at least three hours at room temperature. Subsequently, the blood was centrifuged at 2000g for 10 min at 4°C. The resulting serum was carefully extracted and stored at -80°C for IgE ELISA analysis.

3.6.4(b)   Bronchoalveolar lavage fluid (BALF) collection

Following the mice sacrifice, BALF was obtained from the trachea using an 18G cannula by instillation and aspiration with 0.4 ml of 1% fetal bovine serum in PBS, three times. The BALF was then transferred into a 1.5 ml centrifuge tube and centrifuged at 2000g for 5 min at 4°C. The resulting supernatant was collected and stored at -80°C for the analysis of Th2 cytokines, while the BALF pellet was used for differential leucocyte count.

3.6.4(c)   Lung tissue collection

Following the collection of BALF, the lungs of the mice were carefully removed via a midline incision, cutting through the rib cage along the medio sternum. The left lung lobe was then washed with PBS and fixed in 10% formalin for histological staining, while the other lung lobes were first washed with PBS solution and placed in an RNA stabilising reagent (RNA-hold, TransGen) for gene expression analysis.

3.6.5   Histopathological analysis of the lungs tissue

Following sacrifice, lung tissues were fixed with 10% formalin overnight. Subsequently, the entire left lung lobe was placed in a tissue cassette for processing. The lung tissues were placed in 10% formalin for one hour, followed by graded dehydration, clearing, and paraffin wax infiltration or impregnation. A series of procedures were performed to clearing the tissue for histological examination. Initially, the tissues were placed inside tissue cassettes and immersed in 50% ethanol and xylene, followed by two separate xylene treatments, each step for one hour duration. The subsequent infiltration or embedding phase involved the immersion of the tissues in paraffin wax for one hour. This process ensured that the tissues maintained their structural firmness and integrity, and could be sectioned consistently. Upon completion, lung tissue samples were embedded in paraffin blocks and sectioned using a microtome. Paraffin-embedded tissue sections were trimmed to a thickness of 3-5 μm on microscope slides using a microtome.

3.6.5(a)   BALF differential leucocyte count (DLC)

BALF pellets were washed twice by re-suspending them in 200 μl of PBS and undergoing centrifugation in a microcentrifuge before discarding the supernatant. The cells were then resuspended in 100 μl of PBS, and a drop of approximately 30-50 μl

of the resuspended cells was smeared on clean microscope slides. The slides were fixed with methanol for 2 min, air-dried at room temperature (RT), and stained with diluted Giemsa stain (1:19 in PBS) for 8-10 minutes. Then 200 inflammatory cells were identified by their standard morphological criteria at x100 magnification using a light microscope under oil immersion. The relative DLC of various white blood cells was calculated as a percentage of total leucocytes counted.

3.6.5(b)   Haematoxylin and Eosin (H&E) staining

H&E staining of lung tissue sections was carried out in accordance with the following steps, the sequence and duration of which was determined after optimisation runs (Table 3.8).

Table 3.8   H&E Staining protocol

Reagent	Condition
Slide warming	55^0C 60 -90 min
Xylene I	5 min
Xylene II	5 min
100% alcohol	2 min
90% alcohol	2 min
80% alcohol	2 min
70% alcohol	2 min
50% alcohol	2 min
Tap water (flow)	5 min
Haematoxylin	15 min
Tap water (flow)	5 min
1% acid alcohol (or few dips)	10 sec
Tap water (rinse)	30 sec

Table 3.8 Continued

Reagent	Condition
Ammonia water	10 sec
Tap water (flow)	5 min
Eosin	5 min
100% alcohol (dip slide one by one)	30-60 sec
100% alcohol (dip slide one by one)	30-60 sec
Xylene I	2 min
Xylene II	2 min
DPX and coverslip mount	

Lung tissue sections were hand-picked from a water bath, transferred to labelled glass slides, and allowed to desiccate for 24 h. Subsequently, the dried slides were warmed by placing them on a hot plate for one hour at 55°C. Deparaffinization was performed by immersing the slides in two changes of xylene for 5 min to remove paraffin. The slides were then rehydrated in five decreasing ethanol concentrations, from absolute ethanol to a 50% ethanol solution. Tissue slides were fully rehydrated in tap water for 5 min. Haematoxylin staining was conducted by immersing the slides in haematoxylin stain for 15 min to stain the nuclei blue, followed by rinsing with several changes of water. The slides were then immersed in 1% acid alcohol for 10 s for differentiation and to remove excess haematoxylin stain, followed by rinsing with water for 5 min. Blueing was performed in ammonia water for 10 s to neutralise the acid and turn the nuclei blue, followed by rinsing with flowing tap water for 5 min. Eosin staining was performed by immersing the slides in eosin Y-solution aqueous for 5 min to stain the cytoplasm pink. Finally, the tissue slides were dehydrated with two changes of absolute alcohol for 1 min and cleared with two changes of xylene for 2

min. The slides were then mounted with DPX and cover slipped and avoiding air bubbles. The slides were then dried and stored in slide boxes.

Analysis of the H&E-stained slides (n=7 per mouse) for airway tissue structure and morphometric features of peribranchial and perivascular inflammatory cell infiltrates on whole sections was conducted. Photographs were taken using a bright light microscope (Olympus, BX41) at 10x and 40x magnifications. The number of cell layers surrounding the vessels or bronchioles was considered when scoring the tissue slides, and this method was based on the work of (Myou *et al.*, 2003; Kim, Song and Lee, 2019). The hotspot area of the lung sections was then assigned a score on a scale of 0 to 4, as follows:

Table 3.9   Lung inflammatory cells infiltration scoring

Score	Inflammatory Cell Infiltration
0	Normal
1	Few inflammatory cells
2	A ring of inflammatory cells 1 cells layer deep
3	A ring of inflammatory cells 2–4 cells deep
4	A ring of inflammatory cells of >4 cells deep

(Adopted from Myou et al. (2003) and Kim, Song and Lee (2019)).

3.6.5(c)   Periodic-acid Schiff (PAS) staining

Similarly, PAS staining of lung tissue sections was performed in accordance with the following steps, the duration of which was determined through optimisation runs (Table 3.10). Lung tissue sections were prepared, air-dried, warmed, deparaffinized, and rehydrated, as described in the aforementioned H&E procedure. Tissue rehydration was performed before immersing the slides in periodic acid for 5 min, followed by rinsing with several changes in water. The slides were then immersed

in Schiff's reagent for 15 min and rinsed with warm water for 5 min. Nuclei staining

was performed by immersing the slides in haematoxylin for 1 min, and the nuclei were

Table 3.10   PAS staining protocol

Reagent/condition	Condition
Slide warming	55^0C 60 -90 min
Xylene I	5 min
Xylene II	5 min
100% alcohol	2 min
90% alcohol	2 min
80% alcohol	2 min
70% alcohol	2 min
50% alcohol	2 min
Tap water (flow)	5 min
Periodic Acid solution	5 min
Tap water rinse	Several changes
Schiff's reagent	15 - 20 min
Warm water flow	5 min
Hematoxylin counterstaining	10-30 sec
Tap water (flow)	5 min
80% alcohol	30 sec
90% alcohol	30 sec
100% alcohol	30 sec
Xylene III	1-2 min
Xylene IV	1- 2 min
DPX and cover slip mount	

blued by immersing the slides in ammonium water for 1 min, followed by rinsing with flowing tap water for 1 min. Finally, the tissue slides were dehydrated, immediately mounted with DPX, cover slipped, dried, and stored in slide boxes.

Analysis of PAS-stained slides (n=7 per mouse) for airway tissue structure and morphometric features of goblet cell hyperplasia in whole sections was performed. The percentage of stained goblet cells in the airway epithelium was assessed as an indicator of mucus production, which was denoted as goblet cell hyperplasia in the airway epithelium. The slides were evaluated and graded on a semi-quantitative basis, as previously described (Mäkelä *et al.*, 2002; Myou *et al.*, 2003; Kim, Song and Lee, 2019) (Table 3.11). Photographs were taken using a bright light microscope at 10x and 40x magnifications.

Table 3.11   Lung goblet cells hyperplasia scoring

Score	Percentage of PAS positive cells
0	< 5 %
1	5 - 25%
2	25 - 50%
3	50 - 75%
4	>75%

(Adopted from Myou et al. (2003) and Kim, Song and Lee (2019)).

Assessment of airway inflammation in both H&E and PAS tissue stains was performed by two independent reviewers using a double-blind scoring method. The pathologist validated the findings by examining a random selection of 20% slides. The mean semi-quantitative scores of the airway sections in the lungs for each experimental group were calculated.

3.6.6 Th2 cytokine analysis from BALF using Luminex multiplex immunoassay

The levels of interleukin-5 (IL-5) and interleukin-13 (IL-13) in BALF were determined using the Mouse Magnetic Luminex Screening Assay 4-plex kit. The kit reagents and samples were thawed to room temperature and centrifuged, and the provided standards were reconstituted according to the Standard Value Card. The standards and samples were diluted at a ratio of 1:2 using calibrator diluents. The standards were serially diluted to achieve a 2-fold increase in cytokine concentration. Fifty microlitres of the diluted microparticle cocktail from both samples and standards was loaded into a 96-well plate, and the assay was conducted in accordance with the manufacturer's instructions, involving several steps of a Biotin-Antibody cocktail, Streptavidin-PE, and incubation on a horizontal microplate shaker. Between each step, the plate was washed with a magnetic washer in washing steps.

Each sample was tested in triplicate on a Luminex 200 system, and the data were analysed by fitting a five-parameter curve using the xPonent software (Luminex, Inc., Austin, TX, USA).

3.6.7 Serum immunoglobulin-E (IgE) and BALF IL-4 ELISA assay

The concentration of total IgE in the serum and IL-4 in BALF were determined using a mouse IgE BioLegend and IL-4 Quantikine™ ELISA kits, following the manufacturer's instructions. Briefly, a 96-well ELISA plate was coated with 100 μl of diluted capture antibody and incubated overnight at 4°C. The plate was subsequently washed four times with washing buffer and then blocked with 200 μl of assay diluent A for one hour at room temperature with shaking. After blocking, 100 μl of diluted standards and serum samples (1:100) and BALF were added to the respective wells and incubated for two hours at room temperature with shaking. The plates were then washed with wash buffer four times, and 100 μl of diluted detection antibody was

added to each well and incubated for one hour with shaking. Following four washes, 100 µl of diluted avidin-HRP solution was added and incubated for 30 min. Subsequently, five washes were performed, and 100 µl of freshly mixed substrate solution was added to each well and incubated in the dark for 20 min. Finally, 100 µl of stop solution was added to stop the reaction in each well. Optical density (OD) was measured at 450 nm using a microplate reader and corrected by subtracting the 570 nm readings. IgE and IL-4 levels were extrapolated from the OD absorbance standard curve.

3.6.8 Inflammatory gene expression

The RT-qPCR results of this study were reported according to The MIQE Guidelines" (MIQE 2009).

3.6.8(a) Experimental design and sample processing

A true experimental design was employed, with random allocation of mice into six distinct groups, as outlined in **Error! Reference source not found.**. Lung tissue s amples were obtained from each mouse, placed in RNA preservative (RNA-hold, TransGen), and stored at -80°C. These samples were maintained for one month prior to RNA extraction. It is important to note that the samples were not fixed in formaldehyde before being placed in the RNA preservative. Mouse lung tissue (100 mg) was placed in a chilled mortar and ground into micropieces using a pestle and liquid nitrogen. The resulting tissue was placed into a 1.5-milliliter centrifuge tube.

RNA extraction was performed in a laminar flow cabinet that was cleaned and decontaminated with RNase Quiet Spray Surface Decontaminant (Nacalai Tesque). One millilitre of TRIzol was added to each centrifuge tube and mixed with the tissue samples by gentle inversion. Subsequently, 200 µL of chloroform was added to each tissue sample, which was mixed and incubated for 2-5 minutes at room temperature.

RNA was precipitated using 500 µL isopropanol, incubated for 10 min, and then centrifuged at 12000 g for 10 min at 4°C. The supernatant was discarded, and the pellet was resuspended in 1 ml of 75% alcohol, followed by a 5-minute centrifugation at 7500 g at 4°C.

The isolated RNA pellets were resuspended in 40 µL RNase-free water by pipetting up and down and placed on a 55°C heat block for 10 min to rehydrate and completely dissolve the pellet. The extracted RNA was stored at -80°C for cDNA synthesis the following day, and 5 µL aliquots were taken for nanodrop RNA concentration and purity estimation. The absorbance at 260 nm provided the total nucleic acid content, whereas the absorbance ratio at 280 nm determined the sample purity (A260/A280).

3.6.8(b) Reverse transcription

cDNA synthesis was performed using the HiScript III 1st Strand cDNA Synthesis Kit VazymE, according to the manufacturer's instructions. Briefly, the kit components were thawed to room temperature, mixed, and centrifuged. Master mix components, including RNase-free water, HiScript Enzyme Mix, Oligo (dT)23VN, and random hexamers, was prepared. Equivalent amounts of 1 ng of RNA template from each sample were then added to the respective 100 µL tubes to make up to a volume of 20 µL. The tubes were then placed in a heat block at 25°C for 5 min, 50°C for 15 min, and 85°C for 2 min. The synthesised cDNA samples were stored at -20°C for downstream qPCR.

3.6.8(c) qPCR oligonucleotides and primer sequence

Prior to commencing the qPCR protocol, the primers were validated and optimized using a two-fold serial dilution of 100 ng of cDNA template copies per microliter across five distinct concentrations, including the NTC control. Primer

amplifications were conducted in duplicate using calibrator sample (OVA group) for the primer optimization.

The RT-qPCR analysis focused on the following genes, and their respective primer sequences are provided in Table 3.12.

Table 3.12   qPCR Primer sequences used

Gene	Primer sequence
IL-22 Mouse qPCR Primer	Forward: GCTTGAGGTGTCCAACTTCCAG Reverse: ACTCCTCGGAACAGTTTCTCCC
ADAM33 Mouse qPCR Primer	Forward: CTTGGAAGCAGGAGAAGAGTGC Reverse: CAGCAATCACCGTGGGCACATT
iNOS Mouse qPCR Primer	Forward: GAGACAGGGAAGTCTGAAGCAC Reverse: CCAGCAGTAGTTGCTCCTCTTC
COX-2 Mouse qPCR Primer	Forward: ACC AGC AGT TCC AGT ATC AGA Reverse: CAG GAG GAT GGA GTT GTT GTA G
GAPDH Mouse qPCR Primer	Forward: ATG TGT CCG TCG TGG ATC TGA C Reverse: AGA CAA CCT GGT CCT CAG TGT AG

GAPDH was used as the reference gene. The primer sequences were adapted from OriGene mouse primer sets (https://www.origene.com/catalog/gene-expression/qpcr-primer-pairs). Oligonucleotides were supplied by Integrated DNA Technologies (Science Park II, Singapore) with standard desalting purification.

3.6.8(d)   qPCR protocol

In this study, the RT-qPCR method was performed using Luna® Universal qPCR Master Mix. The components of the kit were thawed to room temperature Primer pairs were initially dissolved in RNase-free water and diluted to 7 μM before incorporation into the master mix. The reaction master mix was prepared in a 1.5 ml tube, and 19 μL of the reaction master mix was dispensed into individual PCR tubes. Each primer optimisation was conducted with five dilution cDNA concentrations (100

– 6.25 ng cDNA) to determine the optimum cDNA template concentration; consequently, 50 ng cDNA template was subsequently used for qPCR runs.

The reaction mixtures were prepared according to the kit specifications as listed in Table 3.13.

Table 3.13   Volume and concentration of qPCR reaction mixtures.

Components	Volume/reaction	concentration
Luna® Universal qPCR Master Mix	10 µl	1x
Forward Primer	1 µl	0.35 µM
Reverse primer	1 µl	0.35 µM
RNase water	7 ul	-
cDNA template	1 µl	50 ng per reaction
Total reaction volume	**20 µl**	

Subsequently, 50 ng of the cDNA template was added to each PCR tube containing the reaction master mix to achieve a total volume of 20 µL per qPCR tube. NTC tubes containing a master mix without a cDNA template were also prepared. All tubes were prepared in duplicates. The qPCR tubes were briefly vortexed and centrifuged to remove air bubbles and then placed in a Bio-Rad real-time cycler. The cycler program was set up in accordance with the specifications listed in Table 3.14. The CFX96 machine was switched on, and the CFX Maestro software was initiated on a computer connected to the Bio-Rad thermocycler. From the Run set-up menu, the user-defined protocol was set up (Table 3.14), with 1 min initial activation at 95°C, 15 s denaturation, and 30 s extension at 60°C, with plate reading and melting curve analysis configured. The plate layout was configured with each well labelled according to the sample ID, SYBR green fluorophore, sample type, target names, and biological group in two technical replicates. The qPCR tubes were carefully positioned in the machine to ensure the correct orientation.

Table 3.14   qPCR thermocycler program used.

Step	time	Temperature
PCR Initial Activation	1 min	95^0C
Denaturation	15s	95^0C
Combined Annealing/Extension	30s	60^0C
Number of Cycles	**43**	
	Plus Melting Curve Analysis	

3.7   Effect of LRP on guinea pig trachea contractility

This study investigated the effect of LRP on three airway receptors, muscarinic, histamine, and beta receptor responses, using isolated guinea pig tracheal (GPT) rings in a water bath myograph. To determine the inhibitory concentrations 50% (IC_{50}) of the respective receptor antagonists, atropine, cimetidine, and the beta-agonist salbutamol, the agonist-antagonist Dose-Response Curve (DRC) was analysed and compared with the effects of LRP. Additionally, the involvement of the beta receptor in LRP was tested in GPT rings preincubated with propranolol. The experimental design for the effect of LRP on guinea pig trachea contractility is described in Figure 3.6.

```
                    ┌─────────────────┐
                    │  LRP Fraction   │
                    │    Isolation    │
                    └────────┬────────┘
                    ┌────────┴────────┐
                    │ Myograph Set-up &│
                    │   callibration   │
                    └────────┬────────┘
               ┌─────────────┴─────────────┐
               │ Guinea Pig Dissection &   │
               │     trachea Isolation     │
               └─────────────┬─────────────┘
               ┌─────────────┴─────────────┐
               │ Cleaning, preparation of  │
               │  GPT rings and Mounting   │
               └─────────────┬─────────────┘
               ┌─────────────┴─────────────┐
               │ Agonist Dose Response     │
               │ Study (Carbachol, Histamine)│
               └─────────────┬─────────────┘
```
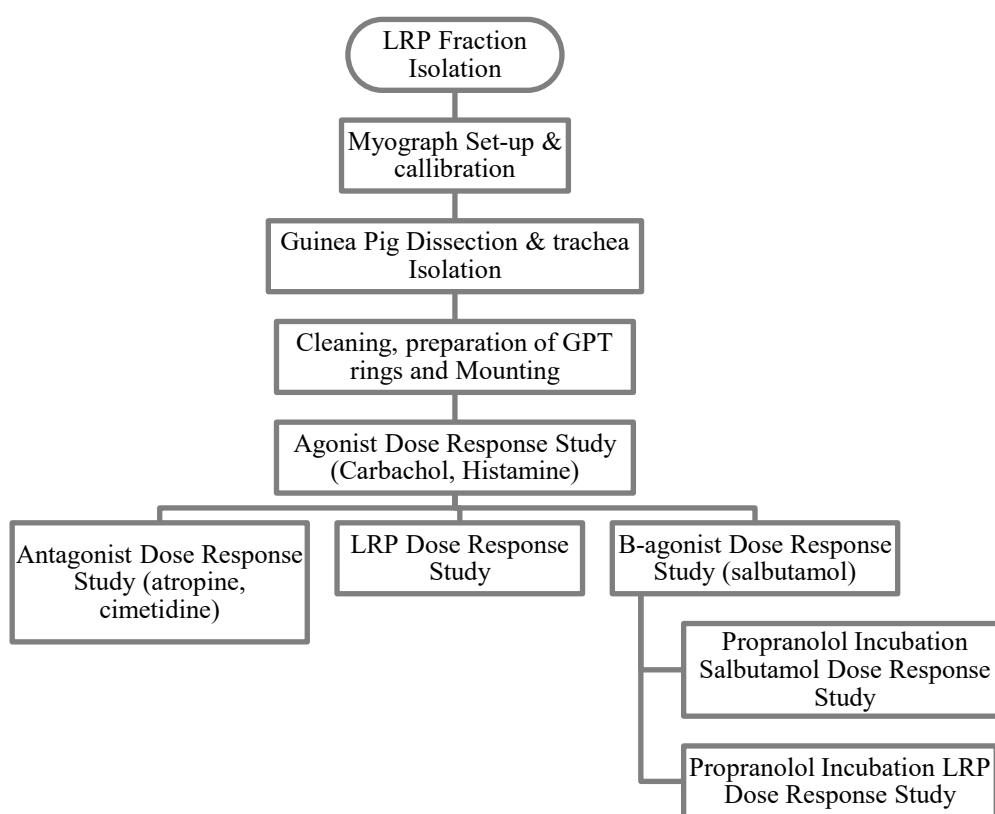
Figure 3.6   Experimental design of the GPT airway receptor study

Antagonist Dose Response Study (atropine, cimetidine)

LRP Dose Response Study

B-agonist Dose Response Study (salbutamol)

Propranolol Incubation Salbutamol Dose Response Study

Propranolol Incubation LRP Dose Response Study

3.7.1 Animals

3.7.1(a) Animal holding

Seven (7) short-haired albino male guinea pigs weighing 300–400 g was used in this study. The animals were housed in polypropylene cages at the Animal Research and Service Centre (ARASC), Universiti Sains Malaysia Health Campus, Kubang Kerian Kelantan. The animals were kept in a stable 12-hour light-dark cycles and fed on standard feed pallets (Raspberry, Malaysia) with unlimited access to clean drinking water. The animal experimental protocol was approved by the Institution Animal Care and Use Committee of Universiti Sains Malaysia (USM/IACUC/2017/(109)(878)).

3.7.1(b) Animal dissection

Guinea pigs were euthanised with sodium pentobarbital 100mg/kg intraperitoneal (IP) injection. After passing out GPs were immediately dissected with

a midline incision in the neck to expose the trachea, about 2cm of the cervical trachea was isolated and carefully removed, transferred into pre-warmed Kreb–Henseleit's solution for further cleaning. Excess fat and connective tissues were removed from the GPT under a dissecting microscope and sectioned into 2-3 tracheal ring-length sections.

3.7.2 Myograph preparation

3.7.2(a) Myograph organ bath

Prior to tissue mounting, myograph calibration was always performed using a 2 g standard weight and unit conversion to express muscle tension in grams (g). Two ending trachea rings were discarded from the dissected GPT sections, and the remaining middle rings were sectioned into 2-3 ring lengths per section. These sections were then carefully mounted on myograph pins in each chamber. The organ bath used for this study was a four-chamber multichannel myograph (DMT-620M; Danish Myo Technology A.S, Denmark), each chamber preloaded with 10 ml Kreb–Henseleit's solution continuously aerated using carbogen gas, with the myograph heating system turned on at 37°C.

GPT relaxation and contraction changes were recorded using a force transducer data acquisition system (PowerLab, AD instrument) and recorded using the data acquisition software LabChart (LabChat 7, AD instrument) on a desktop computer system (Hewlett Packard). The LRP airway contractility experiment protocol on GPT rings was described in Figure 3.7.
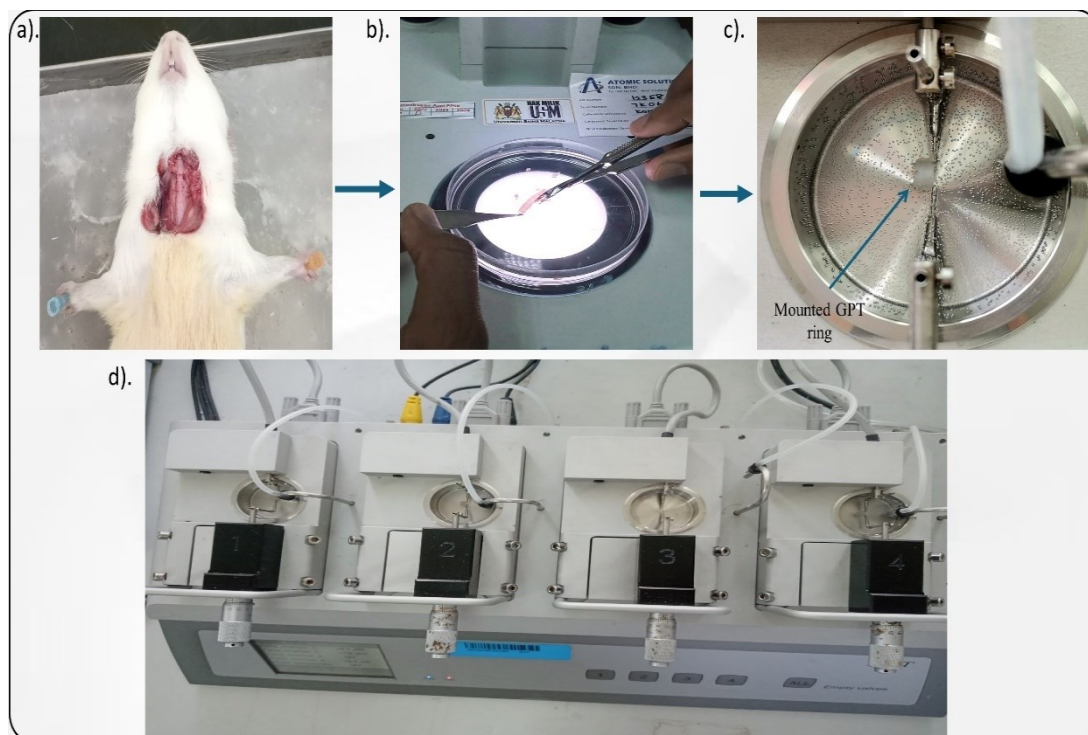
Figure 3.7   Airway contractility experiment protocol: **a)** Isolation of guinea pig trachea (GPT) **b)** Cleaning and removal of excess fat and connective tissue under a dissecting microscope. **c)** The mounting of GPT rings to the pin in the myograph chamber **d)** Multichannel myograph used to detect changes in ASM tone.

3.7.3   Myography experiment protocol

After setting a 2 g resting tension and allowing for tissue normalisation, GPT rings were evaluated for tissue viability twice in response to 40 nM-KCl high-potassium depolarization. Tissues were then washed three times with prewarmed Krebs solution before being tested for agonist-antagonist response.

3.7.3(a)   Effect of carbachol on GPT contractility

An increasing concentration series of carbachol from 1 nM (10^{-9}) to 300 mM ($3x10^{-3}$) was added cumulatively at 3-5 min intervals to construct a carbachol dose-response curve after the final concentration. Each myograph chamber was then washed three times to bring the trachea contraction back to resting tension.

3.7.3(b)   Effect of histamine on GPT contractility

In addition, an increasing concentration series of histamine from 1 nM (10^{-9}) to 300 mM (3×10^{-3}) was added cumulatively at intervals to construct a histamine dose-response curve, after which each myograph chamber was washed three times to relax the trachea back to resting tension.

3.7.3(c)   Effect of atropine on GPT relaxation

To assess the effect of atropine on GPT, each tracheal ring was contracted with EC_{40} carbachol to achieve a 2–4 g submaximal contraction. After stable contraction, increasing concentrations of atropine 3 nM-300 μM were added cumulatively to construct an atropine drug response curve. Upon complete relaxation, the GPT rings were washed thrice. The effect of atropine on GPT relaxation was computed as a percentage fraction of EC_{40} carbachol precontraction.

3.7.3(d)   Effect of cimetidine on GPT relaxation

The cimetidine effect on histamine contracted GPT was carried out with each trachea ring contracted with EC_{50} histamine, after stable contraction increasing concentrations of cimetidine 1μM-10mM were added cumulatively to construct the cimetidine drug response curve, and after adding the concentrations GPT rings were washed 3 times. The cimetidine effect on GPT relaxation was computed as a percentage fraction of EC_{50} histamine precontraction.

3.7.3(e)   Effect of LRP on contracted GPT

Similarly, GPT rings were each pre-contracted with EC_{40} carbachol or EC_{50} histamine per channel to achieve a submaximal contraction of 2–4 g. Following stable contraction, a series of increasing LRP concentrations 10μg/ml-100 mg/ml were added cumulatively at 3-5 min intervals, after which each channel was washed three times.

The effect of LRP on GPT was computed and expressed as a percentage reduction of carbachol and histamine precontraction.

3.7.3(f)   Involvement of β-receptor in LRP relaxation

To determine the involvement of β-receptors in LRP relaxation, the presence and blockage of β-receptors on the GPT rings was first determined. Fresh GPT rings were pre-contracted with carbachol (EC_{40}) or histamine (EC_{50}), after which serial concentrations of salbutamol 3μM-30mM were added. Relaxation by salbutamol was expressed as a percentage fraction of the carbachol or histamine precontraction, and the salbutamol IC_{50} was calculated.

To achieve beta receptor blockade in this experiment, the beta receptor antagonist propranolol was used, which is consistent with previous studies (Memarzia *et al.*, 2019; Chen *et al.*, 2020). Preincubation with propranolol for 30 min was performed, after which the GPT rings were precontracted with carbachol EC_{40} or histamine EC_{50} and subsequently relaxed with salbutamol IC_{50}. To assess the involvement of the β-receptor in LRP relaxation, separate GPT rings were preincubated with propranolol for 30 min and precontracted with carbachol or histamine. After stable contraction, IC_{50} LRP was added to each GPT ring.

3.8   Data analysis

A comparative analysis of the total carbohydrate and protein contents of LR and LRP was conducted using an unpaired t-test. In the inhalation formulation section, the aerodynamic properties of the nebulised LRP mist were assessed according to the protocol outlined in the United States Pharmacopoeia's General Chapter 1601 (Products for Nebulisation – Characterisation Tests: Apparatus 5).

In this study, Shapiro-Wilk normality test, one-way analysis of variance (ANOVA), with Tukey's and Šídák post hoc test were performed using GraphPad Prism software to examine the histological and immunological parameters measured in the asthma experiment section. Comparisons were made between the normal group, untreated (OVA) group, LRP treatment groups, and dexamethasone group.

qPCR data were analysed using the qPCR analysis program Bio-Rad CFX Maestro 2.3 (version 5.3.022.1030). The software was used to open and edit the plate settings according to the specific setup of each qPCR run. Target names, sample names, biological groups, and technical replicates were set for each plate for each qPCR run. The results of multiple qPCR runs and gene expression were combined and analysed using a gene study file.

For the airway receptor GPT myograph analysis, data were collected and extracted from LabChart. The contractility response to carbachol and histamine was measured as the increase in tension in grams from the resting tension, whereas the relaxation response to atropine, cimetidine, salbutamol, and LRP was measured as the percentage reduction in the fraction of carbachol and histamine pre-contraction. From the collected data, a normalised dose-response non-linear sigmoidal curve was fitted. Each drug dose-response curve is presented as mean ± standard deviation (SD), and the data were also analysed using ANOVA with Tukey's post hoc test.

All statistical analyses of the datasets obtained in this study were performed using GraphPad Prism (version 8, Dotmatics, US), and statistical significance difference was set at α-level ≤ 0.05.

CHAPTER 4

RESULTS

4.1   *Lignosus rhinocerotis* polysaccharides (LRP) fractionation

Lignosus rhinocerotis extract (LRE) was obtained by Soxhlet hot aqueous extraction of LR sclerotia powder. Subsequently, the LR polysaccharides was fractionated from LRE using ion-exchange chromatography (DEAE-cellulose) and size-exclusion chromatography (Sephadex G-100) (Figure 4.1). The phytochemical characteristics of the resulting LRP were subsequently investigated.

Following Soxhlet extraction, approximately 16.1% (w/w) of the crude LR extract was obtained from 40 g of LR sclerotia powder. Using distilled water elution on the DEAE column, a symmetrical peak of polysaccharides elution was observed; however, upon elution with increasing ionic concentration of the NaCl solution, no detectable sugar was eluted, as determined by the phenol-sulfuric acid method. The fractionated polysaccharides were subsequently concentrated using rotary evaporator at 45°C for subsequent purification on a Sephadex-G100 column. Furthermore, the Sephadex G-100 column elution exhibited a single symmetrical peak elution profile, representing LRP homogeneity (Figure 4.1). Column fractions were collected in bottles and freeze-dried.

The yield of LRP from the initial LR powder was approximately 7.3%. The powder was lyophilised and stored at -20°C for further use. The fractionated LRP fraction was obtained as a light yellowish powder, with a yield of 7.6 µg/mg (7.3% yield).
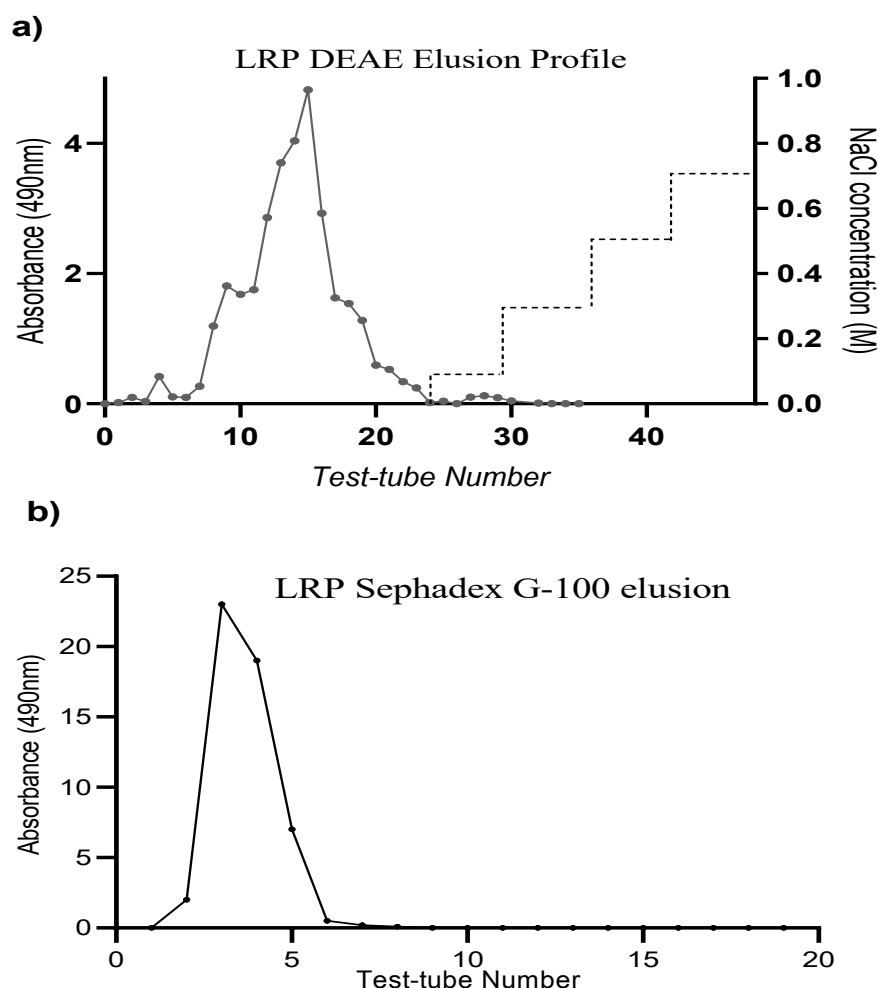
Figure 4.1   Elution profiles of LRP using a) DEAE-cellulose column followed by column b) Sephadex G-100 column.

4.2   Estimation of LRP total carbohydrate and protein content

The estimation of the carbohydrate and protein contents of the LRP fraction was carried out using the phenol-sulfuric acid and Bradford methods, with glucose and bovine serum albumin as standards. Carbohydrate and protein levels were extrapolated from the respective standard curves. The carbohydrate concentration in the crude extract was determined to be 0.838 ± 0.01 mg/ml, which increased to 1.920 ± 0.02 mg/ml ($p < 0.0001$) in LRP, as demonstrated in Figure 4.2a. This suggests that the fractionation process has a significant impact on carbohydrate concentration. However, less protein was extracted from the crude extract, with the protein

concentration decreasing from 0.090 ± 0.001 to 0.081 ± 0.003 mg/ml (w/v), which was not statistically significant (Figure 4.2b).
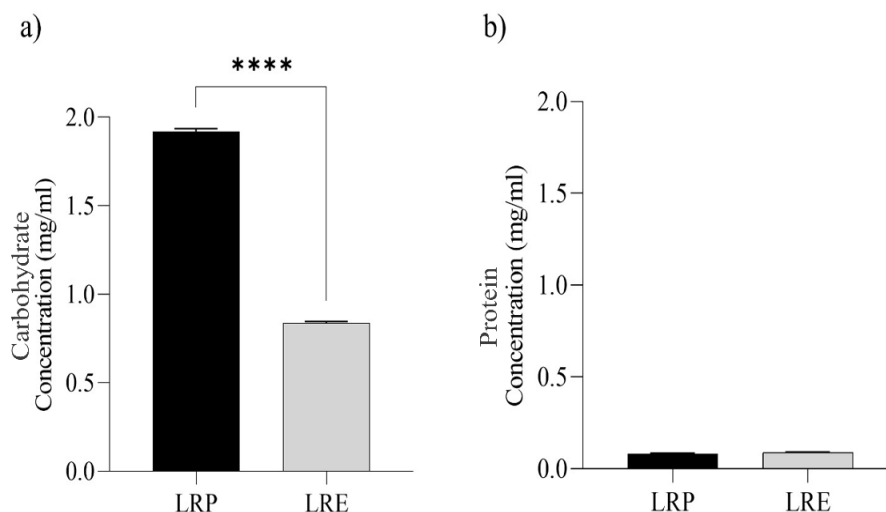
Figure 4.2   LRP comparative analysis of a) total carbohydrate concentration and b) total protein concentration between the crude extract and LRP. Values are presented as mean $\pm$ SEM (n=3). Statistical differences were assessed using unpaired t-tests. ****$p < 0.0001$.

4.2.1   LRP monosaccharides composition analysis by HPLC

Eight PMP derivatives of monosaccharide standards were separated within 45 min, and quantitative analysis of LRP's monosaccharide components of LRP revealed that it is a typical heteropolysaccharide composed of mannose, ribose, rhamnose, glucose, galactose, xylose, and arabinose (Figure 4.3). The contents of monosaccharide compounds found in LRP were calculated as 832.64, 236.53, 159.45, 46577.12, 144.03, 12.63, and 37.90 (μg/ml), with content percentages of 1.73%, 0.49%, 0.33%, 96.90%, 0.30%, 0.03%, 0.08%, and 0.14%, respectively (Table 4.1).
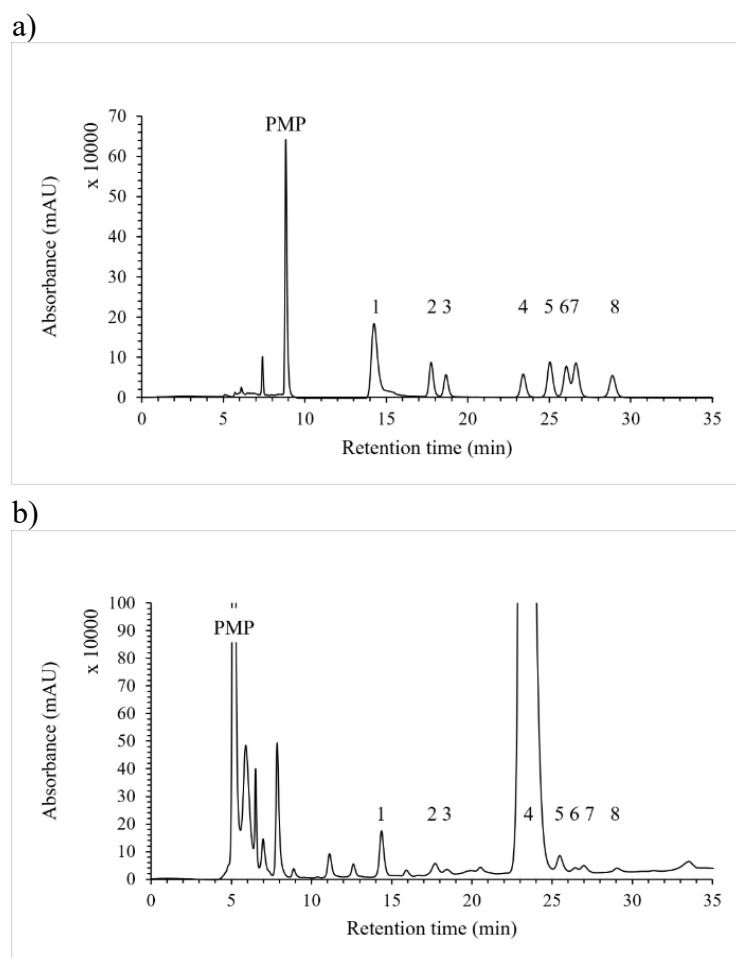
Figure 4.3   HPLC chromatogram of (a) synthetic mixture of eight standard monosaccharides and (b) monosaccharide components present in LR with pre-column PMP derivatisation. LRP peaks were identified as mannose (1), ribose (2), rhamnose (3), glucose (4), galactose (5), xylose (6), arabinose (7), and fucose (8), with fucose serving as an internal standard.

Table 4.1   Monosaccharide composition and concentrations of LRP

	Carbohydrate	Retention time	LRP Peak areas	LRP monosaccharide content (µg/ml)	Percentage of monosaccharides (%)
1	Mannose	14.25	13018165	832.64	1.73
2	Ribose	17.752	14204573	236.53	0.49
3	Rhamnose	18.663	7935603	159.45	0.33
4	Glucose	23.398	7078539	46577.12	96.90
5	Galactose	25.042	9818045	144.03	0.30
6	Xylose	26.049	11732232	12.63	0.03
7	Arabinose	26.634	15164453	37.90	0.08

4.2.2   LRP total glucan and β-glucan content

The Megazyme kit total glucan and α-glucan assays were conducted using 50 mg LRP, LRE, and the kit control. The assay was performed through acid and enzyme hydrolysis of glucans, followed by stoichiometric quantification of the released d-glucose using spectrophotometry in accordance with the manufacturer's protocol. The β-D-glucan content (% w/w) was determined from the MegaCalc sheet, and the results are presented in Table 4.2.

The Megazyme β-glucans assay revealed that the percentage of α- and β-glucans in LRE were 25.847 ± 2.397 % and 17.452 ± 1.123 %, respectively, whilst those in LRP were 21.515 ± 0.531 % and 21.074 ± 2.193 %, respectively (Figure 4.4).

Table 4.2   LRP glucan content assay

Sample	Total glucan ± SD (% w/w)	α-Glucan ± SD (% w/w)	β-Glucan ± SD (% w/w)
Control	45.981 ± 3.353	1.177 ± 0.071	44.871 ± 3.307
LRE	45.966 ± 1.797	25.847 ± 2.397	17.452 ± 1.123
LRP	42.588 ± 2.619	21.515 ± 0.531	21.074 ± 2.193
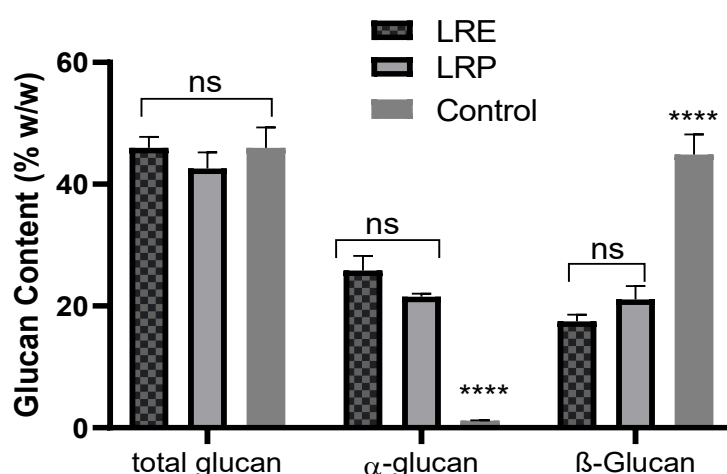
Figure 4.4   Comparative glucan contents of LR crude extract and LRP. Values are presented as mean ± SD (n=3). Statistical differences were assessed using ANOVA with Sidak post hoc. ****$p < 0.0001$.

4.3 LRP inhalation formulation and characterization

Two formulations of fractionated LRP were attempted: dry powder inhalation and nebulization. To evaluate their potential for inhalation delivery, the aerodynamic properties of the selected formulation was characterised using a next-generation impactor (NGI).

4.3.1 LRP dry powder inhalation (DPI) formulation

LRP was initially developed as a dry powder inhalation formulation. To achieve this, spray drying was employed to convert the LRP solution into a dry powder using two distinct approaches. In the first approach, the LRP solution was spray-dried without excipients.

Following the spray drying process, the yield of LRP dry powder from formulation 'a' (200 mg LRP + 200mg lactose in 200 mL dH_2O) was only 4%, while formulation 'b' (400 mg LRP in 200 mL dH_2O) yielded 13%. Additionally, the powder was found to be hygroscopic, sticky, difficult to collect, and expressed a low yield (Figure 4.5).

Figure 4.5   LRP exhibiting adhesive properties, adhering to the walls of the spray dryer cyclone and even the collection vessel.

From this experiment, it can be inferred that the LRP powder exhibits propensity to agglomerate and absorb atmospheric moisture upon spray drying (Figure 4.5). This instability and hygroscopic nature present challenges for the LRP DPI approach. Consequently, a modification of the initial approach was considered for subsequent LRP SD.

In the second approach, it was discovered subsequently that the melting point of the freeze-dried LRP was found to be between 97-99°C when measured using the Gallenhamp melting point apparatus (SCS.0/M.07.A/10). Consequently, in response to this finding, the inlet temperature was reduced in the next approach. For the hygroscopicity of dry powder formulations, excipients such as L-leucine, L-isoleucine, L-phenylalanine (Chang *et al.*, 2014; Otake, Okuda and Okamoto, 2016), and sodium stearate (Yu *et al.*, 2018) can be incorporated into formulations to achieve stable dry powder inhalation. To address the hygroscopicity issue, 20% w/v L-leucine was added to the solution, and the inlet temperature was lowered to 105°C to address its volatility issue (Chang *et al.*, 2014). The following are the modified spray-drying parameters

used to dry the LRP solution in the second approach (Table 4.3). The yield obtained

from the second spray-drying process was 3% of LRP powder.

Table 4.3   LRP spray drying parameters

Parameters	Conditions
Inlet temperature	105°C
Outlet temperature	80°C
Spray gas flow	60L
Pump	5%
Aspirator	100%
Feed flow rate	2 mL/min
Solution concentration	2 mg/mL LRP + 20 % w/v L-leucine (400 mg LRP and 40 g L-leucine dissolved in 200 mL distilled water)

4.3.2   LRP nebulisation solution

A second alternative delivery method was pursued when the spray-drying

method failed to successfully prepared LRP into a dry powder formulation. The

nebulisation inhalation method was utilised to administer the LRP solution in the form

of a nebulisation solution. This solution was prepared by dissolving 80 mg of LRP in

20 mL of distilled water to a concentration of 4 mg/ml. This solution was used

immediately after the preparation.

4.3.2(a)   Quantification of LRP in the nebulisation solution

Quantification of polysaccharides in the LRP solution was performed to

determine the amount of polysaccharides in the sample during characterisation.

Quantification was conducted using the phenol-sulfuric acid test (Dubois *et al.*, 1956),

followed by measurement of absorbance using a UV spectrophotometer at a

wavelength of 490 nm (Table 4.4). A standard calibration curve was established using

two-fold increasing concentrations of the LRP standard solutions. The measurements

were conducted in triplicate, and the resulting curve was linear within the specified

concentration range, as shown in Figure 4.6.

4.3.2(b) *In vitro* **aerosol deposition characterisation of nebulized LRP solution**

The LRP solution was nebulised using a RossMax N80 jet-nebuliser, and the aerodynamic properties of the nebulised mist were characterised using a next-generation impactor (NGI). Under the utilised conditions, the cut-off diameter for each NGI stage is tabulated in Table 4.5. A 6 ml solution of LRP was nebulised to complete dryness at a flow rate of 0.3 ml/min. The NGI's maximum stage volume capacity (T_0) was established at 19 min to prevent overflow of stages. Subsequently, the nebuliser bottle, induction port, stages 1-8, and micro-orifice filter were rinsed with 3 ml of distilled water. Each NGI component, including the nebuliser and aerosol conduction tube, were rinsed with 3-5 ml of distilled water, and the polysaccharides content of each was quantified using the phenol-sulfuric acid test and compared to the LRP standard curve, as depicted in Figure 4.6.

The NGI device comprises seven stages that simulate the various components of the respiratory system. The deposition of nebulized LRP along the NGI was collected and quantified (Figure 3.2). Each component from the nebulizer bottle, induction port, stages 1-7, and micro-orifice filter was washed with 3-5 ml distilled water, and the deposited LRP concentration was estimated by considering the distilled water dilution factor. The deposition concentration was extrapolated using an LRP phenol-sulfuric acid standard curve (Table 4.4; Figure 4.6). The NGI *in vitro* LRP nebulization characterization was conducted in three replicate experiments, and the average mean value and standard deviation were recorded. Figure 4.7 illustrates the mean LRP concentration deposition at each stage and the MOC of the NGI across the three experimental trials, indicating elevated LRP deposition from stages 3 to 4 compared to other stages of the NGI. The results of the three experiments are summarized in Table 4.6.

Based on the NGI LRP nebulization results, the Aerodynamic Particle Size Distribution (APSD) properties of the LRP nebulization were calculated, including the Emitted Fraction (EF), Median Mass Aerodynamic Diameter (MMAD), and Geometric Standard Deviation (GSD), as presented in Table 4.6.

Table 4.4   LRP phenol-sulfuric sugar estimation OD readings

Concentration of LRP solution (mg/ml)	Abs 1	Abs 2	Abs 3	Mean ± S.D.
3.0	3.474	3.363	3.170	3.336 ± 0.154
2.5	2.762	2.800	2.820	2.794 ± 0.029
2.0	2.353	2.334	2.100	2.262 ± 0.141
1.5	1.656	1.922	1.773	1.784 ± 0.133
1.0	1.172	1.348	1.098	1.206 ± 0.128
0.5	0.743	0.614	0.667	0.675 ± 0.065
0.25	0.260	0.259	0.266	0.262 ± 0.004
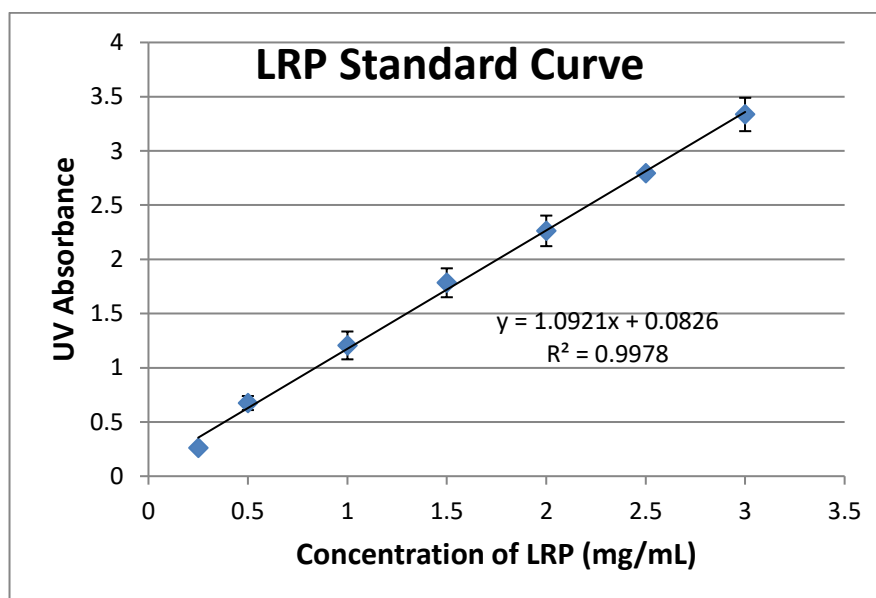
Figure 4.6   LRP phenol-sulfuric sugar estimation standard curve

Table 4.5   NGI cut-off size at 15 L/min flow rate

Stage	Cut-off Diameter (μm)
1	14.1
2	8.61
3	5.39
4	3.30
5	2.08
6	1.36
7	0.98
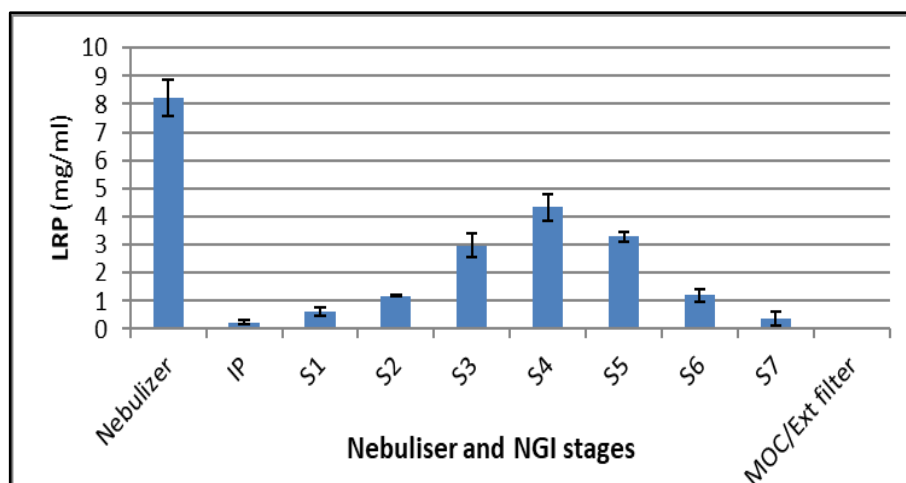
Figure 4.7   Quantification of LRP concentration deposition across the nebulizer, NGI stages 1-7 and MOC of nebulized LRP deposition.

4.3.2(b)(i)   Fine particle fraction (FPF)

The fine particle fraction is the proportion of particles smaller than 5.0 μm in size (Van Holsbeke *et al.*, 2014). Herein, by plotting a graph of the cumulative mass of the LRP against the cut-off diameter of each stage, the FPF value of 62.84% was extrapolated as the percentage intercept of 5 μm on the APSD curve, as depicted in Figure 4.8.

4.3.2(b)(ii)   Mass median aerodynamic diameter (MMAD)

MMAD represents the average size of the particles collected in the impactor, indicating that half of the aerosolised particle mass falls below the estimated aerodynamic diameter (Sheth, Stein and Myrdal, 2014). In this study, LRP MMAD was calculated to be 4.16 ± 0.19 (Figure 4.8).

MMAD = d_{50} (Particle diameter intercepts at cumulative mass 50%)
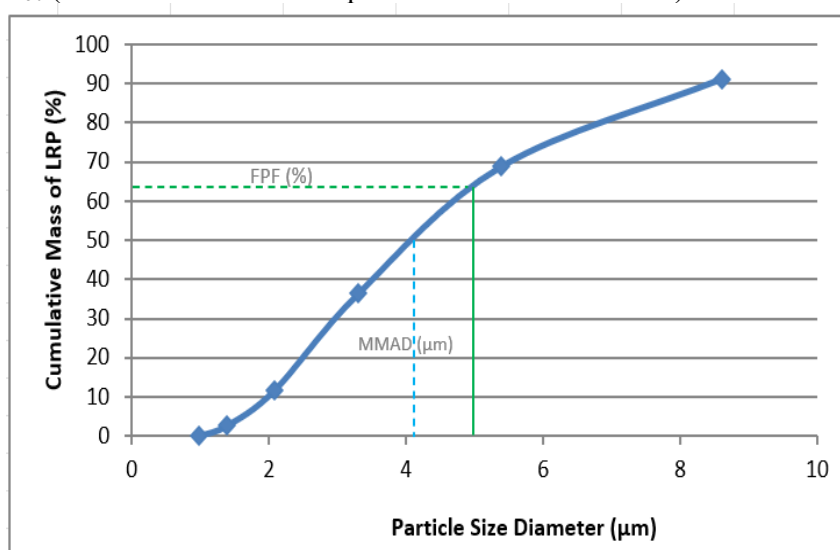
Figure 4.8   Nebulized LRP APSD curve.

4.3.2(b)(iii)   Geometric standard deviation

The Geometric Standard Deviation (GSD) is a measure of the sharpness of the collection efficiency curve, which is analogous to the spread of its log-normal distribution function (Marple, Olson, *et al.*, 2003). A larger GSD value indicates a wider spread of particle sizes (Sheth et al., 2014). LRP GSD was calculated to be 1.83 ± 0.08 (Table 4.6).

The MMAD diameter of the nebulised aerosols was 4.16 µm (Table 4.6), which falls within the optimal size range for effective inhalation and lung deposition of 1–5 µm (Verma *et al.*, 2011). Smaller particles within this range have a high probability of being deposited in the lungs, with the potential to penetrate deep into the lung tissue (Sheth, Stein and Myrdal, 2014). Analysis of LRP nebulization indicated that approximately 62.8% (Table 4.6) of the particles were smaller than 5 µm and may be deposited deep in the lung.

Table 4.6   Average LRP nebulized APSD

Parameters	Experiment 1	Experiment 2	Experiment 3	Mean ± S.D.
Nebulisation Rate (mL/min)	3.30	3.19	3.22	3.24 ± 0.06
Mass Balance (%)	93.68	94.70	92.11	93.50 ± 1.30
EF (%)	66.54	61.26	62.24	63.34 ± 2.81
FPF (%)	61.37	62.17	64.99	62.84 ± 1.90
MMAD (μm)	4.29	4.26	3.94	4.16 ± 0.19
GSD	1.78	1.79	1.92	1.83 ± 0.08

4.3.3   Short stability study of the LRP nebulisation solution

As part of this study, a short-term stability assessment was carried out to evaluate the stability of freeze-dried LRP in solution form. LRP was dissolved in distilled water at a concentration of 1 mg/mL, and 3 mL of the solution was stored in 12 glass vials for each storage condition at room temperature and 4°C. The stability of the LRP solution was assessed by testing its total polysaccharides content, pH, and physical appearance at predetermined intervals (Table 4.7; Figure 4.9). It was found that the LRP solution was stable at 4°C from first day (1.46 ± 0.05) to day 11 (1.36 ± 0.17). However, the stability was compromised at room temperature during the storage time first day (1.46 ± 0.05) to day 11 (0.62 ± 0.12; $p < 0.0001$). This was also shown by cloudy appearance containing particle suspension for solution stored at room temperature, as early as day 3 (Figure 4.10). The free dried LRP powder is usually kept in -20^0C freezer and dissolved in water before nebulisation process.

This study revealed that the LRP solution was stable at 4°C over a period of 11 days based on the polysaccharide content, pH and physical appearance of the LRP solution. However, its stability is compromised when stored at room temperature during the same timeframe. This was evident from the cloudy appearance of the

solution, which contained a particle suspension, as early as day 3 of storage at room

temperature (Figure 4.10).

Table 4.7   Physicochemical properties of stored LRP solution

Evaluated parameters	Storage Conditions / Sampling time (days)	Room Temperature (27^{0}C)							
		1	2	3	ANOVA (P-Value)	1	2	3	ANOVA (P-Value)
Total polysaccharide content in the solution (mg)	0	1.41	1.50	1.46		1.51	1.46	1.42	
	1	1.33	1.25	1.13	0.1605	1.22	1.03	1.11	0.0153
	5	1.27	1.21	1.20	0.1351	1.21	0.93	0.77	0.0007
	11	1.25	1.26	1.55	0.7281	0.69	0.69	0.48	< 0.0001
pH	0	4.34				4.62			
	1	4.40				4.36			
	11	3.72				2.81			
Physical appearance	0				Clear				Clear
	1				Clear				Clear
	5				Clear				Cloudy
	11				Clear				Cloudy

135

Short-LRP Stability
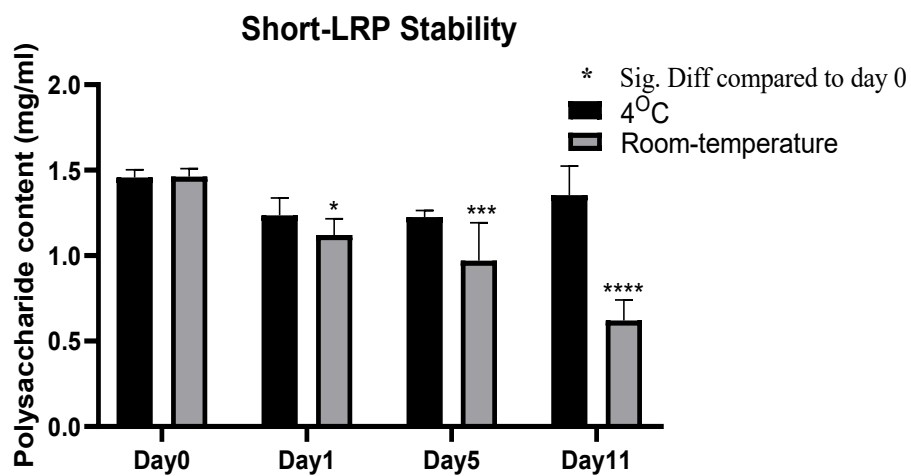
Figure 4.9   Comparative polysaccharide concentration of LRP solution at 4^0C and room temperature between day 0 to 11. Values are presented as mean ± SD (n=3). Statistical differences were assessed using 2-way ANOVA with tukey's post hoc. *$p < 0.5$ ***$p < 0.001$****$p < 0.0001$.
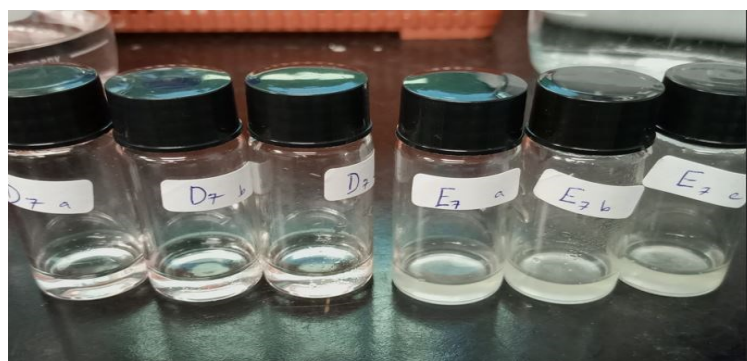
Figure 4.10   Short stability of LRP solution in 4°C (3 vials on the left) and room temperature (3 vials on the right) on day 7

4.4   Anti-asthmatic effect of LRP in ovalbumin asthma mice model

4.4.1   Preliminary anti-asthmatic study in ovalbumin asthma mice model

A major objective of this study was to evaluate the anti-asthmatic properties of a polysaccharides extract from the *L. rhinocerotis* mushroom. To accomplish this, the present study utilised an ovalbumin (OVA)-challenged asthmatic mouse model, assessing the effect of LRP treatment in this model, comparing results between different experimental groups. This study was designed to analyse the potential therapeutic effects of LRP in the context of asthma.

From results of the pilot study, lung tissue of OVA-challenged mice exhibited a notably higher infiltration of inflammatory cells score (3.25 ± 0.353) compared to the normal group (0.25 ± 0.353; $p < 0.001$). LRP administration resulted in a significant decrease in inflammatory cell infiltration score at concentrations of 4 mg (15 min) (2.250 ± 0.353), 4 mg (30 min) (2 ± 0.0; $p < 0.05$), 8 mg (15 min) (2.25 ± 0.353), and 40 mg/ml (1 ± 0.0; $p < 0.01$). Similarly, dexamethasone treatment effectively lowered the inflammatory cell infiltration score (0.50 ± 0.707; $p < 0.01$) to levels approaching those of the normal group (Figure 4.11).
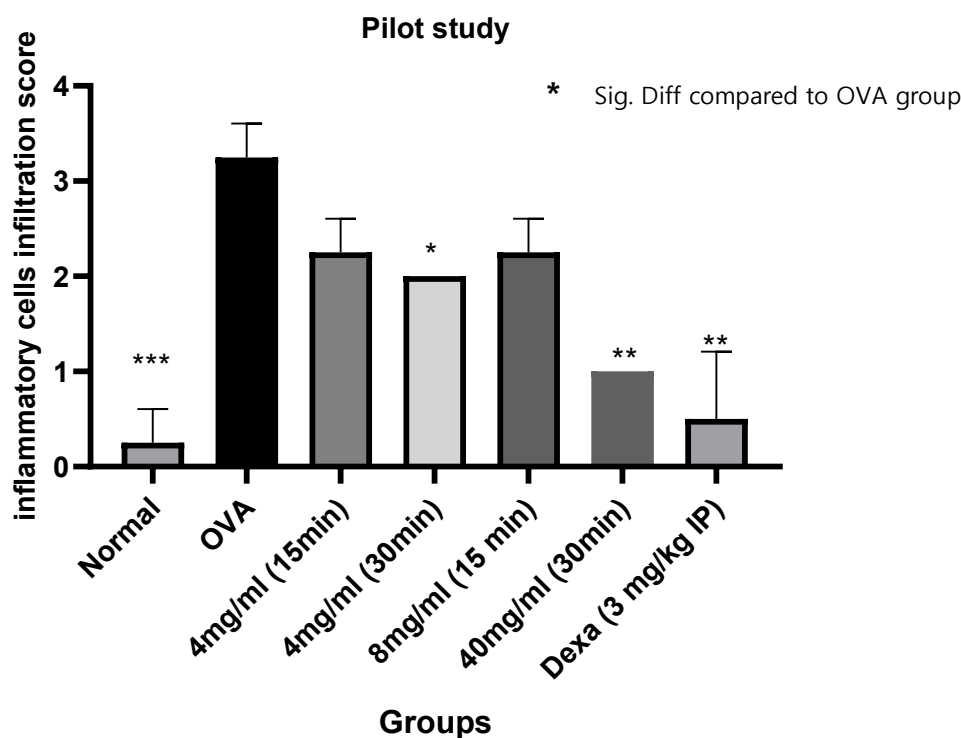
Figure 4.11   Effects of LRP on OVA-challenge induced lung inflammatory cells infiltration score from pilot study. Values are expressed as the mean ± SD (n=2 per group). Statistical differences were assessed using one-way ANOVA with tukey's post hoc. *p < 0.05, **p<0.01, and ***p<0.001.

4.4.2   Main study on anti-asthmatic effect of LRP in ovalbumin asthma mice model

In the main study, LRP treatments were administered concomitantly with 20-minute OVA-challenges from days 21 to 27 of the asthma study to assess their effects on asthma pathophysiology parameters. Based on the findings of this pilot study, a 30-minute inhalation duration and LRP concentrations of 4, 8, and 40 mg/ml were selected for the main study.

4.4.2(a)   LRP attenuate increased differential leucocyte count in OVA-challenged mice

In order to investigate the bioactive effects of LRP on airway inflammation, a differential leucocyte count (DLC) was conducted on the BALF that had been obtained 24 hours after the final aerosol challenge and treatment. BALF was centrifuged, and the resulting pellets were smeared on slides and stained with Giemsa reagent to observe inflammatory cells.

Individual white blood cells were counted based on their cellular morphology and the relative DLC was estimated accordingly (Figure 4.12; Figure 4.13).

4.4.2(a)(i)   Effects of LRP on eosinophil count in BALF

In this study, eosinophils count comparison between mice from the OVA group (11.45 ± 1.938%) and normal group (4.914 ± 1.054%; $p < 0.0001$) revealed that the OVA group exhibited a significantly higher eosinophil count in BALF. Following treatment, 4mg/ml (8.681 ± 1.233%; $p < 0.05^*$), 8mg/ml (8.109 ± 1.074%; $p < 0.01$), 40 mg/ml of LRP (8.263 ± 1.279%; $p < 0.01$) and dexamethasone (7.35 ± 1.279%; $p < 0.001$) groups expressed a significant reduction in eosinophil levels (Figure 4.12 a).

4.4.2(a)(ii)   Effects of LRP on lymphocyte count in BALF

The percentage of lymphocyte cells was significantly higher in OVA-challenged mice (59.36 ± 4.889%) compared to the normal control group (36.70±4.428%; $p < 0.0001$). OVA challenge led to a statistically significant increase in the percentage of lymphocyte cells. Furthermore, LRP treatment resulted in a statistically significant decrease in the percentage of lymphocyte cells in both the 8 mg/ml (45.12 ± 3.078%; $p < 0.01$) and 40 mg/kg (46.66 ± 4.037%; $p < 0.01$) treatment groups, and a significant decrease in the dexamethasone-treated group (48.77 ± 2.450%; $p < 0.001$) was also observed (Figure 4.12b).

4.4.2(a)(iii)   Effects of LRP on macrophage count in BALF

The results revealed that the percentage of macrophages was significantly higher in mice challenged with OVA (11.37 ± 1.583%) than in the normal control (6.688±1.409%; $p < 0.0001$) groups. Treatment with LRP resulted in a statistically significant reduction in the percentage of macrophage cells in the 4 mg/ml (8.523±1.409%; $p < 0.05$), 8 mg/kg (7.924 ± 1.476%; $p < 0.01$) and 40 mg/kg (7.816 ± 1.366%; $p < 0.01$) LRP treatment groups, together with dexamethasone-treated (6.780 ± 1.519%; $p < 0.001$) mice (Figure 4.12c).

4.4.2(a)(iv)   Effects of LRP on neutrophils count in BALF

The OVA challenge resulted in a slight increase in neutrophils ($30.35 \pm 4.068\%$); however, this increase was not statistically significant. On average, neutrophil levels in OVA-challenged mice were marginally higher than those in the other groups, except for the 8 mg/ml group ($22.19 \pm 3.547\%$; $p < 0.05$) which showed statistically significant lower neutrophil counts. The study findings demonstrated that the percentage of neutrophils in the BALF was relatively consistent across the groups (Figure 4.12d).
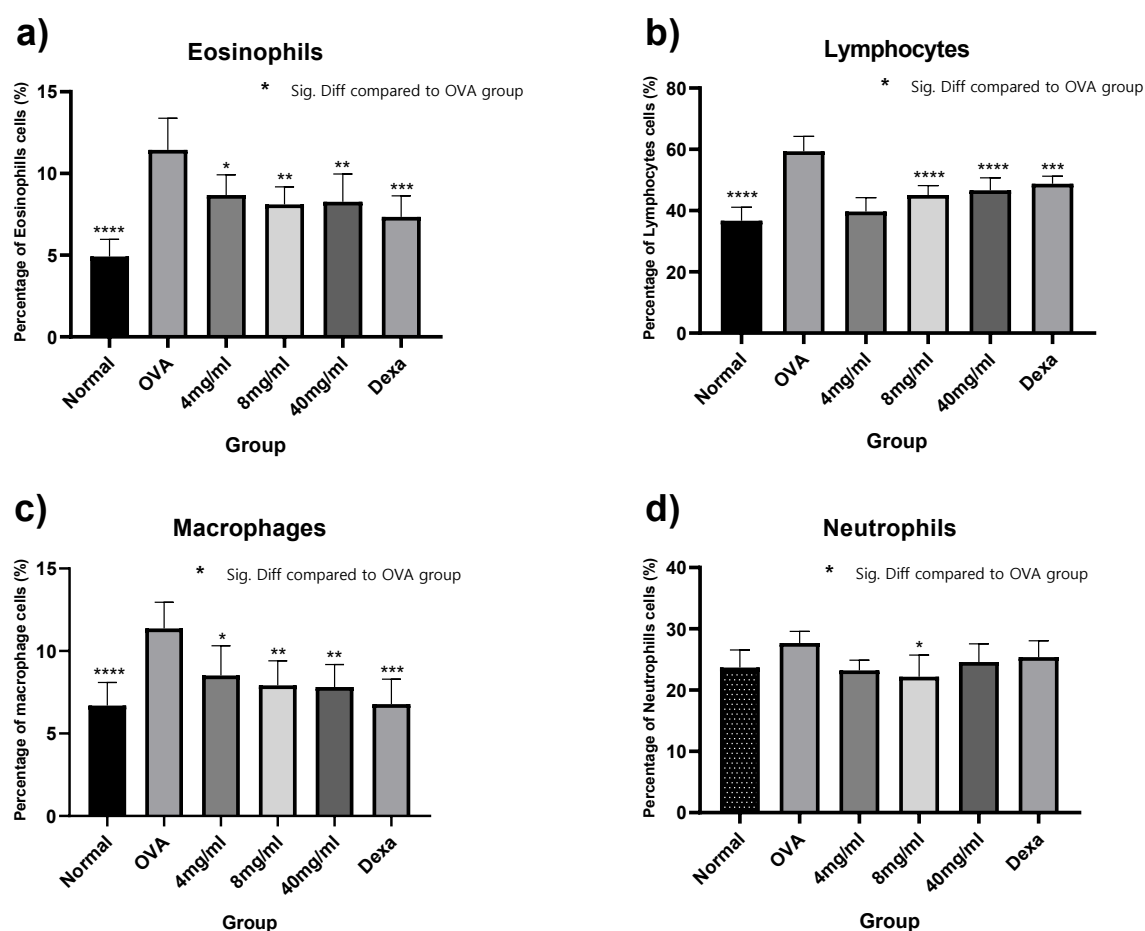
Figure 4.12   Effects of LRP on OVA-challenge induced leucocytes infiltration in BALF. Values are expressed as mean ± SD (n=7 per group). Statistical differences were assessed using one-way ANOVA with tukey's post hoc. *p < 0.05, **p<0.01, ***p<0.001 and ****p<0.0001.
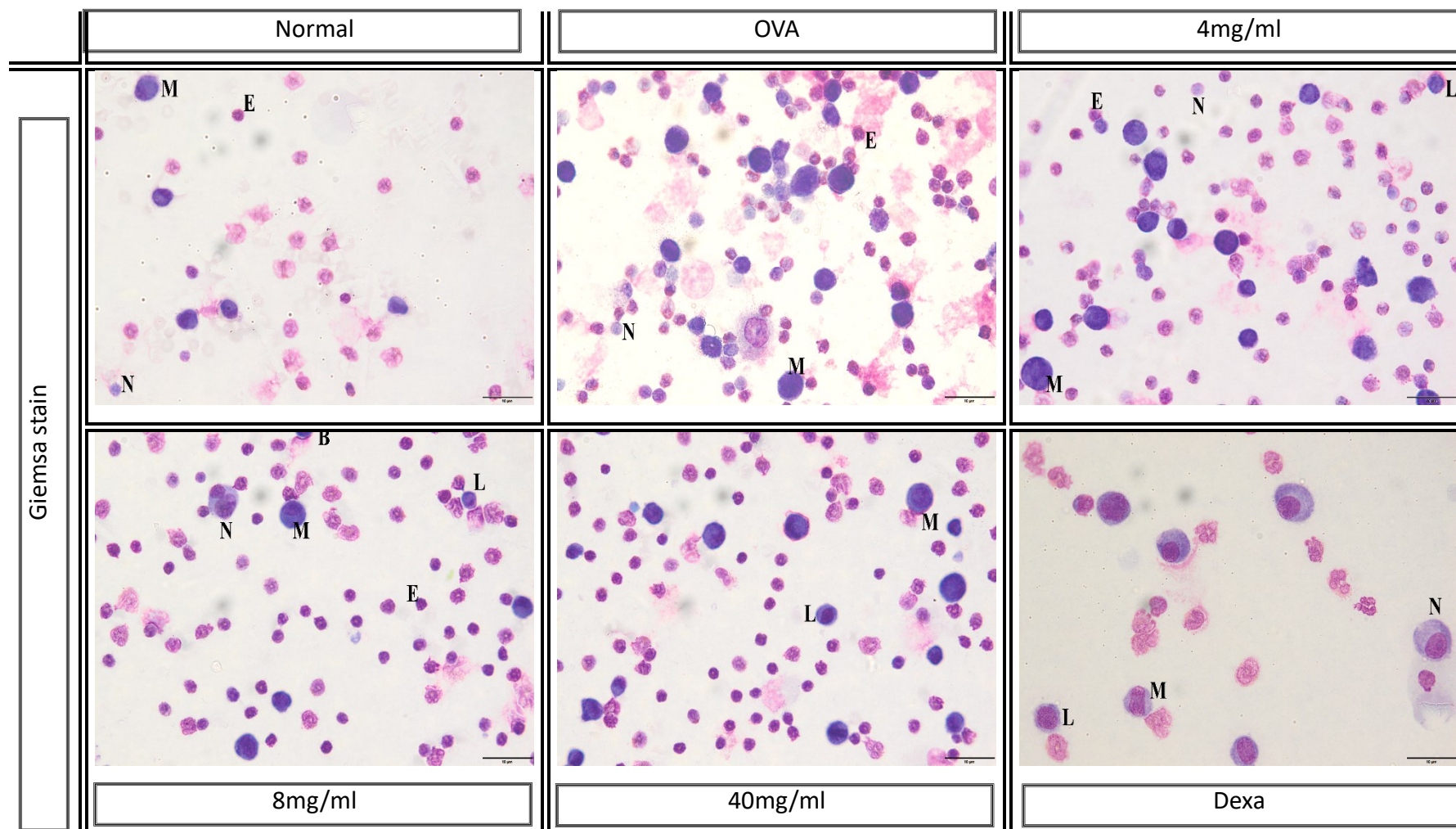
Figure 4.13   Representative Giemsa-stained BALF smear showing inflammatory cells from normal control, OVA-challenged, LRP-, and dexamethasone-treated mice. **E**= eosinophils; **L**= lymphocytes; **M**= macrophages; **N**= neutrophils. LRP attenuate increased eosinophil, lymphocyte and macrophage counts in OVA-challenged mice

4.4.2(b)   LRP reduced serum immunoglobulin-E (IgE)

To evaluate the potential impact of LRP on an established OVA-specific Th2 response *in vivo*, the study quantified the serum IgE levels in murine blood samples. Elevated IgE levels, a hallmark of allergic asthma, indicate inflammation and bronchial hyperresponsiveness. Mouse serum IgE levels were evaluated using ELISA.

The level of serum IgE was significantly higher in mice subjected to the OVA challenge (7.268 ± 0.889) than in the normal group (2.261 ± 0.9281; $p < 0.001$). A marked and considerable reduction in IgE levels was evident in the 4 mg/ml (2.665 ± 0.8114; $p < 0.001$) and 8 mg/kg (1.437 ± 0.3871; $p < 0.001$) treatment groups, while a less significant reduction was observed in the 40 mg/ml (3.403 ± 1.554; $p < 0.01$) and dexamethasone-treated groups (3.831 ± 0.2693; $p < 0.01$) (Figure 4.14).
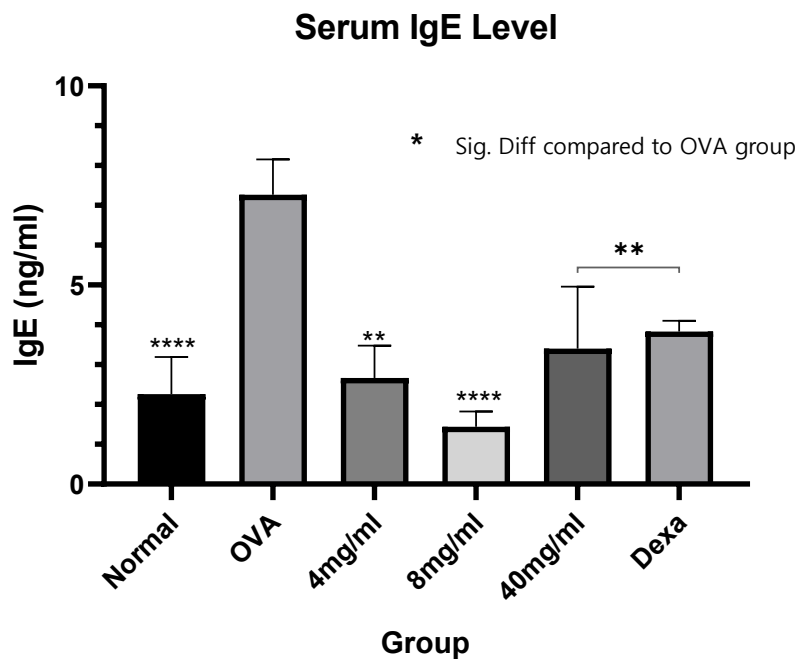
Figure 4.14   Effects of LRP on serum IgE in OVA-challenged mice. Values are expressed as mean ± SD (n=7 per group). Statistical differences were assessed using one-way ANOVA with tukey's post hoc. **p<0.01 and ****p<0.0001.

4.4.2(c)   Effects of LRP on Th2 cytokines in BALF

Elevated levels of Th2 cytokines are indicative of an atopic allergic response. In this study, concentrations of Th2-associated cytokines implicated in asthma, specifically IL-5 and IL-13 using Luminex immunoassay and IL-4 using ELISA methods were estimated. In the OVA-challenged asthma mouse model, the response to OVA challenges is characterised by a substantial increase in the levels of IL-4, IL-5, and IL-13 in BALF. However, because a substantial proportion of the sample values fell below the standard curve and detection limit of the Luminex assay, quantitative analysis based on extrapolated concentrations was not feasible. This constraint necessitated an alternative approach; consequently experimental group comparisons were performed using raw mean fluorescence intensity (MFI) values as a relative measure of analyte abundance, rather than extrapolated analyte concentrations (Breen, Polaskova and Khan, 2015; Sullivan, Gebel and Bray, 2017). This methodology allowed the identification trends in analyte expression, despite the limitations imposed by the assay. Consistent with the established mechanism of OVA-challenged asthma, this study demonstrated that OVA-challenged mice exhibited significantly elevated levels of IL-4, IL-5 and IL-13 cytokines compared to the normal control group (Figure 4.15).

4.4.2(c)(i)   Effects of LRP on BALF IL-5 level

Notably, levels of IL-5 were markedly increased in OVA-challenged mice (30.96 ± 3.19) in comparison to the normal group (6.667 ± 2.60; $p < 0.0001$). Significant differences in mean values were detected between treatment groups, with more significant IL-5 reduction in the 40 mg/ml (8.50 ± 2.51; $p < 0.01$) and dexamethasone (13.44 ± 5.05; $p < 0.01$) groups than in the 4 mg/ml (14.62 ± 5.04; $p < 0.05$) and 8 mg/ml (23.17 ± 2.45; $p < 0.01$) treatment groups when compared to OVA group (Figure 4.15a).

4.4.2(c)(ii)   Effects of LRP on BALF IL-13 level

OVA challenge caused a significant increase in the level of IL-13, as it was significantly elevated in OVA-challenged mice (11.38 ± 1.89) in comparison to the normal group (3.45 ± 1.83; p < 0.001). There was also a significant difference in the level of IL-13 among the treatment groups, with a marked reduction among the 40 mg/ml LRP (4.87 ± 1.23; p < 0.01) and dexamethasone (3.16 ± 1.65**) groups, whereas a less significant reduction in IL-13 values was observed in the 4 mg/ml (7.08 ± 2.42) and 8 mg/ml (9.04 ± 1.73) treatment groups (Figure 4.15b).

4.4.2(c)(iii)   Effects of LRP on BALF IL-4 level

Similarly, OVA challenge resulted in a significant increase in the BALF level of IL-4, which was observed to be elevated in OVA-challenged mice (17.80 ± 3.75) compared to the normal group (6.94 ± 1.09; p < 0.0001). There was also a significant difference in the level of IL-4 among the treatment groups, with a marked reduction in 4 mg/ml (11.20 ± 2.17; p < 0.01), 8 mg/ml (9.72 ± 3.71; p < 0.001) and 40 mg/ml LRP (8.89 ± 2.51; p < 0.001) as well as dexamethasone (11.06 ± 3.07; p < 0.01) treatment groups (Figure 4.15c).
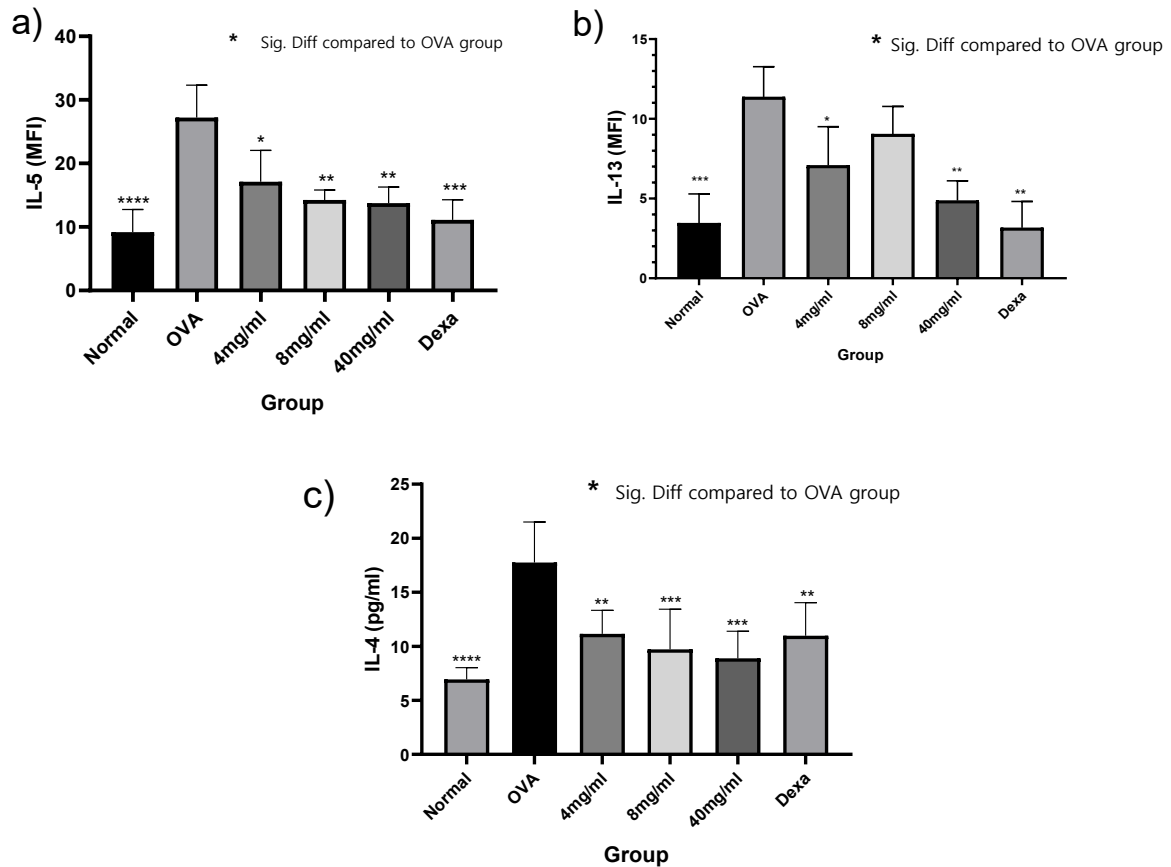
Figure 4.15   Effects of LRP on a) IL-5, b) IL-13 and c) IL-4 in BALF of OVA-challenged mice. Values are expressed as mean ± SD (n=7 per group). Statistical differences were assessed using one-way ANOVA with tukey's post hoc. *p < 0.05, **p<0.01, ***p<0.001 and ****p<0.0001.

### 4.4.2(d)   Effects of LRP on inflammatory genes expressions

Following primer optimization using a two-fold serial dilution of 100 ng to 6.25 ng of cDNA template copies per microliter across five distinct concentrations, as demonstrated in the amplification plots presented in (Figures 4.16-4.20), and the gene expression levels were normalized to GAPDH as a reference gene. Inflammatory cytokine gene expression results further strengthened the effectiveness of asthma induction in this model, where OVA-challenged mice showed increased gene expression of Th2-related pro-inflammatory cytokines Cox-2, iNOS, IL-22, and ADAM33 in lung tissue homogenates (Figure 4.21).
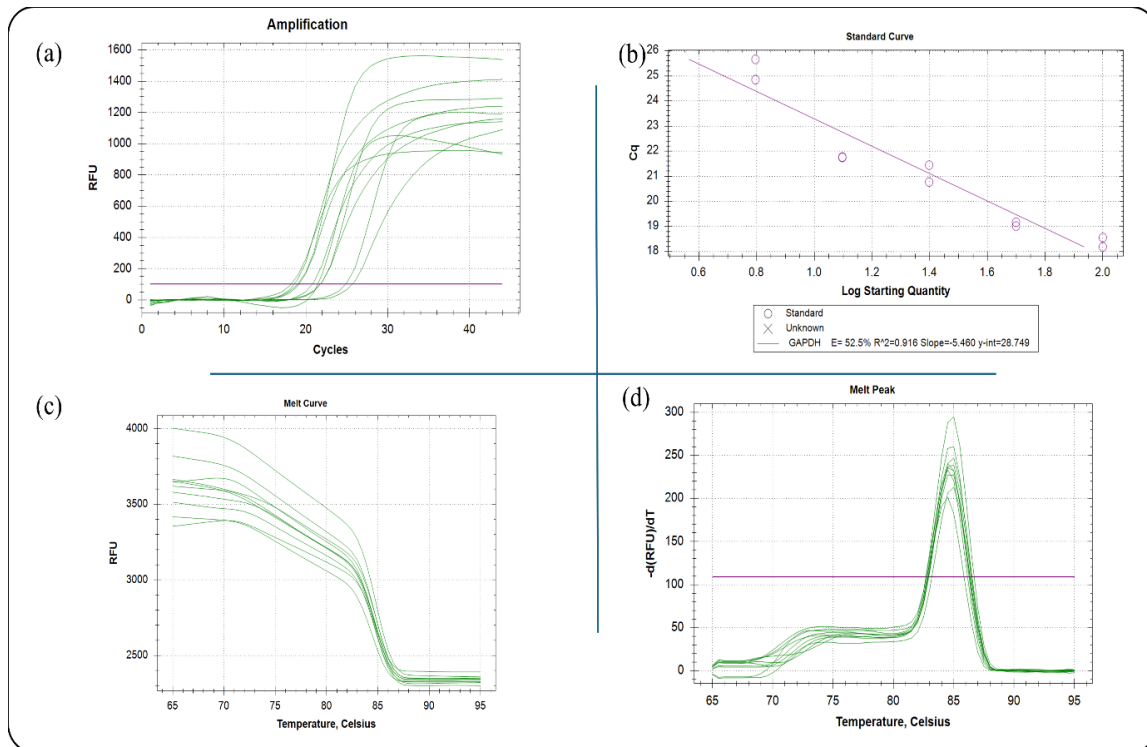
Figure 4.16   GAPDH primer optimisation: **a)** GAPDH amplification **b)** GAPDH standard curve **c)** GAPDH melt curve **d)** GAPDH melt peak.

4.4.2(d)(i)   COX-2 gene expression

Relative gene expression levels of COX-2 were markedly increased in OVA-challenged mice (6.60 ± 1.02) in comparison to the mean values expressed between treatment groups, with more significant COX-2 expression reduction in the 40 mg/ml (2.55 ± 0.417; $p < 0.001$), 8 mg/ml (2.43 ± 0.138; $p < 0.001$) and dexamethasone (2.08 ± 0.299; $p < 0.0001$) groups than in the 4 mg/ml (4.10 ± 0.457; $p < 0.05$) treatment groups (Figure 4.21a).
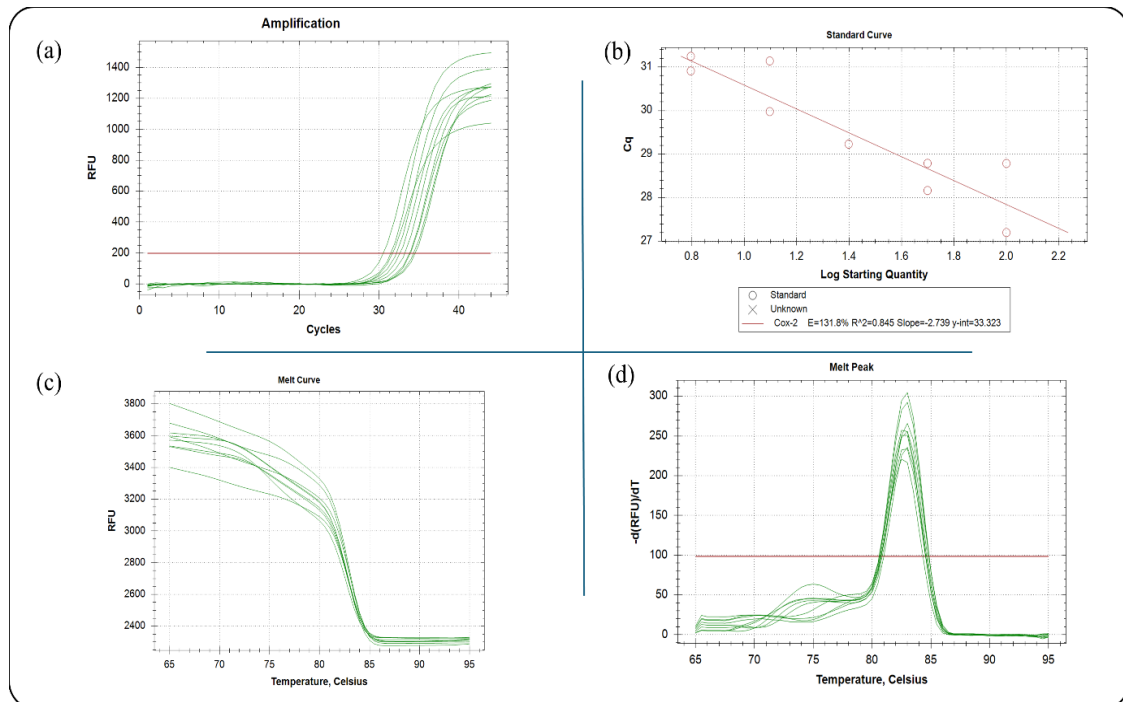
Figure 4.17   Cox-2 primer optimisation: **a)** Cox-2 amplification **b)** Cox-2 standard curve **c)** Cox-2 melt curve **d)** Cox-2 melt peak.

4.4.2(d)(ii)   iNOS gene expression

Relative gene expression levels of iNOS were also increased in OVA-challenged mice (3.32±0.480) in comparison to the mean values expressed between treatment groups, with significant in iNOS expression reduction in the 4 mg/ml ($1.62.10 \pm 0.289$; $p < 0.01$), 8 mg/ml (1.97 ± 0.520; $p < 0.05$), 40 mg/ml (1.67 ± 0.219; $p < 0.01$), and dexamethasone (1.52 ± 0.215; $p < 0.01$) treatment groups (Figure 4.21b).
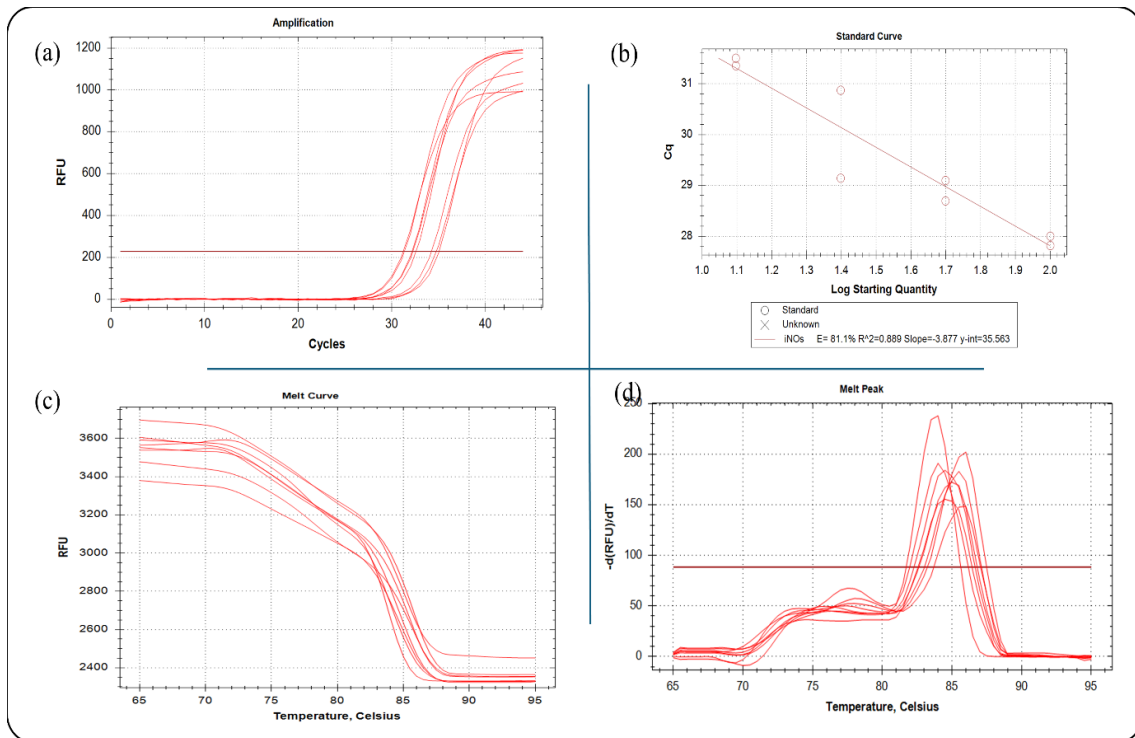
Figure 4.18   iNOS primer optimisation: **a)** iNOS amplification **b)** iNOS standard curve **c)** iNOS melt curve **d)** iNOS melt peak.

4.4.2(d)(iii)   IL-22 gene expression

OVA challenge caused a significant increase in lung gene expression levels of IL-22, as it was significantly elevated in OVA-challenged mice (3.15 ± 0.251) with a significant reduction in the 40 mg/ml LRP (1.77 ± 0.333; $p < 0.05$). However, there was relative reduction among the treatment groups, dexamethasone (2.37 ± 1.41), 4 mg/ml (2.20 ± 0.498) and 8 mg/ml (2.06 ± 0.204) treatment groups (Figure 4.21c).
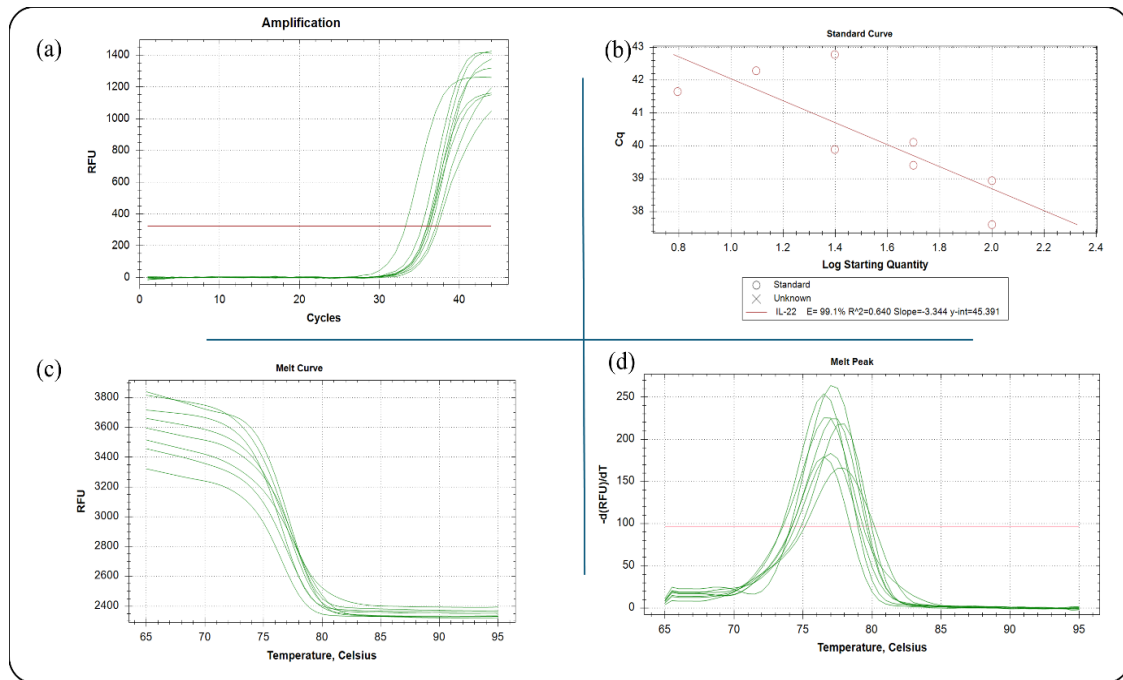
Figure 4.19   IL-22 primer optimisation: **a)** IL-22 amplification **b)** IL-22 standard curve **c)** IL-22 melt curve **d)** IL-22 melt peak.

4.4.2(d)(iv)   ADAM33 gene expression

OVA-challenged mice exhibited increased ADAM33 relative gene expression levels (2.68 ± 0.236), while a significant decrease was observed in the 40 mg/ml $(1.28 \pm 0.133$; $p < 0.01)$, 8 mg/ml $(1.52 \pm 0.813$; $p < 0.05)$ LRP groups and dexamethasone $(1.35 \pm 0.126$; $p < 0.05)$, while relative reduction in 4 mg/ml (1.86 ± 0.326) (Figure 4.21d).
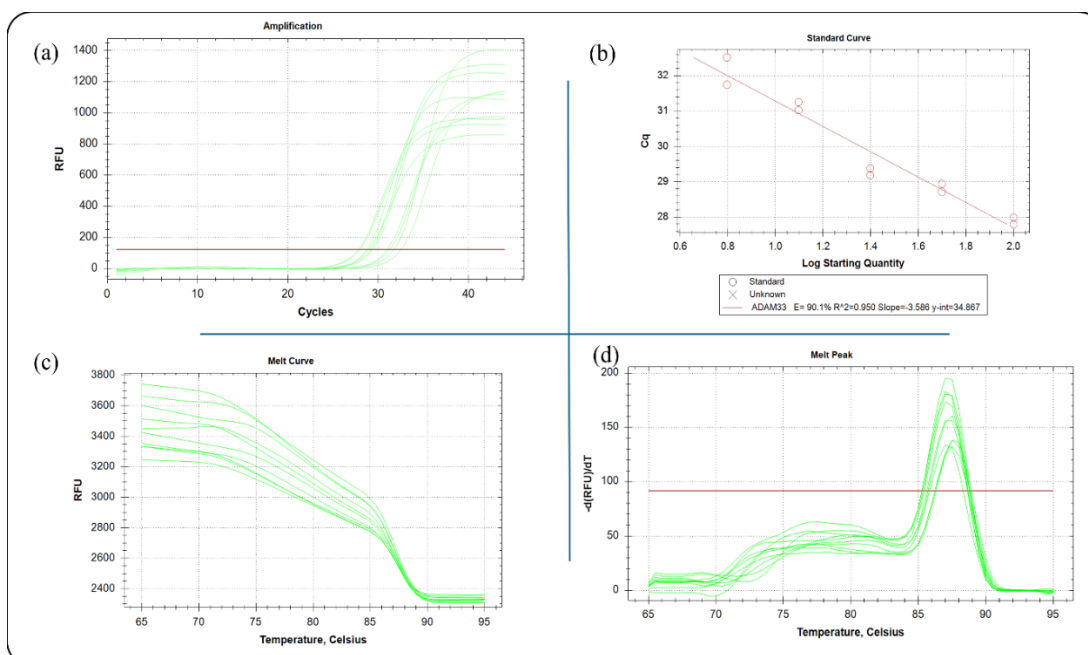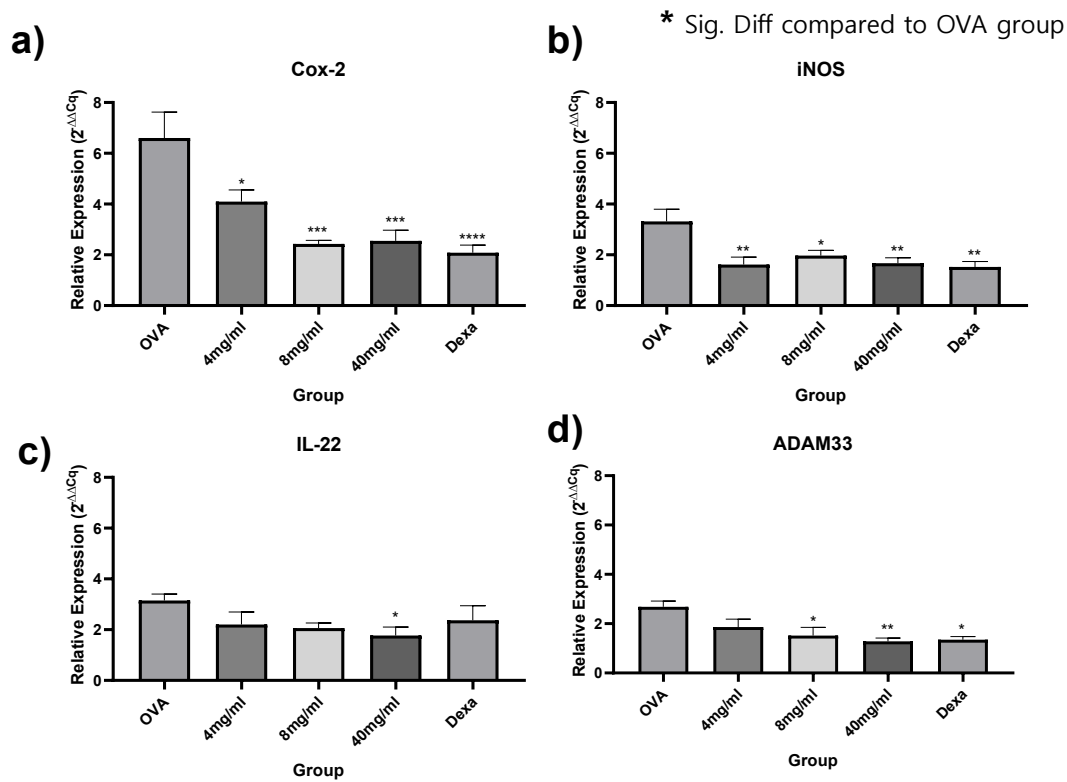
Figure 4.21 Relative lung expression of Cox-2, iNOS, IL-22, and ADAM33 target genes, normalized to the expression levels in control group mice. Values presented as mean ± SEM (n=5 per group). Statistical differences were assessed using one-way ANOVA with tukey's post hoc. *$p < 0.05$, **$p<0.01$, ***$p<0.001$ and ****$p<0.0001$.

4.4.3 Histopathological analysis of lung tissues

4.4.3(a) LRP reduced airway inflammatory cells infiltration in the lungs

To study the effects of LRP on airway inflammatory cells infiltration, lung tissues were collected 24 h after the last aerosol challenge and treatment. The lung tissues were stained with H&E for visualisation of infiltrating cells and estimated according to the Myou *et al.* (2003) and Kim *et al.* (2019) scoring method.

There was significantly higher inflammatory cells infiltration in the lungs of OVA-challenged mice (2.25±0.689) than in the normal group (0.25±0.274; p < 0.0001). Following

LRP treatment, 4 mg/ml (1.643 ± 0.556; $p < 0.05$), 8 mg/ml (1.00 ± 0.764), and 40 mg/ml (1.00 ± 0.288; $p < 0.01$) of LRP significantly reduced inflammatory cells infiltration. Dexamethasone also significantly suppressed the level of inflammatory cells infiltration score (1.00 ± 0.50; $p < 0.001$) close to the normal group value (Figure 4.22). Figure 4.23 shows the inflammatory cells infiltration in lung tissue slides.
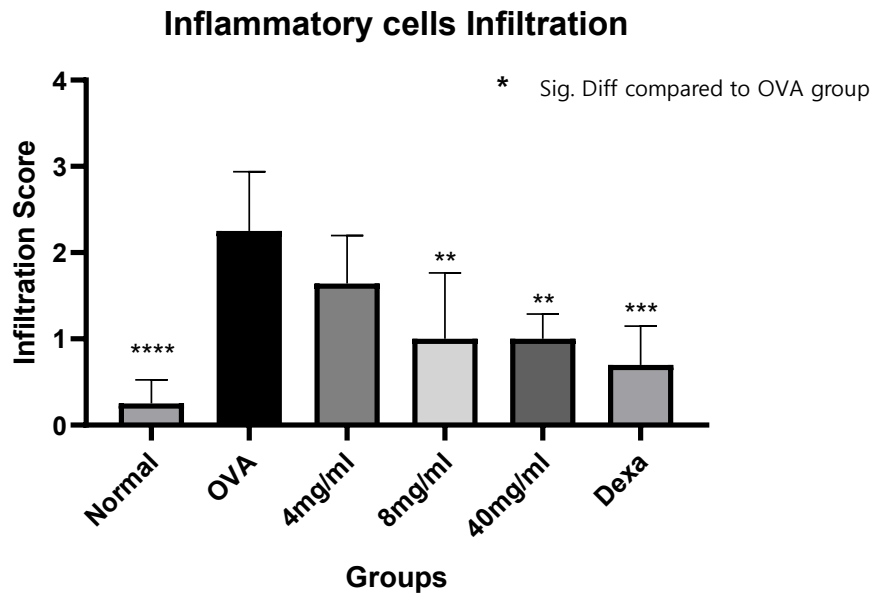
Figure 4.22   Effects of LRP on OVA-challenged induced lung inflammatory cells infiltration. Values are expressed as mean ± SD (n=7 per group). Statistical differences were assessed using one-way ANOVA with tukey's post hoc. *p < 0.05, **p<0.01, ***p<0.001 and ****p<0.0001.

	H&E				
	100	20	100	20	
Normal					8 mg/ml
OVA					40 mg/ml
4 mg/ml					Dexa
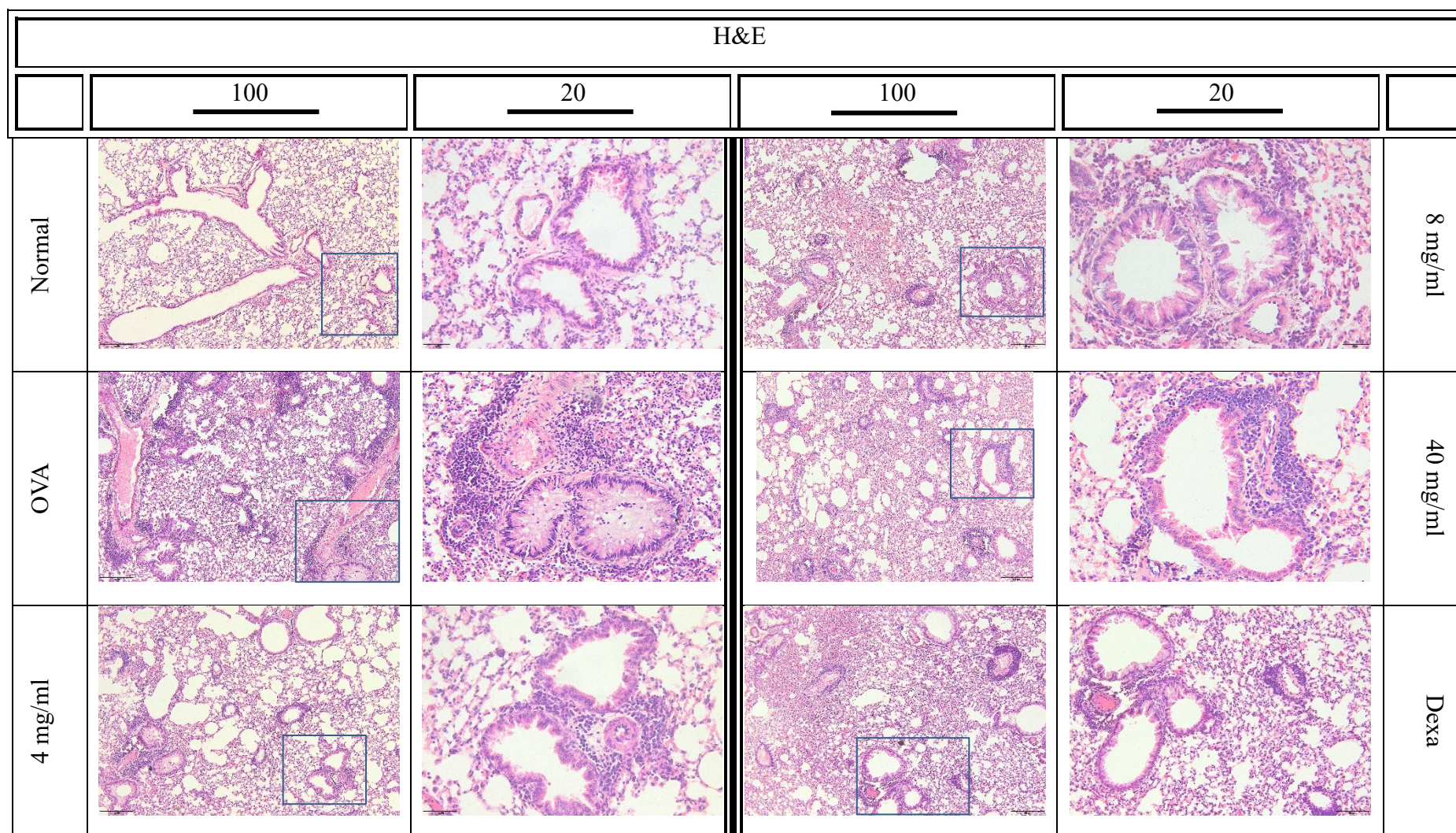
Figure 4.23   Representative H&E-stained sections of lung showing infiltration of inflammatory cells in lung tissue from normal control, OVA-sensitized and challenged, LRP and dexamethasone treated mice.

4.4.3(b)   LRP reduced mucus hypersecretion in the lung tissue

Mucus hypersecretion is a characteristic of airway remodelling. To assess mucus secretion and goblet cells hyperplasia in lung tissues collected 24 h after the last aerosol challenge and treatment. The tissues were stained with PAS for visualisation of mucus secretion and goblet cells. From the PAS-stained slides, the percentages of stained areas of mucus secretion and goblet cells in each mouse lung slides across all experimental groups were estimated according to the Myou *et al.* (2003) and Kim *et al.* (2019) scoring method.

There was a significant increase in goblet cells in OVA-challenged mice (1.583±0.376) compared to the normal group (0.50±0.447; $p < 0.0001$). Following inhalation treatment, the treated groups showed significantly reduced PAS staining scores ($p < 0.01$): 4 mg/ml (0.80±0.288), 8 mg/ml (0.88±0.250), and dexamethasone (0.833±0.288) groups. Interestingly, the 40 mg/ml treatment (0.571±0.345; $p < 0.001$) markedly reduced mucus secretion and goblet hyperplasia compared to the other treatment groups (Figure 4.24). Figure 4.25 shows goblet cell and mucus secretion in the lung tissue slides.
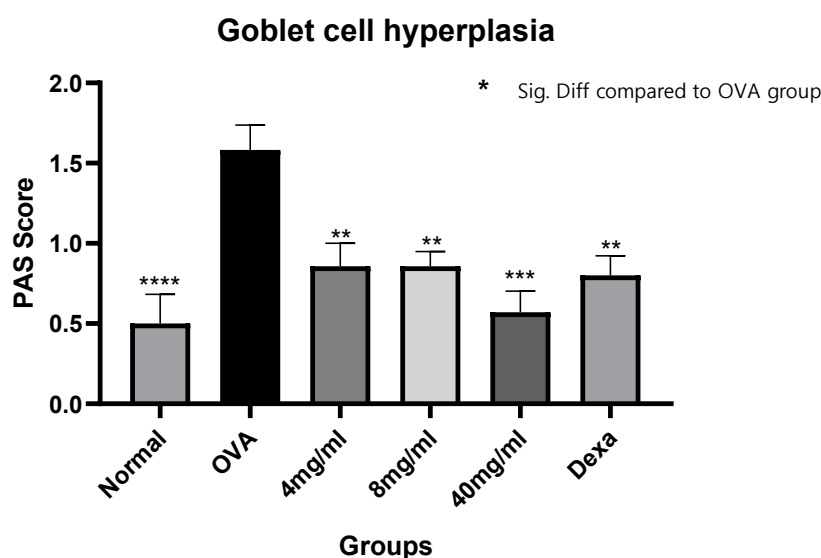
Figure 4.24   Effects of LRP on goblet cells hyperplasia in lungs of OVA-challenged mice. Values are expressed as mean ± SE (n=7 per group). Statistical differences were assessed using one-way ANOVA with tukey's post hoc. **p<0.01, ***p<0.001 and ****p<0.0001.
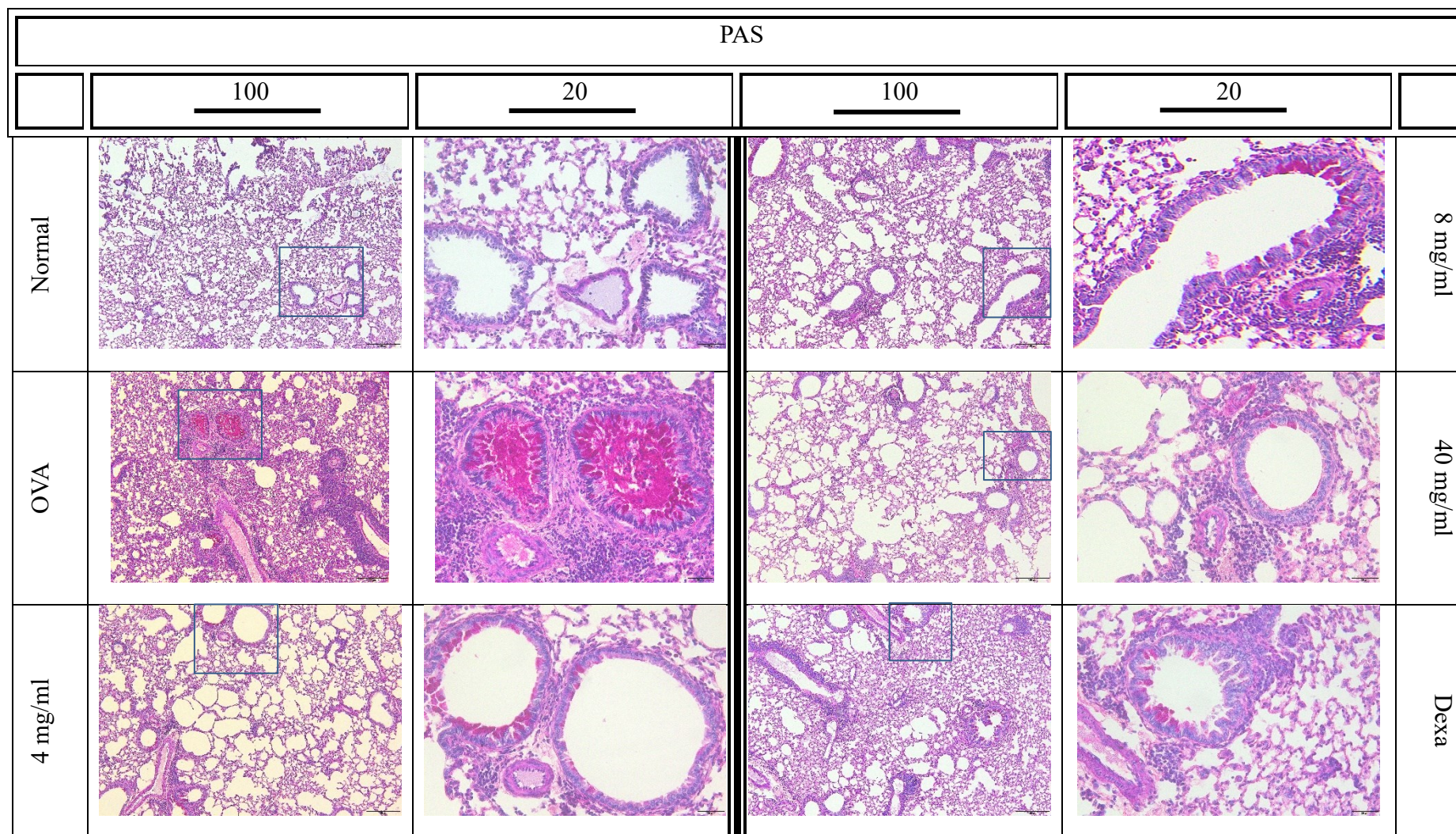
Figure 4.25   Representative PAS-stained sections of lung showing PAS positive goblet cells and mucus secretion in lung tissue from normal control, OVA-sensitized and challenged, LRP and dexamethasone treated mice.

4.5   Effect of LRP on guinea pig trachea contractility

The effect of fractionated LRP on the activity of three airway receptors, namely muscarinic, histamine, and beta receptors, was assessed on isolated guinea pig trachea (GPT) rings in a water bath myograph. The respective receptor antagonists, atropine and cimetidine, and the β-antagonist salbutamol were used to determine their pIC_{50} values from the dose-response curve (DRC), which were subsequently compared to the effects of LRP. The involvement of beta receptors in the LRP response was also examined in GPT rings preincubated with propranolol. The primary objective of the experimental protocol was to evaluate the influence of LRP on the contractility of GPT via muscarinic, histamine, and β-airway receptor pathways.

4.5.1   Agonist (carbachol and histamine) contractile response on GPT

GPT ring contraction response to the cumulative addition series of carbachol and histamine concentrations were measured using LabChart-obtained data (LabChat 7, ADInstruments, US). Dose-response curves for the receptor agonists carbachol and histamine were constructed. Using GraphPad Prism software, a variable-slope sigmoidal curve was generated, plotting log [agonist/inhibitor] concentration against the variable response (g). The contractility response curve was constrained to 0% (bottom) and 100% (top). From the DRC, the EC_{50} and IC_{50} concentrations were extrapolated. The EC50 represents the concentration of the agonist that elicits a 50% maximal response, while the IC_{50} denotes the concentration of the antagonist that achieves a 50% maximal response.

The maximal contraction responses (Emax) of carbachol and histamine were measured to be 7.94 ± 3.56 g and 3.32 ± 0.85 g, respectively. Both carbachol and histamine contracted the GPT rings in a concentration-dependent manner. The EC_{40}

concentration for carbachol was calculated to be 300nM, while the EC_{50} for histamine was determined to be 1.24nM. These values were used in subsequent GPT ring contractions to achieve submaximal contractions of 2–4 g (Figure 4.26; Figure 4.27;).
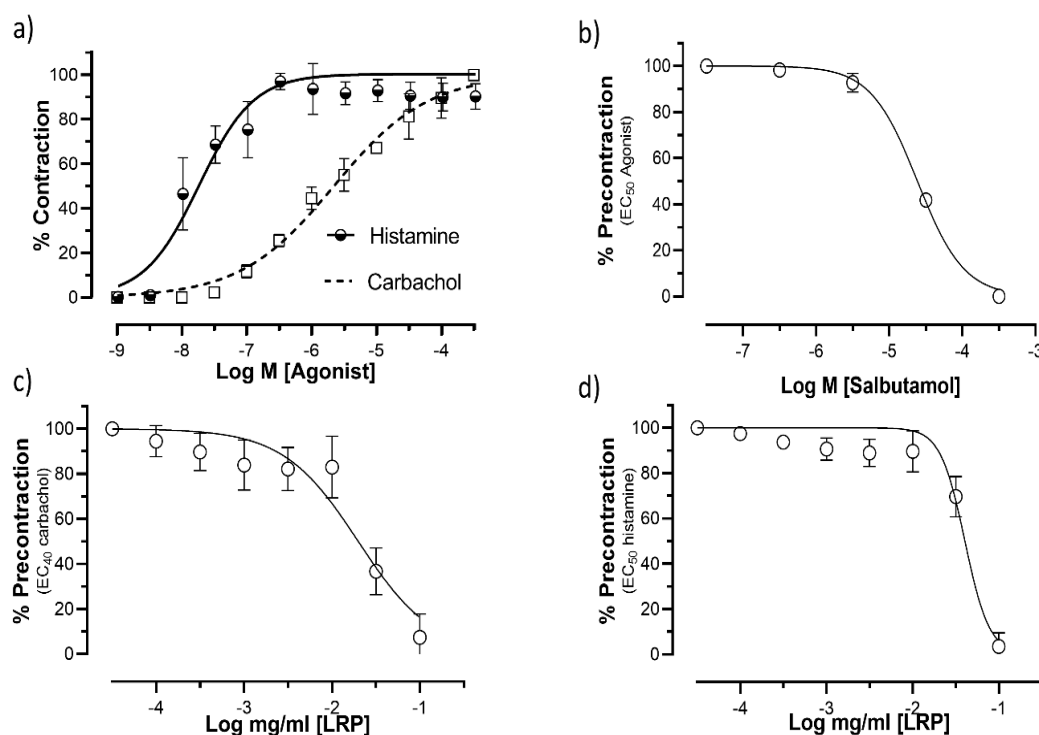
Figure 4.26   Effects of LRP on the contractile response of muscarinic and histamine receptors on GPT. **a)** Concentration-response curve of carbachol and histamine cumulative dose on GPT (n=12); **b)** Concentration-response curve of cumulative salbutamol against carbachol-induced contraction in GPT (n = 6); **c)** Concentration-response curve of cumulative LRP against carbachol -induced contraction in GPT (n = 8); **d)** Concentration-response curve of LRP cumulative against histamine -induced contraction on GPT (n = 8).

4.5.2   Antagonist (atropine, cimetidine) and β-agonist (salbutamol) relaxation response on GPT

Using the collected data, dose-response curves for the muscarinic-antagonists atropine and histamine-antagonist cimetidine were constructed and expressed as a percentage reduction in agonist pre-contraction achieved by 300nM (EC_{40} carbachol) and 1.24nM (EC_{50} histamine) contractions.

Atropine was observed to fully relax carbachol-induced contractions in a concentration-dependent manner. However, cimetidine partially relaxed the histamine-contracted GPT rings. Nonlinear regression analysis was used to determine the inhibition concentration at 50% (IC_{50}). The pIC_{50} values of atropine and cimetidine were calculated to be 3.537 and 2.116, respectively (Figure 4.27).
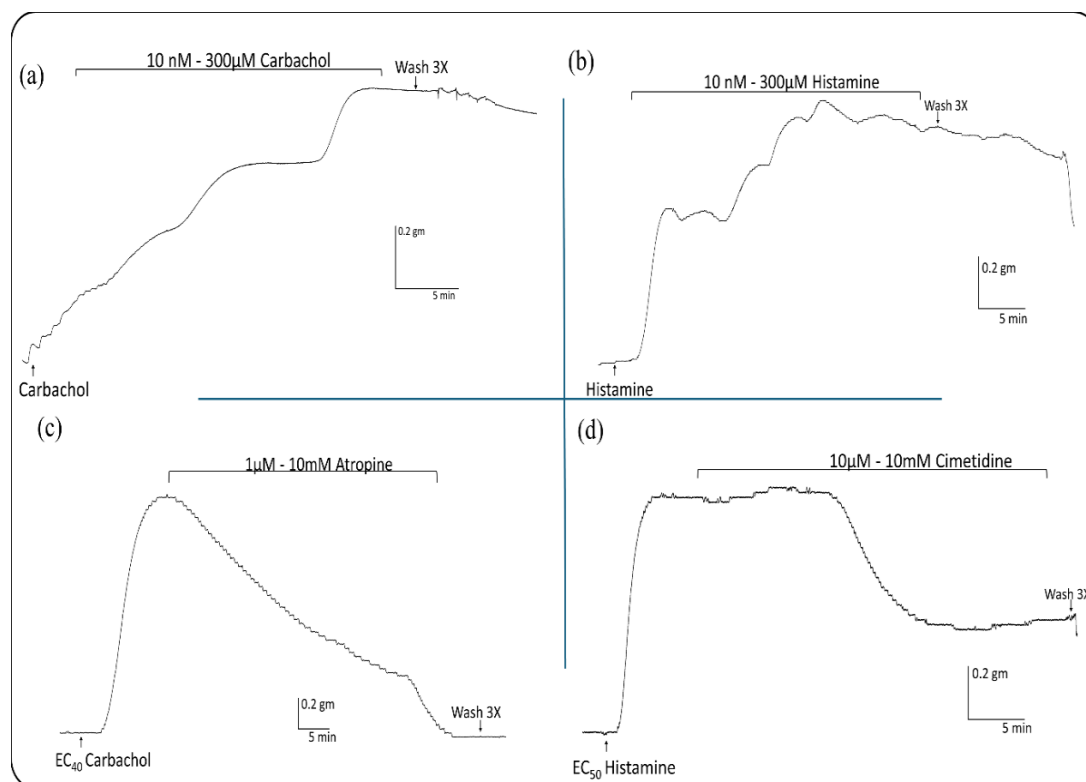
Figure 4.27   Real tracing of GPT agonist-antagonist contractility myograph (a) Real tracing of carbachol cumulative dose response on the GPT rings. (b) Real tracing of histamine cumulative dose response on GPT rings. (c) Real tracing of the atropine relaxation effect on isolated GPT pre-contracted with EC_{40} carbachol. (d) Real tracing of cimetidine relaxation effect on isolated GPT pre-contracted with EC_{50} Histamine.

4.5.3   Effect of LRP on contracted GPT

Similarly, the LRP dose-response curve was fitted using the obtained data, extrapolated as the percentage fraction reduction of the pre-contraction achieved by EC_{40} carbachol and EC_{50} histamine contractions. A comparison of LRP relaxation response was conducted with the receptor antagonists atropine and cimetidine to estimate the potency of LRP in relaxing the agonist-induced contraction of GPT. LRP

157

was observed to reduce the carbachol- and histamine- induced contractions in a concentration dependent manner. Non-linear regression analysis was used to calculate the pIC_{50} values, the LRP pIC_{50} was determined to be 1.702 for carbachol-precontracted GPT and 1.394 for histamine-precontracted GPT (Figure 4.28).

To investigate the involvement of β-receptors in LRP relaxation, GPT rings were pre-incubated with 30mM propranolol for 30 min for adequate blocking of GPT β-receptors, following which they underwent carbachol or histamine pre-contraction. Once stable contraction was achieved, 30 mg/ml LRP (IC_{50} LRP) was added, resulting in relaxation of the GPT rings, as depicted in Figure 4.29.

GPT rings were demonstrated to restore their resting tension after the washout procedure with Krebs solution, and tissue viability was still observed after the agonist contractions based on the tissue responses to 40 mM KCl.
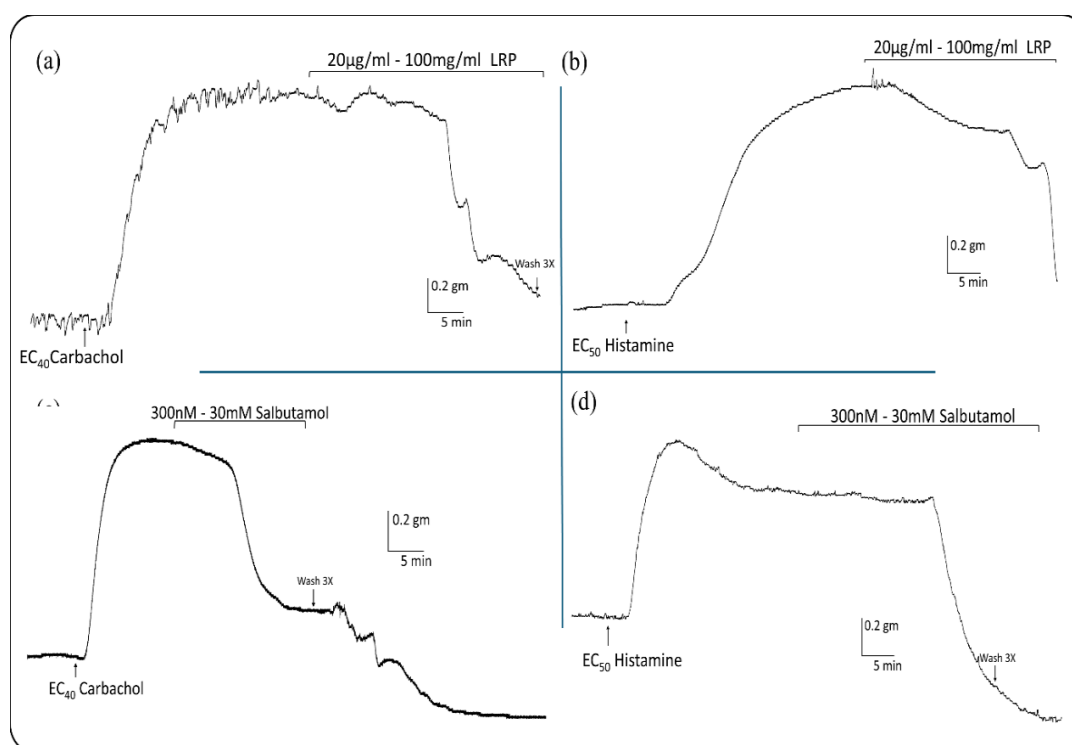
Figure 4.28   Real tracing of LRP on GPT contractility myograph (a) Real tracing of the LRP relaxation effect on isolated GPT pre-condensed with EC_{40} carbachol. (b) Real tracing of the LRP relaxation effect on isolated GPT pre-contracted with

EC$_{50}$ histamine. (C) Real tracing of the salbutamol relaxation effect on isolated GPT pre-contracted with EC$_{40}$ carbachol. (d) Real tracing of salbutamol relaxation effect on isolated GPT pre-contracted with EC$_{50}$ histamine.
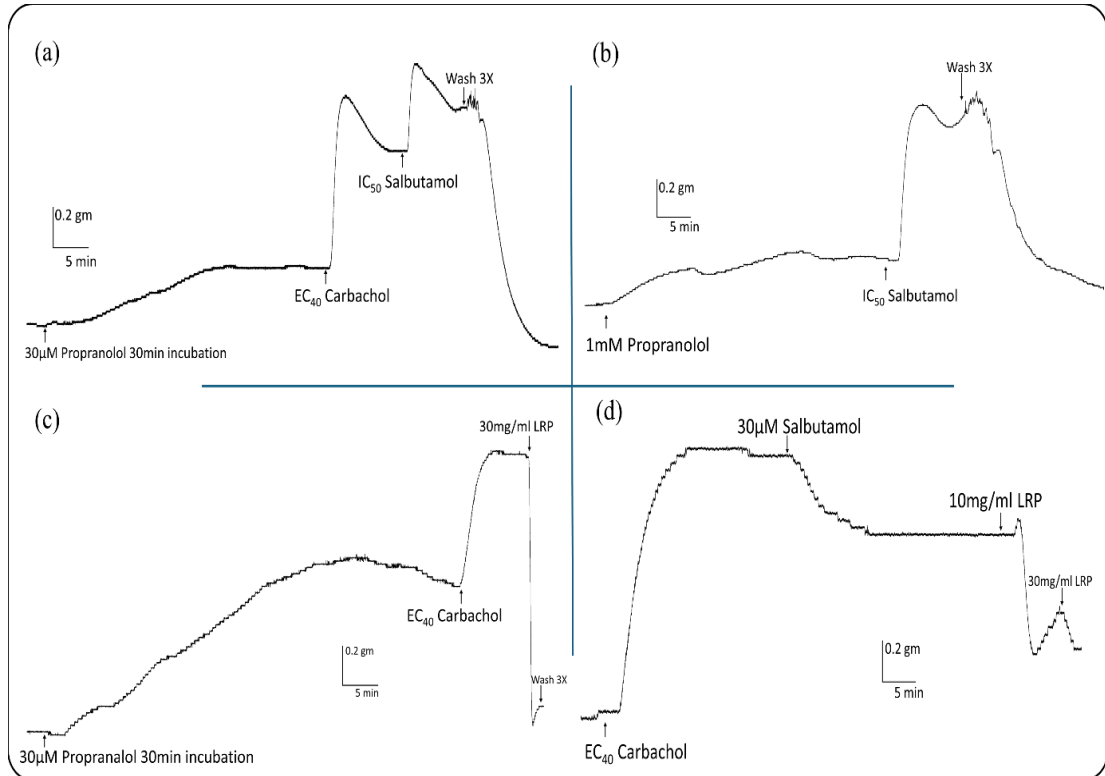
Figure 4.29   Real tracing of LRP and propranolol incubation on GPT contractility myograph (a) Real tracing of propranolol pre-incubation with EC$_{40}$ carbachol contraction on isolated GPT (b) Real tracing of propranolol pre-incubation effect on isolated GPT (c) Real tracing of LRP relaxation effect on isolated GPT pre-incubated with propranolol (d) Real tracing of salbutamol-LRP relaxation effect on isolated GPT pre-contracted with EC$_{40}$ carbachol

CHAPTER 5

DISCUSSION

This section discusses on the isolation of the LR polysaccharides, its inhalation formulation, the anti-asthmatic effects of inhaled LRP in an asthma model and its effects on GPT airway receptor contractility. The study evaluates the effect of LRP inhalation treatment on BALF inflammatory cells counts, lung inflammatory cells infiltration, mucus secretion, goblet cells hyperplasia, serum IgE, BALF levels of Th2 interleukins, and inflammatory genes expressions in an OVA-challenged asthma model.

Mushrooms contain a diverse array of phytochemicals, which exhibit numerous bioactivities. These fungi are rich in bioactive compounds such as polysaccharides, terpenoids, phenolic compounds, and proteins that contribute to various biological effects. One of the most prevalent and efficacious clinical applications of medicinal mushrooms is their utilization as dietary supplements for the prevention and treatment of immune system disorders, particularly in patients with compromised or suppressed immune function (Wasser, 2014). In particular, inflammation and oxidative stress have been implicated in various pathological conditions, and mushroom polysaccharide compounds have demonstrated broad-spectrum bioactivities in mitigating inflammation and oxidative stress. Mushroom polysaccharides exhibit antioxidant properties (Ahmad Usuldin *et al.*, 2020; Wang *et al.*, 2022) and have been demonstrated to reduce inflammation in various studies as well (Zheng *et al.*, 2020; Li *et al.*, 2024). Consequently, these extensive bioactive effects may contribute to the reported overall health benefits of MP.

Importantly, considering the traditional use of LR mushrooms in respiratory ailments and the significant bioactive role of MP, this study aimed to elucidate on the

bioactive compounds of LR and test its polysaccharide isolates exploring its alternative medicinal potential in asthma. The study builds upon previous research on the anti-asthmatic properties of the LR crude extract. This study represents an initial examination of the effect of LR polysaccharides on asthma pathophysiology and their nebulization for inhalation lung delivery in a murine asthma model.

5.1   LR extraction, isolation and β-D-glucan assays

5.1.1   Lignosus rhinocerotis extraction

Previous chemical composition studies on LR mushrooms have revealed that polysaccharides, proteins, peptides, and polysaccharide-protein complexes are major constituents of their sclerotia aqueous extracts, as well as low-molecular-weight secondary metabolites such as alkaloids, flavonoids, mucilage gum (Lau *et al.*, 2015), phenolics, and triterpenes (Lau *et al.*, 2013). The presence of alkanes, fatty acids, benzene, phenol, dicarboxylic acid, and high concentrations of linoleic acid indicated by GC-MS analysis were reported from LR sequential extract (Johnathan *et al.*, 2016).

Because MP macromolecules are attached to the mushroom cell wall, energy-efficient extraction methods are required to penetrate tight canals, solubilise, and extract these metabolites (Zhang *et al.*, 2016). Therefore, hot water extraction (HWE) is the most commonly used method for extracting polysaccharides from mushrooms. Hot aqueous extraction also offers the advantages of inexpensive operation and minimal equipment requirement (Parniakov *et al.*, 2014). In addition, a higher solvent-to-solid ratio is essential for creating concentration gradients that facilitate mass transfer, whereas elevated temperatures enhance molecular mobility, thereby increasing the molecular movement and material solubility (Prakash Maran *et al.*, 2017). An extraction yield of approximately 11.3% w/w from LR hot aqueous

extraction (LR-HA) has been reported to be significantly higher than that of the cold water extract (4.5% w/w) (Lau *et al.*, 2013). Similarly, soluble polysaccharides derived from the hot water fraction of LR (*Polyporus rhinocerotis* Cooke) exhibited antitumor activity against leukemic cell lines *in vitro*, demonstrating significant growth inhibition, whereas the cold isolates did not exhibit such inhibitory effects (Lai, Wong and Cheung, 2008). This suggests that high-temperature extraction provides superior extraction yield and bioactivity compared to cold extraction methods. Consequently, the selection of the hot aqueous Soxhlet extraction method from cultivated TM-02 powder for this investigation was based on previous literature on LR and MP extraction. In this study, following Soxhlet extraction, approximately 16.1% (w/w) of the crude LR extract was obtained from LR sclerotia powder, which is consistent with ranges previously reported for hot aqueous extractions of LR.

5.1.2 *Lignosus rhinocerotis* polysaccharides isolation

Previous studies have reported that LR-grown strains exhibited higher levels of protein and water-soluble components than the wild type and that their sclerotia powder contains a higher proportion of carbohydrates but a lower proportion of fat (Yap *et al.*, 2013). In this study, TM02 which is a standardised grown strain of LR sclerotia powder produced using proprietary solid-state fermentation technology was used. The phenol sulfuric test results revealed that the carbohydrate concentration of LR crude extract was 0.838 mg/ml (w/v), which increased to 1.920 mg/ml (w/v) in LRP. This significant increase in carbohydrate concentration from the crude extract to the fractionated polysaccharides fraction suggests that the fractionation process exerts a substantial influence on carbohydrate concentration. Conversely, a slight reduction in protein concentration was observed, with the protein concentration in crude extract being 0.090 ± 0.001 and subsequently decreasing to 0.081 ± 0.003 mg/ml (w/v) in the

fractionated LRP fraction. Comparable concentrations of carbohydrate (7.76±0.04 mg/g w/w) and protein (1.38±0.02 mg/g w/w) were also reported in cultivated LR sclerotia extracts of TM02 (Yap *et al.*, 2013). The high molecular weight (HMW) fraction of the LR cold water extract, fractionated by Sephadex G50 gel filtration, was reported to contain 79% carbohydrates and 4% protein by dry weight (w/w) (Lee *et al.*, 2014). Lee et al. (2012) reported that the high-molecular-weight Sephadex G-50 fractions of LR sclerotia predominantly contain carbohydrates (68.7%) and a small amount of protein (3.6%), whereas the low-molecular-weight fraction contains 31% carbohydrates and is devoid of protein. Hot water extracts of LR were reported to contain higher concentrations (mg/g w/w) of carbohydrate (130.50±7.35) and protein (392.50±3.13) than those obtained through cold water extraction (37.70±1.11) and (196.67±11.39) respectively (Lau *et al.*, 2013).

Mushrooms possess various types of polysaccharides which are predominantly acidic and neutral MPs (Gunasekaran, Govindan and Ramani, 2021; Liu *et al.*, 2022; Zhang *et al.*, 2023). Polysaccharides obtained through hot- or cold-water extraction are typically crude and contain multiple, structurally distinct polysaccharides (Smiderle *et al.*, 2017). In contrast, LRP exhibited a single virtually symmetrical peak elution profile of polysaccharides from the DEAE column and subsequent Sephadex G-50 column elution, indicating LRP homogeneity. The absence of polysaccharide detection with increasing NaCl concentration suggests a weak affinity of LRP for the positively charged DEAE-cellulose resin. Based on the observed elution behaviour, LRP was fractionated as a neutral water-soluble polysaccharide, consistent with other reported neutral mushroom polysaccharides elution (Gunasekaran et al., 2011; Gunasekaran et al., 2021; Liu et al., 2016; Song et al., 2018).

Numerous studies have explored various extraction methods, their optimization, and their impact on the resulting polysaccharide types and yields. For instance, polysaccharide yields obtained using ultrasonic enzyme assistance have been reported to be higher than those obtained using hot water, enzyme-, and ultrasonic-assisted methods (Li and Wang, 2016). Zhu et al. (2016) examined five different MPs extraction techniques (RWE, HWE, MAE, UAE, and CAE) and determined that MAE produced higher extraction yields; UAE application significantly increased *Agaricus bisporus* polysaccharide (ABPS) yields up to 155.08% higher than HWE at even lower temperatures and shorter extraction times (Tian *et al.*, 2012). It is crucial to recognize that no single extraction method is universally applicable for the general isolation of mushroom polysaccharides, or across species. Previous studies have shown that the polysaccharide yields from mushroom species vary significantly. These variations can be attributed to several factors but are mainly due to differences in specie, extraction and isolation methods.

Nevertheless, comprehensive reviews of MP extraction methods are available (Ruthes, Smiderle and Iacomini, 2015; Gong *et al.*, 2020), including emerging techniques in this field (Leong, Yang and Chang, 2021). Recently, green extraction methods for polysaccharide extraction, such as subcritical water technology, pressurized hot water, and deep eutectic solvents, may offer benefits such as improved yields, higher purity, lower energy costs, and environmental friendliness (Barbosa, 2023).

5.1.3 LRP monosaccharide composition and β-D-glucan assay

Polysaccharides are complex carbohydrates composed of multiple monosaccharide units linked by glycosidic bonds. Mushroom polysaccharides in particular are known for their unique composition and often contain special glucans,

especially β-glucans. β-glucans are of particular interest because of their potential bioactive properties. However, the extraction methods can significantly affect the yield and structure of the obtained polysaccharides. For instance, a peak resembling lentinan-like β-D-glucan was observed when extracted using hot water rather than in alkali LR extracts, suggesting a higher concentration of these compounds in LR hot water extracts. Although alkaline solutions may enhance β-D-glucan extraction, but possess the potential to alter the extracted MP, resulting in variations in retention time during column isolation and conformational changes to the MP structure (Mohd Jamil *et al.*, 2013). This underscores the importance of judiciously selecting extraction method and solvents to optimize both the yield and structural integrity of mushroom polysaccharides.

The most abundant polysaccharides in mushrooms are glycogen-like glucans, which function as storage components, whereas others are heteropolysaccharides rich in various monomers (Smiderle *et al.*, 2017). In this study, the HPLC results indicated that LRP contained 96.90% glucose as the predominant monosaccharide. Correspondingly, previous studies have elucidated the monosaccharide composition of LR, revealing that glucose constitutes more than 90% of its fractionated polysaccharide (Liu *et al.*, 2016; Lee, Li, *et al.*, 2018) . Additionally, minor quantities of galactose and mannose as well as certain pentoses such as fucose, xylose, and arabinose have been reported (Sum *et al.*, 2020). The findings of the present study demonstrated that LRP is a heteropolysaccharide composed of mannose, ribose, rhamnose, glucose, galactose, xylose, and arabinose monomers. LRP was determined to be a neutral, water-soluble polysaccharide-protein complex, and the fraction was obtained as a light yellowish powder, with a 7.3% yield of 7.6μg/mg w/w dry weight of the initial LR TM02 powder.

Meanwhile, for mushroom glucans estimation, McCleary & Draga, (2016) evaluated various acid- and enzyme-based techniques for glucan hydrolysis in mushroom samples. Enzymatic-based hydrolysis methods demonstrated substantially lower glucan values than those obtained through combined acid- and enzyme-based approaches, resulting in a significant underestimation of β-glucan content across all mushroom samples examined. Their findings indicated that the most efficacious method was H_2SO_4 hydrolysis, which yielded significantly better results than HCl, trifluoroacetic acid, and other enzyme-based procedures. In this study, the Megazyme kit was used to determine the total glucan and α-glucan contents of LRE, LRP, and a control sample. This methodology encompasses the sulfuric acid and enzymatic hydrolysis of glucans, followed by spectrophotometric quantification of liberated d-glucose in accordance with the manufacturer's protocol.

Abdullah et al. (2017) reported B-glucan content in various mushrooms, which they found to ranging from $0.51 \pm 0.11\%$ w/w in *Termitomyces heimii* extract to as high as $18.94 \pm 1.53\%$ w/w in *Pleurotus eryngii*. Their study also observed a correlation between the β-glucan content of mushrooms and their immunostimulatory effects, with those exhibiting higher percentages of β-glucan content demonstrating greater immunomodulatory properties. The results of present study demonstrated that total glucan content of LRE and LRP was 45.966 ± 1.797 and 42.588 ± 2.619 % w/w, respectively. LR extracts exhibited moderate β-glucan content, the β-glucan content of LRE was 17.452 ± 1.123 % w/w, which increased to 21.074 ± 2.193 % w/w in LRP after polysaccharides isolation. In support of this, glucan content of hot water LR sclerotium extracts was previously reported to be around 38.93 ± 9.65 (mg/g) (Lau *et al.*, 2013), and its fractionated polysaccharide *β*-D-glucan content was found to be approximately 33.950% (Mohd Jamil *et al.*, 2013). Utilising a similar megazyme

assay, Usuldin (2020) reported that the total glucan, α-glucan, and β-D-glucan contents from the mycelium of LR were determined to be 40.49 ± 5.7% (w/w), 4.19 ± 2.6% (w/w) and 36.3 ± 1.50% (w/w), respectively.

The LRP glucan assay indicated a substantial proportion of total glucans (42.588%, w/w). However, HPLC analysis demonstrated that 96.90% of monosaccharides were glucose. The portion of glucose that was not accounted for may have been present in association with other polysaccharides, proteins, or other compounds that were not detected in the glucan assay. Furthermore, the presence of small quantities of galactose, ribose, and mannose could be attributed to polysaccharides other than glucans or suggest the potential existence of glucan-branching structures involving these other sugars. After the isolation and purification of LRP from the aqueous LR extract, a pattern was observed, indicating an increase in polysaccharide levels, including β-glucan, while the protein content decreased.

In overall, mushroom polysaccharides containing β-glucans exhibit a broad spectrum of biological activities. These β-glucan-rich mushroom polysaccharides have shown potential in boosting natural defence mechanisms through their immunomodulatory effects. The extraction, isolation, and subsequent analysis of LRP revealed that it is a β-glucan-rich mushroom polysaccharide fraction. Subsequently, the effect of the fractionated β-glucan-rich LR heteropolysaccharide-protein complex on the pathophysiology of asthma was further examined.

5.2   LRP inhalation formulation

Targeted drug delivery involves the administration of a drug or therapeutic agent with a relatively higher specificity to certain tissues or organs than to others. The pulmonary drug delivery route offers several advantages, including direct drug

delivery to lung tissues with the ability to provide both local and systemic effects. PDD offers rapid absorption and onset of action, as well as the non-invasive nature of the approach and ease of administration of inhalable formulations (Jawahar and Gowtham, 2012; Kaur *et al.*, 2012; Da-Silva *et al.*, 2013). Also investigating the inhalation of phytochemical extracts may offer possible therapeutic benefits and applications for disorders of the respiratory system.

5.2.1   LRP dry powder formulation

Spray drying (SD) is a commonly employed technique for producing respirable powders that are suitable for pulmonary delivery. This study endeavour to formulate fractionated LRP into a dry powder using SD. In SD procedure, a solvent is used to dissolve desired solutes, and compressed gas (typically air or N_2) is used to disperse the liquid body through a nozzle into fine droplets that are subsequently dried, resulting in the formation of minute particles that are collected in a dry powder form (Sou *et al.*, 2013; Büchi, 2020). Upon incorporation into spray drying feed solution, lactose functions as a bulking agent to enhance spray-dried powder flowability, which is essential for filling and emptying the spray-drying device, as well as for inhalation deposition of the active therapeutic compound (Hebbink *et al.*, 2022). LRP was initially formulated as a dry powder for DPI using spray drying of two solutions: LRP only and LRP with lactose as the bulking agent. However, the spray-drying process was shown to be unsuitable for LRP owing to its volatility and hygroscopicity.

Spray drying offers the advantage of modifying composition of the feed solution with excipients that alter the properties of the dry powder formulation, thereby enabling the generation of diverse DPI formulations (Sou *et al.*, 2013). To address the hygroscopicity of the dry powder formulations, agents such as L-leucine, L-isoleucine, and L-phenylalanine (Chang *et al.*, 2014; Otake, Okuda and Okamoto, 2016) and

sodium stearate (Yu *et al.*, 2018) are added in formulations to achieve stable powder inhalations. In addition, Lakio et al. (2015) and Kaialy and Nokhodchi (2016) indicated that leucine improves spray-dried powder yields, enhances powder handling and aerosolization, and reduces powder moisture absorption. Therefore to address moisture-induced aerosol performance deterioration could be reduced by adding 10-20% (w/w) L-leucine to bulk powders (Li *et al.*, 2016). The principle behind is magnesium stearate and leucine are both soft lamellar waxy solids that attach to particle surfaces as coating additives and excipients in SD powder formulations (Lakio *et al.*, 2015). Specific to phytochemical extracts for DPI formulations, L-leucine has been reported to improve powder flowability, retain particle shape and integrity under moisture stress, and exert anti-caking effects (Chang *et al.*, 2014) by reducing the hygroscopicity of the powder and increasing the yield, these also enhances the recovery of spray-dried powder particles (Sou *et al.*, 2013). In this study, L-leucine was added to LRP powder formulation to address the aforementioned challenges of LRP hygroscopicity.

Afterwards, the melting point of the freeze-dried LRP powder was determined to be 97-99°C using a Gallenhamp melting point apparatus (SCS.0/M.07.A/10). Therefore, in a second attempt to overcome the initial challenges of the LRP DPI formulation, L-leucine was added to the solution to address the hygroscopicity problem and the inlet temperature was reduced to 105°C to address the volatility issue. However, the incorporation of leucine and the reduction in inlet temperature marginally decreased LRP powder agglomeration but failed to adequately address the issue of LRP volatility. Given that the solution contained water evaporating at 100°C, further reduction of the inlet temperature was avoided to ensure the proper desiccation of the produced powder. It was determined that the addition of agents such as leucine

to mitigate LRP powder hygroscopicity and lowering the spray-drying inlet temperature to reduce LRP powder volatility did not resolve the hygroscopicity and volatility challenges associated with the spray-dried LRP powder. Consequently, as LRP was obtained as water-soluble polysaccharides, it was deemed suitable for solution nebulization.

Despite the advantages of the SD method, spray-dried DPI formulation present challenges and drawbacks. The finding of LRP moisture absorption in this study was not unexpected, given that certain mono- and disaccharides, especially fructose, are known to promote hygroscopicity of SD powders (Feng *et al.*, 2022). Likewise, previous studies demonstrated that the hygroscopicity of L-arginine persists even with the addition of L-leucine (Lakio *et al.*, 2015), as L-leucine particle surface coverage may be insufficient for highly hygroscopic powders and may only provide short-term protection against moisture upon powder dispersion (Li *et al.*, 2016). Nevertheless, other studies have suggested the use of spray freeze-drying methods to dry volatile carbohydrate-protein formulations (Maa *et al.*, 1999; Liang *et al.*, 2018), and this method could be more suitable for powders that are sensitive to high temperatures (Chaurasiya and Zhao, 2021).

5.2.2   LRP nebulization characterization

Various methods and devices have been developed to characterise and determine the suitability of formulations intended for inhalation delivery. For this, inhalation formulation evaluation protocols and approaches have been standardised for various formulation types and devices, with prominent examples being those outlined in the United States and European pharmacopoeias products for inhalation. In this study, nebulised LRP aerosol deposition was characterised using a Next-Generation Impactor, in accordance with the protocol outlined in General Chapter 1601 of the

United States Pharmacopoeia. The NGI is a high-performance cascade impactor for classifying aerosol particles into size fractions for testing inhalation formulations and devices, including metered-dose inhalers, dry-powder inhalers, and nebulisers. The LRP solution was nebulized using a nebulizer and characterised for *in vitro* aerosol deposition on the NGI. LRP APSD were determined to be: Nebulisation Rate (3.33 ml/min), Fine Particle Fraction (62.84), Mean Median Aerodynamic Diameter (4.16), and Geometric Standard Deviation (1.83). Based on the obtained results, nebulization of the LRP solution produced aerosols within the inhalable range for lung delivery, as 1-5 μm size range for optimal inhalation (Verma *et al.*, 2011). FPF denotes the fraction of particles smaller than 5μm, this particle size exhibits a high probability of lung deposition, and particles of even smaller dimensions could penetrate further into the pulmonary region (Sheth, Stein and Myrdal, 2014), indicating that approximately 62.8% of LRP nebulised aerosols may be deposited in the deep lung.

An additional advantage of the nebulization inhalation delivery method is that nebulizers do not require any propellant, which could potentially compound or interfere with the extract activity, thus enabling the assessment of the bioactivity of phytochemical compounds in isolation. Consequently, the bioactive effects of LRP alone can be evaluated without the influence of other substances. In this study, inhalable LRP nebulisation was used to investigate lung delivery of LRP for pulmonary administration. Meanwhile, for laboratory animal inhalation studies, several previous investigations have employed nebulisation inhalation of a few milligrams of drug and extract compound solutions, such as 1 mg/mL salbutamol (Chang *et al.*, 2019), 1 mg/mL dornase alfa (Chang *et al.*, 2020), 2.5 mg/mL salbuterol (Song et al., 2016), 5 mg/ml salbutamol (Sarhan *et al.*, 2018), 10 mg/ml sodium fluoride (Adorni *et al.*, 2019) and so forth. For this study, a nebulizer feed

concentration of 4 mg/ml was utilized, which is within the range reported in previous nebulization studies and is deemed suitable for quantifying LRP depositions along the NGI. Overall, doses of nebulizer feed ranging from 1 mg/mL for potent compounds to 40 mg/mL for less potent compounds have been utilized for inhalation studies (Phillips, Zhang and Johnston, 2017).

5.2.3   Short-stability of LRP nebulization solution

The development of inhalation formulations presents certain challenges, a major one is assuring therapeutic delivery to target regions of the lungs, which can be addressed by optimizing the formulation and delivery system to produce particles with the required particle size and aerodynamic diameter on a consistent basis. Another challenge is the drug or compound stability within the formulation, where the therapeutic agent should be stable during the shelf life, during use, and throughout storage. Because the freeze-dried LRP powder was dissolved in the solution for nebulization, a short stability study was performed to determine the stability of the LRP solution under two different conditions: room temperature and 4°C. It was observed that the LRP solution remained stable at 4°C for up to 11 days, but degraded at room temperature over time, as evidenced by the cloudy appearance of the particle suspension, declining polysaccharide concentration, and pH of the solution stored at room temperature as early as day 3. Therefore, the LRP solution was found to be stable at 4°C for at least 11 days and possibly beyond. Subsequently, the effects of inhalable LRP nebulisation for pulmonary delivery on asthma pathophysiology in a murine OVA asthma model was investigated.

5.3 Anti-asthmatic effect of LRP in OVA-challenged asthma mice model

Asthma is associated with various airway disorders, including bronchoconstriction, vasodilatation, airway oedema, and activation of sensory nerve endings causing airway hypersensitivity (Barnes, 2016). The recognition and presentation of antigen derivatives to Th2 cells triggers Th2 secretion, which facilitates the activation and migration of eosinophils (Barnes, 2016; Athari *et al.*, 2017), mast cells, and basophils into the airways as well as the production of IgE (Caminati *et al.*, 2018). While the underlying mechanisms of asthma involve a complex interplay between genetic susceptibility and exaggerated immune reactions to environmental triggers, certain factors are recognized as crucial in initiating the characteristic pathological inflammatory response. Key environmental triggers such as air pollutants, pollen, and house dust mites exacerbate immune-mediated inflammatory processes in predisposed individuals.

Various medications for asthma are available and prescribed for quick relief and long-term control, including oral and intravenous corticosteroids for severe exacerbations. Additionally, some medications, such as biologics that target specific inflammatory pathways and gene therapies, are currently under development and investigation. However, long-term use of asthma medications such as systemic corticosteroids (SCS), which are essential for treating moderate-to-severe asthma, is associated with numerous adverse effects of tachycardia, anxiety, osteoporosis, cataract and cardiotoxicity (Newnham, 2001; Lefebvre *et al.*, 2015; Price *et al.*, 2018; Haida *et al.*, 2020). These concerns have prompted investigations into safe alternative and complementary anti-asthmatic measures to mitigate these exaggerated immune responses. Researchers have extensively investigated the polysaccharide content of numerous mushroom species and recognised their wide-ranging therapeutic potential.

Studies and reviews of mushroom polysaccharides (MPs) have been conducted using various *in vitro* and *in vivo* investigations, demonstrating their broad bioactivity, as evidenced in the literature (Ruthes, Smiderle and Iacomini, 2015, 2016; Wang *et al.*, 2017).

On the other hand, the use of a prevalent human allergen egg ovalbumin (OVA), makes OVA-challenged asthma models highly relevant to asthma research. Also, the ability of mice to exhibit differential responses between strains for a given antigen sensitization and challenge protocol, coupled with extensive knowledge of mouse genetics, makes mice asthma models suitable species for asthma research (Zosky and Sly, 2007). Therefore, among the animal models for studying allergic airway responses, mice have emerged as the predominant choice and are most frequently used for asthma studies. BALB/c mice exhibit a predisposition to allergic inflammation, demonstrates consistent T helper 2 (Th2)-biased responses and a propensity to produce high levels of OVA allergen-specific antibodies which are characteristic of human allergic asthma (Kodama *et al.*, 2010). These attributes render BALB/c mice a suitable model for studying asthma pathophysiology and evaluating potential treatments. OVA-challenged mouse models have been extensively utilised for decades, resulting in a substantial corpus of data and established protocols, thereby facilitating the straightforward interpretation of outcomes. Analogous to this study, ovalbumin asthma model has been effectively utilized to investigate a diverse range of potential asthma treatments, including natural phytochemical products (Li and Zhang, 2013; Kamaruzaman *et al.*, 2014; Bai *et al.*, 2019; Li *et al.*, 2021; Muhamad *et al.*, 2023).

Furthermore, Kim et al. (2019) compared intranasal and inhalation challenges in OVA mouse models of asthma and demonstrated that inflammation of pulmonary

vessels, alveolar ducts, alveoli, and Th2 cytokine levels were enhanced by inhaled OVA challenge compared with intranasal administration challenge. Ovalbumin's accessibility, cost-effectiveness all contribute to the model's viability and selection. In this study, to established an OVA-challenged asthma model, mice initially received three intraperitoneal OVA/aluminium hydroxide (100 µg/4 mg) sensitizations on days 0, 7, and 14, followed by OVA inhalation challenge and treatment (Jin et al., 2019; Song et al., 2023). In this study, OVA-challenged mice exhibited typical asthma characteristics, including airway inflammatory cell infiltration, goblet cell hyperplasia, elevated serum IgE levels, and increased BALF IL-4, IL-5, and IL-13 levels.

Dexamethasone (Dexa) is a commonly used glucocorticoid that exhibits potent anti-inflammatory and immunosuppressive properties, making it an ideal positive control for asthma studies such as those induced by OVA allergen. This corticosteroid drug has been extensively used in numerous asthma studies (Johnathan *et al.*, 2016; Yu and Chen, 2018; Muhamad *et al.*, 2023), and its inclusion here provides a reliable benchmark for comparing LRP effects in this study. Dexamethasone has been reported to exhibit a preference or greater specificity for inhibiting ovalbumin-induced asthma. Dexamethasone decrease number of eosinophils, airway inflammation, early asthmatic responses (EAR) and elevate levels of T helper (Th)2 cytokines in BALF compared to LPS- or combined OVA and LPS-induced asthma models (Lowe *et al.*, 2017; Yu and Chen, 2018). Dexamethasone was chosen in this study due to its proven efficacy in reducing airway inflammation, aligning with the specific objectives of the study in assessing the anti-asthmatic effect of the experimental compound LRP.

Among the various mushroom polysaccharides investigated, to date only a limited number of studies have examined the bioactive effects of LR mushroom polysaccharides, and minimal research has been conducted on the anti-asthmatic

bioactivity of LR. LR polysaccharides and polysaccharide-protein complexes have been proposed in previous studies as the primary active components determining LR bioactivity. For instance, LR β-glucan-rich polysaccharides have demonstrated antioxidant effects (Ahmad Usuldin *et al.*, 2020) and their antiproliferative activity has been shown to inhibit the growth of lung cancer and leukemic cell lines (Lai, Wong and Cheung, 2008; Lee *et al.*, 2012; Lai, Zainal and Daud, 2014; Jamil *et al.*, 2018).

Meanwhile, human pulmonary delivery requires particle aerodynamic sizes of 0.5 to 5 m, whereas the rodent upper respiratory tract cannot be penetrated by particles larger than 3 μm. Therefore, the particle size must be ≤3μm in investigating the biological effects of inhaled particulate matter in rodents (Asgharian *et al.*, 2014). Rodents, including rats, mice, and guinea pigs, have an oropharynx that does not connect to the lower airway due to the anatomical position of their epiglottis relative to the soft palate (Grimaud and Murthy, 2018). As obligate nasal breathers, these rodents in preliminary studies exhibit a physiological preference for nasal airflow, making the nasal route particularly relevant for assessing pulmonary drug delivery in these animals. Commonly used experimental PDD methods for laboratory animal aerosolization include nose-only and whole-body chamber exposure due to their physiological and non-invasive nature. These techniques allow for repeated and long-duration dosing without the need for sedation (Ehrmann *et al.*, 2020).

Comparative studies in rodents have shown that nasal administration results in higher lung depositions than whole-body chamber delivery (Oyabu *et al.*, 2015; Kogel *et al.*, 2021). Nasal delivery was chosen as the primary route of LRP administration in this study due to the selected animal model and its direct targeting of the respiratory tract, the primary site of asthmatic inflammation. The use of phytochemical extracts for inhalation presents a promising avenue of research with potential benefits in the

treatment of respiratory conditions. In this study, LRP-nebulised aerosols were examined in an OVA-challenged murine model to further elucidate it's *in vivo* anti-asthmatic effects. The administration of LRP to OVA-challenged asthmatic mice in this study employed the inhalation design of Kaur et al. (2020), which constitutes a simple, reliable, and cost-effective nose-only inhalation chamber for rodent nebulization.

Furthermore, nebuliser delivery offers the advantage of continuous generation of a respirable aerosol for an extended duration, which is essential for depositing an effective medication dose into the lungs of a spontaneously nose-only breathing animal in an inhalation exposure study (Snipes *et al.*, 1989).

5.3.1 Effect of LRP inhalation on BALF differential leucocyte count

Inflammatory cells play a pivotal role in asthma pathogenesis, with the characteristic mobilization and migration of inflammatory cells into the airways and peribronchiolar and perivascular regions (Curtis *et al.*, 1990; Barnes, 2016). This study evaluated the anti-inflammatory potential of LRP, examining the differential leukocyte count in the collected BALF of OVA-challenged asthmatic mice.

The results of this study demonstrated OVA group exhibited significantly higher eosinophil, lymphocyte, and macrophage counts in the BALF. However, neutrophil counts did not show significant differences among the experimental groups, except for the 4 mg/ml treatment group, which showed a slight reduction in neutrophil count. LRP and dexamethasone treatment significantly reversed the increase in eosinophil, lymphocyte, and macrophage counts in the LRP and dexamethasone groups. These results indicate that inhalation of LRP in an ovalbumin-induced asthma model could potentially ameliorate the elevated macrophage and eosinophil levels in

the BALF. These findings were further corroborated by the results of H&E and PAS staining of the lung sections from the experimental groups.

Similar studies on the anti-asthmatic effects of LR extract have been reported. Intranasal administration of LR crude extract significantly suppressed BALF inflammatory cells counts and CD4^{+} T-cells in lung draining lymph nodes in an OVA-challenged asthma model, in addition to ameliorating leukocyte infiltration (Muhamad *et al.*, 2019, 2023). LRE administration significantly reduced the number of eosinophils and neutrophils observed in BALF. Notably, a substantial decrease in FOXP3^{+} regulatory T lymphocytes was observed following OVA induction. However, these cells exhibited a significant increase subsequent to LRE treatment (Johnathan *et al.*, 2021).

5.3.2   Effect of LRP inhalation on serum IgE level

Serum IgE level is a well-established biomarker of allergic sensitisation and asthma pathogenesis. B-lymphocytes are a major source of IgE production in asthmatic airway inflammation (Lambrecht and Hammad, 2015; Barnes, 2016; Athari *et al.*, 2017; Lambrecht, Hammad and Fahy, 2019). IgE binds to high-affinity IgE receptors on activated mast cells and basophils, resulting in their infiltration into the airway surface and smooth muscle (Barnes, 2016). This study measured serum IgE levels in mice to evaluate their allergic response to OVA challenge. Enzyme-linked immunosorbent assay (ELISA) results demonstrated that OVA exposure significantly elevated serum IgE levels compared to the control group, indicating successful induction of allergic asthma. Conversely, dexamethasone and LRP treatment significantly reduced the serum IgE levels.

Previous studies have demonstrated that the administration of LR extract reduces serum IgE levels (Johnathan et al., 2016; Muhamad et al., 2019; Muhamad et

al., 2023). This effect can be attributed to the potential influence of the extract on B-cells function, possibly leading to a decrease in the production of IgE antibodies, which are implicated in allergic reactions.

5.3.3   Effect of LRP inhalation on BALF Th2 cytokines levels

Th2 inflammatory cytokines are key mediators involved in eosinophilic allergic asthma inflammation, and contribute to the promotion of airway eosinophil differentiation and recruitment. In OVA-sensitized asthma model, allergen exposure induced dendritic cells activation of Th-2 cells, leading to the release of IL-4, IL-5, and IL-13 cytokines (Shin, Takeda and Gelfand, 2009). This study measured IL-4, IL-5, and IL-13 levels in BALF by Luminex and ELISA assays to compare their levels between the study groups.

Bead-based multiplex immunoassays have been analyzed and presented based on either raw median fluorescence intensities (MFI) or derived absolute concentration values (ACV). However, a common problem of this assay is the selection of the appropriate standard dilution series; frequently, concentrations that are either excessively high or low cause unknown test samples to fall outside the range of the standard curve, resulting in large unbalanced datasets (Breen, Polaskova and Khan, 2015). In general, MFI produced significant differences, similar to those observed using absolute concentration values. Of great significance, MFI-based analysis could prove advantageous for extensive experimental or longitudinal studies employing multiple microtiter plates, as MFI has the potential to mitigate repeated-measure variability attributable to technician and instrument factors (Davis *et al.*, 2001; Breen, Polaskova and Khan, 2015; Sullivan, Gebel and Bray, 2017). Breen *et al.* (2015) studied the variance of MFI versus ACV, and demonstrated a background subtraction procedure to reduce the number of out-of-range values by 50%. They argued that MFI

is a more suitable choice than absolute concentration values for the analysis of protein expression, thereby offering higher statistical power, less reliance on analyte standards, and improved cost-effectiveness.

In this study, because a significant portion of BALF sample values fell below the standard curve, it was not feasible to extrapolate the absolute concentration values for the IL-5 and IL-13 quantitative analyses. Consequently, comparisons were conducted using MFI readings as relative indicators of the analyte abundance. The results demonstrated that OVA challenge significantly increased the BALF levels of IL-4, IL-5, and IL-13 compared with those in the normal control groups. Conversely, inhalation of LRP at 8 mg/ml and 40 mg/ml, as well as dexamethasone treatment, decreased BALF cytokine levels, therefore indicating the anti-inflammatory properties of LRP.

This finding aligns with previous studies that reported that the hot water extract of LR significantly ameliorated elevated serum IgE, Th2 cytokines IL-4, IL-5 and IL-13 levels, and eosinophil levels in BALF in an OVA-challenged asthma rat model (Johnathan *et al.*, 2016). LR crude extract significantly suppressed Th2 cytokine levels in BALF and serum IgE in an OVA-challenged asthma model (Muhamad *et al.*, 2019, 2023). Furthermore, administration of LRE significantly reduced the elevated levels of IgE in serum, as well as the cytokines IL-4, IL-5, and IL-13 in BALF (Johnathan *et al.*, 2021).

5.3.4 Effect of LRP inhalation on lung inflammatory gene expression

Asthma is a chronic inflammatory disease characterised by the release of several inflammatory cytokines and mediators that are crucial for the pathological inflammatory response. To evaluate the immunomodulatory effects of LRP, the study examined the expression of inflammatory cytokines IL-22, COX-2, iNOS, and the

asthma susceptibility gene ADAM33 using RT-qPCR. Expression levels were quantified using the $2^{-\triangle\triangle Ct}$ method, with all values normalized to the normal control group, using GAPDH as the reference gene. The findings showed the relative expression of COX-2, iNOS, IL-22 was significantly increased in OVA-challenged mice relative to the normal control group. This indicated enhanced signalling for inflammation in the mouse model, as evidenced by the elevated levels of inflammatory cytokine mRNA measured by qPCR.

Ovalbumin-induced asthma models have revealed significant changes in the expression of various inflammatory genes that contribute to the pathogenesis of allergic airway inflammation. Studies have demonstrated upregulation of genes associated with inflammatory mediators, cytokines, and cellular immune responses in these models. ADAM33 is implicated in the genetic predisposition to allergic hypersensitivity, airway inflammation, and asthma susceptibility. In this study, RT-qPCR results demonstrated that the expression of ADAM33 mRNA was slightly elevated in OVA-challenged mice compared with that in the control group, with a marginal difference in ADAM33 expression observed between the OVA and treatment groups. This finding aligns with that of a previous study that reported the modulation of several key genes, including ADAM33, as demonstrated by gene expression analysis in OVA-challenged asthmatic SD rats. PCR arrays revealed a significant increase in the expression of 16 genes associated with asthma, including IL17A, ADAM33, CCL5, IL4, CCR3, CCL22, and IFNG, following sensitization with OVA. However, these genes were downregulated after treatment with LRE (Johnathan *et al.*, 2021).

Although there is limited research on the effect of LR extracts on asthma model inflammatory gene expression, the effects of other extracts on OVA-challenged asthma models have been reported in the literature. As demonstrated in the literature, COX-2 and iNOS gene expression is significantly affected in OVA-challenged asthma models. Chestnut inner shell extract (CIE) attenuated OVA-challenged airway inflammation in the mouse model. The expression of COX-2, iNOS, and matrix metalloproteinase-9 (MMP-9) was sequentially decreased in lung tissues. This attenuation occurs through the inhibition of NF-κB phosphorylation, subsequently reducing the expression of iNOS and COX-2, which ultimately leads to decreased MMP-9 expression (Kim *et al.*, 2022). Previous study utilizing the flavonoid compound Tilianin demonstrated that the expressions of TGF-β1, iNOS, and COX-2 were significantly suppressed by Tilianin in ovalbumin (OVA)-challenged asthma in mice. Furthermore, Tilianin treatment substantially reduces the levels of IL-4, IL-5, IL-13, IFN-γ, eotaxin, and IgE (Zhang *et al.*, 2022).

5.3.5 Effect of LRP inhalation on lung inflammatory cells infiltration and goblet cells hyperplasia

Inflammatory cells are pivotal in asthma pathophysiology, particularly in allergic asthma, once activated, these cells release numerous inflammatory mediators including leukotrienes, prostaglandins, and interleukins, which sustain the inflammatory response (Fahy, 2015; Barnes, 2016; Lambrecht, Hammad and Fahy, 2019). Histopathological examination of the lung tissue remains important for evaluating asthma-induced airway inflammation, mucus secretion, and goblet cells hyperplasia. To assess the extent of airway inflammation and mucus hypersecretion, mouse lung tissue sections were stained with haematoxylin and eosin (H&E) and periodic acid-Schiff (PAS). The present study demonstrated that OVA challenge

significantly promoted airway inflammation and mucus hypersecretion compared with the normal control group. However, inhalation of dexamethasone and LRP significantly reduced lung inflammatory cells infiltration and goblet cells hyperplasia.

Previous studies have demonstrated that the administration of LRE mitigated the histological alterations induced by OVA in rats by reducing pulmonary inflammation, excessive mucus production, and goblet cell proliferation (Johnathan *et al.*, 2021). Similarly, LRE also diminished the infiltration of eosinophils and hyperplasia of goblet cells in lung tissues. Furthermore, it ameliorated airway remodeling by reducing smooth muscle thickness and decreasing the expression of TGF-β1 and Activin A positive cells in lung tissues (Muhamad *et al.*, 2019, 2023).

A notable finding in the H&E-stained sections was the presence of a perivascular inflammatory infiltrate, which exhibited greater prominence around pulmonary vessels than around airways. The staining results indicated that the OVA-challenged group exhibited a pronounced perivascular and peribronchial inflammatory infiltrate, characterized by marked inflammatory cells layers and increased goblet cells as well as mucus production inside the airways. The distribution pattern of inflammatory cells infiltration surrounding the airways demonstrated heterogeneity, with airways in close proximity to blood vessels displaying a higher frequency of inflammatory cells rings. This observation suggests a potential association between vascular inflammation and airway involvement, wherein inflammatory cells may migrate from the vasculature to the airway epithelium. In contrast, the LRP and dexamethasone treatment groups demonstrated a significant reduction in mucus production and inflammatory cells infiltration, with mild-to-moderate perivascular and peribronchial inflammations. In some lung tissue spots only patchy or incomplete rings of inflammatory cells were observed around the airways, as illustrated in

representative images (Figure 4.23) and quantified using semiquantitative scoring (Figure 4.22).

Furthermore, in this study, histopathological examination revealed a mixed inflammatory pattern characterised by both acute and chronic features. The predominance of eosinophils and lymphocytes within the inflammatory infiltrate indicated an acute phase. The presence of giant cells, macrophages, plasma cells infiltration, and mitotic figures suggested a chronic inflammatory response. However, the airway epithelium was observed to remain intact with no evidence of epithelial flattening or significant damage, which is typical of the acute exposure model utilized in this study.

5.3.6   The anti-asthmatic effect of LRP inhalation

In this study, OVA-challenged mice exhibited typical asthma characteristics, including airway inflammatory cell infiltration, goblet cell hyperplasia, elevated serum IgE levels, and increased BALF IL-4, IL-5, and IL-13 levels. Inhalation of LRP and dexamethasone attenuated these asthmatic inflammatory changes in the treatment groups. The observed ameliorative effect of LRP on immunohistopathological changes in this study was consistent with previous research findings on the anti-asthmatic effect of LR extracts, which reduced serum IgE levels and significantly suppressed the counts of inflammatory cells in BALF, as well as Th2 cytokines(Muhamad *et al.*, 2019, 2023; Johnathan *et al.*, 2021). Additionally, LRE ameliorated airway remodelling by decreasing smooth muscle thickness and reducing the expression of TGF-β1 and Activin A-positive cells in lung tissues (Muhamad *et al.*, 2019, 2023; Johnathan *et al.*, 2021). A related study revealed that honey inhalation (50% solution) treatment successfully suppressed OVA-challenged airway inflammation by mitigating asthma-related histological changes in the airway, effectively reducing hyperplasia of mucus-

producing goblet cells, and preventing asthma onset in a rabbit asthma model (Kamaruzaman *et al.*, 2014).

The bioactivities of mushroom polysaccharides have been extensively investigated in the literature with various receptor targets and mechanisms proposed for MPs; the most commonly reported MP-interacting receptors include Dectin-1 receptors (Lee and Hong, 2011; Lee and Kim, 2014), toll-like receptors (TLR-2,-4,-6) (Li *et al.*, 2021), and complement receptor 3 (CR3) (Barsanti *et al.*, 2011). These PRRs are widely present in innate immune cells (Kim *et al.*, 2000), and could be a possible rationale immunomodulation remains a central bioactivity of many MPs *in vivo* bioactive effects. MPs exert immunomodulatory effects by enhancing various immune functions, including increasing lymphocyte proliferation (Pan *et al.*, 2015; Hu *et al.*, 2015; Jeff *et al.*, 2016; Zhu *et al.*, 2016; Gao *et al.*, 2022), macrophage activity (Hu *et al.*, 2015; Yang, Liu and Zhang, 2019), spleen and thymus indices (Chai *et al.*, 2013; Fang *et al.*, 2016; Awadasseid *et al.*, 2017; Liu *et al.*, 2019; Sun *et al.*, 2021). These effects are thought to be mediated via TLR4 (Fang *et al.*, 2016; Tian *et al.*, 2019) and Dectin-1/Syk/NF-κB pathways (Fang *et al.*, 2012). Given that LR extract and mushroom polysaccharides have been reported to exhibit anti-inflammatory effects, it is plausible that the anti-asthmatic effects of LRP are closely associated with the known anti-inflammatory and immunomodulatory properties of LR mushroom and its mushroom polysaccharides.

In addition, the literature has documented the anti-asthmatic effects of other mushroom polysaccharides and protein fractions. Abdelmawgood et al. (2024) demonstrated that chaga mushroom alkali-extracted β-glucan substantially suppressed IgE production, airway inflammation, and the infiltration of inflammatory cells in a mouse model of OVA-challenged asthma. The study reported that the anti-asthmatic

effect of chaga mushroom β-glucan was also involved in suppressing the infiltration of CD8$^+$ T cells and oxidative stress, suggesting the potential involvement of CD8$^+$ T lymphocytes in allergic asthma pathophysiology. Also, LR hot aqueous extract has been reported to suppress CD4$^+$ T-cells counts in lung-draining lymph nodes (Muhamad *et al.*, 2019). The observed effects of LRP can be attributed to its immunomodulatory and anti-inflammatory effects, LR extracts likely inhibits the activation and differentiation of Th2 cells, which are key mediators of allergic inflammation that produce cytokines responsible for recruiting inflammatory cells into the lungs. Also, orally administered fungal immunomodulatory protein (FIP-fve) isolated from *Flammulina velutipes* has demonstrated anti-asthmatic effects. This protein inhibits lung inflammatory cells infiltration, reduces OVA-specific IgE levels in the serum, and significantly decreases the secretion of cytokines and chemokines in BALF by Th2 cells (Lee *et al.*, 2013; Wu *et al.*, 2020). Lee et al. (Lee *et al.*, 2014) reported protein fractions of LR cold water extract exhibit substantial anti-inflammatory activity that significantly inhibits TNF-α production. Likewise, the hot water extract of the LR sclerotia polysaccharide-protein complex demonstrated distinctive immunomodulatory effects by eliciting a significant increase in spleen weight in both healthy BALB/c mice and healthy athymic nude mice through innate immune cells and T-helper cells activation (Wong, Lai and Cheung, 2011).

Considering the reported literature that mushroom beta-glucans and LR extract effects lead to suppression of CD4$^+$ and CD8$^+$ T lymphocytes(Muhamad *et al.*, 2019; Abdelmawgood *et al.*, 2024), and given the observed attenuation of goblet cell hyperplasia, the observed suppression of Th2 cytokines in BALF, and decreased lung airway inflammation by LRP, as demonstrated in this study, the anti-asthmatic mechanism of LRP can be ascribed to the suppression of cellular immune responses

in the ovalbumin mouse model. These are likely the mechanisms underlying the anti-asthmatic effects of LRP demonstrated in this study. Moreover, considering the reported anti-inflammatory effects of LR protein fractions (Lee *et al.*, 2014), the synergistic effects of LR proteins and polysaccharides in LRP cannot be excluded as components of the anti-asthma mechanism.

Furthermore, oxidative stress has been implicated in the pathophysiology of asthma, wherein the excessive production of reactive oxygen species (ROS) is associated with inflammation. Studies have reported the antioxidant properties of LR mushrooms, which contain antioxidant effects. LR extracts demonstrate antioxidant properties by decreasing intracellular ROS through the DAF-16/FOXO pathway in juglone-induced oxidative stress in *Caenorhabditis elegans* (Kittimongkolsuk, Roxo, *et al.*, 2021). LR-isolated glucans exhibit significant antioxidative properties, as demonstrated by DPPH and ferric-reducing assays (Usuldin, 2020). These factors may contribute to the potential anti-asthmatic effects of LR extract and LRP reported.

Meanwhile, comparing positive control animal group that received inhaled dexamethasone with those given systemic dexamethasone from the pilot study, it was observed that intraperitoneal dexamethasone administration demonstrated greater efficacy than inhaled dexamethasone. In support of this, Lowe et al. (2017) reported that combined OVA and LPS–induced functional and inflammatory responses are insensitive to inhaled dexamethasone but are partially sensitive to systemic dexamethasone. The study highlights that the route of corticosteroid administration is significant in determining the corticosteroid sensitivity of asthmatic responses (Lowe *et al.*, 2017). Inhaled CS treatment is less curative, as airway inflammation, Th2 effector cells function, and eosinophils reappear when therapy is discontinued in an OVA-challenged asthma mouse model (Kerzerho *et al.*, 2011). While inhaled

corticosteroids are a cornerstone of asthma management, the study findings, coupled with previous literature, suggest that inhaled dexamethasone may exhibit reduced efficacy compared to systemic dexamethasone administered intraperitoneally. This discrepancy may be attributed to pharmacokinetic factors such as airway first-pass metabolism, low-dose nature of inhalations, and incomplete lung deposition, as well as potential pharmacodynamic differences in inhibiting inflammatory cells migration to the lung and the signalling pathways. Therefore, further investigation is warranted to elucidate the underlying mechanisms and optimise inhaled corticosteroid therapy in OVA-challenged asthma models.

In summary, the pronounced inflammatory response observed in the OVA-challenged group aligns with previous studies on OVA-challenged allergic airway inflammation, characterized by the infiltration of inflammatory cells, such as eosinophils and lymphocytes, into the airway wall, a hallmark feature of allergic asthma (Lowe *et al.*, 2017; Yu and Chen, 2018; Jin *et al.*, 2019; Song *et al.*, 2023). The patchy or incomplete rings of inflammatory cells observed in the treatment groups may indicate partial resolution of the inflammatory process, and that LRP modulates the inflammatory response, corroborating the anti-inflammatory bioactivity of LRP. The results indicate that LRP has a significant anti-inflammatory effect on asthma pathogenesis, as evidenced by the suppression of serum IgE, lung inflammatory cells infiltration, BALF Th2 cytokine levels, and lung inflammatory gene expression, with more pronounced positive outcomes observed in the 8 mg/ml and 40 mg/ml LRP groups.

5.4 Effect of LRP on guinea pig trachea contractility

The pathophysiology of asthma is multifactorial involving several pathway mechanisms. Therefore, asthma management employs various medications, including antimuscarinics, antihistamines, beta-agonists, corticosteroids, and leukotriene receptor antagonists (GINA, 2024) as preventive medications and symptom relievers. Muscarinic and histamine receptors play significant roles in the pathophysiology of asthma by influencing airway smooth muscle tone, inflammation, and hyperresponsiveness. Moreover the E-prostanoid receptor (Säfholm *et al.*, 2015), Cysteinyl LT receptor 1 (Okunishi and Peters-Golden, 2011), and the downstream central role of phosphodiesterase (PDE) (Rehman *et al.*, 2022) have been identified to influence airway contractility. Consequently, the regulation of airway contractility, particularly in asthma-related conditions with complex regulatory mechanisms involving interacting receptor pathways and intertwined biological processes, presents challenges in identifying specific targets or attributing particular responses to definitive effects that influence this autonomous process.

Notwithstanding the complexity, airway bronchoconstriction is a cardinal symptom of respiratory diseases such as asthma, limiting breathing, and oxygen distribution in the body; thus, bronchodilation agents play a vital role in these respiratory conditions. To determine and measure muscle contractility, myography assess *ex vivo* muscle responses to various agents and stimuli, whereby their pharmacological responses are evaluated to compare the bioactivity and potency of these agents in determining the therapeutic role of drugs and phytochemical extracts.

Considering the traditional use of LR in respiratory illness (Nallathamby *et al.*, 2018; Tan, Leo and Tan, 2021), its reported anti-asthmatic effects (Johnathan *et al.*, 2016; Muhamad *et al.*, 2019), and the need for natural alternatives to mitigate the

adverse effects of long-term dependency on asthma drug medications. This study evaluated the bioactivity of the LR polysaccharides fraction on airway contractility, with a specific focus on airway muscarinic, histamine, and beta receptors, which are major pathway receptors involved in airway contractility and are significantly implicated in the pathophysiology of asthma.

The influence of muscarinic receptors on airway smooth muscle contraction is predominantly mediated by M_3 via Phospholipase C (PLC) and Inositol Phosphate activation for intracellular Ca^{2+} release and protein kinase C (PKC) activation for diacylglycerol formation, all together causing airway constriction (Dale *et al.*, 2014). In this study, a dose-dependent increase in the contraction of the GPT rings was observed in response to series of increasing carbachol concentrations. Stimulation of airway histamine receptors also induces airway contractions. Airway histamine receptors are largely H_1 receptors that stimulate airway contraction via inositol-trisphosphate (IP3) activation and subsequent Ca^{2+} release (Dale *et al.*, 2018; Ince and Ruether, 2021). Similar dose-dependent GPT contractions were observed in response to increasing histamine concentrations in the organ bath chamber (Figure 4.26). Thus, these tissue responses to carbachol and histamine imply the presence and function of muscarinic and histamine receptors in the GPT airway tissue, as previously reported (Dudášová *et al.*, 2013; Vasconcelos *et al.*, 2019; Chen *et al.*, 2020). Furthermore, carbachol elicited more pronounced airway contractions than histamine, while comparing both pEC_{50} values, histamine exhibited greater potency as a bronchoconstrictor in the GPT airways than carbachol.

On the other hand, airway β-receptors influence the relaxation of airway smooth muscles; β-receptor relaxation pathway is mediated via cAMP activation and protein kinase A (PKA) (Dale *et al.*, 2018). In this study, the carbachol-contracted

GPT rings were fully relaxed by atropine, salbutamol also caused relaxed the carbachol- and histamine-contracted GPT rings (Figure 4.27). Other studies have reported atropine antagonises muscarinic receptor stimulation causing airway relaxation in GPT (Xiao *et al.*, 2009; Mans *et al.*, 2015; Menchi *et al.*, 2022),.

For cimetidine, a partial relaxation of the histamine-contracted GPT ring was observed, more so as it being a H_2 antagonist than to H1 histamine receptors. Meanwhile, more potent antihistamine relaxation was reported with chlorpheniramine (Mans *et al.*, 2015) to relax histamine pre-contraction of the GPT rings. In comparison, atropine and salbutamol showed more potent GPT relaxation than cimetidine. Altogether, the contraction response to carbachol and histamine, and the relaxation response to atropine, cimetidine, and salbutamol substantiate the presence and influence of muscarinic, histamine, and beta receptors on GPT ring contractility, and further support the suitability of GPT in airway receptor studies, as previously reported (Vasconcelos *et al.*, 2019; Adner *et al.*, 2020).

For alternative medicinal purpose, which is widely gaining recognition, mushrooms have been a source of organic remedies, with many mushroom species being considered based on their traditional use and proven bioactivity. In this study, the LRP fraction caused relaxation of the carbachol- and histamine-precontracted GPT rings (Figure 4.28). Similarly, other organic extracts, such as fenchone, *Aster tataricus*, *Napoleona vogelii* and Surinamese (Mans *et al.*, 2015; Adejayan *et al.*, 2019; Chen *et al.*, 2020; Rehman *et al.*, 2022), have been reported to relax muscarinic contracted airways in normal and diseased animal models in *ex vivo* myography studies. Prior study has demonstrated that the administration of LRE at various concentrations (125, 250, and 500 mg/kg) effectively reduced methacholine-induced airway resistance and AHR in mice exposed to house dust mites (HDM), as measured by whole-body

plethysmography (Johnathan *et al.*, 2021). Furthermore, to determine whether LRP relaxation occurs through a beta receptor influence, beta-receptor blockage was first verified with a 30 min propranolol incubation. LRP caused relaxation of the GPT rings, even with beta receptor blockage (Figure 4.29).

Finally, in asthma management, corticosteroids play a central role in reducing the markers of type-2 inflammation (GINA, 2017; Busby, Khoo, Pfeffer, Mansur, & Heaney, 2020), whereas β-2 receptor agonists and muscarinic receptor antagonists are essential for reducing bronchoconstriction and improving lung function in asthma. It is determined from results of this study that LRP influences GPT airway contractility, possibly by antagonising muscarinic and histamine receptors independent of β-receptors influence, comparison of the LRP pIC_{50} values, LRP demonstrated superior antihistamine receptor potency relative to its antimuscarinic activity.

The safety of both LR mycelial and sclerotia extracts has been corroborated by several studies. LR has been known to be consumed as food and traditional medicine, its non-toxicity has been studied and reported. Jhou *et al.* (2017) reported that rats exposed to doses of up to 3400 mg/kg/day of LRE did not display any adverse reproductive or developmental effects. Prior studies have demonstrated that chronic exposure study (180 days) conducted on rats at LR extract doses exceeding 1000 mg/kg revealed no observable adverse effect level (NOAEL) for fertility, teratogenic, or genotoxic effects (Lee *et al.*, 2013). Thus, in light of the advantages associated with direct pulmonary administration, the demonstrated anti-asthmatic efficacy of LRP inhalation, and the LRP airway receptor effects elucidated in this investigation, coupled with its established safety profile, this study suggest that LRP inhalation may offer potential as a complementary therapeutic approach in asthma management.

5.5　Significance of the study findings

This study demonstrated the isolation of LR polysaccharides and its inhalation formulation, and elucidated the effects of LRP inhalation on airway inflammation and airway relaxation in an OVA-challenged murine asthma model and guinea pig trachea. Treatment with inhaled LRP (8 and 40 mg/ml) attenuated OVA-induced airway inflammation, reduced serum IgE, BALF Th2 cytokine levels, and lung inflammatory gene expression in an OVA-challenged asthma mouse model. LRP induces GPT airway relaxation, which is independent of beta receptors, potentially via muscarinic and histamine receptor antagonisms. The present study indicates a potential anti-asthmatic effect of LRP on allergic asthma airway inflammation, supporting the management of respiratory disorders, such as asthma. The study highlights the polysaccharides as significance phytochemical constituent of LR responsible for its anti-asthmatic effects. These findings may contribute significantly to future clinical investigations of the potential of LRP formulation as an adjunctive therapy in asthmatic individuals. Figure 5.1. summarise and illustrates the findings of this study.
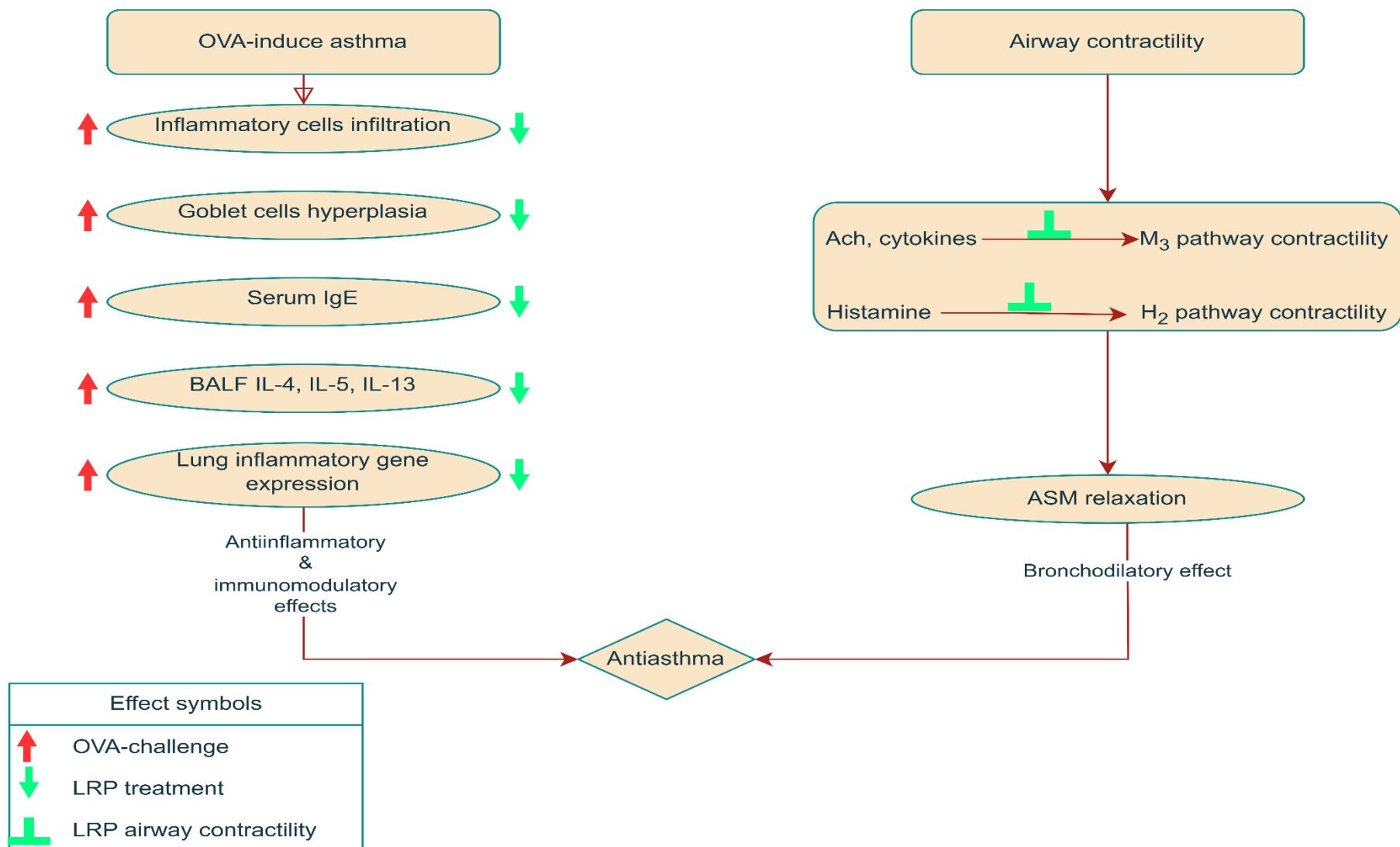
Figure 5.1   Summary of the study findings.

CHAPTER 6

CONCLUSION, LIMITATIONS AND RECOMMENDATIONS

6.1   Conclusion

LRP was fractionated as a water-soluble neutral polysaccharide-protein complex. Its carbohydrate concentration increased from 0.838 ± 0.01 mg/ml in the crude extract to 1.920 ± 0.02 mg/ml in LRP. Conversely, the protein concentration decreased slightly from 0.090 ± 0.001 to 0.081 ± 0.003 mg/ml, a change that was not statistically significant. The megazyme β-glucans assay revealed that the percentage of α- and β-glucans in LRE were 25.847 ± 2.397 % and 17.452 ± 1.123 %, respectively, whilst those in LRP were 21.515 ± 0.531 % and 21.074 ± 2.193 %, respectively

The LRP spray-dried powder formulation was volatile and hygroscopic, rendering it unsuitable for optimal DPI use. Nebulisation of LRP in solution form produced aerosols with a mass median aerodynamic diameter (MMAD) of 4.16 μm and a 62.8% fine particle fraction, thus falling within the inhalable range for lung delivery. Ovalbumin sensitisation and challenge result in airway inflammation characterized by infiltration of inflammatory cells and goblet cell hyperplasia, increased serum IgE and Th2 cytokine (IL-4, IL-5, IL-13) levels in BALF. The expression of COX-2, iNOS, IL-22, and ADAM33 in the lung tissue was significantly elevated in OVA-challenged mice, indicating enhanced signalling for inflammation. Treatment with inhaled LRP (4, 8, and 40 mg/ml) for 30 min attenuated airway inflammation in a dose dependent manner, with 8 and 40 mg/ml treatment groups expressing the most significant effect.

Furthermore, LRP induces GPT airway relaxation, which is independent of beta receptors, possibly via muscarinic and histamine receptor antagonisms.

6.2   Limitations and Recommendations

This study was limited to hot aqueous LR extraction, and it is important to note that different extraction methods can yield varying yields and properties of extracted compounds. Therefore, future studies should consider other extraction methods and employ optimization techniques, such as the Box-Behnken design and response surface methodology, to improve extraction efficiency.

It has been postulated that the presence of certain mono- and disaccharides, particularly fructose, promotes hygroscopicity in spray-dried powders, as observed for LR polysaccharides. Previous research has suggested the use of spray freeze-drying methods for drying volatile carbohydrate-protein formulations. Given that this study employed conventional spray drying, which proved inadequate, as evidenced by the LRP volatility and hygroscopic nature, alternative drying methods such as spray freeze-drying are recommended for future investigations. Future studies should explore the use of stabilizers, such as amino acids, cyclodextrins, and buffering agents, to improve LRP nebulisation solution stability. In addition, the inhalation study was conducted on small animals, specifically mice, considering that only low-MMAD particles will be deposited and reach the lungs. Therefore, the utilization of larger animal models, such as the rabbit asthma model, is recommended in future studies to achieve higher lung deposition and improved bioactive effect performance of nebulized LRP. Another limitation of the present study was the inability to further elucidate the involvement of other asthma-related genes responsible for asthma predisposition, such as ADAM8, RORA, ORMDL3, and GATA3. However, this limitation needs to be addressed in future studies.

Furthermore, this investigation focused on the specific receptors involved in airway smooth muscle contraction, the LRP bronchorelaxation study are limited to

muscarinic, histamine, and beta receptor regulation of airway smooth muscle tone. Considering the possibility that other mechanisms may contribute to the bronchodilator effects of LRP, future studies should explore additional potential mechanisms, such as the involvement of other airway contractility pathways and modulation of ion channels.

Meanwhile, formulation and delivery methods can significantly influence the efficacy and bioavailability of LRP, and formulating LRP into nanoparticles or other delivery systems to enhance its therapeutic potential is recommended. Considering its anti-asthmatic effects, it is recommended to explore the development of LRP-based therapeutic formulations.

In conclusion, the findings of this study underscore the need for further research to fully optimize the formulation and delivery of LRP and to elucidate the therapeutic potential of LRP as a natural source to support the management of respiratory disorders such as asthma.

REFERENCES

Abdelmawgood, I.A. *et al.* (2024) 'β-glucan mitigates ovalbumin-induced airway inflammation by preventing oxidative stress and CD8+ T cell infiltration', *International Immunopharmacology*, 132(April), p. 111985. Available at: https://doi.org/10.1016/j.intimp.2024.111985.

Abdullah, N. *et al.* (2013) 'Domestication of a wild medicinal sclerotial mushroom, Lignosus rhinocerotis (Cooke) Ryvarden', *Industrial Crops and Products*, 47, pp. 256–261. Available at: https://doi.org/10.1016/j.indcrop.2013.03.012.

Abdullah, N. *et al.* (2017) 'Immune-stimulatory potential of hot water extracts of selected edible mushrooms', *Food and Agricultural Immunology*, 28(3), pp. 374–387. Available at: https://doi.org/10.1080/09540105.2017.1293011.

Adejayan, A.A. *et al.* (2019) 'Evaluation of the anti-asthmatic and antitussive potentials of methanol leaf extract of Napoleona vogelii in rodents', *Biomedicine & Pharmacotherapy*, 109, pp. 120–126. Available at: https://doi.org/10.1016/J.BIOPHA.2018.10.058.

Adner, M. *et al.* (2020) 'Back to the future: Re-establishing Guinea pig in vivo asthma models', *Clinical Science*, 134(11), pp. 1219–1242. Available at: https://doi.org/10.1042/CS20200394.

Adorni, G. *et al.* (2019) 'pharmaceutics Aerosolization Performance of Jet Nebulizers and Biopharmaceutical Aspects'. Available at: https://doi.org/10.3390/pharmaceutics11080406.

Ahmad Usuldin, S.R. *et al.* (2020) 'In-depth spectral characterization of antioxidative (1,3)-β-D-glucan from the mycelium of an identified tiger milk mushroom Lignosus rhinocerus strain ABI in a stirred-tank bioreactor', *Biocatalysis and Agricultural Biotechnology*, 23, p. 101455. Available at: https://doi.org/10.1016/j.bcab.2019.101455.

Akira, S. and Takeda, K. (2004) 'Toll-like receptor signalling', *Nature Reviews Immunology*, 4, pp. 499–511.

Akira, S., Uematsu, S. and Takeuchi, O. (2006) 'Pathogen recognition and innate immunity', *Cell* , 124, pp. 783–801.

Al-sajee, D., Yin, X. and Gauvreau, G.M. (2019) 'Expert opinion on pharmacotherapy an evaluation of roflumilast and PDE4 inhibitors with a focus on the treatment of asthma asthma', *Expert Opinion on Pharmacotherapy*, pp. 1–12. Available at: https://doi.org/10.1080/14656566.2019.1570132.

Alangari, A.A. (2014) ' Corticosteroids in the treatment of acute asthma. ', *Annals Thoracic Medicine*, 9(4), pp. 187–192.

Albertine, K.H. *et al.* (2002) 'Temporal correlation of measurements of airway hyperresponsiveness in ovalbumin-sensitized mice.', *American journal of physiology. Lung cellular and molecular physiology*, 283(1 27-1). Available at: https://doi.org/10.1152/AJPLUNG.00324.2001.

Alhajery, M.A. (2024) 'The Overlap Syndrome: A Combination of Chronic Obstructive Pulmonary Disease and Obstructive Sleep Apnea.', *Cureus*, 16. Available at: https://doi.org/10.7759/CUREUS.52349.

Aminu, N. *et al.* (2020) 'The influence of nanoparticulate drug delivery systems in drug therapy', *Journal of Drug Delivery Science and Technology*, 60, p. 101961. Available at: https://doi.org/https://doi.org/10.1016/j.jddst.2020.101961.

Andrew, P.H., Brian, D.K. and David, J.J. (2020) 'Biologic treatment options for severe asthma', *Current Opinion in Immunology*, 66, pp. 151–160. Available at: https://doi.org/10.1016/j.coi.2020.10.004.

Annadurai, G. *et al.* (2024) 'A review of experimental methods to determine bioaerosol transfer in energy recovery ventilators', *Applied Thermal Engineering*, 240. Available at: https://doi.org/10.1016/j.applthermaleng.2023.122322.

Anto, J.M. *et al.* (2017) 'Mechanisms of the Development of Allergy (MeDALL): Introducing novel concepts in allergy phenotypes', *Journal of Allergy and Clinical Immunology*, 139(2), pp. 388–399. Available at: https://doi.org/10.1016/j.jaci.2016.12.940.

Antoniu, S.A. (2011) 'Roflumilast for the treatment of respiratory disease: review of the Phase II and III trials 1', pp. 1413–1419.

Ari, A. and Alhamad, B.R. (2023) 'Evaluating dry powder inhalers: From in vitro studies to mobile health technologies', *Respiratory Medicine*, 215, p. 107281. Available at: https://doi.org/10.1016/J.RMED.2023.107281.

Asgharian, B. *et al.* (2014) 'Computational modeling of nanoscale and microscale particle deposition, retention and dosimetry in the mouse respiratory tract', *Inhalation toxicology*, 26(14), pp. 829–842. Available at: https://doi.org/10.3109/08958378.2014.935535.

Asher, M.I. (2010) 'Recent perspectives on global epidemiology of asthma in childhood', *Allergol Immunopathology (Madr)*, 38(2), pp. 83–87. Available at: https://doi.org/10.1016/j.aller.2009.11.002.

Athari, S.S. *et al.* (2017) 'Critical role of Toll-like receptors in pathophysiology of allergic asthma', *European Journal of Pharmacology*, 808, pp. 21–27. Available at: https://doi.org/10.1016/j.ejphar.2016.11.047.

Atkinson, R.W. *et al.* (2006) 'Temporal associations between daily counts of fungal spores and asthma exacerbations', *Occupational and Environmental Medicine*, 63, pp. 580–590.

Aun, M.V. *et al.* (2017) 'Animal models of asthma: utility and limitations', *Journal of Asthma and Allergy*, pp. 293–301. Available at: https://doi.org/10.2147/JAA.S121092.

Awadasseid, A. *et al.* (2017) 'Purification, characterization, and antitumor activity of a novel glucan from the fruiting bodies of Coriolus Versicolor', *PLOS ONE*, 12(2), p. e0171270. Available at: https://doi.org/10.1371/JOURNAL.PONE.0171270.

Bai, F. *et al.* (2019) 'Vanillic acid mitigates the ovalbumin (OVA)-induced asthma in rat model through prevention of airway inflammation', *Bioscience, Biotechnology, and Biochemistry*, 83(3), pp. 531–537. Available at: https://doi.org/10.1080/09168451.2018.1543015.

Bakakos, P., Patentalakis, G. and Papi, A. (2016) 'Vascular Biomarkers in Asthma and COPD', *Current topics in medicinal chemistry*, 16(14), pp. 1599–1609. Available at: https://doi.org/10.2174/1568026616666150930121157.

Barbosa, J.R. (2023) 'Recovery of natural polysaccharides and advances in the hydrolysis of subcritical, supercritical water and eutectic solvents', in T.A. Dr. Inamuddin (ed.) *Green Sustainable Process for Chemical and Environmental Engineering and Science: Green Solvents and Extraction Technology*. Elsevier, pp. 239–268. Available at: https://doi.org/10.1016/B978-0-323-95156-2.00009-X.

Barisione, G. *et al.* (2010) 'Beta-adrenergic agonists', *Pharmaceuticals*, 3(4), pp. 1016–1044. Available at: https://doi.org/10.3390/ph3041016.

Barnes, P.J. (2008) 'The cytokine network in asthma and chronicobstructive pulmonary disease', *Journal of Clinical Investigation*, 118, p. 3546-3556.

Barnes, P.J. (2012) 'Severe asthma: advances in current management and future therapy', *The Journal of allergy and clinical immunology*, 129(1), pp. 48–59. Available at: https://doi.org/10.1016/J.JACI.2011.11.006.

Barnes, P.J. (2016) 'Asthma mechanisms', *Medicine (United Kingdom)*, 44(5), pp. 265–270. Available at: https://doi.org/10.1016/j.mpmed.2016.02.020.

Barnes, P.J. and Adcock, I.M. (2003) 'How do corticosteroids work in asthma?', *Annals of Internal Medicine*, 139, pp. 359–370.

Barr, R.D. *et al.* (2004) 'Prospective study of postmenopausal hormone use and newly diagnosed asthma and chronic obstructive pulmonary disease', *Archives of International Medicine*, 164, pp. 379–386.

Barsanti, L. *et al.* (2011) 'Chemistry, physico-chemistry and applications linked to biological activities of β-glucans', *Natural Product Reports*, 28(3), pp. 457–466. Available at: https://doi.org/10.1039/C0NP00018C.

Bateman, E.D. *et al.* (2019) 'Global strategy for asthma management and prevention: GINA executive summary', *European Respiratory Journal*, 31(1), pp. 143–178. Available at: https://doi.org/10.1183/09031936.00138707.

Benetti, L.R. *et al.* (2013) 'Hydrogen sulfide inhibits oxidative stress in lungs from allergic mice in vivo', *European Journal of Pharmacology*, 698(1–3), pp. 463–469. Available at: https://doi.org/10.1016/j.ejphar.2012.11.025.

Black, J.L. *et al.* (2012) 'Airway smooth muscle in asthma: just a target for bronchodilation?', *Clin Chest Med*, 33, pp. 543–558.

Boberg, M. *et al.* (2019) 'Characterization of acoustic emission analysis in applications for inhalation device performance assessment', *International Journal of Pharmaceutics*, 563, pp. 304–313. Available at: https://doi.org/10.1016/J.IJPHARM.2019.04.011.

Bodkhe, S. *et al.* (2020) 'Current insights on clinical efficacy of roflumilast for treatment of COPD, asthma and ACOS', *International Immunopharmacology*, 88, p. 106906. Available at: https://doi.org/10.1016/j.intimp.2020.106906.

Borges, R. (2022) 'The rebirth of isolated organ contraction studies for drug discovery and repositioning', *Drug Discovery Today*, 27(4), pp. 1128–1131. Available at: https://doi.org/10.1016/j.drudis.2021.11.016.

Boulet, L.P. (2009) ' Influence of comorbid conditions on asthma', *European Respiratory Journal*, 33, pp. 897–906.

Bradding, P., Walls, A.F. and Holgate, S.T. (2006) 'The role of the mast cell in the pathophysiology of asthma', *Journal of Allergy and Clinical Immunology*, 117, pp. 1277–1284. Available at: https://doi.org/10.1016/j.jaci.2006.02.039.

Breen, E.J., Polaskova, V. and Khan, A. (2015) 'Bead-based multiplex immuno-assays for cytokines, chemokines, growth factors and other analytes: Median fluorescence intensities versus their derived absolute concentration values for statistical analysis', *Cytokine*, 71(2), pp. 188–198. Available at: https://doi.org/10.1016/J.CYTO.2014.10.030.

Brightling, C., Saha, S. and Hollins, F. (2010) 'Interleukin-13: Prospects for new treatments', *Clinical & Experimental Allergy*, 40, p. 42-49.

Büchi (2020) 'B-290 Mini Spray Dryer Operation Manual', *Büchi*, pp. 1–82. Available at: https://static1.buchi.com/sites/default/files/downloads/B-290_OM_en_I_0.pdf?b0ba59e782a99211b159d5a83189e1e223038cbe (Accessed: 13 July 2023).

Buels, K.S. and Fryer, A.D. (2012) 'Muscarinic receptor antagonists: Effects on pulmonary function', *Handbook of Experimental Pharmacology*, 208(208), pp. 317–341. Available at: https://doi.org/10.1007/978-3-642-23274-9_14.

Burrows. B. et al. (1989) 'Association of asthma with serum IgE levels and skin-test reactivity to allergens', *New England Journal of Medicine*, 271–277, p. 320.

Busby, J. *et al.* (2020) 'The effects of oral corticosteroids on lung function, type-2 biomarkers and patient-reported outcomes in stable asthma: A systematic review and meta-analysis', *Respiratory Medicine*, 173, p. 106156.

Bushra, S.M.R., Bakar, R.A. and Nurul, A.A. (2025) 'Analytical method development and validation for monosaccharide profiling in Lignosus rhinocerotis using rP-HPLC.', *Journal of Asian natural products research*, pp. 1–14. Available at: https://doi.org/10.1080/10286020.2025.2453852.

Cai, W. *et al.* (2018) 'Effect of ultrasound on size, morphology, stability and antioxidant activity of selenium nanoparticles dispersed by a hyperbranched polysaccharide from Lignosus rhinocerotis', *Ultrasonics Sonochemistry*, 42, pp. 823–831. Available at: https://doi.org/10.1016/J.ULTSONCH.2017.12.022.

Calzetta, L. *et al.* (2024) 'Use of human airway smooth muscle in vitro and ex vivo to investigate drugs for the treatment of chronic obstructive respiratory disorders', *British Journal of Pharmacology*, 181(5), pp. 610–639. Available at: https://doi.org/10.1111/bph.16272.

Caminati, M. *et al.* (2018) 'Type 2 immunity in asthma', *World Allergy Organization Journal*, 11(13).

Del Campo, L. and Ferrer, M. (2015) 'Wire myography to study vascular tone and vascular structure of isolated mouse arteries', *Methods in Molecular Biology*, 1339, pp. 255–276. Available at: https://doi.org/10.1007/978-1-4939-2929-0_18/FIGURES/10.

Canning, B.J. and Chou, Y. (2008) 'Using guinea pigs in studies relevant to asthma and COPD', *Pulmonary pharmacology & therapeutics*, 21(5), pp. 702–720. Available at: https://doi.org/10.1016/J.PUPT.2008.01.004.

Chai, R. *et al.* (2013) 'β-Glucan Synthase Gene Overexpression and β-Glucans Overproduction in Pleurotus ostreatus Using Promoter Swapping', *PLOS ONE*, 8(4), p. e61693. Available at: https://doi.org/10.1371/JOURNAL.PONE.0061693.

Chandel, A. *et al.* (2019) 'Recent advances in aerosolised drug delivery', *Biomedicine & Pharmacotherapy*, 112, p. 108601. Available at: https://doi.org/10.1016/J.BIOPHA.2019.108601.

Chang, K.H. *et al.* (2019) 'Comparison of salbutamol delivery efficiency for jet versus mesh nebulizer using mice', *Pharmaceutics*, 11(4). Available at: https://doi.org/10.3390/pharmaceutics11040192.

Chang, K.H. *et al.* (2020) 'Aerosol Delivery of Dornase Alfa Generated by Jet and Mesh Nebulizers.', *Pharmaceutics*, 12(8), pp. 1–14. Available at: https://doi.org/10.3390/pharmaceutics12080721.

Chang, Y.S. and Lee, S.S. (2004) 'Utilisation of macrofungi species in Malaysia', *Fungal Diversity*, 15, pp. 15–22.

Chang, Y.X. *et al.* (2014) 'Anti-hygroscopic effect of leucine on spray-dried herbal extract powders', *Powder Technology*, 266, pp. 388–395. Available at: https://doi.org/10.1016/J.POWTEC.2014.06.058.

Chaurasiya, B. and Zhao, Y.Y. (2021) 'Dry powder for pulmonary delivery: A comprehensive review', *Pharmaceutics*, 13(1), pp. 1–28. Available at: https://doi.org/10.3390/PHARMACEUTICS13010031.

Chen, T.-I. *et al.* (2013) 'Mutagenicityandgenotoxicityeffectsof Lignosus rhinocerotis mushroommycelium', *Journal of Ethnopharmacology*, 149, pp. 70–74. Available at: https://doi.org/10.1016/j.jep.2013.06.001.

Chen, X. *et al.* (2023) 'Global, regional, and national burden of chronic respiratory diseases and associated risk factors, 1990–2019: Results from the Global Burden of Disease Study 2019', *Frontiers in Medicine*, 10, p. 1066804. Available at: https://doi.org/10.3389/FMED.2023.1066804/BIBTEX.

Chen, Y. *et al.* (2020) 'Aster tataricus attenuates asthma efficiently by simultaneously inhibiting tracheal ring contraction and inflammation', *Biomedicine and Pharmacotherapy*, 130(August), p. 110616. Available at: https://doi.org/10.1016/j.biopha.2020.110616.

Chipps, B.E. *et al.* (2018) 'More than a decade follow-up in patients with severe or difficult-to-treat asthma: The Epidemiology and Natural History of Asthma: Outcomes and Treatment Regimens (TENOR) II', *Journal of Allergy and Clinical Immunology*, 141(5), pp. 1590–1597. Available at: https://doi.org/10.1016/j.jaci.2017.07.014.

Choong, Y.K. *et al.* (2016) 'Differential identification of mushrooms sclerotia by IR macro-fingerprint method', *Spectrochimica Acta Part A: Molecular and Biomolecular Spectroscopy*, 152, pp. 34–42. Available at: https://doi.org/10.1016/j.saa.2015.07.054.

Clement, A. and Eber, E. (2008) 'Interstitial lung diseases in infants and children', *The European respiratory journal*, 31(3), pp. 658–666. Available at: https://doi.org/10.1183/09031936.00004707.

Collins, P. *et al.* (1995) 'Cooperation between interleukin-5 and the chemokine eotaxin to induce eosinophil accumulation in vivo', *Journal of Experimental Medicine*, 182(4), pp. 1169–1174.

Copley, M. (2018) 'Variability in cascade impaction: Sources, impact and strategies for reduction', *ONdrugDelivery*, 2018(92), pp. 60–65. Available at: https://www.ondrugdelivery.com/variability-in-cascade-impaction-sources-impact-and-strategies-for-reduction/ (Accessed: 30 September 2022).

Copley Scientific (2024) *Brochure Next Generation Impactor*. Available at: https://www.sanyo-si.com/wp-content/uploads/NGI.pdf.

Côté, A., Godbout, K. and Boulet, L.-P. (2020) 'The management of severe asthma in 2020', *Biochemical Pharmacology*, 179, p. 114112. Available at: https://doi.org/10.1016/j.bcp.2020.114112.

Curtis, J.L. *et al.* (1990) 'Histologic analysis of an immune response in the lung parenchyma of mice. Angiopathy accompanies inflammatory cell influx', *American Journal of Pathology*, 137, p. 689-699.

Cyr, M. and Tagnit-Hamou, A. (2001) 'Particle size distribution of fine powders by LASER diffraction spectrometry. Case of cementitious materials', *Materials and Structures/Materiaux et Constructions*, 34(6), pp. 342–350. Available at: https://doi.org/10.1007/BF02486485/METRICS.

Da-Silva, A.L. *et al.* (2013) 'Nanoparticle-based therapy for respiratory diseases', *Annals of the Brazilian Academy of Sciences*, pp. 1–10.

Dale, P. *et al.* (2018) 'Selective inhibition of histamine-evoked Ca2+ signals by compartmentalized cAMP in human bronchial airway smooth muscle cells', *Cell Calcium*, 71(December 2017), pp. 53–64. Available at: https://doi.org/10.1016/j.ceca.2017.12.002.

Dale, P.R. *et al.* (2014) 'The pharmacological rationale for combining muscarinic receptor antagonists and β-adrenoceptor agonists in the treatment of airway and bladder disease', *Current Opinion in Pharmacology*, 16(1), pp. 31–42. Available at: https://doi.org/10.1016/j.coph.2014.03.003.

Davis, D. *et al.* (2001) *Selection of Standards for Bio-Plex Cytokine Assays*, *Technical Article, Bio-Rad Laboratories, Hercules, CA*. Tech Note 2900.

Debeuf, N. *et al.* (2016) 'Mouse Models of Asthma', *Current protocols in mouse biology*, 6(2), pp. 169–184. Available at: https://doi.org/10.1002/CPMO.4.

Demenais, F. *et al.* (2018) 'Multiancestry association study identifies new asthma risk loci that colocalize with immune-cell enhancer marks', *Nature Genetics*, 50, pp. 42–50.

Denning. D.W. et al. (2009) 'Randomized controlled trial of oral antifungal treatment for severe asthma with fungal sensitization:The Fungal Asthma Sensitization Trial (FAST) study', *American Journal of Respiratory and Critical Care Medicine*, 179, pp. 11–18.

Dixon, C.E., Bedenice, D. and Mazan, M.R. (2021) 'Comparison of Flowmetric Plethysmography and Forced Oscillatory Mechanics to Measure Airway Hyperresponsiveness in Horses', *Frontiers in Veterinary Science*, 7, p. 511023. Available at: https://doi.org/10.3389/FVETS.2020.511023/BIBTEX.

Dolovich, M.B. and Bailey, D.L. (2012) 'Positron emission tomography (PET) for assessing aerosol deposition of orally inhaled drug products', *Journal of aerosol medicine and pulmonary drug delivery*, 25 Suppl 1(SUPPL.1). Available at: https://doi.org/10.1089/JAMP.2012.1SU6.

Domingo, C. *et al.* (2018) 'The prostaglandin D2 receptor 2 pathway in asthma: a key player in airway inflammation', *Respiratory research*, 19(1). Available at: https://doi.org/10.1186/S12931-018-0893-X.

Dubois, M. *et al.* (1956) 'Colorimetric Method for Determination of Sugars and Related Substances', *Analytical Chemistry*, 28(3), pp. 350–356. Available at: https://doi.org/10.1021/ac60111a017.

Dudášová, A. *et al.* (2013) 'The effects of cannabidiol on the antigen-induced contraction of airways smooth muscle in the guinea-pig', *Pulmonary Pharmacology and Therapeutics*, 26(3), pp. 373–379. Available at: https://doi.org/10.1016/j.pupt.2013.02.002.

Dweik, R.A. *et al.* (2011) 'American thoracic society committee on interpretation of exhaled nitric oxide levels (FENO) for clinical applications: an official ATS clinical practice guideline: interpretation of exhaled nitric oxide levels (FeNO) for clinical applications', *American Journal of Respiratory and Critical Care Medicine*, 184, pp. 602–615.

Dykewicz, M.S. and Hamilos, D.L. (2010) 'Rhinitis and sinusitis', *Journal of Allergy and Clinical Immunology*, 125(2), pp. S103–S115. Available at: https://doi.org/10.1016/J.JACI.2009.12.989.

Ehrmann, S. *et al.* (2020) 'Innovative preclinical models for pulmonary drug delivery research', *Expert opinion on drug delivery*, 17(4), p. 463. Available at: https://doi.org/10.1080/17425247.2020.1730807.

Ehteshami-Afshar, S. *et al.* (2016) 'The global economic burden of asthma and chronic obstructive pulmonary disease', *International Journal of Tuberculosis and Lung Disease*, 20(1), pp. 11–23. Available at: https://doi.org/10.5588/ijtld.15.0472.

Eik, L.F. *et al.* (2012) 'Lignosus rhinocerus (Cooke) Ryvarden: A medicinal mushroom that stimulates neurite outgrowth in PC-12 cells.', *Evid Based Complement Alternat Med*, 2012. Available at: https://doi.org/10.1155/2012/320308.

Elkholy, S.M.H. *et al.* (2019) 'Serum Vascular Endothelial Growth Factor Levels in Asthmatic Children', *The Egyptian Journal of Hospital Medicine*, 75(1), pp. 2007–2012. Available at: https://doi.org/10.21608/EJHM.2019.29398.

Ellan, K. *et al.* (2019) 'Anti-viral activity of culinary and medicinal mushroom extracts against dengue virus serotype 2: an in-vitro study', *BMC complementary and alternative medicine*, 19(1). Available at: https://doi.org/10.1186/S12906-019-2629-Y.

Emala, C.W., Clancy-Keen, J. and Hirshman, C.A. (2000) 'Decreased adenylyl cyclase protein and function in airway smooth muscle by chronic carbachol pretreatment', *American Journal of Physiology - Cell Physiology*, 279(4 48-4). Available at: https://doi.org/10.1152/AJPCELL.2000.279.4.C1008/ASSET/IMAGES/LARGE/H01000116007.JPEG.

Enerback, L., Pipkorn, U. and Granerus, G. (1986) 'Intraepithelial migration of nasal mucosal mast cells in hay fever', *International Archive in Allergy Applied Immunology*, 80(1), pp. 44–51.

Erick Bateman (2016) *Global Strategy for Asthma Management and Prevention*, *Global Iniciative for Asthma*. Edited by M.D. Bethsda. NIH publication, : U.S. Dept. of Health and Human Services, Public Health Service. Available at:

http://ginasthma.org/wp-content/uploads/2016/04/GINA-2016-main-report_tracked.pdf.

Erle, D.J. and Sheppard, D. (2014) 'The cell biology of asthma', *Journal of Cell Biology*, 205, pp. 621–631.

Escamilla-Gil, J.M., Fernandez-Nieto, M. and Acevedo, N. (2022) 'Understanding the Cellular Sources of the Fractional Exhaled Nitric Oxide (FeNO) and Its Role as a Biomarker of Type 2 Inflammation in Asthma', *BioMed research international*, 2022. Available at: https://doi.org/10.1155/2022/5753524.

Fahy, J. V. (2015) 'Type 2 inflammation in asthma-present in most, absent in many', *Nature Reviews Immunology*, 15(1), pp. 57–65. Available at: https://doi.org/10.1038/nri3786.

Fang, J. *et al.* (2012) 'Structure of a β-glucan from Grifola frondosa and its antitumor effect by activating Dectin-1/Syk/NF-κB signaling', *Glycoconjugate Journal 2012 29:5*, 29(5), pp. 365–377. Available at: https://doi.org/10.1007/S10719-012-9416-Z.

Fang, L. *et al.* (2016) 'Royal Sun Medicinal Mushroom, Agaricus brasiliensis (Agaricomycetidae), Derived Polysaccharides Exert Immunomodulatory Activities *In Vitro* and *In Vivo*', *International Journal of Medicinal Mushrooms*, 18(2), pp. 123–132. Available at: https://doi.org/10.1615/INTJMEDMUSHROOMS.V18.I2.30.

Farache, J. *et al.* (2013) 'Luminal bacteria recruit CD103+ dendritic cells into the intestinal epithelium to sample bacterial antigens for presentation', *Immunity*, 38, pp. 581–595.

Farahi, N. *et al.* (2007) 'Eotaxin-1/CC chemokine ligand 11: a novel eosinophil survival factor secreted by human pulmonary artery endothelial cells', *Journal of Immunology*, 179(2), pp. 1264–1273.

Feng, S. *et al.* (2022) 'Cell wall polysaccharides and mono-/disaccharides as chemical determinants for the texture and hygroscopicity of freeze-dried fruit and vegetable cubes', *Food Chemistry*, 395, p. 133574. Available at: https://doi.org/10.1016/J.FOODCHEM.2022.133574.

Fish, S.C. *et al.* (2005) 'IgEgeneration and mast cell effector function in mice deficient in IL-4 and IL-13', *Journal Immunology*, 74, pp. 7716–7724.

Foley, S.C. *et al.* (2007) 'Increased expression of ADAM33 and ADAM8 with disease progression in asthma', *The Journal of allergy and clinical immunology*, 119(4), pp. 863–871. Available at: https://doi.org/10.1016/J.JACI.2006.12.665.

Foster, J.M. *et al.* (2020) 'Patient experiences of as-needed budesonide-formoterol by Turbuhaler® for treatment of mild asthma; a qualitative study', *Respiratory Medicine*, 175, p. 106154. Available at: https://doi.org/10.1016/j.rmed.2020.106154.

Gan, D. *et al.* (2011) 'Production, preliminary characterization and antitumor activity in vitro of polysaccharides from the mycelium of Pholiota dinghuensis Bi', *Carbohydrate Polymers*, 84(3), pp. 997–1003. Available at: https://doi.org/10.1016/J.CARBPOL.2010.12.058.

Gans, M.D. and Gavrilova, T. (2020) 'Understanding the immunology of asthma: Pathophysiology, biomarkers, and treatments for asthma endotypes', *Paediatric Respiratory Reviews*, 36, pp. 118–127. Available at: https://doi.org/10.1016/j.prrv.2019.08.002.

Gao, X. *et al.* (2022) 'Immunoregulatory activity of a low-molecular-weight heteropolysaccharide from Ganoderma leucocontextum fruiting bodies in vitro and in vivo', *Food chemistry: X*, 14. Available at: https://doi.org/10.1016/J.FOCHX.2022.100321.

Generoso, A. and Oppenheimer, J. (2020) 'Asthma/obstructive pulmonary disease overlap: update on definition, biomarkers, and therapeutics, ', *Current Opinion in Allergy and Clinical Immunology*, 20, pp. 43–47. Available at: https://doi.org/10.1097/ACI.0000000000000596.

GINA (2024) *Global Initiative for Asthma. 2024 GINA Main Report.*, *Global Initiative for Asthma*. Available at: https://ginasthma.org/2024-report/ (Accessed: 29 July 2024).

Glaab, T. *et al.* (2001) 'Tidal midexpiratory flow as a measure of airway hyperresponsiveness in allergic mice.', *American journal of physiology. Lung cellular and molecular physiology*, 280(3 24-3). Available at: https://doi.org/10.1152/AJPLUNG.2001.280.3.L565.

Gon, Y. (2008) 'Toll-like receptors and airway inflammation', *Allergol Int*, 57, pp. 33–37.

Gong, P. *et al.* (2020) *Extraction methods, chemical characterizations and biological activities of mushroom polysaccharides: A mini-review*, *Carbohydrate Research*. NLM (Medline). Available at: https://doi.org/10.1016/j.carres.2020.108037.

Goral, V. *et al.* (2011) 'Agonist-Directed Desensitization of the β2-Adrenergic Receptor', *PLOS ONE*, 6(4), p. e19282. Available at: https://doi.org/10.1371/JOURNAL.PONE.0019282.

Gordon, E.D. *et al.* (2016) 'Alternative splicing of interleukin-33 and type 2 inflammation in asthma', *Proc Natl Acad Sci U S A*, 113, pp. 8765–8770.

Gosens, R. *et al.* (2006) 'Muscarinic receptor signaling in the pathophysiology of asthma and COPD', *Respiratory Research*. Respir Res. Available at: https://doi.org/10.1186/1465-9921-7-73.

Gregory, L.G. and Lloyd, C.M. (2011) 'Orchestrating house dust miteassociated allergy in the lung', *Trends in Immunology*, 32, pp. 402–411.

Grimaud, J. and Murthy, V.N. (2018) 'How to monitor breathing in laboratory rodents: a review of the current methods', *Journal of Neurophysiology*, 120(2), p. 624. Available at: https://doi.org/10.1152/JN.00708.2017.

Grotenboer, N.S. *et al.* (2013) 'Decoding asthma: translating genetic variation in IL33 and IL1RL1 into disease pathophysiology', *The Journal of allergy and clinical immunology*, 131(3), pp. 856-865.e9. Available at: https://doi.org/10.1016/J.JACI.2012.11.028.

Gui, Y. *et al.* (2011) 'Uridine adenosine tetraphosphate induces contraction of airway smooth muscle', *American journal of physiology. Lung cellular and molecular physiology*, 301(5). Available at: https://doi.org/10.1152/AJPLUNG.00203.2011.

Guilliams, M., Lambrecht, B.N. and Hammad, H. (2013) 'Division of labor between lung dendritic cells and macrophages in the defense against pulmonary infections', *Mucosal Immunol* , 6, pp. 464–473.

Gunasekaran, S., Govindan, S. and Ramani, P. (2021) 'Investigation of chemical and biological properties of an acidic polysaccharide fraction from Pleurotus eous (Berk.) Sacc.', *Food Bioscience*, 42, p. 101209. Available at: https://doi.org/10.1016/J.FBIO.2021.101209.

Guo, C., Wong, K.H. and Cheung, P.C.K. (2011) 'Hot water extract of the sclerotium of Polyporus rhinocerus Cooke enhances the immune functions of murine macrophages', *International journal of medicinal mushrooms*, 13(3), pp. 237–244. Available at: https://doi.org/10.1615/INTJMEDMUSHR.V13.I3.30.

Haida, M. *et al.* (2020) 'Detection of Adrenal Insufficiency in Moderate to Severe Asthma', *Journal of Allergy and Clinical Immunology*, AB208.

Hallworth, G.W. and Westmoreland, D.G. (1987) 'The twin impinger: a simple device for assessing the delivery of drugs from metered dose pressurized aerosol inhalers', *Journal of Pharmacy and Pharmacology*, 39(12), pp. 966–972. Available at: https://doi.org/10.1111/j.2042-7158.1987.tb03142.x.

Halwani, R., Al-Muhsen, S. and Hamid, Q. (2013) 'T helper 17 cells in airway diseases: from laboratory bench to bedside', *Chest*, 143, pp. 494–501.

Hamelmann, E. *et al.* (1997) 'Noninvasive measurement of airway responsiveness in allergic mice using barometric plethysmography.', *American Journal of Respiratory and Critical Care Medicine*, 156(3 I), pp. 766–775. Available at: https://doi.org/10.1164/AJRCCM.156.3.9606031.

Hammad, H. and Lambrecht, B.N. (2015) 'Barrier epithelial cells and the control of type 2 immunity', *Immunity* , 43, pp. 29–40.

Hamzah, Z.B. *et al.* (2022) 'Evaluation of the Male and Female Fertility and Teratogenic Effects of Lignosus rhinocerotis (Cooke) Ryvarden in Rats', *Sains Malaysiana*, 51(1), pp. 297–306. Available at: https://doi.org/10.17576/jsm-2022-5101-24.

Hardman, C.S., Panova, V. and McKenzie, A.N. (2012) 'IL-33 citrine reporter mice reveal the temporal and spatial expression of IL-33 during allergic lung inflammation', *European Journal of Immunology*, 43, pp. 488–498.

Hebbink, G.A. *et al.* (2022) 'Recent developments in lactose blend formulations for carrier-based dry powder inhalation', *Advanced Drug Delivery Reviews*, 189, p. 114527. Available at: https://doi.org/10.1016/J.ADDR.2022.114527.

Henseleit, K. and Adolf Krebs, H. (1932) 'Untersuchungen uber die Harnstoffbildung im Tierkörper', *Hoppe-Seyler's Zeitschrift fur Physiologische Chemie*, 210(1–2), pp. 33–66. Available at: https://doi.org/10.1515/BCHM2.1932.210.1-2.33/MACHINEREADABLECITATION/RIS.

Hikichi, M., Hashimoto, S. and Gon, Y. (2018) 'Asthma and COPD overlap pathophysiology of ACO', *Allergology International*, 67, pp. 179–186. Available at: https://doi.org/10.1016/j.alit.2018.01.001.

Högman, M. *et al.* (2018) '2017 global initiative for chronic obstructive lung disease reclassifies half of COPD subjects to lower risk group', *International Journal of COPD*, 13, pp. 165–173. Available at: https://doi.org/10.2147/COPD.S151016.

Holgate, S. *et al.* (2005) 'The anti-inflammatory effects of omalizumab confirm the central role of IgE in allergic inflammation', *Journal of Allergy and Clinical Immunology*, 115(3), pp. 459–465. Available at: https://doi.org/10.1016/j.jaci.2004.11.053.

Van Holsbeke, C. *et al.* (2014) 'Median mass aerodynamic diameter (MMAD) and fine particle fraction (FPF): Influence on lung deposition?', *Eur. Respir. J.*, 44(Suppl_58), pp. P912-. Available at: http://erj.ersjournals.com/content/44/Suppl_58/P912 (Accessed: 10 November 2022).

Hsu, K.-D. and Cheng, K.-C. (2018) 'From nutraceutical to clinical trial: frontiers in Ganoderma development.', *Applied microbiology and biotechnology*, 102(21), pp. 9037–9051. Available at: https://doi.org/10.1007/s00253-018-9326-5.

Hu, S.H. *et al.* (2015) 'Antitumor and Immunomodulating Activities of Exopolysaccharide Produced by Big Cup Culinary- Medicinal Mushroom *Clitocybe maxima* (Higher Basidiomycetes) in Liquid Submerged Culture', *International Journal of Medicinal Mushrooms*, 17(9), pp. 891–901. Available at: https://doi.org/10.1615/INTJMEDMUSHROOMS.V17.I9.90.

Hu, T., Huang, Q., Wong, K., Yang, H., *et al.* (2017) 'A hyperbranched β-d-glucan with compact coil conformation from Lignosus rhinocerotis sclerotia', *Food Chemistry*, 225, pp. 267–275. Available at: https://doi.org/10.1016/J.FOODCHEM.2017.01.034.

Hu, T., Huang, Q., Wong, K. and Yang, H. (2017) 'Structure, molecular conformation, and immunomodulatory activity of four polysaccharide fractions from Lignosus rhinocerotis sclerotia', *International Journal of Biological*

Macromolecules, 94, pp. 423–430. Available at: https://doi.org/10.1016/j.ijbiomac.2016.10.051.

Hu, X. *et al.* (2015) 'Toxicity evaluation of exposure to an atmospheric mixture of polychlorinated biphenyls by nose-only and whole-body inhalation regimens HHS Public Access Author manuscript', *Environ Sci Technol*, 49, pp. 11875–11883. Available at: https://doi.org/10.1021/acs.est.5b02865.

Hwang, S.S. *et al.* (2013) 'Transcription factor YY1 is essential for regulation of the Th2 cytokine locus and for Th2 cell differentiation', *Proceedings of the National Academy of Science of the United States of America*, 110, p. 276-281.

Ince, M. and Ruether, P. (2021) 'Histamine and antihistamines', *Anaesthesia and Intensive Care Medicine*, 22(11), pp. 749–755. Available at: https://doi.org/10.1016/j.mpaic.2021.07.025.

IPH (2008) *The Third National Health and Morbidity Survey (NHMSIII) 2006, Asthma*, *Asthma Children (Aged below 18 years)*. Ministry of Health, Malaysia.

Ito, T., Hirose, K. and Nakajima, H. (2019) 'Bidirectional roles of IL-22 in the pathogenesis of allergic airway inflammation', *Allergology International*, 68(1), pp. 4–8. Available at: https://doi.org/10.1016/J.ALIT.2018.10.002.

Izuhara, K. *et al.* (2016) 'Roles of periostin in respiratory disorders', *American Journal of Respiratory and Critical Care Medicine*, 193(9), pp. 949–956. Available at: https://doi.org/10.1164/rccm.201510-2032PP.

Jackson, D.J. *et al.* (2019) 'Serum IL-6: A biomarker in childhood asthma?', *Journal of Allergy and Clinical Immunology*, 145(6), p. LETTERS TO THE EDITOR 1701-1703.

Jamil, N.A.M. *et al.* (2018) 'Comparative nutritional and mycochemical contents, biological activities and LC/MS screening of tuber from new recipe cultivation technique with wild type tuber of tiger's milk mushroom of species Lignosus rhinocerus', *World Journal of Microbiology and Biotechnology*, 34(1), p. 0. Available at: https://doi.org/10.1007/s11274-017-2385-4.

Jawahar, N. and Gowtham, R. (2012) 'Nanoparticles: A Novel Pulmonary Drug Delivery System for Tuberculosis', *Journal of Pharmaceutical Sciences & Research*, 4(88), pp. 1901–1906.

Jeff, I.B.I.B. *et al.* (2016) 'In vivo anticancer and immunomodulating activities of mannogalactoglucan-type polysaccharides from Lentinus edodes (Berkeley) Singer.', *Central-European journal of immunology*, 41(1), pp. 47–53. Available at: https://doi.org/10.5114/ceji.2015.56962.

Jhou, B.-Y. *et al.* (2017) 'Oral reproductive and developmental toxicity of Lignosus rhinocerotis mycelium in rat', *Journal of Ethnopharmacology*, 208, pp. 66–71. Available at: https://doi.org/10.1016/j.jep.2017.06.029.

Jiang, T. *et al.* (2021) 'Lipid metabolism and identification of biomarkers in asthma by lipidomic analysis', *BBA - Molecular and Cell Biology of Lipids*, 1866, p. 158853. Available at: https://doi.org/10.1016/j.bbalip.2020.158853.

Jin, H. *et al.* (2019) 'Modified Si-Jun-Zi-Tang attenuates airway inflammation in a murine model of chronic asthma by inhibiting Teff cells via the mTORC1 pathway', *Frontiers in Pharmacology*, 10(febuary), p. 423923. Available at: https://doi.org/10.3389/FPHAR.2019.00161/BIBTEX.

Johnathan, M. *et al.* (2016) 'Phytochemical profiles and inhibitory effects of Tiger Milk mushroom (Lignosus rhinocerus) extract on ovalbumin-induced airway inflammation in a rodent model of asthma', *BMC Complementary and Alternative Medicine*, 16(1). Available at: https://doi.org/10.1186/s12906-016-1141-x.

Johnathan, M. *et al.* (2021) 'Lignosus rhinocerotis Cooke Ryvarden ameliorates airway inflammation, mucus hypersecretion and airway hyperresponsiveness in a murine model of asthma', *PLoS ONE*, 16(3 March), pp. 1–16. Available at: https://doi.org/10.1371/journal.pone.0249091.

Johnston NW *et al.* (2005) 'The September epidemic of asthma exacerbations in children: a search for etiology', *Journal of Allergy and Clinical Immunology*, 115, pp. 132–138.

Joks, R., Lee, L. and Vastardi, M.-A. (2020) 'The Relationship Between Family History of Cancer and Prevalence of Asthma and Allergies in Pediatric Patients in an inner-city minority population.', *Journal of Allergy and Clinical Immunology*, p. AB208.

Kabesch M. et al. (2006) 'IL-4/IL-13 pathway genetics strongly influence serum IgE levels and childhood asthma', *Journal of Allergy and Clinical Immunology*, 117, pp. 269–274.

Kaialy, W. and Nokhodchi, A. (2016) 'The use of freeze-dried mannitol to enhance the in vitro aerosolization behaviour of budesonide from the Aerolizer®', *Powder Technology*, 288, pp. 291–302. Available at: https://doi.org/10.1016/j.powtec.2015.11.016.

Kamal, S. *et al.* (2013) 'The anti-asthma herbal medicine ASHMI acutely inhibits airway smooth muscle contraction via prostaglandin E2 activation of EP2/EP4 receptors', *American Journal of Physiology - Lung Cellular and Molecular Physiology*, 305(12), pp. 1002–1010. Available at: https://doi.org/10.1152/ajplung.00423.2012.

Kamaruzaman, N.A. *et al.* (2014) 'Inhalation of honey reduces airway inflammation and histopathological changes in a rabbit model of ovalbumin-induced chronic asthma', *BMC Complementary and Alternative Medicine*, 14(1), pp. 1–11. Available at: https://doi.org/10.1186/1472-6882-14-176.

Kang, X. *et al.* (2018) 'Molecular architecture of fungal cell walls revealed by solid-state NMR', *Nature Communications 2018 9:1*, 9(1), pp. 1–12. Available at: https://doi.org/10.1038/s41467-018-05199-0.

Kaur, G. *et al.* (2012) 'Advances in Pulmonary Delivery of Nanoparticles', *Artificial Cells, Blood Substitutes, and Biotechnology*, 40, pp. 75–96. Available at: https://doi.org/10.3109/10731199.2011.592494.

Kaur, R. *et al.* (2020) 'An Efficient and Cost-Effective Nose-Only Inhalational Chamber for Rodents: Design, Optimization and Validation', *AAPS PharmSciTech 2020 21:3*, 21(3), pp. 1–10. Available at: https://doi.org/10.1208/S12249-019-1608-4.

Kawamatawong, T. (2017) 'Roles of roflumilast, a selective phosphodiesterase 4 inhibitor, in airway diseases', *Journal of Thoracic Disease*, 9, pp. 1144–1154. Available at: https://doi.org/10.21037/jtd.2017.03.116.

Kerzerho, J. *et al.* (2011) 'Effects of systemic versus local administration of corticosteroids on mucosal tolerance', *Journal of Immunology (Baltimore, Md. : 1950)*, 188(1), p. 470. Available at: https://doi.org/10.4049/JIMMUNOL.1101405.

Keshavarz-Rezaei, M. *et al.* (2022) 'The HbA1c and blood glucose response to selenium-rich polysaccharide from Fomes fomentarius loaded solid lipid nanoparticles as a potential antidiabetic agent in rats', *Biomaterials Advances*, 140(July), p. 213084. Available at: https://doi.org/10.1016/j.bioadv.2022.213084.

Kim, C.Y. *et al.* (2022) 'Inner Shell of the Chestnut (Castanea crenatta) Suppresses Inflammatory Responses in Ovalbumin-Induced Allergic Asthma Mouse Model', *Nutrients*, 14(10). Available at: https://doi.org/10.3390/nu14102067.

Kim, D.I., Song, M.K. and Lee, K. (2019) 'Comparison of asthma phenotypes in OVA-induced mice challenged via inhaled and intranasal routes', *BMC Pulmonary Medicine*, 19(1), pp. 1–11. Available at: https://doi.org/10.1186/s12890-019-1001-9.

Kim, Y.G. *et al.* (2008) 'The Cytosolic Sensors Nod1 and Nod2 Are Critical for Bacterial Recognition and Host Defense after Exposure to Toll-like Receptor Ligands', *Immunity*, 28(2), pp. 246–257. Available at: https://doi.org/10.1016/j.immuni.2007.12.012.

Kim, Y.S. *et al.* (2000) 'Gram-negative bacteria-binding protein, a pattern recognition receptor for lipopolysaccharide and β-1,3-glucan that mediates the signaling for the induction of innate immune genes in Drosophila melanogaster cells', *Journal of Biological Chemistry*, 275(42), pp. 32721–32727. Available at: https://doi.org/10.1074/JBC.M003934200.

Kistemaker, L.E.M. *et al.* (2014) 'Muscarinic M3 receptors contribute to allergen-induced airway remodeling in mice', *American Journal of Respiratory Cell and Molecular Biology*, 50(4), pp. 690–698. Available at: https://doi.org/10.1165/rcmb.2013-0220OC.

Kittimongkolsuk, P., Roxo, M., *et al.* (2021) 'Extracts of the tiger milk mushroom (Lignosus rhinocerus) enhance stress resistance and extend lifespan in caenorhabditis elegans via the daf-16/foxo signaling pathway',

Pharmaceuticals, 14(2), pp. 1–22. Available at: https://doi.org/10.3390/ph14020093.

Kittimongkolsuk, P., Pattarachotanant, N., *et al.* (2021) 'Neuroprotective effects of extracts from tiger milk mushroom lignosus rhinocerus against glutamate-induced toxicity in HT22 hippocampal neuronal cells and neurodegenerative diseases in caenorhabditis elegans', *Biology*, 10(1), pp. 1–16. Available at: https://doi.org/10.3390/biology10010030.

Klein, W.R.G. *et al.* (2012) 'Pulmonary innate lymphoid cells are major producers of IL-5 and IL-13 in murine models of allergic asthma', *European Journal of Immunology*, 42, pp. 1106–1116.

Koarai, A. and Ichinose, M. (2018) 'Possible involvement of acetylcholine-mediated inflammation in airway diseases', *Allergology International*, 67(4), pp. 460–466. Available at: https://doi.org/10.1016/j.alit.2018.02.008.

Kodama, M. *et al.* (2010) 'Strain-Specific Phenotypes of Airway Inflammation and Bronchial Hyperresponsiveness Induced by Epicutaneous Allergen Sensitization in BALB/c and C57BL/6 Mice', *International Archives of Allergy and Immunology*, 152(Suppl. 1), pp. 67–74. Available at: https://doi.org/10.1159/000312128.

Kogel, U. *et al.* (2021) 'Impact of whole-body versus nose-only inhalation exposure systems on systemic, respiratory, and cardiovascular endpoints in a 2-month cigarette smoke exposure study in the ApoE−/− mouse model', *Journal of Applied Toxicology*, 41(10), p. 1598. Available at: https://doi.org/10.1002/JAT.4149.

Kolahian, S. and Gosens, R. (2012) 'Cholinergic Regulation of Airway Inflammation and Remodelling', *Journal of Allergy*, 2012, p. 681258. Available at: https://doi.org/10.1155/2012/681258.

Komalla, V. *et al.* (2023) 'Advances in soft mist inhalers', *Expert Opinion on Drug Delivery*, 20(8), pp. 1055–1070. Available at: https://doi.org/10.1080/17425247.2023.2231850.

Lai, C.K.M., Wong, K.H. and Cheung, P.C.K. (2008) 'Antiproliferative effects of sclerotial polysaccharides from Polyporus rhinocerus cooke (Aphyllophoromycetideae) on different kinds of leukemic cells', *International Journal of Medicinal Mushrooms*, 10(3), pp. 255–264. Available at: https://doi.org/10.1615/IntJMedMushr.v10.i3.60.

Lai, K. (2016) 'Comparison of Clinical Characteristics and Pathophysiology of Cough Predominate Asthma and Noncough Predominate Asthma', *Journal of Allergy and Clinical Immunology*, 137(2), p. SUPLEMENT AB101. Available at: https://doi.org/10.1016/j.jac.2015.12.457.

Lai, W.H. *et al.* (2011) 'Optimal Culture Conditions for Mycelial Growth of Lignosus rhinocerus', *Mycobiology*, 39(2), p. 92. Available at: https://doi.org/10.4489/MYCO.2011.39.2.092.

Lai, W.H. *et al.* (2013) 'Molecular phylogenetic analysis of wild Tiger's milk mushroom (Lignosus rhinocerus) collected from Pahang, Malaysia and its nutritional value and toxic metal content', *International Food Research Journal*, 20, pp. 2301–2307.

Lai, W.H., Zainal, Z. and Daud, F. (2014) *Preliminary study on the potential of polysaccharide from indigenous tiger's milk mushroom (Lignosus rhinocerus) as anti-lung cancer agent*, *AIP Conference Proceedings*. Available at: https://doi.org/10.1063/1.4895252.

Lakio, S. *et al.* (2015) 'Optimizing aerosolization of a high-dose L-arginine powder for pulmonary delivery', *Asian Journal of Pharmaceutical Sciences*, 10(6), pp. 528–540. Available at: https://doi.org/10.1016/j.ajps.2015.08.001.

Lallukka, T. *et al.* (2017) 'GBD 2015 mortality and causes of death collaborators. Global, regional, and national life expectancy, all-cause mortality, and cause-specifi c mortality for 249 causes of death, 1980-2015: a systematic analysis for the global burden of disease study 2015 ', *Lancet*, 389(10064), pp. E1–E1.

Lambrecht, B.N. and Hammad, H. (2012) 'Lung dendritic cells in respiratory viral infection and asthma: from protection to immunopathology', *Annual Review of Immunology* , 30, pp. 243–270.

Lambrecht, B.N. and Hammad, H. (2015) 'The immunology of asthma', *Nature Immunology*, 16(1), pp. 45–56. Available at: https://doi.org/10.1038/ni.3049.

Lambrecht, B.N., Hammad, H. and Fahy, J. V (2019) 'The cytokines of asthma', *Immunity*, 50, pp. 975–991.

Lau, B.F. *et al.* (2013) 'Chemical composition and cellular toxicity of ethnobotanical-based hot and cold aqueous preparations of the tiger's milk mushroom (Lignosus rhinocerotis)', *Journal of Ethnopharmacology*, 150(1), pp. 252–262. Available at: https://doi.org/10.1016/j.jep.2013.08.034.

Lau, B.F. *et al.* (2014) 'The potential of mycelium and culture broth of Lignosus rhinocerotis as substitutes for the naturally occluding sclerotium with regard to antioxidant capacity, cytotoxic effect, and low-molecular-weight chemical constituents', *PloSOne*, 9(7), p. e102509. Available at: https://doi.org/10.1371/journal.pone.0102509.

Lau, B.F. *et al.* (2015) 'Ethnomedicinal uses, pharmacological activities, and cultivation of Lignosus spp. (tiger′s milk mushrooms) in Malaysia - A review.', *Journal of ethnopharmacology*, 169, pp. 441–458. Available at: https://doi.org/10.1016/j.jep.2015.04.042.

Lau, B.F., Abdullah, N. and Aminudin, N. (2013) 'Chemical composition of the tiger's milk mushroom, Lignosus rhinocerotis (Cooke) Ryvarden, from different developmental stages', *Journal of Agricultural and Food Chemistry*, 61(20), pp. 4890–4897. Available at: https://doi.org/10.1021/jf4002507.

Lavorini, F. (2013) 'The challenge of delivering therapeutic aerosols to asthma patients', *ISRN Allergy*, 102418. Available at: https://doi.org/10.1155/2013/102418. 2013.

Lee, D.H. and Kim, H.W. (2014) 'Innate immunity induced by fungal β-glucans via dectin-1 signaling pathway', *International journal of medicinal mushrooms*, 16(1), pp. 1–16. Available at: https://doi.org/10.1615/INTJMEDMUSHR.V16.I1.10.

Lee, J.S. and Hong, E.K. (2011) 'Immunostimulating activity of the polysaccharides isolated from Cordyceps militaris', *International Immunopharmacology*, 11(9), pp. 1226–1233. Available at: https://doi.org/10.1016/J.INTIMP.2011.04.001.

Lee, M.K., Li, X., *et al.* (2018) 'Airway relaxation effects of water-soluble sclerotial extract from Lignosus rhinocerotis', *Frontiers in Pharmacology*, 9(MAY). Available at: https://doi.org/10.3389/fphar.2018.00461.

Lee, M.K., Lim, K.H., *et al.* (2018) 'Bronchodilator effects of Lignosus rhinocerotis extract on rat isolated airways is linked to the blockage of calcium entry', *Phytomedicine*, 42, pp. 172–179. Available at: https://doi.org/10.1016/j.phymed.2018.03.025.

Lee, M.L. *et al.* (2012) 'The antiproliferative activity of sclerotia of Lignosus rhinocerus (tiger milk mushroom). . ', *Evidence Based Complement Alternative Medicine*, 2012, pp. 5–9. Available at: https://doi.org/http://dx.doi.org/10.1155/2012/697603.

Lee, S.S. *et al.* (2011) 'Evaluation of the sub-acute toxicity of the sclerotium of Lignosus rhinocerus (Cooke), the Tiger Milk mushroom', *Journal of Ethnopharmacology*, 138, pp. 192–200. Available at: https://doi.org/10.1016/j.jep.2011.09.004.

Lee, S.S. *et al.* (2013) 'Preclinical toxicological evaluations of the sclerotium of Lignosus rhinocerus (Cooke), the Tiger Milk mushroom', *Journal of Ethnopharmacology*, 147(1), pp. 157–163. Available at: https://doi.org/10.1016/j.jep.2013.02.027.

Lee, S.S. *et al.* (2014) 'Anti-inflammatory effect of the sclerotium of Lignosus rhinocerotis (Cooke) Ryvarden, the Tiger Milk mushroom', *BMC Complementary and Alternative Medicine*, 14(1), pp. 1–8. Available at: https://doi.org/10.1186/1472-6882-14-359.

Lee, S.S., Chang, Y.S. and Noraswati, M.N.R. (2009) 'Utilization of macrofungi by some indigenous communities for food and medicine in Peninsular Malaysia', *Forest Ecology and Management*, 257(10), pp. 2062–2065. Available at: https://doi.org/10.1016/j.foreco.2008.09.044.

Lee, Y.T. *et al.* (2013) 'Effect of the fungal immunomodulatory protein FIP-fve on airway inflammation and cytokine production in mouse asthma model', *Cytokine*, 61(1), pp. 237–244. Available at: https://doi.org/10.1016/J.CYTO.2012.09.024.

Lefebvre, P. *et al.* (2015) 'Acute and chronic systemic corticosteroid-related complications in patients with severe asthma', *The Journal of allergy and clinical immunology*, 136(6), pp. 1488–1495. Available at: https://doi.org/10.1016/J.JACI.2015.07.046.

Leong, Y.K., Yang, F.C. and Chang, J.S. (2021) 'Extraction of polysaccharides from edible mushrooms: Emerging technologies and recent advances', *Carbohydrate Polymers*. Elsevier, p. 117006. Available at: https://doi.org/10.1016/j.carbpol.2020.117006.

Levine, S. *et al.* (2021) *Forum of International Respiratory Societies. The Global Impact of Respiratory Disease. Second, The Global Impact of Respiratory Disease - Second Edition. Sheffield, European Respiratory Society*. Second. Sheffield: European Respiratory Society. Available at: https://alatorax.org/es/firs/el-impacto-global-de-las-enfermedades-respiratorias-3ra-edicion-espanol-y-portugues.

Li, H. *et al.* (2024) 'Polysaccharides from an edible mushroom, Hericium erinaceus, alleviate ulcerative colitis in mice by inhibiting the NLRP3 inflammasomes and reestablish intestinal homeostasis', *International Journal of Biological Macromolecules*, 267(P1), p. 131251. Available at: https://doi.org/10.1016/j.ijbiomac.2024.131251.

Li, J. and Zhang, B. (2013) 'Apigenin protects ovalbumin-induced asthma through the regulation of Th17 cells', *Fitoterapia*, 91, pp. 298–304. Available at: https://doi.org/10.1016/J.FITOTE.2013.09.009.

Li, L.-F.F. *et al.* (2021) 'Rubinoboletus ballouii polysaccharides exhibited immunostimulatory activities through toll-like receptor-4 via NF-κB pathway', *Phytotherapy Research*, 35(4), pp. 2108–2118. Available at: https://doi.org/10.1002/ptr.6958.

Li, L. *et al.* (2016) 'L-Leucine as an excipient against moisture on in vitro aerosolization performances of highly hygroscopic spray-dried powders', *European Journal of Pharmaceutics and Biopharmaceutics*, 102, pp. 132–141. Available at: https://doi.org/10.1016/j.ejpb.2016.02.010.

Li, M. *et al.* (2015) 'UDP-glucose pyrophosphorylase influences polysaccharide synthesis, cell wall components, and hyphal branching in Ganoderma lucidum via regulation of the balance between glucose-1-phosphate and UDP-glucose', *Fungal Genetics and Biology*, 82, pp. 251–263. Available at: https://doi.org/10.1016/J.FGB.2015.07.012.

Li, Q. *et al.* (2021) 'Ginsenoside Rh1 attenuates ovalbumin-induced asthma by regulating Th1/Th2 cytokines balance', *Bioscience, Biotechnology, and Biochemistry*, 85(8), pp. 1809–1817. Available at: https://doi.org/10.1093/BBB/ZBAB099.

Li, X. and Wang, L. (2016) 'Effect of extraction method on structure and antioxidant activity of Hohenbuehelia serotina polysaccharides', *International Journal of*

Biological Macromolecules, 83, pp. 270–276. Available at: https://doi.org/10.1016/j.ijbiomac.2015.11.060.

Li, X.M. (2011) 'Treatment of asthma and food allergy with herbal interventions from traditional Chinese medicine', *Mount Sinai Journal of Medicine*, 78, pp. 697–716.

Li, Y. *et al.* (2020) 'ORMDL3 modulates airway epithelial cell repair in children with asthma under glucocorticoid treatment via regulating IL-33', *Pulmonary Pharmacology & Therapeutics*, 64, p. 101963. Available at: https://doi.org/10.1016/j.pupt.2020.101963.

Liang, W. *et al.* (2018) 'Spray freeze drying of small nucleic acids as inhaled powder for pulmonary delivery', *Asian Journal of Pharmaceutical Sciences*, 13(2), pp. 163–172. Available at: https://doi.org/10.1016/J.AJPS.2017.10.002.

Liang, Y. *et al.* (2020) 'Short-term oral corticosteroids for initial treatment of moderate-to-severe persistent asthma: A double-blind, randomized, placebo-controlled trial', *Respiratory Medicine*, 172, p. 106126. Available at: https://doi.org/10.1016/j.rmed.2020.106126.

Liu, C. *et al.* (2016) 'Immunomodulatory Activity of Polysaccharide-Protein Complex from the Mushroom Sclerotia of Polyporus rhinocerus in Murine Macrophages', *Journal of Agricultural and Food Chemistry*, 64(16), pp. 3206–3214. Available at: https://doi.org/10.1021/acs.jafc.6b00932.

Liu, G. and Liu, F. (2022) 'Bach2: A Key Regulator in Th2-Related Immune Cells and Th2 Immune Response', *Journal of Immunology Research*, 2022(1), p. 2814510. Available at: https://doi.org/10.1155/2022/2814510.

Liu, H. *et al.* (2022) 'Different exposure modes of PM2.5 induces bronchial asthma and fibrosis in male rats through macrophage activation and immune imbalance induced by TIPE2 methylation', *Ecotoxicology and Environmental Safety*, 247, p. 114200. Available at: https://doi.org/10.1016/J.ECOENV.2022.114200.

Liu, Q. *et al.* (2022) 'Neutral Polysaccharides From Hohenbuehelia serotina With Hypoglycemic Effects in a Type 2 Diabetic Mouse Model', *Frontiers in Pharmacology*, 13(May), pp. 1–10. Available at: https://doi.org/10.3389/fphar.2022.883653.

Liu, Y. *et al.* (2016) 'Purification, characterization and antioxidant activity of polysaccharides from Flammulina velutipes residue', *Carbohydrate Polymers*, 145, pp. 71–77. Available at: https://doi.org/10.1016/J.CARBPOL.2016.03.020.

Liu, Y. *et al.* (2019) 'Immunomodulatory Activities of Polysaccharides from White Button Mushroom, *Agaricus bisporus* (Agaricomycetes), Fruiting Bodies and Cultured Mycelia in Healthy and Immunosuppressed Mice', *International Journal of Medicinal Mushrooms*, 21(1), pp. 13–27. Available at: https://doi.org/10.1615/INTJMEDMUSHROOMS.2018029648.

Loftus, P.A. and Wise, S.K. (2015) 'Epidemiology and economic burden of asthma', *International forum of allergy & rhinology*, 5 Suppl 1, pp. S7–S10. Available at: https://doi.org/10.1002/ALR.21547.

Lowe, A.P.P. *et al.* (2017) 'Route of Administration Affects Corticosteroid Sensitivity of a Combined Ovalbumin and Lipopolysaccharide Model of Asthma Exacerbation in Guinea Pigs', *The Journal of pharmacology and experimental therapeutics*, 362(2), pp. 327–337. Available at: https://doi.org/10.1124/JPET.117.241927.

Luk, K.H. *et al.* (2023) 'Selenium nanoparticles functionalized by mushroom polysaccharide-protein complex: A novel nano-mineral for managing postmenopausal osteoporosis', *Journal of Functional Foods*, 110(July), p. 105832. Available at: https://doi.org/10.1016/j.jff.2023.105832.

Ma, G. (2024) 'Stationary phases for the separation of biopolymers by ion-exchange chromatography', *Ion-Exchange Chromatography and Related Techniques*, pp. 69–90. Available at: https://doi.org/10.1016/B978-0-443-15369-3.00021-3.

Maa, Y.F. *et al.* (1999) 'Protein inhalation powders: spray drying vs spray freeze drying', *Pharmaceutical research*, 16(2), pp. 249–254. Available at: https://doi.org/10.1023/A:1018828425184.

Mäkelä, M.J. *et al.* (2002) 'The failure of interleukin-10-deficient mice to develop airway hyperresponsiveness is overcome by respiratory syncytial virus infection in allergen-sensitized/challenged mice', *American journal of respiratory and critical care medicine*, 165(6), pp. 824–831. Available at: https://doi.org/10.1164/AJRCCM.165.6.2105062.

Mallol, J. *et al.* (2013) 'The International Study of Asthma and Allergies in Childhood (ISAAC) Phase Three: A global synthesis', *Allergologia et Immunopathologia*, 41(2), pp. 73–85. Available at: https://doi.org/10.1016/j.aller.2012.03.001.

Mans, D.R.A. *et al.* (2015) 'Evaluation of surinamese medicinal plants for their potential bronchospasmolytic effects in isolated guinea pig tracheal chains', *Research Journal of Medicinal Plant*, 9(1), pp. 14–23. Available at: https://doi.org/10.3923/rjmp.2015.14.23.

Marks, G.B. *et al.* (2001) 'Thunderstorm outflows preceding epidemics of asthma during spring and summer', *Thorax*, 56, pp. 468–471.

Marple, V.A., Hochrainer, D., *et al.* (2003) 'Next generation pharmaceutical impactor (a new impactor for pharmaceutical inhaler testing). Part I: Design', *Journal of aerosol medicine : the official journal of the International Society for Aerosols in Medicine*, 16(3), pp. 283–299. Available at: https://doi.org/10.1089/089426803769017659.

Marple, V.A., Olson, B.A., *et al.* (2003) 'Next Generation Pharmaceutical Impactor (a new impactor for pharmaceutical inhaler testing). Part II: Archival calibration', *Journal of Aerosol Medicine: Deposition, Clearance, and Effects in the Lung*,

16(3), pp. 301–324. Available at: https://doi.org/10.1089/089426803769017668.

McCleary, B. V. and Draga, A. (2016) 'Measurement of β-Glucan in Mushrooms and Mycelial Products', *Journal of AOAC International*, 99(2), pp. 364–373. Available at: https://doi.org/10.5740/JAOACINT.15-0289.

Mehtaa, P. *et al.* (2018) 'Phytoconstituent based dry powder inhalers as biomedicine for the management of pulmonary diseases', *Biomedicine & Pharmacotherapy*, 108, pp. 828–837. Available at: https://doi.org/https://doi.org/10.1016/j.biopha.2018.09.094.

Memarzia, A. *et al.* (2019) 'The contribution of beta-2 adrenergic, muscarinic and histamine (H1) receptors, calcium and potassium channels and cyclooxygenase pathway in the relaxant effect of Allium cepa L. on the tracheal smooth muscle', *Journal of Ethnopharmacology*, 241(June), p. 112012. Available at: https://doi.org/10.1016/j.jep.2019.112012.

Menchi, E. *et al.* (2022) 'Optimization of Long-Acting Bronchodilator Dose Ratios Using Isolated Guinea Pig Tracheal Rings for Synergistic Combination Therapy in Asthma and COPD', *Pharmaceuticals*, 15(8). Available at: https://doi.org/10.3390/ph15080963.

Menzies-Gow, A. *et al.* (2019) 'An expert consensus framework for asthma remission as a treatment goal', *Journal of Allergy and Clinical Immunology*, 145(3), pp. 757–765. Available at: https://doi.org/10.1016/j.jaci.2019.12.006.

MERUERT, E.B. *et al.* (2023) 'Experimental Bronchial Asthma in Different Laboratory Animal Models (Review Article)', *Vestnik*, (1(64)), pp. 145–165. Available at: https://doi.org/10.53065/kaznmu.2023.90.52.012.

Michele, T.M., Zhao, L. and Sahajwalla, C.G. (2012) 'Tachyphylaxis With Scheduled Use Of Short-Acting Beta-Agonists In Patients With Asthma', *American Journal of Respiratory and Critical Care Medicine*, 185(A3955), p. A3955. Available at: https://doi.org/10.1164/ajrccm-conference.2012.185.1_meetingabstracts.a3955.

Miller, N.C. *et al.* (1992) 'Assessment of the twin impinger for size measurement of metered-dose inhaler sprays', *Pharmaceutical research*, 9(9), pp. 1123–1127. Available at: https://doi.org/10.1023/A:1015835301929.

MM, B. and Bradford, M.M. (1976) 'A rapid and sensitive method for the quantitation of microgram quantities of protein utilizing the principle of protein-dye binding', 72(1–2), pp. 248–254. Available at: https://pubmed.ncbi.nlm.nih.gov/942051/ (Accessed: 11 September 2022).

Mohanarji, S., Dharmalingam, S. and Kalusalingam, A. (2012) 'Screening of Lignosus rhinocerus Extracts as Antimicrobial Agents against Selected Human Pathogens', *Journal of Pharmaceutical and Biomedical Sciences© (JPBMS)*, 2012(11), p. 18. Available at: www.jpbms.info (Accessed: 26 July 2024).

Mohd Jamil, N.A. *et al.* (2013) ' LCMS-QTOF Determination of Lentinan-Like β - D-Glucan Content Isolated by Hot Water and Alkaline Solution from Tiger's Milk Mushroom, Termite Mushroom, and Selected Local Market Mushrooms ', *Journal of Mycology*, 2013, pp. 1–8. Available at: https://doi.org/10.1155/2013/718963.

Momtazmanesh, S. *et al.* (2023) 'Global burden of chronic respiratory diseases and risk factors, 1990–2019: an update from the Global Burden of Disease Study 2019', *eClinicalMedicine*, 59. Available at: https://doi.org/10.1016/j.eclinm.2023.101936.

Montalbano, A.M. *et al.* (2016) 'Autocrine Acetylcholine, Induced by IL-17A via NFκB and ERK1/2 Pathway Activation, Promotes MUC5AC and IL-8 Synthesis in Bronchial Epithelial Cells', *Mediators of inflammation*, 2016. Available at: https://doi.org/10.1155/2016/9063842.

Moon, S.M. *et al.* (2013) 'Purification and characterization of a novel fibrinolytic α chymotrypsin like serine metalloprotease from the edible mushroom, Lyophyllum shimeji', *Journal of Bioscience and Bioengineering*, 117(5), pp. 544–550. Available at: https://doi.org/10.1016/J.JBIOSC.2013.10.019.

Morgan, S.J. *et al.* (2014) 'β-agonist-mediated relaxation of airway smooth muscle is protein kinase A-dependent', *Journal of Biological Chemistry*, 289(33), pp. 23065–23074. Available at: https://doi.org/10.1074/jbc.M114.557652.

Mowbray, F.I. *et al.* (2020) 'Examining the clinical management of asthma exacerbations by nurse practitioners in a pediatric emergency department', *International Emergency Nursing*, 50, p. 100844. Available at: https://doi.org/10.1016/j.ienj.2020.100844.

Muhamad, S. *et al.* (2019) 'Intranasal administration of Lignosus�rhinocerotis (Cooke) Ryvarden (Tiger Milk mushroom) extract attenuates airway inflammation in murine model of allergic asthma', *Experimental and Therapeutic Medicine*, 17, pp. 3867–3876. Available at: https://doi.org/10.3892/etm.2019.7416.

Muhamad, S.A. *et al.* (2023) 'Lignosus rhinocerotis extract ameliorates airway inflammation and remodelling via attenuation of TGF-β1 and Activin A in a prolonged induced allergic asthma model', *Scientific Reports*, 13(1), pp. 1–16. Available at: https://doi.org/10.1038/s41598-023-45640-z.

Muralidharan, P. *et al.* (2014) 'Inhalable PEGylated phospholipid nanocarriers and PEGylated therapeutics for respiratory delivery as aerosolized colloidal dispersions and dry powder inhalers', *Pharmaceutics*, 6(2), pp. 333–353.

Murphy, K.R. *et al.* (2020) 'Nebulized Inhaled Corticosteroids in Asthma Treatment in Children 5 Years or Younger: A Systematic Review and Global Expert Analysis', *J Allergy Clin Immunol Pract*, 8(1), pp. 815–827. Available at: https://doi.org/10.1016/j.jaip.2020.01.042.

Murray, C.S. *et al.* (2006) 'Study of modifiable risk factors for asthma exacerbations: virus infection and allergen exposure increase the risk of asthma hospital admissions in children', *Thorax* , 61, pp. 376–382.

Murray, C.S., Simpson, A. and Custovic, A. (2004) 'Allergens, viruses, and asthma exacerbations ', *Proceedings of the American Thoracic Society*, 1, pp. 99–104.

Myou, S. *et al.* (2003) 'Blockade of Inflammation and Airway Hyperresponsiveness in Immune-sensitized Mice by Dominant-Negative Phosphoinositide 3-Kinase-TAT', *Journal of Experimental Medicine*, 198(10), pp. 1573–1582. Available at: https://doi.org/10.1084/jem.20030298.

Naclerio, R.M. (1991) ' Allergic rhinitis', *New England Journal of Medicine*, 325(12), pp. 860–869.

Nallathamby, N. *et al.* (2018) 'A status review of the bioactive activities of tiger milk mushroom Lignosus rhinocerotis (Cooke) Ryvarden', *Frontiers in Pharmacology*, 8(JAN), p. 998. Available at: https://doi.org/10.3389/fphar.2017.00998.

Narendra, D., Blixt, J. and Hanania, N.A. (2019) 'Immunological biomarkers in severe asthma', *Seminars in Immunology*, 46, p. 101332. Available at: https://doi.org/10.1016/j.smim.2019.101332.

Nathan, C. and Xie, Q. (1994) 'Regulation of biosynthesis of nitric oxide', *Journal of Biological Chemistry*, 269, pp. 13725–13728.

Network GA (2018) *The Global Asthma Report*, *Auckland, New Zealand*. http://www.globalasthmareport.org.

Newnham, J.P. (2001) 'Is prenatal glucocorticoid administration another origin of adult disease?', *Clinical and Experimental Pharmacology and Physiology*, 28(11), pp. 957–961. Available at: https://doi.org/10.1046/j.1440-1681.2001.03559.x.

Nguyen Hoang, A.T. *et al.* (2012) 'Dendritic cell functional properties in a three-dimensional tissue model of human lung mucosa', *American Journal Physiology-Lung Cellular and Molecular Physiology*, 302, pp. L226–L237.

Ochiai, K. *et al.* (1994) 'A review on FceRI on human epidermal Langerhans cells. ', *Intional Archive on Allergy Immunology*, 104, pp. 63–64.

Okunishi, K. and Peters-Golden, M. (2011) 'Leukotrienes and airway inflammation', *Biochimica et Biophysica Acta - General Subjects*. NIH Public Access, pp. 1096–1102. Available at: https://doi.org/10.1016/j.bbagen.2011.02.005.

Omer, H., Husein, N. and Hamadameen, H. (2019) 'Comparison between the next generation impactor and the twin glass impinge as model pulmonary drug delivery devices', *Zanco Journal of Medical Sciences*, 23(1), pp. 74–80. Available at: https://doi.org/10.15218/ZJMS.2019.010.

OMS (2013) *Asthma : Fact Sheet no.307.* Available at: https://doi.org/http://www.who.int/mediacentre/factsheets/fs307/en/.

Otake, H., Okuda, T. and Okamoto, H. (2016) 'Development of spray-freeze-dried powders for inhalation with high inhalation performance and antihygroscopic property', *Chemical and Pharmaceutical Bulletin*, 64(3), pp. 239–245. Available at: https://doi.org/10.1248/cpb.c15-00824.

Oyabu, T. *et al.* (2015) 'Comparison between whole-body inhalation and nose-only inhalation on the deposition and health effects of nanoparticles', *Environmental Health and Preventive Medicine*, 21(1), p. 42. Available at: https://doi.org/10.1007/S12199-015-0493-Z.

Pan, H. *et al.* (2015) 'Purification and identification of a polysaccharide from medicinal mushroom Amauroderma rude with immunomodulatory activity and inhibitory effect on tumor growth', *Oncotarget*, 6(19), p. 17777. Available at: https://doi.org/10.18632/ONCOTARGET.4397.

Paranjpe, M. and MüllerGoymann, C.C. (2014) 'Nanoparticle-Mediated Pulmonary Drug Delivery: A Review', *International Journal of Molecular Sciences*, 15, pp. 5852–5873. Available at: https://doi.org/10.3390/ijms15045852.

Parniakov, O. *et al.* (2014) 'Pulsed Electric Field Assisted Pressure Extraction and Solvent Extraction from Mushroom (Agaricus Bisporus)', *Food and Bioprocess Technology*, 7(1), pp. 174–183. Available at: https://doi.org/10.1007/S11947-013-1059-Y/METRICS.

Pascoe, C.D., Vaghasiya, J. and Halayko, A.J. (2020) 'Oxidation specific epitopes in asthma: New possibilities for treatment', *International Journal of Biochemistry and Cell Biology*, 129, p. 105864. Available at: https://doi.org/10.1016/j.biocel.2020.105864.

Pasqualotto A.C. et al. (2009) 'The effects of antifungal therapy on severe asthma with fungal sensitization and allergic bronchopulmonary aspergillosis', *Respirology*, 14, pp. 1121–1127.

Pattni, B.S. and Torchilin, V.P. (2015) 'Targeted Drug Delivery Systems: Strategies and Challenges', pp. 3–38. Available at: https://doi.org/10.1007/978-3-319-11355-5_1.

Peden, D.B. (2003) 'Air pollution: indoor and outdoor', in N.F.J. Adkinson et al. (eds) *Middleton's allergy: principles and practice*. Philadelphia: Mosby, pp. 515–528.

Peden, D.B. (2005) 'The epidemiology and genetics of asthma risk associated with air pollution', *Journal of Allergy and Clinical Immunology*, 115, pp. 213–219.

Pera, T. and Penn, R.B. (2014) 'Crosstalk between beta-2-adrenoceptor and muscarinic acetylcholine receptors in the airway', *Current Opinion in Pharmacology*. NIH Public Access, pp. 72–81. Available at: https://doi.org/10.1016/j.coph.2014.03.005.

Perrigoue, J.G. *et al.* (2009) 'MHC class II-dependent basophil-CD4+ T cell interactions promote T(H)2 cytokine-dependent immunity. ', *Nature Immunology*, 10, pp. 697–705.

Phillips, J.E., Zhang, X. and Johnston, J.A. (2017) 'Dry powder and nebulized aerosol inhalation of pharmaceuticals delivered to mice using a nose-only exposure system', *Journal of Visualized Experiments*, 2017(122), p. e55454. Available at: https://doi.org/10.3791/55454.

Pieper, M.P. (2012) 'The non-neuronal cholinergic system as novel drug target in the airways', *Life sciences*, 91(21–22), pp. 1113–1118. Available at: https://doi.org/10.1016/J.LFS.2012.08.030.

Porter, P.C. *et al.* (2011) 'Seeking common pathophysiology in asthma, atopy and sinusitis', *Trends in Immunology*, 32(2). Available at: https://doi.org/10.1016/j.it.2010.11.007.

Powell, C., White, R. and Primhak, R. (1993) *Asthma management guidelines.*, *BMJ (Clinical research ed.)*. National Asthma Education and Prevention Program Coordinating Committee. Available at: https://doi.org/10.1136/bmj.306.6885.1132-b.

Prado, C.M. *et al.* (2006) 'Effect of nitric oxide synthases in chronic allergic airway inflammation and remodeling', *American Journal of Respiratory Cell and Molecula Biology*, 35, pp. 457–465.

Prakash Maran, J. *et al.* (2017) 'Ultrasound assisted extraction of bioactive compounds from Nephelium lappaceum L. fruit peel using central composite face centered response surface design', *Arabian Journal of Chemistry*, 10, pp. S1145–S1157. Available at: https://doi.org/10.1016/j.arabjc.2013.02.007.

Price, D.B. *et al.* (2018) 'Adverse outcomes from initiation of systemic corticosteroids for asthma: long-term observational study', *Journal Asthma Allergy*, 11, pp. 193–204.

Qin, D.W. and Han, C. (2014) 'Medicinal and edible fungi as an alternative medicine for treating age-related disease', *Evidence-based Complementary and Alternative Medicine*, 2014. Available at: https://doi.org/10.1155/2014/638561.

Ramet M et al. (2001) 'Drosophila scavenger receptor CI is a pattern recognition receptor for bacteria', *Immunity*, 15, pp. 1027–1038.

Rawy, A.M. and Mansour, A.I. (2015) 'Fraction of exhaled nitric oxide measurement as a biomarker in asthma and COPD compared with local and systemic inflammatory markers', *Egyptian Journal of Chest Diseases and Tuberculosis*, 64, pp. 13–20. Available at: https://doi.org/10.1016/j.ejcdt.2014.09.004.

Reed, C.E. (2010) 'Asthma in the elderly: Diagnosis and management', *Journal of Allergy and Clinical Immunology*, 126(4), pp. 681–687. Available at: https://doi.org/10.1016/j.jaci.2010.05.035.

Rehman, N.U. *et al.* (2022) 'In Silico and Ex Vivo Studies on the Spasmolytic Activities of Fenchone Using Isolated Guinea Pig Trachea', *Molecules*, 27(4), pp. 1–14. Available at: https://doi.org/10.3390/molecules27041360.

Ressmeyer, A.R. *et al.* (2006) 'Characterisation of guinea pig precision-cut lung slices: Comparison with human tissues', *European Respiratory Journal*, 28(3), pp. 603–611. Available at: https://doi.org/10.1183/09031936.06.00004206.

Roberts, D.L. and Mitchell, J.P. (2019) 'Measurement of Aerodynamic Particle Size Distribution of Orally Inhaled Products by Cascade Impactor: How to Let the Product Specification Drive the Quality Requirements of the Cascade Impactor', *AAPS PharmSciTech*, 20(2), pp. 1–10. Available at: https://doi.org/10.1208/s12249-018-1276-9.

Roffel, A.F. *et al.* (1988) 'Muscarinic M2 receptors in bovine tracheal smooth muscle: discrepancies between binding and function', *European Journal of Pharmacology*, 153(1), pp. 73–82. Available at: https://doi.org/10.1016/0014-2999(88)90589-4.

Roffel, A.F., Elzinga, C.R.S. and Zaagsma, J. (1990) 'Muscarinic M3 receptors mediate contraction of human central and peripheral airway smooth muscle', *Pulmonary pharmacology*, 3(1), pp. 47–51. Available at: https://doi.org/10.1016/0952-0600(90)90009-8.

Rosdan Bushra, S.M. and Nurul, A.A. (2022) 'Bioactive mushroom polysaccharides: The structure, characterization and biological functions', *Journal of Liquid Chromatography and Related Technologies*, 45(13–16), pp. 174–190. Available at: https://doi.org/10.1080/10826076.2023.2182317.

Rose, G. (1992) 'The strategy of preventive medicine', in. Oxford: Oxford University Press.

Rovati, G.E. *et al.* (2006) 'Cysteinyl-leukotrienes in the regulation of β2-adrenoceptor function: an in vitro model of asthma', *Respiratory Research*, 7(1), p. 103. Available at: https://doi.org/10.1186/1465-9921-7-103.

Roviezzo, F. *et al.* (2015) 'Hydrogen sulfide inhalation ameliorates allergen induced airway hypereactivity by modulating mast cell activation', *Pharmacological Research*, 100, pp. 85–92.

Russjan, E. and Kaczyńska, K. (2018) 'Murine models of hapten-induced asthma', *Toxicology*, 410, pp. 41–48. Available at: https://doi.org/10.1016/J.TOX.2018.09.001.

Ruthes, A.C., Smiderle, F.R. and Iacomini, M. (2015) 'D-Glucans from edible mushrooms: A review on the extraction, purification and chemical characterization approaches', *Carbohydrate Polymers*, 117, pp. 753–761. Available at: https://doi.org/10.1016/j.carbpol.2014.10.051.

Ruthes, A.C., Smiderle, F.R. and Iacomini, M. (2016) 'Mushroom heteropolysaccharides: A review on their sources, structure and biological

effects', *Carbohydrate Polymers*, 136, pp. 358–375. Available at: https://doi.org/10.1016/j.carbpol.2015.08.061.

Sabaratnam, V. *et al.* (2013) 'Neuronal health - Can culinary and medicinal mushrooms help?', *Journal of Traditional and Complementary Medicine*, 3(1), pp. 62–68. Available at: https://doi.org/10.4103/2225-4110.106549.

Sabat, R., Ouyang, W. and Wolk, K. (2013) 'Therapeutic opportunities of the IL-22–IL-22R1 system', *Nature Reviews Drug Discovery 2014 13:1*, 13(1), pp. 21–38. Available at: https://doi.org/10.1038/nrd4176.

Säfholm, J. *et al.* (2015) 'Prostaglandin E2 inhibits mast cell–dependent bronchoconstriction in human small airways through the E prostanoid subtype 2 receptor', *Journal of Allergy and Clinical Immunology*, 136(5), pp. 1232-1239.e1. Available at: https://doi.org/10.1016/j.jaci.2015.04.002.

Sandberg, S. *et al.* (2004) 'Asthma exacerbations in children immediately following stressful life events: a Cox's hierarchical regression', *Thorax*, 59, pp. 1046–1051.

Sarhan, R.M. *et al.* (2018) 'Effect of a nebulizer holding chamber on aerosol delivery', *Respiratory Care*, 63(9), pp. 1125–1131. Available at: https://doi.org/10.4187/respcare.06061.

Schatz, M., Clark, S. and Camargo, C.A. (2006) 'Sex differences in the presentation and course of asthma hospitalizations. ', *Chest*, 129, pp. 50–55.

Schears, G. *et al.* (1997) 'Chronic carbachol pretreatment decreases adenylyl cyclase activity in airway smooth muscle', *The American journal of physiology*, 273(3 Pt 1). Available at: https://doi.org/10.1152/AJPLUNG.1997.273.3.L640.

Schleich, F., Demarche, S. and Louis, R. (2016) 'Biomarkers in the management of difficult asthma', *Current Topics Medicinal Chemistry*, 16(14), pp. 1561–1573.

Schuijs, M.J. *et al.* (2013) 'Cytokine targets in airway inflammation', *Curr Opin Pharmacol*, 13, pp. 351–361.

Schuschnig, U., Heine, B. and Knoch, M. (2022) 'How Cold Is Cold Enough? Refrigeration of the Next-Generation Impactor to Prevent Aerosol Undersizing', *Journal of Aerosol Medicine and Pulmonary Drug Delivery*, 35(1), pp. 25–31. Available at: https://doi.org/10.1089/jamp.2021.0015.

Scott, G.D. and Fryer, A.D. (2012) 'Role of parasympathetic nerves and muscarinic receptors in allergy and asthma', *Chemical Immunology and Allergy*, 98, pp. 48–69.

Sears, M.R. (2008) 'Epidemiology of asthma exacerbations', *Journal of Allergy and Clinical Immunology*, 122(4), pp. 662–668. Available at: https://doi.org/10.1016/j.jaci.2008.08.003.

Seedevi, P. *et al.* (2019) 'Chemical structure and biological properties of a polysaccharide isolated from Pleurotus sajor-caju', *RSC advances*, 9(35), pp. 20472–20482. Available at: https://doi.org/10.1039/C9RA02977J.

Seow, S.L.S. *et al.* (2015) 'Lignosus rhinocerotis (Cooke) Ryvarden mimics the neuritogenic activity of nerve growth factor via MEK/ERK1/2 signaling pathway in PC-12 cells', *Scientific Reports*, 5, p. 16349. Available at: https://doi.org/10.1038/SREP16349.

Seow, S.L.S. *et al.* (2017) 'Tiger's milk medicinal mushroom, Lignosus rhinocerotis (Agaricomycetes) sclerotium inhibits nitric oxide production in LPS-stimulated BV2 microglia', *International Journal of Medicinal Mushrooms*, 19(5), pp. 405–418. Available at: https://doi.org/10.1615/IntJMedMushrooms.v19.i5.30.

Seumois, G. *et al.* (2014) 'Epigenomic analysis of primary human T cells reveals enhancers associated with TH2 memory cell differentiation and asthma susceptibility', *Nature Immunology*, 15, pp. 777–788.

Sheth, P., Stein, S.W. and Myrdal, P.B. (2014) 'Factors Influencing Aerodynamic Particle Size Distribution of Suspension Pressurized Metered Dose Inhalers', *AAPS PharmSciTech*, 16(1), pp. 192–201. Available at: https://doi.org/10.1208/s12249-014-0210-z.

Shin, Y.S., Takeda, K. and Gelfand, E.W. (2009) 'Understanding asthma using animal models', *Allergy, Asthma & Immunology Research*, 1(1), p. 10-18. Available at: https://doi.org/10.4168/AAIR.2009.1.1.10.

Shur, J. *et al.* (2012) 'Effect of device design on the in vitro performance and comparability for capsule-based dry powder inhalers', *AAPS Journal*, 14(4), pp. 667–676. Available at: https://doi.org/10.1208/s12248-012-9379-9.

Sillapachaiyaporn, C. and Chuchawankul, S. (2020) 'HIV-1 protease and reverse transcriptase inhibition by tiger milk mushroom (Lignosus rhinocerus) sclerotium extracts: In vitro and in silico studies', *Journal of Traditional and Complementary Medicine*, 10(4), pp. 396–404. Available at: https://doi.org/10.1016/j.jtcme.2019.08.002.

Simcock, D.E. *et al.* (2012) 'Induction of Angiogenesis by Airway Smooth Muscle From Patients with Asthma', *https://doi.org/10.1164/rccm.200707-1046OC*, 178(5), pp. 460–468. Available at: https://doi.org/10.1164/RCCM.200707-1046OC.

Singh, S. *et al.* (2023) 'Airway Epithelium: A Neglected but Crucial Cell Type in Asthma Pathobiology', *Diagnostics 2023, Vol. 13, Page 808*, 13(4), p. 808. Available at: https://doi.org/10.3390/DIAGNOSTICS13040808.

Sinyor, B. and Perez, L.C. (2023) 'Pathophysiology Of Asthma', *StatPearls* [Preprint]. Available at: https://www.ncbi.nlm.nih.gov/books/NBK551579/ (Accessed: 22 July 2024).

Smiderle, F.R. *et al.* (2017) 'Evaluation of microwave-assisted and pressurized liquid extractions to obtain β-d-glucans from mushrooms', *Carbohydrate Polymers*, 156, pp. 165–174. Available at: https://doi.org/10.1016/J.CARBPOL.2016.09.029.

Snipes, M.B. *et al.* (1989) 'Retention patterns for inhaled particles in the lung: Comparisons between laboratory animals and humans for chronic exposures', *Health Physics*, 57, pp. 69–78. Available at: https://doi.org/10.1097/00004032-198907001-00008.

Song, P. *et al.* (2022) 'Global, regional, and national prevalence of asthma in 2019: a systematic analysis and modelling study', *Journal of global health*, 12. Available at: https://doi.org/10.7189/JOGH.12.04052.

Song, X. *et al.* (2016) 'Effects of Temperature and Humidity on Laser Diffraction Measurements to Jet Nebulizer and Comparison with NGI', *AAPS PharmSciTech*, 17(2), pp. 380–388. Available at: https://doi.org/10.1208/s12249-015-0346-5.

Song, X. *et al.* (2018) 'Anti-inflammatory and hepatoprotective effects of exopolysaccharides isolated from Pleurotus geesteranus on alcohol-induced liver injury', *Scientific Reports*, 8(1). Available at: https://doi.org/10.1038/s41598-018-28785-0.

Song, Y. *et al.* (2023) 'Gene expression profiles and bioinformatics analysis in lung samples from ovalbumin-induced asthmatic mice', *BMC Pulmonary Medicine*, 23(1), pp. 1–13. Available at: https://doi.org/10.1186/S12890-023-02306-W/FIGURES/5.

Sou, T. *et al.* (2013) 'Designing a Multicomponent Spray-Dried Formulation Platform for Pulmonary Delivery of Biomacromolecules: The Effect of Polymers on the Formation of an Amorphous Matrix for Glassy State Stabilization of Biomacromolecules', *Drying Technology*, 31(13–14), pp. 1451–1458. Available at: https://doi.org/10.1080/07373937.2013.788019.

Steinke, J.W. and Borish, L. (2001) ' Th2 cytokines and asthma. Interleukin-4: Its role in the pathogenesis of asthma, and targeting it for asthma treatment with interleukin-4 receptor antagonists. , ', *Respiratory Research* , 2, p. 66-70.

Sullivan, H.C., Gebel, H.M. and Bray, R.A. (2017) 'Understanding solid-phase HLA antibody assays and the value of MFI', *Human Immunology*, 78(7–8), pp. 471–480. Available at: https://doi.org/10.1016/J.HUMIMM.2017.05.007.

Sum, A.Y.C. *et al.* (2020) 'The immunomodulating properties of tiger milk medicinal mushroom, lignosus rhinocerus tm02® cultivar (Agaricomycetes) and its associated carbohydrate composition', *International Journal of Medicinal Mushrooms*, 22(8), pp. 803–814. Available at: https://doi.org/10.1615/IntJMedMushrooms.2020035658.

Sun, F.J. *et al.* (2017) 'Association between ADAM metallopeptidase domain 33 gene polymorphism and risk of childhood asthma: A meta-analysis', *Brazilian*

Journal of Medical and Biological Research, 50(10), pp. 1–7. Available at: https://doi.org/10.1590/1414-431x20176148.

Sun, J. *et al.* (2021) 'Pulmonary rehabilitation focusing on the regulation of respiratory movement can improve prognosis of severe patients with COVID-19', *Annals of palliative medicine*, 10(4), pp. 4262–4272. Available at: https://doi.org/10.21037/apm-20-2014.

Sunther, M., Marchon, K. and Gupta, A. (2021) 'Tiotropium in the management of paediatric and adolescent asthma: Systematic review', *Paediatric Respiratory Reviews*, 38, pp. 58–62. Available at: https://doi.org/10.1016/j.prrv.2020.08.003.

Suziana Zaila, C.F. *et al.* (2013) 'Anti proliferative effect of Lignosus rhinocerotis, theTiger Milk mushroom on HCT 116 human colorectal cancer cells.', *Open Conference Proceedings Journal*, 4(2), pp. S65–S70.

Suzuki, Y. *et al.* (2021) 'Hydrogen sulfide as a novel biomarker of asthma and chronic obstructive pulmonary disease', *Allergology International*, 70(2), pp. 181–189. Available at: https://doi.org/10.1016/j.alit.2020.10.003.

Tan, C.S. *et al.* (2010) 'Genetic markers for identification of a Malaysian medicinal mushroom, Lignosus rhinocerus (Cendawan Susu Rimau)', *Acta Horticulturae*, 859, pp. 161–168. Available at: https://doi.org/10.17660/actahortic.2010.859.19.

Tan, E.S.S., Leo, T.K. and Tan, C.K. (2021) 'Effect of tiger milk mushroom (Lignosus rhinocerus) supplementation on respiratory health, immunity and antioxidant status: an open-label prospective study', *Scientific Reports*, 11(1), pp. 1–10. Available at: https://doi.org/10.1038/s41598-021-91256-6.

Tan, K.S., McFarlane, L.C. and Lipworth, B.J. (1997) 'Modulation of airway reactivity and peak flow variability in asthmatics receiving the oral contraceptive pill', *American Journal of Respiratory and Critical Care Medicine*, 155(4), pp. 1273–1277. Available at: https://doi.org/10.1164/ajrccm.155.4.9105066.

Tan, M.M.C. *et al.* (2022) 'Prevalence of and factors associated with multimorbidity among 18 101 adults in the South East Asia Community Observatory Health and Demographic Surveillance System in Malaysia: a population-based, cross-sectional study of the MUTUAL consortium', *BMJ Open*, 12, p. 68172. Available at: https://doi.org/10.1136/bmjopen-2022-068172.

Tang, D. *et al.* (2020) 'All-trans-retinoic acid shifts Th1 towards Th2 cell differentiation by targeting NFAT1 signalling to ameliorate immune-mediated aplastic anaemia', *British Journal of Haematology*, 191(5), pp. 906–919. Available at: https://doi.org/10.1111/bjh.16871.

Thakur, V.R. *et al.* (2019) 'An experimental model of asthma in rats using ovalbumin and lipopolysaccharide allergens', *Heliyon*, 5(11), p. e02864. Available at: https://doi.org/10.1016/j.heliyon.2019.e02864.

Thorat, S.R. and Meshram, S.M. (2015) 'Formulation and product development of pressurised metered dose inhaler: An overview', *Pharma Tutor*, Volume 3(Issue 9), pp. 58–59. Available at: https://www.pharmatutor.org/pdf_download/pdf/Vol. 3, Issue 9, September 2015, PharmaTutor, Paper-7.pdf.

Tian, H. *et al.* (2019) 'Immunomodulatory effects exerted by Poria Cocos polysaccharides via TLR4/TRAF6/NF-κB signaling in vitro and in vivo', *Biomedicine & Pharmacotherapy*, 112, p. 108709. Available at: https://doi.org/10.1016/J.BIOPHA.2019.108709.

Tian, M. *et al.* (2012) 'Correlation between serum H2S and pulmonary function in children with bronchial asthma', *Molecular Medicine Reports*, 6, pp. 335–338.

Tian, Y. *et al.* (2012) 'Ultrasonic-assisted extraction and antioxidant activity of polysaccharides recovered from white button mushroom (Agaricus bisporus)', *Carbohydrate Polymers*, 88(2), pp. 522–529. Available at: https://doi.org/10.1016/j.carbpol.2011.12.042.

To, T. *et al.* (2012) 'Globma prevalence in adults: findings from the cross-sectional world health survey', *BMC Public Health*, 12(204).

Townsend, E.A. and Emala, C.W. (2013) 'Quercetin acutely relaxes airway smooth muscle and potentiates β-agonist-induced relaxation via dual phosphodiesterase inhibition of PLCβ and PDE4', *American journal of physiology. Lung cellular and molecular physiology*, 305(5). Available at: https://doi.org/10.1152/AJPLUNG.00125.2013.

Trifilieff, A., El-Hashim, A. and Bertrand, C. (2000) 'Time course of inflammatory and remodeling events in a murine model of asthma: effect of steroid treatment', *American Journal of Physiology-Lung Cellular and Molecular Physiology*, 279(6), pp. L1120–L1128.

Trifunovic, A. *et al.* (2020) 'The potential of microRNAs as noninvasive biomarkers in acute pediatric asthma', *Journal of Allergy and Clinical Immunology*, LETTERS TO, pp. 1706–1708. Available at: https://doi.org/10.1016/j.jaci.2020.01.032.

Tripathi, P. *et al.* (2013) 'Increased expression of ADAM33 protein in asthmatic patients as compared to non-asthmatic controls', *The Indian Journal of Medical Research*, 137(3), p. 507. Available at: https://pmc.ncbi.nlm.nih.gov/articles/PMC3705658/ (Accessed: 17 November 2024).

Troisi, R.J. *et al.* (1995) 'Menopause, postmenopausal estrogen preparations and the risk of adult-onset asthma: a prospective cohort study', *Am J Respir Crit Care Medicine*, 152, pp. 1183–1188.

Tsai, M.J. *et al.* (2015) 'Aryl hydrocarbon receptor agonists upregulate VEGF secretion from bronchial epithelial cells', *Journal of molecular medicine (Berlin, Germany)*, 93(11), pp. 1257–1269. Available at: https://doi.org/10.1007/S00109-015-1304-0.

Tsai, W.C. *et al.* (2022) 'Lignosus rhinocerus attenuates non-alcoholic fatty liver induced by plant-based high-fat diet in hamster', *Electronic Journal of Biotechnology*, 58, pp. 46–54. Available at: https://doi.org/10.1016/j.ejbt.2022.05.004.

Uchida, A., Sakaue, K. and Inoue, H. (2018) 'Epidemiology of asthma-chronic obstructive pulmonary disease overlap (ACO)', *Allergology International*, 67, pp. 165–171. Available at: https://doi.org/10.1016/j.alit.2018.02.002.

Usuldin, S.R.A. (2020) 'Identification of a Malaysian Tiger Milk Mushroom Specimen and Characterisation of Its Mycelial (1,3)-B-D-Glucan'.

Usuldin, S.R.A. *et al.* (2021) 'In vivo toxicity of bioreactor-grown biomass and exopolysaccharides from Malaysian tiger milk mushroom mycelium for potential future health applications', *Scientific Reports*, 11(1), pp. 1–13. Available at: https://doi.org/10.1038/s41598-021-02486-7.

van-Helden, M.J. and Lambrecht, B.N. (2013) 'Dendritic cells in asthma', *Current Opinion in Immunology*, 25, pp. 745–754. Available at: https://doi.org/10.1016/j.coi.2013.10.002.

Vasconcelos, L.H.C. *et al.* (2019) 'A Guinea pig model of airway smooth muscle hyperreactivity induced by chronic allergic lung inflammation: Contribution of epithelium and oxidative stress', *Frontiers in Pharmacology*, 9(JAN), pp. 1–15. Available at: https://doi.org/10.3389/fphar.2018.01547.

Verma, R.K. *et al.* (2011) 'Inhaled therapies for tuberculosis and the relevance of activation of lung macrophages by particulate drug-delivery systems', *Therapeutic Delivery*, 2(6), pp. 753–768. Available at: https://doi.org/10.4155/TDE.11.34/ASSET/IMAGES/LARGE/FIGURE1.JPEG.

Verstraete, K. *et al.* (2017) 'Structure and antagonism of the receptor complex mediated by human TSLP in allergy and asthma', *Nature Communications*, 8, p. 14937.

Vicencio. A.G. et al. (2010) 'Severe asthma with fungal sensitization in a child: response to itraconazole therapy', *Pediatrics*, 125, pp. e1255–e1258.

Volman, J.J. *et al.* (2010) 'Effects of mushroom-derived β-glucan-rich polysaccharide extracts on nitric oxide production by bone marrow-derived macrophages and nuclear factor-κB transactivation in Caco-2 reporter cells: Can effects be explained by structure?', *Molecular Nutrition & Food Research*, 54(2), pp. 268–276. Available at: https://doi.org/10.1002/MNFR.200900009.

Wang, H. *et al.* (2022) 'Current advances and potential trends of the polysaccharides derived from medicinal mushrooms sanghuang', *Frontiers in Microbiology*, 13(1968). Available at: https://doi.org/10.3389/fmicb.2022.965934.

Wang, J. *et al.* (2020) 'Physicochemical properties and bioactivities of Lentinula edodes polysaccharides at different development stages.', *International*

journal of biological macromolecules, 150, pp. 573–577. Available at: https://doi.org/10.1016/j.ijbiomac.2020.02.099.

Wang, Q. *et al.* (2017) 'Bioactive mushroom polysaccharides: A review on monosaccharide composition, biosynthesis and regulation', *Molecules*, 22(6). Available at: https://doi.org/10.3390/molecules22060955.

Wang, X.H. *et al.* (2022) 'Antioxidant and anti-aging effects of polysaccharide LDP-1 from wild Lactarius deliciosus on Caenorhabditis elegans', *Food and Nutrition Research*, 66(6), pp. 1–12. Available at: https://doi.org/10.29219/fnr.v66.8110.

Wasser, S.P. (2014) 'Medicinal mushroom science: Current perspectives, advances, evidences, and challenges', *Biomedical Journal*, 37(6), pp. 345–356. Available at: https://doi.org/10.4103/2319-4170.138318.

Williams, D.M. and Rubin, B.K. (2018) 'Clinical Pharmacology of Bronchodilator Medications', 63(6), pp. 641–654. Available at: https://doi.org/10.4187/RESPCARE.06051.

Wills-Karp, M. *et al.* (1998) 'Interleukin-13: central mediator of allergic asthma', *Science*, 282(5397), pp. 2258–2261.

Wills-Karp, M. (2004) ' Interleukin-13 in asthma pathogenesis', *Immunological Reviews*, 202, pp. 175–190.

Wills-Karp, M. (2010) 'Allergen-specific pattern recognition receptor pathways , .', *Current Opinion in Immunology*, 22, pp. 777–782.

Wong, K.H. and Cheung, P.C.K. (2008) 'Sclerotia: emerging functional food derived from mushrooms', in P.C.K. Cheung (ed.) *Mushrooms as Functional Food*. New Jersey: John Wiley and Sons Inc, pp. 111–146.

Wong, K.H., Lai, C.K.M. and Cheung, P.C.K. (2009) 'Stimulation of human innate immune cells by medicinal mushroom sclerotial polysaccharides', *International Journal of Medicinal Mushrooms*, 11(3), pp. 215–223. Available at: https://doi.org/10.1615/INTJMEDMUSHR.V11.I3.10.

Wong, K.H., Lai, C.K.M. and Cheung, P.C.K. (2011) 'Immunomodulatory activities of mushroom sclerotial polysaccharides', *Food Hydrocolloids*, 25(2), pp. 150–158. Available at: https://doi.org/10.1016/j.foodhyd.2010.04.008.

Wright, D. *et al.* (2013) 'Models to study airway smooth muscle contraction in vivo, ex vivo and in vitro: Implications in understanding asthma', *Pulmonary Pharmacology and Therapeutics*, 26(1), pp. 24–36. Available at: https://doi.org/10.1016/j.pupt.2012.08.006.

Wu, C.T. *et al.* (2020) 'Role of biomarkers and effect of FIP-fve in acute and chronic animal asthma models', *Journal of Microbiology, Immunology and Infection*, 53(6), pp. 996–1007. Available at: https://doi.org/10.1016/j.jmii.2020.07.006.

Wu, R. *et al.* (2008) 'Plasma level of endogenous hydrogen sulfide in patients with acute asthma', *Beijing Da Xue Xue Bao Yi Xue Ban*, 40:, pp. 505–508.

Wynn, T.A. (2015) 'Type 2 cytokines: mechanisms and therapeutic strategies', *Nature Reviews Immunology*, 15, pp. 271–282.

Xiao, H. *et al.* (2009) 'Effects of the selective muscarinic receptor antagonist penehyclidine hydrochloride on the respiratory tract', *Pharmazie*, 64, pp. 337–341. Available at: https://doi.org/10.1691/ph.2009.8764.

Xu, Y. (2019) 'Pulmonary function test and pulmonary interstitial disease', *Chinese Journal of Applied Clinical Pediatrics*, 34. Available at: https://doi.org/10.3760/CMA.J.ISSN.2095-428X.2019.16.002.

Xue, L. *et al.* (2014) 'Prostaglandin D2 activates group 2 innate lymphoid cells through chemoattractant receptor-homologous molecule expressed on TH2 cells', *The Journal of allergy and clinical immunology*, 133(4). Available at: https://doi.org/10.1016/J.JACI.2013.10.056.

Yang, D., Liu, Y. and Zhang, L. (2019) 'Tremella polysaccharide: The molecular mechanisms of its drug action.', *Progress in molecular biology and translational science*, 163, pp. 383–421. Available at: https://doi.org/10.1016/bs.pmbts.2019.03.002.

Yap, H.Y.Y. *et al.* (2013) 'Nutrient composition, antioxidant properties, and anti-proliferative activity of Lignosus rhinocerus Cooke sclerotium', *J. Sci. Food Agric*, 93, pp. 2945–2952. Available at: https://doi.org/10.1002/jsfa.6121.

Yap, H.Y.Y. *et al.* (2018a) 'Inhibition of protein glycation by tiger milk mushroom [Lignosus rhinocerus (Cooke) Ryvarden] and search for potential anti-diabetic activity-related metabolic pathways by genomic and transcriptomic data mining', *Frontiers in Pharmacology*, 9(FEB). Available at: https://doi.org/10.3389/FPHAR.2018.00103/FULL.

Yap, H.Y.Y. *et al.* (2018b) 'Molecular attributes and apoptosisinducing activities of a putative serine protease isolated from Tiger Milk mushroom (Lignosus rhinocerus) sclerotium against breast cancer cells in vitro', *PeerJ*, 2018(6). Available at: https://doi.org/10.7717/PEERJ.4940.

Yeo, Y. *et al.* (2019) 'Human Embryonic Stem Cell-Derived Neural Lineages as In Vitro Models for Screening the Neuroprotective Properties of Lignosus rhinocerus (Cooke) Ryvarden'. Available at: https://doi.org/10.1155/2019/3126376.

Yoshimoto, T. *et al.* (2009) 'Basophils contribute to T(H)2-IgE responses in vivo via IL-4 production and presentation of peptide-MHC class II complexes to CD4+ T cells', *Nature Immunology*, 10, pp. 706–712.

Yu, J. *et al.* (2018) 'Protective effect of sodium stearate on the moisture-induced deterioration of hygroscopic spray-dried powders', *International Journal of Pharmaceutics*, 541(1–2), pp. 11–18. Available at: https://doi.org/10.1016/J.IJPHARM.2018.02.018.

Yu, Q.L. and Chen, Z. (2018) 'Establishment of different experimental asthma models in mice', *Experimental and Therapeutic Medicine*, 15(3), pp. 2492–2498. Available at: https://doi.org/10.3892/ETM.2018.5721/HTML.

Yusuf, F., Prayle, A.P. and Yanney, M.P. (2019) 'β2-agonists do not work in children under 2 years of age: Myth or maxim?', *Breathe*, 15(4), pp. 273–276. Available at: https://doi.org/10.1183/20734735.0255-2019.

Zannetos, S. *et al.* (2017) 'The economic burden of adult asthma in Cyprus; a prevalence-based cost of illness study', *BMC Public Health*, 17(1), pp. 1–9. Available at: https://doi.org/10.1186/S12889-017-4184-0.

Zhang, C. *et al.* (2016) 'Antioxidant and hepatoprotective activities of intracellular polysaccharide from Pleurotus eryngii SI-04', *International Journal of Biological Macromolecules*, 91, pp. 568–577. Available at: https://doi.org/10.1016/J.IJBIOMAC.2016.05.104.

Zhang, G. *et al.* (2013) 'The inhibitory role of hydrogen sulfide in airway hyperresponsiveness and inflammation in a mouse model of asthma', *American Journal Pathology*, 182, pp. 1188–1195.

Zhang, H. *et al.* (2023) 'Preparation and structural characterization of acid-extracted polysaccharide from Grifola frondosa and antitumor activity on S180 tumor-bearing mice', *International Journal of Biological Macromolecules*, 234(29), p. 123302. Available at: https://doi.org/10.1016/j.ijbiomac.2023.123302.

Zhang, L. *et al.* (2022) 'Tilianin alleviates airway inflammation in ovalbumin-induced allergic asthma in mice through the regulation of Th2 cytokines and TGF-β1/Smad markers', *Arabian Journal of Chemistry*, 15(8). Available at: https://doi.org/10.1016/j.arabjc.2022.103961.

Zhang, W. *et al.* (2020) 'Technical evaluation of soft mist inhaler use in patients with chronic obstructive pulmonary disease: A cross-sectional study', *International Journal of COPD*, 15, pp. 1471–1479. Available at: https://doi.org/10.2147/COPD.S253338.

Zhao, S. *et al.* (2019) 'First demonstration of protective effects of purified mushroom polysaccharide-peptides against fatty liver injury and the mechanisms involved.', *Scientific reports*, 9(1), p. 13725. Available at: https://doi.org/10.1038/s41598-019-49925-0.

Zheng, L. *et al.* (2020) 'Distribution of Zinc in Mycelial Cells and Antioxidant and Anti-Inflammatory Activities of Mycelia Zinc Polysaccharides from Thelephora ganbajun TG-01', *Oxidative Medicine and Cellular Longevity*, 2020. Available at: https://doi.org/10.1155/2020/2308017.

Zhou, J. *et al.* (2020) 'A review on mushroom-derived bioactive peptides: Preparation and biological activities', *Food Research International*, 134, p. 109230. Available at: https://doi.org/10.1016/j.foodres.2020.109230.

Zhou, Y., Duan, Q. and Yang, D. (2023) 'In vitro human cell-based models to study airway remodeling in asthma', *Biomedicine & Pharmacotherapy*, 159, p. 114218. Available at: https://doi.org/10.1016/J.BIOPHA.2023.114218.

Zhu, Z.Y. *et al.* (2016) 'Effects of extraction methods on the yield, chemical structure and anti-tumor activity of polysaccharides from Cordyceps gunnii mycelia', *Carbohydrate Polymers*, 140, pp. 461–471. Available at: https://doi.org/10.1016/J.CARBPOL.2015.12.053.

Zosky, G.R. and Sly, P.D. (2007) 'Animal models of asthma', *Clinical and Experimental Allergy*, 37(7), pp. 973–988. Available at: https://doi.org/10.1111/j.1365-2222.2007.02740.x.

Zuo, H. *et al.* (2019) 'Phosphodiesterases as therapeutic targets for respiratory diseases', *Pharmacology and Therapeutics*, 197, pp. 225–242. Available at: https://doi.org/10.1016/j.pharmthera.2019.02.002.

APPENDICES

APPENDIX A   ANTIASTHMATIC STUDY ANIMAL ETHICS APPROVAL

Jawatankuasa Penjagaan dan Penggunaan Haiwan
Institusi USM (JKPPH USM)
USM Institutional Animal Care and Use Committee
(USM IACUC)

Bahagian Penyelidikan & Inovasi (R&I)
Kampus Kesihatan,
Universiti Sains Malaysia
16150, Kubang Kerian, Kelantan

Tel: 09-767 3000 samb. 2364 / 2352
W: www.research.usm.my

11th May 2021

Assoc. Prof. Dr. Nurul Asma Abdullah
School of Health Sciences
Universiti Sains Malaysia
16150 Kubang Kerian
Kelantan.

Dear Assoc. Prof. Dr.,

Animal Ethics Approval

Project title (1139): Study on the Effects of Intranasal Administration of Polysaccharides-Based Fractions (Polysaccharides and Glycolipids) from _Lignosus rhinocerotis_ in Ovalbumin-Induced Airway Inflammation Asthmatic Model

The USM Institutional Animal Care and Use Committee (USM IACUC) has approved the above research project. Principal Investigators are required to submit End of Project Report to USM IACUC within two (2) months after the completion of this project. Attached with this letter is the End of Project Report.

No. of Animal Ethics Approval: USM/IACUC/2021/(128)(1139)

Title	: Study on the Effects of Intranasal Administration of Polysaccharides-Based Fractions (Polysaccharides and Glycolipids) from _Lignosus rhinocerotis_ in Ovalbumin-Induced Airway Inflammation Asthmatic Model
Source of Animals	: Animal Research and Service Centre (ARASC), USM
Location of Animals	: Animal Research and Service Centre (ARASC), USM
Duration	: 01st June 2021 – 31st May 2024
Number of Samples	: 86 BALB/c Mice (Female)
Name of Principal Investigator	: Assoc. Prof. Dr. Nurul Asma Abdullah
Name of Co-Investigator	: Bushra Solehah Binti Mohd Rosdan : Dr. Abubakar Bishir Daku

(Please notify USM IACUC if there are additional staff/students who will be involved in animal handling for this project)

Jawatankuasa Penjagaan dan Penggunaan Haiwan Institusi USM   **JKPPH USM**
USM Institutional Animal Care and Use Committee (USM IACUC)

Jawatankuasa Penjagaan dan Penggunaan Haiwan
Institusi USM (JKPPH USM)
USM Institutional Animal Care and Use Committee
(USM IACUC)

Kampus Kesihatan,
Universiti Sains Malaysia
16150, Kubang Kerian, Kelantan

Tel: 09-767 3000 samb. 2364 / 2352
Email: jkpph@usm.my
W: www.research.usm.my

13 OGOS 2024

Prof. Madya Dr. Nurul Asma Abdullah
Pusat Pengajian Sains Kesihatan
Universiti Sains Malaysia
16150 Kubang Kerian
Kelantan

Prof. Madya Dr.,

PENGAKTIFAN SEMULA DAN PELANJUTAN TEMPOH KELULUSAN ETIKA HAIWAN

Tajuk Projek : Study of the Effects of Intranasal Administration of Polysaccharides-Based Fractions (Polysaccharides and Glycolipids) from *Lignosus rhinocerotis* in Ovalbumin-Induced Airway Inflammation Asthmatic Model [USM/IACUC/2021/(128)(1139)]

Perkara di atas adalah dengan hormatnya dirujuk. Jawatankuasa Penjagaan dan Penggunaan Haiwan Institusi USM (JKPPH) telah meluluskan permohonan pihak Prof. Madya Dr. sebagaimana berikut:

BIL	PERKARA
1.	Pengaktifan Semula dan Pelanjutan Tempoh Kelulusan Etika Haiwan 13 Ogos 2024 – 12 Ogos 2025

Sekian, terima kasih.

"MALAYSIA MADANI"
"BERKHIDMAT UNTUK NEGARA"
Saya yang menjalankan amanah,

PROF. DR. AIDA HANUM GHULAM RASOOL
Pengerusi
Jawatankuasa Penjagaan dan Penggunaan Haiwan Institusi USM (JKPPH USM)

![USM APEX logo]

UNIVERSITI SAINS MALAYSIA

Jawatankuasa Penjagaan dan Penggunaan Haiwan
Institusi USM (JKPPH USM)
USM Institutional Animal Care and Use Committee
(USM IACUC)

Kampus Kesihatan,
Universiti Sains Malaysia
16150, Kubang Kerian, Kelantan

Tel: 09-767 3000 samb. 2364 / 2352
Email: jkpph@usm.my
W: www.research.usm.my

31 MAC 2022

Prof. Madya Dr. Nurul Asma Abdullah
Pusat Pengajian Sains Kesihatan
Universiti Sains Malaysia
16150 Kubang Kerian
Kelantan

Prof. Madya Dr.,

PENGAKTIFAN SEMULA KELULUSAN ETIKA HAIWAN DAN PENAMBAHAN NAMA PENYELIDIK

Tajuk Projek : The Effect of Tiger Milk Mushroom / Lignosus rhinoceros Extract on Airway Smooth Muscle Contractility of Trachea Isolated from Guinea Pig
No. Kelulusan : USM/IACUC/2017/(109)(878)

Perkara di atas adalah dengan hormatnya dirujuk. Jawatankuasa Penjagaan dan Penggunaan Haiwan Institusi USM (JKPPH) telah meluluskan permohonan pihak Prof. Madya Dr. sebagaimana berikut:

BIL	PERKARA
1.	**Pengaktifan Semula Tempoh Kelulusan Etika Haiwan** 31 Mac 2022 – 31 Mac 2024
2.	**Penambahan Nama Penyelidik** Abubakar Bishir Daku

Sekian, terima kasih.

"WAWASAN KEMAKMURAN BERSAMA 2030"

"BERKHIDMAT UNTUK NEGARA"

Saya yang menjalankan amanah,

[signature]

PROF. DR. AIDA HANUM GHULAM RASOOL
Pengerusi
Jawatankuasa Penjagaan dan Penggunaan Haiwan Institusi USM (JKPPH USM)

Jawatankuasa Penjagaan dan Penggunaan Haiwan Institusi USM   **JKPPH USM**
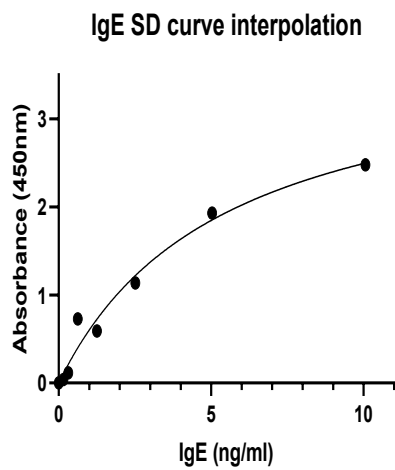USM Institutional Animal Care and Use Committee (USM IACUC)

APPENDIX C   STANDARD CURVES OF ELISA

BALF IL-4 SD curve interpolation
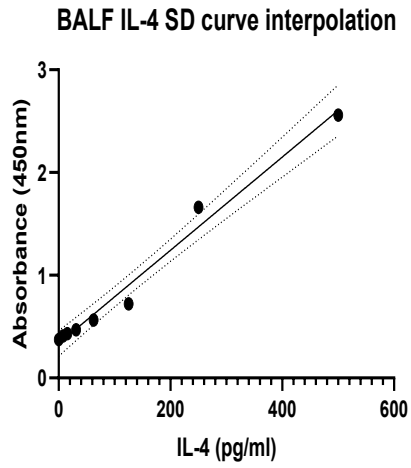
Standard	OD	IL-4 (pg/ml)
S1	2.55975	500
S2	1.66045	250
S3	0.72235	125
S4	0.56415	62.5
S5	0.4678	31.3
S6	0.4319	15.6
S7	0.4077	7.8
Blank	0.3741	0

IgE SD curve interpolation

Standard	OD	IgE (ng/ml)
S1	2.47835	10.065
S2	1.92935	5.0325
S3	1.1362	2.516
S4	0.59185	1.258
S5	0.72655	0.629
S6	0.11505	0.315
S7	0.0392	0.157
Blank	0	0

CERTIFICATE OF ATTENDANCE

this certificate is presented to

Abubakar Bishir Daku

A07399070

For attending the webinar

ANIMAL CARE & MANAGEMENT FOR PRE-CLINICAL STUDY

On July 14, 2021

Assoc. Professor Dr. Badrul Hisham Yahaya
Director

MAVMACPD-2021-118(1POINT)

CERTIFICATE
OF ATTENDANCE

PRESENTED TO:

Abubakar Bishir Daku

...ng a 4th ICSESS Pre-Conference Workshop Title...
...dard Research Paper and Publish in High Impac...
Organised by
...onal Students Society of Nigeria in Conjuction w...
Teknologi Malaysia (UTM) International

Date: 28th November 2021

...nmed
...TM

Mangai Solomon Mahanan
General Secretary ISS-Nigeria
UTM

Certificate of Participation

This Is To Certified That

Abubakar Daku

Has Completed

*Series 1 - ELISA Unveiled: Mastering the
Basics for Biotech Breakthroughs Webinar*

The above person is authorized to perform the assay with appropriate
documentation as specified in the course content.

Organiser: Date of Issue:

Prima Nexus   29-04-2024

Prima Nexus Sdn. Bhd.
28-1B, Jalan Puteri 1/2, Bandar Puteri Puchong, 47100 Selangor, Malaysia.
Co. Reg.: 1055479-X | info@primanexus.com.my

LIST OF PUBLICATIONS

Journal-full text:

1. **A. B. Daku**, S. B. AL-Mhanna, R. Abu Bakar & A. A. Nurul (2023). Glycolipids isolation and characterization from natural source: A review. Journal of Liquid Chromatography & Related Technologies. 45:13-16, 165-173, DOI: 10.1080/10826076.2023.2165097. **(Published)**

2. **Abubakar Bishir Daku**, Bushra Solehah Mohd-Rosdan, Noratiqah Mohtar, Asma Abdullah Nurul. (2024) Advances in polysaccharide-based formulations for intranasal drug delivery: A review, *Journal of Drug Delivery Science and Technology*, (101, Part B), 106266, doi.org/10.1016/j.jddst.2024.106266. **(Published)**

3. Abubakar, B. D, Nurul, A. A., Bushra, S. M. R., Kamaruddin, N. I., & Ahmad, W. A. N. W. (2025). Tiger Milk Medicinal Mushroom Lignosus rhinocerus (Agaricomycetes) Polysaccharides Mediates Airway Smooth Muscle Relaxation Via Muscarinic and Histamine Receptors. International Journal of Medicinal Mushrooms. https://doi.org/10.1615/INTJMEDMUSHROOMS.2025058606. **(Published)**

4. Inhalation characteristics and anti-asthmatic effects of Lignosus rhinocerotis polysaccharides: Potential applications in respiratory drug delivery **(Draft)**

5. In vivo bioactivities of mushroom polysaccharides: A Scoping review **(Draft)**

Book chapter:

Daku, A. B., Nurul, A. A. (2022). Pharmaceutical Nanoscience: Pulmonary Drug Delivery System, Advanced Pharmaceutical and Herbal Nanoscience for Targeted Drug Delivery Systems Part I: pp76-103. https://doi.org/10.2174/9789815036510122010007 **(Published).**